# SENSITIVITY AND UNCERTAINTY ANALYSES OF IMPACTS OF CLIMATE CHANGE ON REGIONAL AIR QUALITY

A Dissertation
Presented to
The Academic Faculty

By

Kuo-Jen Liao

In Partial Fulfillment
of the Requirements for the Degree
Doctor of Philosophy in the
School of Civil and Environmental Engineering

Georgia Institute of Technology
August 2008

# SENSITIVITY AND UNCERTAINTY ANALYSES OF IMPACTS OF CLIMATE CHANGE ON REGIONAL AIR QUALITY

Approved by:


Dr. Armistead G. Russell, Advisor
School of Civil and Environmental Engineering
*Georgia Institute of Technology*

Dr. Mehmet Talat Odman
School of Civil and Environmental Engineering
*Georgia Institute of Technology*

Dr. Michael H. Bergin
School of Civil and Environmental Engineering &
School of Earth & Atmospheric Sciences
*Georgia Institute of Technology*

Dr. Yuhang Wang
School of Earth & Atmospheric Sciences
*Georgia Institute of Technology*

Dr. Athanasios Nenes
School of Chemical & Biomolecular Engineering &
School of Earth & Atmospheric Sciences
*Georgia Institute of Technology*


Date Approved: May 16, 2008

# ACKNOWLEDGEMENTS

I deeply appreciate numerous people for their supports and helps during my Ph.D. studies at Georgia Tech. My greatest appreciation goes to my advisor, Dr. Ted Russell, for his guidance and providing a productive environment in his research group. I thank my committee members - Drs. Mike Bergin, Thanos Nenes, M. Talat Odman and Yuhang Wang - for their time and input to this work. Current and previous group members – especially Yongtao Hu, Thimios Tagaris, Kasemsan Manomaiphiboon, Jaemeen Baek, Burcak Kaynak, Farhan Akhtar, Jorge Pachon, Gretchen Goldman, Di Tian, Sun-Kyoung (Helena) Park, , Sangil Lee, Michelle Bergin, Evan Cobb, and so many others – assisted my research, and their friendship enriched my graduate life at Georgia Tech. My thesis also benefited from Drs. Praveen Amar (NESCAUM), Chien Wang (MIT), L. Ruby Leung (PNNL) and Dr. Loretta Mickley (Harvard University) for providing data used in this study. Furthermore, I would also like to thank the faculty and staff of the School of Civil and Environmental Engineering at Georgia Tech.

Research for this dissertation was mainly conducted with funding from the U.S. Environmental Protection Agency (STAR grant No. RD83096001, RD82897602 and RD83107601), Georgia Power and the Eastern Tennessee State University as well the Air & Waste Management Association – Georgia Chapter scholarship and my thanks also go to them.

# TABLE OF CONTENTS

# LIST OF TABLES

# LISTOF FIGURES

Page

# LIST OF SYMBOLS AND ABBREVIATIONS

Symbols

| | |
|---|---|
| $C_i$ | Concentration of pollutant i |
| $E_j$ | Emission of species j |
| $S_{i,j}$ | First-order sensitivity ($S_{i,j}$) of pollutant concentration $i$ ($C_i$) to source emissions $j$ ($E_j$) |
| ppb | Parts per billion by volume |

Abbreviation

| | |
|---|---|
| AOS | Atmospheric-Ocean System |
| CAIR | Clean Air Interstate Rule |
| CASTNET | Clean Air Status and Trends Network |
| CDF | Cumulative Distribution Function |
| CMAQ | Community Multiple Air Quality Model |
| CO | Carbon Monoxide |
| DDM-3D | Decoupled Direct Method in Three Dimension |
| EI | Emission Inventory |
| EIS | Energy-Industry System |
| GCM | Global Climate Model |
| GHG | Greenhouse Gas |
| GISS | Goddard Institute of Space Studies |
| $HO_2$ | Peroxy Radical |
| IGSM | Integrated Global System Model |
| IMAGE | Integrated Model to Assess the Global Environment |
| IPCC | Intergovermental Penal on Climate Change |
| JJA | June, July and August |
| MCIP | Meteorology Chemistry Interface Processor |
| $M8hO_3$ / MDA8h $O_3$ | Daily Maximum 8-hr Average Ozone |
| MM5 | Generation NCAR/Penn State Mesoscale Model |
| MSA | Metropolitan Statistical Area |

| | |
|---|---|
| NAAQS | National Ambient Air Quality Standards |
| NEI | National Emission Inventory |
| $NH_3$ | Ammonia |
| NH4_NH3 | Sensitivities of Ammonium to Ammonia Emissions |
| $NH_4NO_3$ | Ammonium Nitrate |
| $(NH_4)_2SO4$ | Ammonium Sulfate |
| NMVOC | Nonmethane Volatile Organic Compound |
| NPRI | National Pollution Release Inventory |
| $NO_x$ | Nitrogen Oxides (=NO + $NO_2$) |
| NMIM | National Mobile Inventory Model |
| OC | Organic Carbon |
| OH | Hydroxyl Radical |
| US EPA | United States Environmental Protection Agency |
| PAN | Peroxyacyl Nitrate |
| PDF | Probability Density Function |
| $PM_{2.5}$ | Particulate Matter with an aerodynamic diameter less than 2.5 μm |
| RAQM | Regional Air Quality Model |
| RH | Relative Himudity |
| RPO | Regional Planning Organization |
| VOC | Volatile Organic Compound |
| VMT | Vehicle Miles Traveled |
| SCC | Source Classification Code |
| SIP | State Implementation Plan |
| SMOKE | Sparse Matrix Operator Kernel Emissions Model |
| $SO_2$ | Sulfur Dioxide |
| $S_{4thMDA8hO3, ANOx}$ | Sensitivities of 4th MDA8h O3 to anthropogenic NOx emissions |
| $S_{4thMDA8hO3, AVOC}$ | Sensitivities of 4th MDA8h O3 to anthropogenic VOC emissions |
| $S_{NO3,ANOX}$ | Sensitivities of Nitrate to Anthropogenic Nitrogen Oxides Emissions |
| $S_{NO3,NH3}$ | Sensitivities of Nitrate to Ammonia Emissions |
| $S_{NO3,SO2}$ | Sensitivities of Nitrate to Sulfur Dioxide Emissions |
| $S_{SO4,ANOX}$ | Sensitivities of Sulfate to Anthropogenic Nitrogen Oxides Emissions |

| | |
|---|---|
| $S_{SO4,NH3}$ | Sensitivities of Sulfate to Ammonium Emissions |
| $S_{SO4,SO2}$ | Sensitivities of Sulfate to Sulfur Dioxide Emissions |
| SOA | Secondary Organic Aerosol |
| $S_{SOA,BVOC}$ | Sensitivities of Secondary Organic Aerosols to Biogenic Volatile Organic Compound Emissions |
| SRES | Special Report on Emissions Scenarios |
| SVOC | Semi-volatile Organic Compound |
| TES | Terrestrial Environment System |
| $4^{th}$ MDA8h $O_3$ | $4^{th}$-highest Daily Maximum 8-hr Average Ozone |

# SUMMARY

Climate change is forecast to affect ambient temperatures, precipitation frequency and stagnation conditions, all of which impact regional air quality. An issue of primary importance for policy-makers is how well currently planned control strategies for improving air quality that are based on the current climate will work under future global climate change scenarios. The US EPA's Regional Air Quality Modeling System, CMAQ, with DDM-3D are used to investigate sensitivities of ozone and $PM_{2.5}$ to emissions for current and future scenarios. Sensitivities are predicted to change slightly in response to climate change. In many cases, mass per ton sensitivities to $NO_x$ and $SO_2$ controls are predicted to be greater in the future due to both the lower emissions as well as climate, suggesting that current control strategies based on reducing such emissions will continue to be effective in decreasing ozone and $PM_{2.5}$ levels. Impacts of climate uncertainties on regional air quality predictions are investigated using multiple climate futures in order to evaluate the robustness of currently planned emission controls under impacts of climate change. The results show that planned controls for decreasing regional ozone and $PM_{2.5}$ will continue to be effective in the future under the extreme climate scenarios. However, the impact of climate uncertainties may be substantial in some urban areas and should be included in assessing future regional air quality and emission control requirements. Furthermore, daily cross-responses of ozone and $PM_{2.5}$ to emissions are investigated for current and future scenarios. Planned controls of $NO_x$ emissions are predicted to lead to more positive responses in reducing urban ozone and $PM_{2.5}$ levels in the future. Based on present emission control technologies, cost optimized emission reductions for offsetting impacts of climate change on regional peak fourth-highest daily maximum 8-hr average ozone and yearly average $PM_{2.5}$ are predicted to range from $27 million to $5.9 billion (1999$) per year in 2050s for the cities examined in this study.

# CHAPTER 1

# INTRODUCTION

## 1.1 Overview

Regional air pollution meteorology is forecast to respond to global climate change. Ground-level concentrations of air pollutants are highly sensitive to meteorological conditions, particularly temperature, humidity, precipitation and stagnation events. Mickley et al. (2004) suggest the reduced cyclone frequency in a future warmer climate could increase the severity of summertime pollution in the Northeastern and Midwestern U.S. Holzer and Boer (2001) found that decreases in continental atmospheric transport of the future climate cause stationary-state structure of long-lived passive tracers and hence higher air pollutant concentrations [*Holzer and Boer*, 2001]. Further, changes in precipitation can have a dramatic effect on frequency of washout and fine particle concentrations [*Racherla and Adams*, 2006].

In addition to air pollution meteorology, climate change is forecast to affect chemical and physical mechanisms of air pollutant formation. A number of studies show that peak ozone levels are positively correlated with ambient temperature [*Aw and Kleeman*, 2003; *Baertsch-Ritter, et al.*, 2004; *Menut*, 2003]. Higher temperatures increase decomposition of peroxyacyl nitrates (PANs) and spur the photolysis of nitrogen dioxides ($NO_2$) during the daytime and hence cause higher peak ozone levels [*Sillman*, 1995]. Higher absolute humidity (water vapor concentration), attributed to higher temperature, increases hydroxyl radicals (OH), resulting in faster oxidation of VOCs, forming peroxy

radicals (e.g., $HO_2$, $RO_2$) which react with nitrogen oxides (NO) to form $NO_2$. Moreover, when temperature-induced increases in VOC emissions (especially biogenic VOC emissions) are considered, higher VOC emissions induce more ozone formation in $NO_x$-saturated (or VOC-sensitive) urban areas [*Seinfeld and Pandis*, 1997]. However, recent studies suggest that, at least for ozone, future pollutant concentrations are more sensitive to the expected changes in precursor emissions than to the expected changes in temperature and photolytic flux [*Bergin, et al.*, 1999; *Russell and Dennis*, 2000]. As the amount of ozone formed per $NO_x$ molecule emitted remains somewhat constant [*Kleinman*, 2000], forecast changes in ozone will generally depend on the forecast $NO_x$ emission changes. Global/regional climate change is hypothesized to have relatively less impact on $NO_x$ emissions since they are largely anthropogenic and do not show a strong relationship with temperature.

Another important air pollutant, $PM_{2.5}$ (particulate matter with an aerodynamic diameter less than 2.5 μm), is influenced by climate change in several ways. Higher temperatures favor semi-volatile compounds (e.g., secondary organic aerosols (SOAs) and ammonium nitrate ($NH_4NO_3$)) to remain in the gas phase. On the other hand, increases in temperatures and humidity result in higher emissions of SOA precursors and faster oxidation of $SO_2$, $NO_x$ and VOCs, increasing formation of condensable compounds, such as sulfate, nitrate and Semi-Volatile Organic Compounds (SVOCs).

This study addresses an issue of primary importance for policymakers: how well currently planned control strategies for improving air quality for ozone and $PM_{2.5}$ that are based on the current climate will work under future global climate scenarios. Another

important objective of this study is to investigate impacts of climate change on regional air quality. Of particular interest are the uncertainties associated with the "climate penalty" (increases in levels of air pollutants caused by climate change) [*Mickley, et al.*, 2004] and investigating whether uncertainties in climate predictions suggest alternative emission control strategies. Responses of future ozone and $PM_{2.5}$ levels to both climate change and to emission changes are quantified using historic (2000-2002) and projected future (2049-2051) meteorology. The target future period, 2049-2051, is chosen as a compromise between being far enough in the future to experience non-trivial climate modification yet is still within a reasonable horizon for air quality planning.

For evaluating policy options it is important to investigate the interdependencies between air pollutant formation and how they respond to emission controls currently and as conditions change in the future. Such information can be used to evaluate how controls developed for one pollutant might influence levels for other pollutants. Here we examine daily responses of ozone and $PM_{2.5}$ to emission changes for current and future scenarios, including effects of climate change and currently planned emission controls, and investigate their correlations. Also, under the impacts of future climate change, it is important to quantify the economic impacts of climate change on regional air quality management if potential changes in meteorological fields affect direction and magnitude of currently planned emission controls for improving future air quality.

### 1.2 Sensitivity and Uncertainty Analyses

Sensitivity analysis quantifies the changes in the simulation results when one or multiple parameters are perturbed in the modeling systems. Uncertainty analysis is

important and describes how reliable the modeling results are since model inputs and parameterizations/assumptions lead to uncertainties in the outputs. For air quality management, policy-makers are interested in the sensitivities of air pollutants to changes in physical and chemical mechanisms in the regional air quality models (RAQMs), meteorological conditions and precursor emissions. Results of sensitivity analyses can help us investigate effectiveness of emission control strategies for improving air quality. There are a variety of ways to perform uncertainty analysis. One is an ensemble method, which uses same inputs for running multiple models in order to examine the uncertainties arising from model choice. Another method is to derive probability density functions (PDFs) of variables of interest by taking into account uncertainties in the more influential parameters and inputs.

Sensitivity and uncertainty analyses are used in this study in order to investigate the impacts of global climate change on air quality. Specifically, sensitivities of air pollutants to emission changes and how climate uncertainties affect the predicted impacts of climate change on air quality are investigated. The results are intended to help policy-makers evaluate the effectiveness and robustness of currently planned control strategies for improving air quality and human health in the future. If the pollutant fields and their sensitivities to anthropogenic emissions in the future are similar to current conditions, the conclusion would be that climate considerations will not significantly impact design of current control strategies that deal with ozone and $PM_{2.5}$ as much as if the relative sensitivities changed markedly. If the sensitivities are similar, but the pollutant levels are significantly different, then control strategies should focus on degree of controls rather

than direction. If, however, the sensitivities are significantly different, future control decisions should consider how climate changes.

### 1.3 Scope of This Work

The objectives of this study are to: 1) assess the impacts of global climate change on regional air quality; 2) investigate sensitivities of air pollutants to emissions; 3) quantify impacts of climate uncertainties on air quality forecast; 4) investigate cross-responses of multiple pollutants to emissions; and 5) estimate costs of emission reductions for offsetting climate impacts on air quality. Here, both the direct (impact of climate change alone on meteorology) and indirect impacts (those caused by emission changes due to either/both controls and climate change) of climate change on air quality are investigated. Furthermore, cross-responses of ozone and $PM_{2.5}$ to emission changes for current and future scenarios including effects of climate change and currently planned emission controls are investigated. Economic impacts of climate change on regional air quality management are also examined in this study.

The chapters are organized as follows:

- **Chapter 2**: **Development of North American Emission Inventories for Air Quality Modeling Under Climate Change.** Emissions of U.S., Canada and northern Mexico, consistent with near-term regulations and trends as well as longer-term projections, are developed to assess global climate impacts on regional air quality over North America.

- **Chapter 3: Impacts of Global Climate Change and Emissions on Regional Ozone and Fine Particulate Matter Concentrations over the United States.** Impacts of climate change alone and in combination with currently planned emission control strategies on regional ozone and $PM_{2.5}$ are examined over the continental United States.
- **Chapter 4: The Role of Climate and Emission Changes in Future Air Quality over Southern Canada and Northern Mexico.** Impacts of climate change alone and in combination with currently planned emission control strategies on regional ozone and $PM_{2.5}$ are examined over western and eastern Canada as well as northern Mexico.
- **Chapter 5: Impacts of Future Climate and Emissions Reductions on Nitrogen and Sulfur Reposition over the United States.** Impacts of climate change alone and in combination with currently planned emission control strategies on sulfur and nitrogen deposition are examined over the continental United States.
- **Chapter 6: Sensitivities of Ozone and Fine Particulate Matter Formation to Emissions under the Impact of Potential Future Climate Change.** Impacts of climate change alone and in combination with currently planned emission control strategies on sensitivities of air pollutants to emissions are examined. Results of sensitivity analysis are used to investigate the effectiveness of currently planned emission reductions for decreasing regional air pollutant levels in the future.
- **Chapter 7: Quantification of Impact of Climate Uncertainty on Regional Air Quality.** Given uncertainties in climate forecasts, significance of climate uncertainties and their impacts on air quality are examined in this chapter. The

results of uncertainty analysis are used to evaluate the robustness of currently planned control strategies for improving air quality.

- **Chapter 8: Current and Future Linked Responses of Ozone and $PM_{2.5}$ to Emissions Controls.** Interdependencies between ozone and $PM_{2.5}$ formation and their cross-responses to emission controls are investigated for current and future scenarios. Cross-responses of ozone and $PM_{2.5}$ to emissions are quantified and linked on a daily basis for five cities in the continental United States.
- **Chapter 9: Cost Analysis of Impacts of Climate Change on Regional Air Quality.** Costs of emission reductions for offsetting impacts of climate change on regional air quality are estimated in 2050s using a regional air quality model and cost control tools for five cities in the United States.
- **Chapter 10: Summary and Future Research.** This chapter presents the summary and main findings of this work and recommendations for future research.
- **Appendix A:** Auxiliary material for Chapter 3
- **Appendix B:** Auxiliary material for Chapter 6
- **Appendix C:** Auxiliary material for Chapter 7
- **Appendix D:** Auxiliary material for Chapter 8
- **Appendix E:** Auxiliary material for Chapter 9

# CHAPTER 2

# DEVELOPMENT OF NORTH AMERICAN EMISSION INVENTORIES FOR AIR QUALITY MODELING UNDER CLIMATE CHANGE *

## 2.1 Introduction

Climate change, amongst its many impacts, will affect future regional air quality, which will have potential human health, ecosystem and economic implications. Assessing such impacts is frequently done using regional air quality models which rely on emissions inventories (EIs) of the relevant precursor emissions (e.g., VOCs, $NO_x$, $SO_2$, $NH_3$, primary PM). However, forecasting emissions out to a period far enough into the future so as to result in significant climate change, yet be able to provide consistent emission estimates that reflect various current regulations and trends is challenging.

In the past decade, US EPA has been taking regulatory actions (e.g. Clean Air Interstate Rule (CAIR) [*EPA*, 2005], Regional Haze Rule, etc.) aimed at improving air quality in the US. Finalized in 2005, CAIR would significantly reduce emissions of ozone and PM precursors ($SO_2$ and $NO_x$) from electric generating units across 28 eastern states and the District of Columbia by 2015. In addition, Regional Haze Rule issued in 1999 sets federal requirements targeting reductions in emissions of PM precursors to restore visibility to natural or pristine conditions in national Class I areas by 2064.

---

* This chapter is accepted to publish in the *Journal of the Air & Waste Management Association*. Co-authors are Jung-Hun Woo, Shan He, Efthimios Tagaris, Kasemsan Manomaiphiboon, Praveen Amar and Armistead G. Russell.

These regulatory efforts have resulted in reliable near-future (up to the year 2020) emission inventory for the U.S. Beyond that, IPCC has formulated a wide range of global long-term (up to year 2100) SRES emission scenarios (e.g. A1B, A1T, A2, B1, B2 etc.) [*IPCC*, 2001; *Nakic´enovic´*, 2000]. These long-term emission projections are based on alternate combinations of complex economic/energy/climate assumptions and thus are associated with high level of uncertainty.

The Integrated Model to Assess the Global Environment (IMAGE), developed by Netherlands's National Institute for Public Health and the Environment (RIVM), is one of the more commonly used models to estimate emissions associated with global change (http://www.mnp.nl/en/themasites/image/index.html, last access: May 11, 2008). The main objectives of IMAGE are to contribute to scientific understanding and support decision-making by quantifying the relative importance of major processes and interactions in the society-biosphere-climate system. In the IMAGE 2.2 framework, the general equilibrium economy model, WorldScan, and the population model, PHOENIX, feed the basic information on economic and demographic developments for 17 world regions into the following three linked subsystems. The first subsystem, Energy-Industry System (EIS), calculates regional energy consumption, energy efficiency improvements, fuel substitution, supply and trade of fossil fuels, and renewable energy technologies. On the basis of energy use and industrial production, EIS computes emissions of greenhouse gases (GHGs) (i.e., $CO_2$, $CH_4$ and $N_2O$), ozone precursors ($NO_x$, CO, NMVOC) and $SO_2$. The second subsystem, Terrestrial Environment System (TES), computes land-use changes on the basis of regional consumption, production and trading of food, animal feed, fodder, grass and timber, with consideration of local climatic and terrain properties.

TES computes emissions from land-use changes, natural ecosystems and agricultural production systems, and the exchange of $CO_2$ between terrestrial ecosystems and the atmosphere. Finally, the third subsystem, the Atmospheric-Ocean System (AOS) calculates changes in atmospheric composition using the emissions and other factors (such as land cover change, $CO_2$ uptake, global mean temperature change, moisture availability, etc.) in the EIS and TES, and by taking oceanic $CO_2$ uptake and atmospheric chemistry into consideration. Subsequently, AOS computes changes in climatic properties by resolving the changes in radiative forcing caused by greenhouse gases, aerosols and oceanic heat transport. Historical data for the 1765-1995 period are used to initialize the carbon cycle and climate system. IMAGE 2.2 simulations cover the 1970-2100 period. Data for 1970-1995 are used to calibrate EIS and TES. Simulations up to the year 2100 are made on the basis of scenario assumptions for variables such as demography, food and energy consumption, technology and trade. Although IMAGE 2.2 is global in scope, it performs many of its calculations either on a high-resolution terrestrial 0.5 by 0.5 degree grid (land use and land cover) or for 17 specific world regions (energy, trade and emissions). The energy sectors in the IMAGE are as follows: 1) five energy end-use sectors, i.e. industrial, transport, residential (households), services (commercial and public) and other (agricultural and other), 2) energy consumption by electric power generation, 3) other energy transformation, 4) fossil fuel production (coal production, gas flaring associated with oil production, gas transmission, etc.), and 5) marine bunkers (international shipping). Also, the energy carriers included in IMAGE are: 1) solid fuels (coal and coal products), 2) heavy liquid fuels (diesel, residual fuel oil and crude oil), 3) light liquid fuels (LPG and gasoline), 4) gaseous fuels (natural and

from gasworks), and 5) modern biofuels such as ethanol. The CO, $NO_x$, $SO_2$, and NMVOC are estimated from the model as distinct emission species. The summary of EIS model input, output, and assumptions are described in the Table 2.1.

**Table 2.1: Inputs, outputs, and assumptions of Energy-Industry System (EIS) included in IMAGE**

| | |
|---|---|
| **Model input (energy)** | Income per capita |
| | Energy production and energy end-use consumption (TIMER) |
| | Fraction surface and deep coal mining ($CH_4$) (fossil trade flows) |
| **Submodel assumptions** | Emission factors for energy sectors and carriers (technological and efficiency improvements, structural changes) |
| | Fraction of catalyst-equipped cars |
| | Technological improvements and end-of-pipe control techniques for CO, NMVOC, $NO_x$ and $SO_2$ (FGD in power plants, fuel specification standards for transport, clean-coal technologies industry, etc.) |
| **Model input (industry)** | Regional population |
| | Energy end-use consumption by industry (TIMER) |
| **Submodel assumptions** | Emission factors for industrial sectors and carriers |
| | End-of-pipe control techniques for CO, VOC, $NO_x$ and $SO_2$ |
| | Marine bunkers and feedstocks |
| **Model output** | Emissions of $CO_2$, $CH_4$, $N_2O$, $NO_x$ and $SO_2$, CO, NMVOC and halocarbons. |

The IMAGE thus generates a database using a series of models that allows for the estimation of global emissions with a high degree of internal consistency. This study used emissions data from IMAGE model results for the three regions of interest (Canada, U.S., and Mexico) and for three years (2001, 2020, and 2050) using the A1B scenario. With IPCC A1B as reference scenario, Streets et al. tested the "x1" set of scenarios, which represent globalization scenarios, and are considered to be a much more likely set of futures than the "x2" set of global fragmentation futures [*Streets, et al.*, 2004]. Also, Streets et al. (2004) note that these scenarios are much more in line with recent emission trends in many parts of the world. In a previous research effort they first selected two futures for examination, B1 and A1, and noted a higher level of confidence in the B1 scenario to be realized [*Streets and Fernandes*, 2002]. B1 represents an emphasis on environmental protection, whereas A1 stresses economic development. They eventually selected A1B scenario as the midrange "balanced" scenario.

As part of our more detailed study of climate- regional air quality interactions, a mid-21st century emissions inventory (EI) for North America was required for a modeling study of regional ozone and fine particle matter. Since the time span (about 50 years in the future) of such a long projection is beyond that of regular State Implementation Plan (SIP) EI's used in typical regional air quality modeling (in range of 10~20years), it is necessary to identify a practical approach that allows the future-year projection to account for possible emission controls and climatic and socio-economic changes. However, a technical challenge arises because such an approach requires integration of various different types of information with which emissions from human activities are associated. Often, information given or generated for global-scale studies

has less detail and uses coarser spatial-temporal resolution. This study extensively reviewed and analyzed a number of existing regional and global scale emissions projection efforts, and then developed a method that takes into account up-to-date emission scenarios. Evaluation is based on data availability and accessibility, spatial-temporal coverage and resolution, and future-scenario consistency (i.e. IPCC SRES A1B, the driving future emissions scenario adopted). The method consists of two sequential steps. First step involves the near-future projection of emissions to the year 2020, based closely on both the US EPA CAIR EI and the Environment Canada EI, as well as emissions projections from regional planning organizations (RPOs) in the US. The second step is longer term (to mid-21$^{st}$ century) EI projection, following approaches proposed by the RIVM in its IMAGE model. For Mexico, we update present EI using BRAVO and Mexico NEI, and then project directly to the year 2050 since no intermediate projections are available. Combination of these approaches provides a best-estimate and practical emissions input for regional air quality modeling platform.

Species of interest for regional air quality modeling include carbon monoxide (CO), nitrogen oxides ($NO_x$), sulfur dioxide ($SO_2$), nonmethane volatile organic compounds (NMVOC), ammonia ($NH_3$), and particulate matters ($PM_{2.5}$ and $PM_{10}$). The Sparse Matrix Operator Kernel Emissions (SMOKE) and Community Multiscale Air Quality (CMAQ)-Decoupled Direct Method (DDM) model [*Dunker, et al.*, 2002; *Napelenok, et al.*, 2006] are employed as emissions processing and chemical transport models, respectively, in our modeling platform. This work fills in the gaps in emissions estimates from rather more certain near-term emission scenario (EPA CAIR, year 2020) to less certain distant-future scenarios (e.g., 2050). The resulting inventories have been

used to simulate changes in regional air quality in the U.S. ($O_3$ and $PM_{2.5}$) between now and 2050 [*Liao, et al.*, 2007; *Tagaris, et al.*, 2008; *Tagaris, et al.*, 2007]. Not only this work should provide better emission estimates for climate change impact assessments 50 years down the road, it should also be helpful as a policy-relevant tool and for scientific research.

## 2.2 Methods

### 2.2.1 Emission Inventory for USA

This study develops estimates of future emissions that are as consistent as possible to the Inter governmental Panel on Climate Change SRES A1B scenario, which is the emission scenario that has been used to simulate future climate at global scale, yet also take into account recent emission control efforts in North America. The SRES A1B scenario describes a future world of rapid economic growth and global population that peaks in mid-century and declines thereafter, with rapid introduction of more efficient technologies, and balanced usage between fossil fuels and other energy sources. This study, however, does not restrict itself to the A1B scenario alone and incorporates other information as well.

Salient features of a number of existing regional- and global-scale emissions projection efforts are presented in Figure 2.1. Based on evaluation of a number of factors including data availability and accessibility, spatial-temporal coverage and resolution, and future-scenario consistency (i.e. IPCC SRES A1B, the driving future emissions scenario adopted), an integrated EI is developed. Specific EIs that form the basis of our

forecast, and account for recent control decisions, include the Clean Air Interstate Rule (CAIR) EI from US EPA and the Environment Canada (EC) EI, and the RIVM's IMAGE EI. After considering the factors noted above, the 2001 CAIR EI of EPA was chosen as the base-year inventory for this study. The projection of 2050 emissions from the 2001 base-year consists of two steps: first, collecting and merging projected EI for near-future which already incorporates all of "visible" growth and control (up to year 2020); and then, conducting a distant-future EI projection (up to the mid-century) using a more coarse, but integrated modeling approach. The former is based on the US EPA CAIR 2020 EI while the latter follows approach given by RIVM's IMAGE Model. The year 2020 CAIR EI was selected as the basis for the near-future emissions due to the following advantages. The readily available CAIR EI is the "official" data that is used for the EPA's Rulemaking, and as such, has undergone significant evaluation and quality assurance. It is based on updated growth and control assumptions and has content and format which is most consistent with the needs of this study. In addition, CAIR uses the most recent national database for its base-year 2001, as in this study. The base-year and year-2020 inventories were developed in a "SMOKE-ready" format and include the following pollutants: carbon monoxide (CO), nitrogen oxides ($NO_x$), non-methane volatile organic compounds (NMVOC), sulfur dioxide ($SO_2$), ammonia ($NH_3$), particulate matter with an aerodynamic diameter less than 10 microns ($PM_{10}$), and particulate matter with an aerodynamic diameter less than 2.5 microns ($PM_{2.5}$). As noted earlier, RIVM's IMAGE model was selected to project emissions from year 2020 to year 2050. IMAGE model is the only one available that covers the time horizon of the target future year 2050 (up to year 2100 maximum) as well as the scenarios (i.e. IPCC SRES A1B) which are

consistent with the climate/meteorological scenario of this study. The IMAGE model, as described earlier, has other sub-models which can incorporate interactions among various components. It is readily available and has been used for a US EPA's inter-continental scale transport modeling project.

| Name | Base Year | Future Years | Geographical Domain | Scenario | Source sectors | Chemical species | Model | Availability |
|---|---|---|---|---|---|---|---|---|
| EPA CAIR | 2001 | 2010 /2015 /2020 | Continental US | EPA BASE /CAIR | EGUs, non-EGUs | NOx, VOCs, CO, NH3, SO2, PM | IPM /EGAS/ NMIM | Yes |
| EPA CSI | 1996 | 2010 /2020 | Continental US | EPA BASE /CSI | EGUs, Non-EGUs | NOx, VOCs, CO, NH3, SO2, PM | IPM /EGAS | Yes |
| RPO | 2002 | 2009 /2018 | Continental US | OTB/OTW | EGUs & non-EGUs | NOx, VOCs, CO, NH3, SO2, PM | IPM /EGAS | Partly |
| SAMI | 1990 | 2040 (/10yrs) | 38 States + DC | OTB/OTW/ BWC/BB | EGUs & non-EGUs | NOx, VOCs, CO, NH3, SO2, PM | SAMI | No |
| RIVM* | 1995 | ~2100 (/yr) | World (17 regions) | IPCC SRES(A1, B1, A2, B2) | Energy sector/fuel combination | CO2, CH4, N20, CO, NOx, SO2, NMVOC | IMAGE | Yes |
| NESCAUM /EPA | 1999 | ~2025+ (/3yrs) | Units(EGUs), States(NE), Country | BAU, RGGI | Energy sector/fuel combination | NOx, VOCs, CO, NH3, SO2, PM | MARKAL | 2007 |

Pros Cons Both

RIVM : Netherlands's National Institute for Public Health and the Environment

IMAGE : Integrated Model to Assess the Global Environment

**Figure 2.1: Salient features of a number of existing regional- and global-scale emissions projection efforts**

Integration of the future emissions inventories was done as follows: 1) EPA CAIR inventories for year-2001 and year-2020 were processed with SMOKE programs to ensure consistency in data formatting followed by the generation of an emissions summary by each Source Classification Code (SCC); 2) emissions and "surrogates" (agricultural production and black/organic carbon for $NH_3$ and PM, respectively) from IMAGE and Streets et. al. were estimated for USA/Canada/Mexico and for Y2001/Y2020/Y2050 to generate growth factors for these periods [*Streets, et al.*, 2004];

3) cross-references from US SCC to IMAGE sector/fuel combination were developed, and finally; 4) growth factors were applied to the yearly inventories, using cross references described above to estimate the year-2050 inventory for North America. For on-road mobile sources in the U.S., first the RPO 2018 VMT (vehicle miles traveled) projection and MOBILE6 input scenarios files were used, then IMAGE transportation sector growth factor was used to represent post-2018 change. The forecasting approach accounts for current and expected regulations as well as growth technology advancements, but any forecast over such a long period is open to uncertainties. Finally, emissions were calculated using SMOKE/MOBILE6 with future meteorological (MM5) forecasts.

### 2.2.2 Emission Inventory for Canada and Mexico

In the EPA CAIR work, emissions for Canada and Mexico were held constant for base and future years. This approach may be acceptable for near future (i.e. year 2020), US-based assessments, but is insufficient for more distant periods for climate-related work. Therefore a growth approach was applied for Canada and Mexico even though their emissions information is limited and emission magnitudes are relatively small compared to the US at present. For Canada, the present emissions inventory was updated from US EPA's 1996 Canadian inventory by combining it with Environment Canada (EC)'s emissions inventory (year 2000 for point sources and year 2020 for area, nonroad, on-road mobile, (http://www.epa.gov/ttn/chief/net/canada.html, last access: May 11, 2008) and by using the New York State's Department of Environmental Conservation (NYS DEC)'s point source inventory that includes updated data on Canadian point

sources [*E.H. Pechan & Associates*, 2006c]. For Mexico, the present emissions inventory was updated from US EPA's 1999 BRAVO inventory by combining it with BRAVO EI and Mexico NEI (http://www.epa.gov/ttn/chief/net/mexico.html, last access: May 11, 2008). Since the Mexico NEI (MNEI) only covers six states, it was merged with BRAVO EI to cover the entire modeling domain. Since MNEI does not include emissions of fugitive dust, BRAVO data are used instead for the six-border states. With a merged inventory, growth factors were applied to the datasets.

### 2.3 Results and Discussion

IMAGE-generated emissions estimates for IPCC SRES A1B scenario have been extensively analyzed in this study to provide insights on emissions trends, and to develop growth factors specific to the modeling region. Emissions trends are presented in Figure 2.2 by fuels (left panel) and by source sectors (right panel) for three IMAGE regions (USA/Canada/Mexico) and for three years (Y2001/Y2020/Y2050) for $SO_2$ (top row), $NO_x$ (second row from top), NMVOC (third row from top), and CO (bottom row). For $SO_2$, the dominant fuel is coal (CL) for the US and Canada, and heavy oil (HO) for Mexico (Mexico is part of the Central America region in IMAGE). In the U.S. and Canada, $SO_2$ emissions are forecasted to decline substantially between 2001 and 2020 (~70%) but the rate of decline is lower between 2020 and 2050 (~18%). For Mexico, emissions are forecasted to increase between 2001 and 2020 (~100%) but decline after 2020 (down to 70% of 2020 level by 2050). Power generation (POWGEN) is the dominant sector for $SO_2$ emissions for all three countries (60~80% in US). For $NO_x$, the dominant fuels are light oil (LO) and coal for US and Canada (70~80% overall), but light

oil (LPG and gasoline) and heavy oil (diesel and residual fuel oil) are the important contributors in Mexico (75%). In the U.S., and Canada, $NO_x$ emissions are forecasted to decline throughout all future years. Mexico shows an opposite trend as emissions increase. Transportation (TRA) is dominant sector for Y2001 for all three countries but POWGEN sector becomes more important as total emissions decrease in the future. In U.S. and Canada, $NO_x$ emissions decline because of the implementation of emission controls on vehicles and major stationary sources. But in Mexico, power generation drives an increase in NOx emissions. For NMVOC, the country-by-country emissions trend shows patterns that are similar to $SO_2$ and the dominant fuel is light oil (gasoline) (more than half of emissions from fuel in US, 2001). The transportation, industrial process (INDPRO) and fugitive emissions (LOSS) are the dominant sectors for NMVOC (more than 95% overall). This trend is consistent with high growth rates in such sectors as industrial solvents, paints, glues, and chemicals production. Such industrial commodities are typically associated with economic development. Hydrocarbon emissions from growing transportation fleets of Mexico add to NMVOC emissions. Forecasted CO emissions show a similar pattern to $SO_2$ by countries (2.5 times lower in 2050 compared to 2001). The dominant fuel and sector are, however, light oil and transportation (95% in US, 2001), respectively.

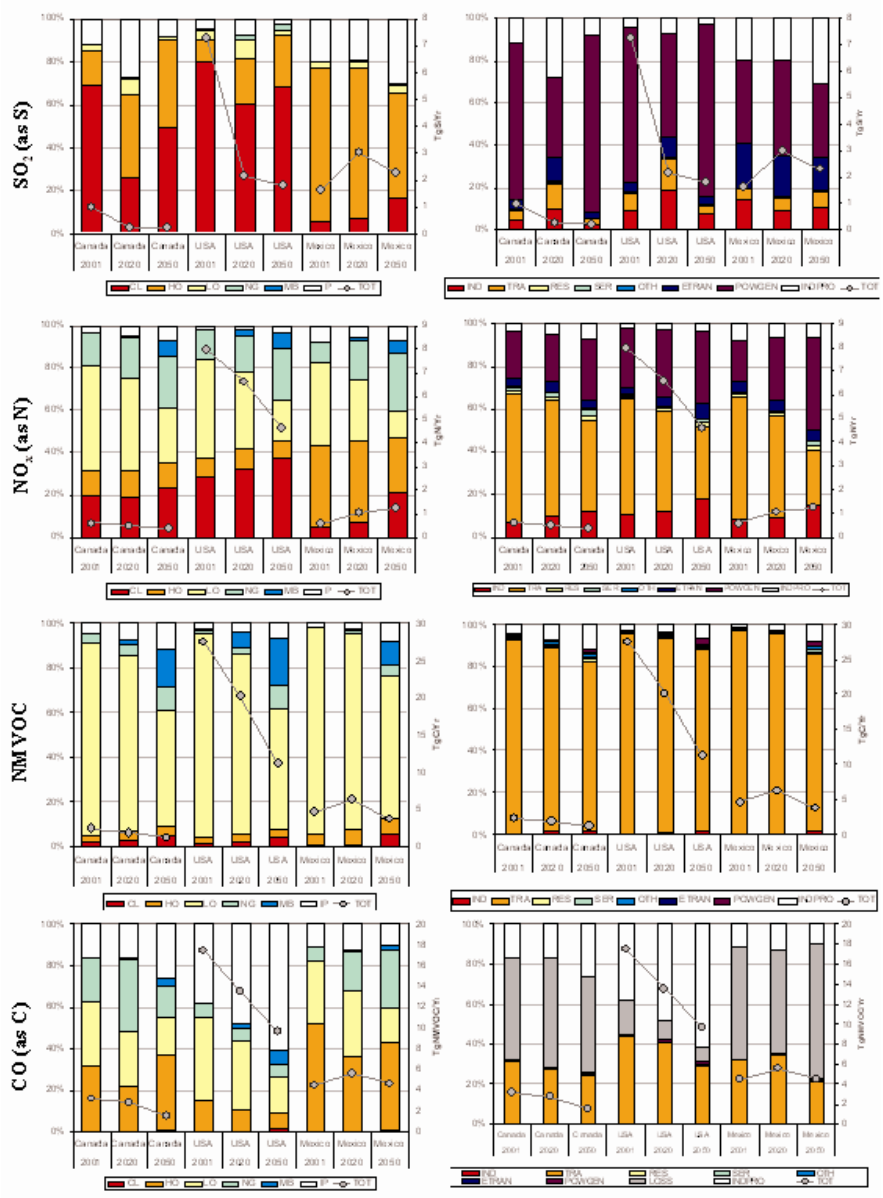


**Figure 2.2: IMAGE emissions (A1B) of $SO_2$, $NO_x$, NMVOC, and CO by fuels (left) and by source sectors (right) for three IPCC regions (USA/Canada/Mexico) and three years (Y2001/Y2020/Y2050) IND : Industrial, TRA : Transportation, RES : Residential, SER :Service, OTH : Other, ETRAN : Energy Transformation, POWGEN : Power Generation, INDPRO : Industrial Processes, LOSS : Loss, CL: Coal, HO: Heavy Oil, LO: Light Oil, NG: Natural Gas, MB : Modern Biofuel, IP : Industrial Processes, TOT : Total**

Ammonia and PM species are treated differently since their emissions are not calculated in the IMAGE model. Agricultural activities were used as the $NH_3$ surrogate. Only livestock production from the IMAGE model was used to "grow" $NH_3$ emissions because $NH_3$ emissions from fertilizer application are held constant through all years in CAIR emissions. Black carbon and organic carbon results from Streets et al. were used as primary PM surrogates [*Streets, et al.*, 2004]. Present and future emissions of two surrogates are shown in Figure 2.3. Agricultural production is projected to increase by more than 30 percent in 50 years for all three countries. PM emission trends show similar patterns as $NO_x$, with a small change in Canada, and a ~40% decrease in the U.S. In Mexico, PM emissions increase by ~20% by 2030 but then decrease by more than 50% by 2050.

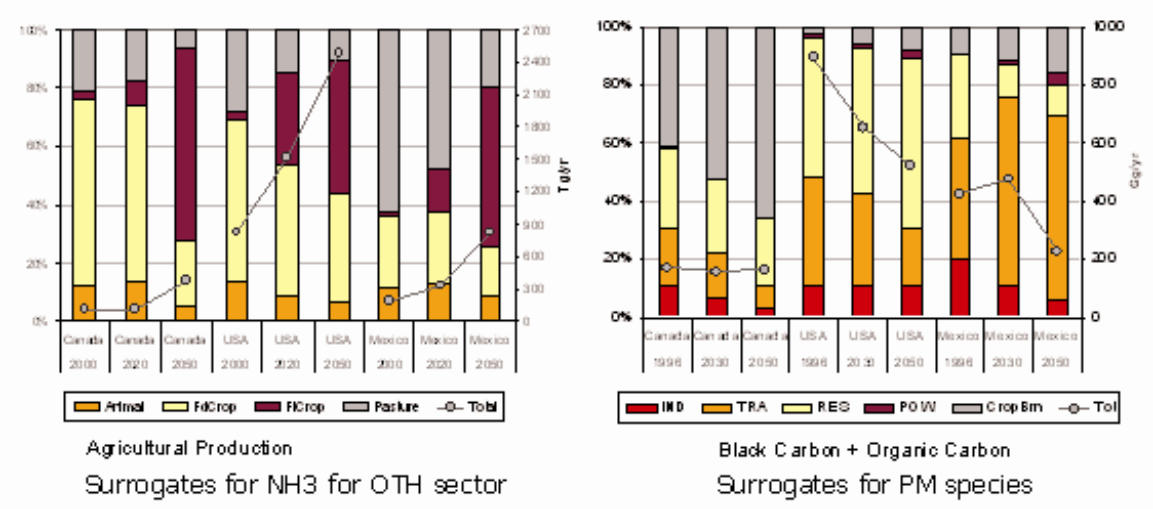


**Figure 2.3: Emissions trends of $NH_3$ and PM under the A1B scenario for three IPCC regions (USA/Canada/Mexico) and three years (Y2001/Y2020/Y2050) FdCrop : Food Crop, FlCrop : Field Crop, CropBrn : Crop Residue Burning**

### 2.3.1 Present and Future Emissions in USA

Since the purpose is to estimate projected emissions, the sectors remaining constant during the years (i.e. fire and fugitive dust) are not included. Figure 2.4 shows US $SO_2$ emissions by state and by source types (point, area, nonroad, and on-road mobile) for years 2001, 2020, and 2050. Based on the CAIR emission inventory, point sources are the dominant source category due to high emissions from the power generation sector. The Midwest region shows higher $SO_2$ emissions due to its substantial coal-fired power generation sector. Area source contributions are relatively high in Northeast compared to other regions due to the higher use of residential oil combustion. Overall, controls and fuel changes by the year 2050 lead to a decrease in $SO_2$ emissions by more than 50% compared to their 2001 level.

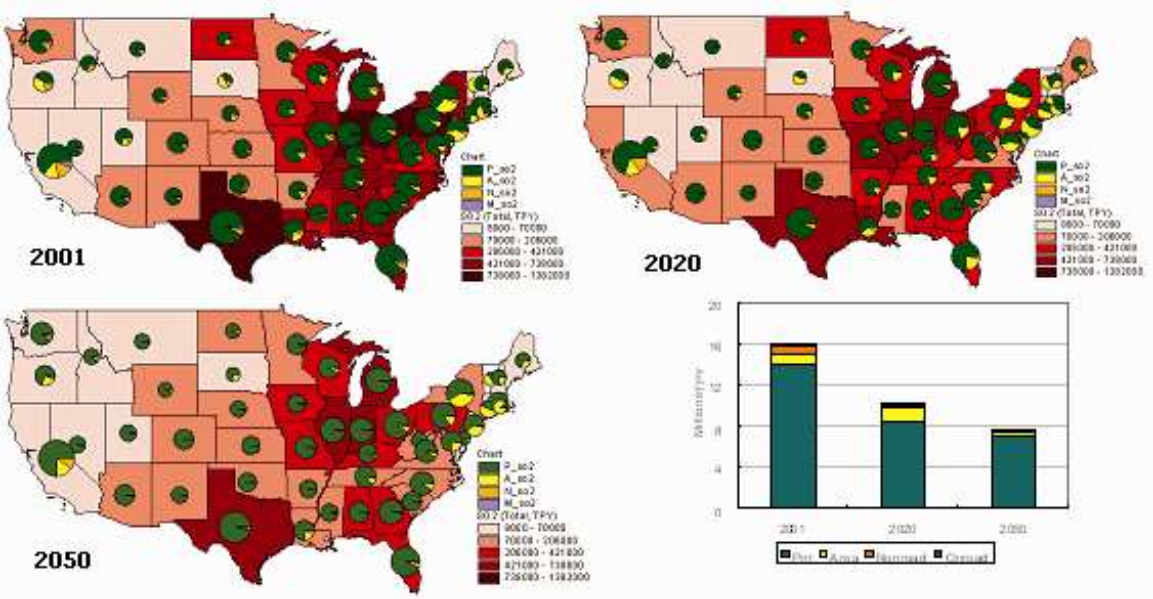


**Figure 2.4: Present and future years $SO_2$ emissions by US states and by source types (P : Point source, A : Area source, N : Nonroad mobile source, M : On-road mobile source)**

Figure 2.5 shows $NO_x$ emissions (in the same format as the $SO_2$ case in Figure 2.4). For $NO_x$, mobile sources (nonroad and on-road) contribute more than half of the total emissions and point sources' portion is about 40%. Emissions decrease throughout the years for mobile and for point sources. On-road mobile emissions show a distinct decrease until the year 2020 due to control programs (e.g. U.S. Tier 2 standards). Note that on-road mobile source emissions estimates are not from SMOKE/MOBILE6 but from National Mobile Inventory Model (NMIM) in CAIR EI [*USEPA*, 2003]. Therefore no growth factor is applied to the on-road mobile source sector beyond 2020. Instead, it is estimated by SMOKE/MOBILE6 with future meteorological fields generated by MM5 model [*Grell, et al.*, 1994; *Seaman*, 2000]. Leung and Gustafson downscaled the GISS simulations for 1995–2005 and 2045–2055 periods using the MM5 to the regional scale [*Leung and Gustafson*, 2005]. MM5 forecasts cover year 2050 but not 2020 since the year 2020 was the future year for the regional regulatory modeling (i.e. CAIR) and not for the climate change. SMOKE/M6 use humidity and temperature data from MM5. Although there are uncertainties in using regionally downscaled climate, we do not consider them here. As for regional distribution, California, Texas and Midwest regions show high $NO_x$ emissions in year-2001 but they are substantially lower in future years.

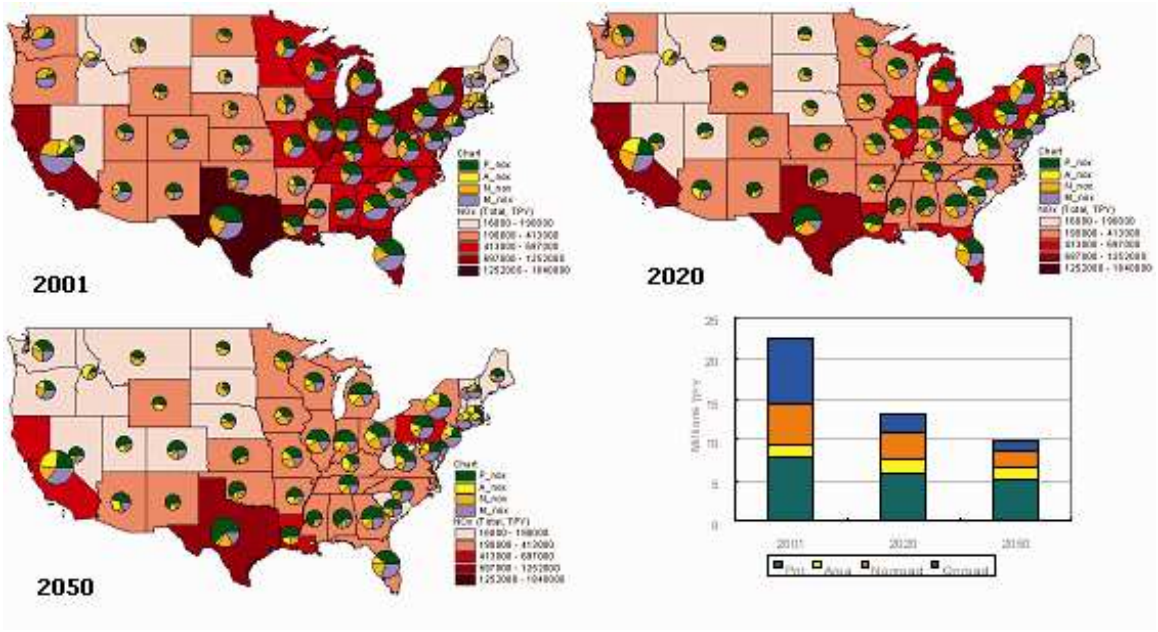


**Figure 2.5: Present and future years $NO_x$ emissions by U.S. states and by source types (P : Point source, A : Area source, N : Nonroad mobile source, M : On-road mobile source)**

Area sources are an important source category for NMVOC (~40%) (Figure 2.6). Emissions decreases are not as significant as $SO_2$ and $NO_x$. Major emissions reductions occur in on-road and nonroad mobile source sectors. The spatial distribution of NMVOC shows a similar pattern to $NO_x$.

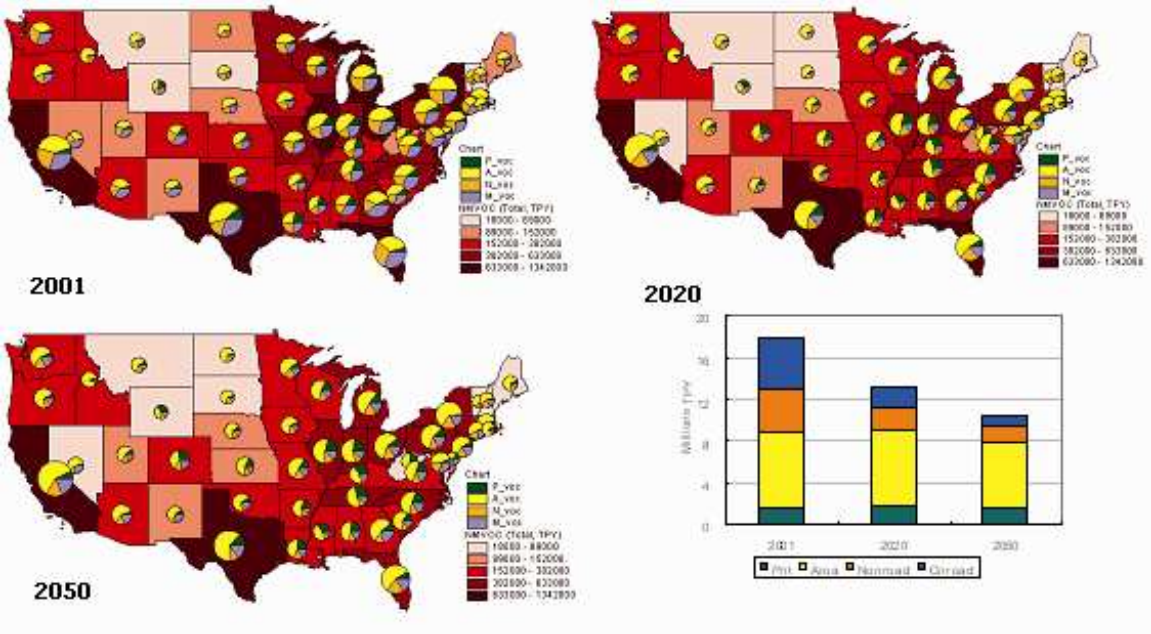


**Figure 2.6: Present and future years NMVOC emissions by U.S. states and by source types (P : Point source, A : Area source, N : Nonroad mobile source, M : On-road mobile source)**

$PM_{2.5}$ emissions (Figure 2.7) indicate point sources as the dominant source category (contributing ~45% $PM_{2.5}$). Overall, $PM_{2.5}$ emissions decrease in the future but point source emissions increase from 2001 to 2020. Note that fugitive dust and fire emissions which comprise about 50% of total $PM_{2.5}$ are not included in this analysis since they are assumed to remain constant through the years. $PM_{2.5}$ emissions are high in California, Texas, Georgia, Florida, and the Midwest region. The area source contribution is high on the west coast, mid-Atlantic and northeast states, whereas the point sources contribution is high in Texas, Midwest and the southern states. $PM_{10}$ and CO emissions (Figure 2.8) show decreases in the future, but $NH_3$ emissions gradually increase due to increased agricultural activities (e.g. livestock feeding). Again, note that

80% of total $PM_{10}$ emissions in the United States are from excluded sources (i.e. fugitive dust and fire emissions).

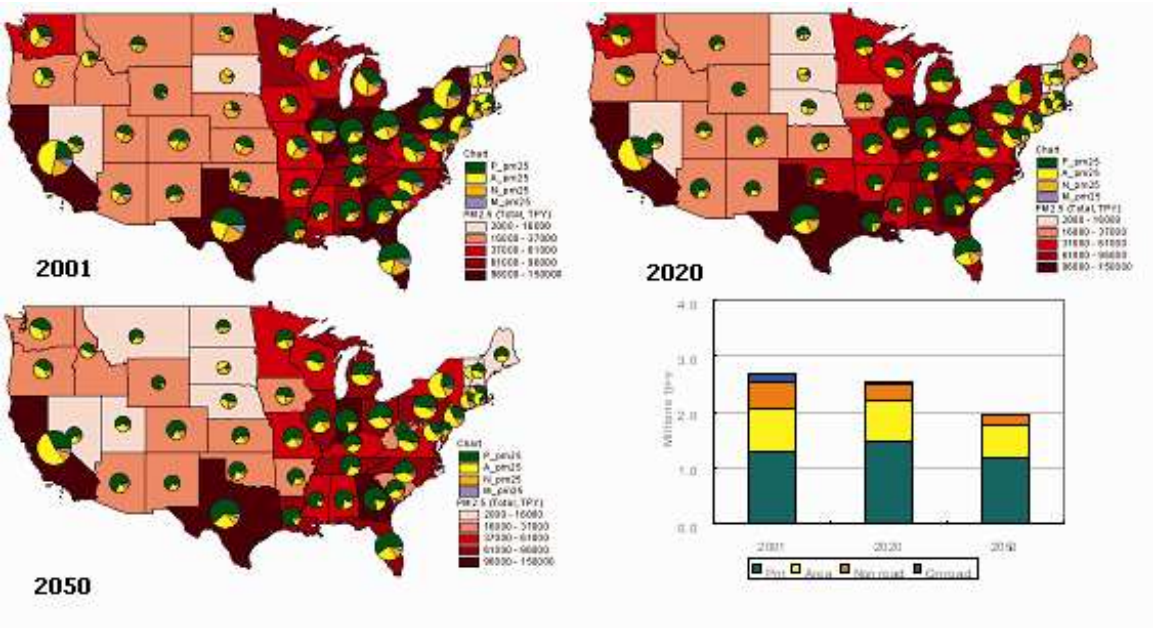


**Figure 2.7: Present and future years $PM_{2.5}$ emissions by U.S. states and by source types (P : Point source, A : Area source, N : Nonroad mobile source, M : On-road mobile source)**

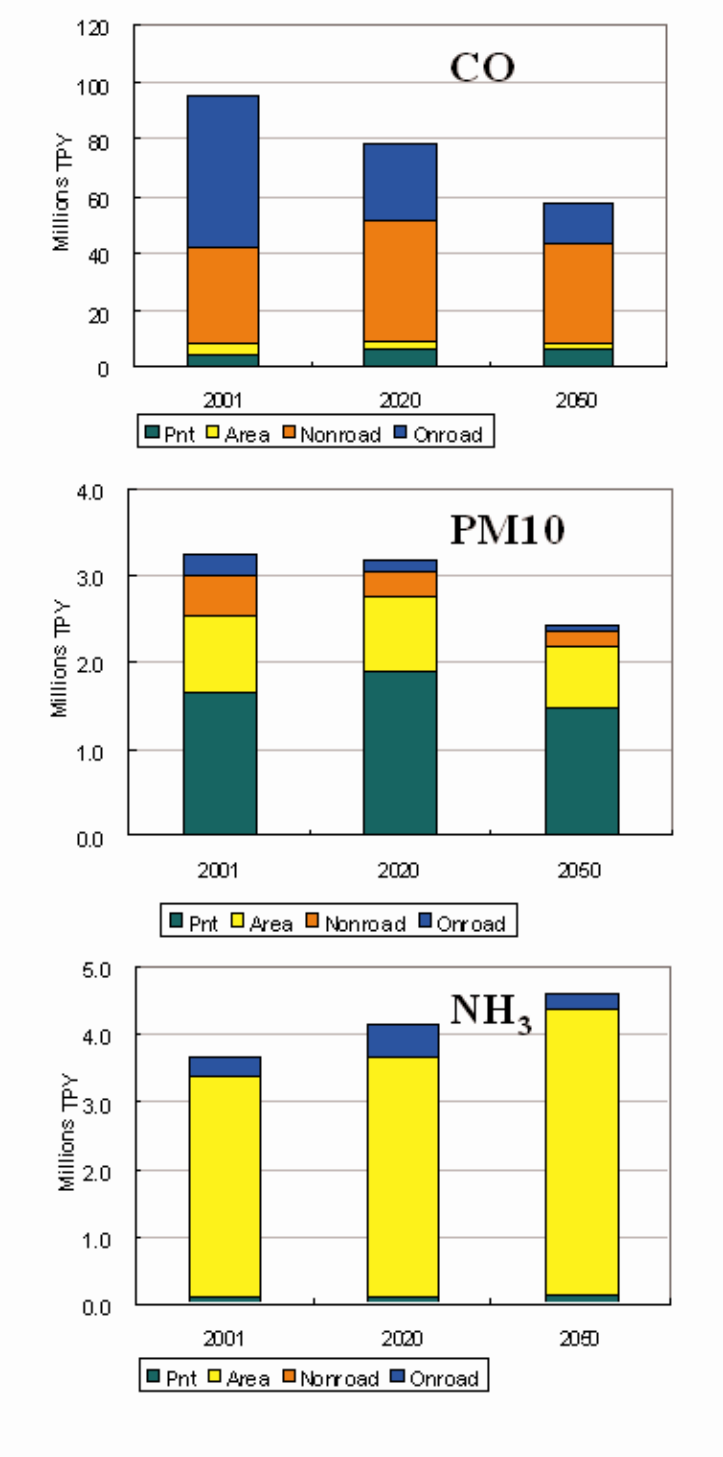


**Figure 2.8: Present and future-years U.S. CO, $PM_{10}$, and $NH_3$ emissions by source types**

As described earlier, future on-road mobile emissions estimates are generated by SMOKE/MOBILE6 and adjusted for daily meteorology. However it is also of interest to investigate impact of VMT vs. controls on future emissions without considering meteorological variable changes in the future. To do that, we conducted one-day SMOKE/MOBILE6 run for base year (2002), near future (2018), and distant future (2050) for 12 Northeast and Mid-Atlantic States. Inventories are developed for each year, and emissions modeling is used to develop day-specific emissions accounting for time of year, weekend-weekday, hourly and meteorological variations on source-by-source basis. Results are shown for August 1 for comparative purposes. Year 2018 is used as near-future year instead of 2020, since 2018 is the future year for regional haze SIP emissions inventory. For this comparison, VMT and planned regulations in the Mobile6 calculation for 2018 are held constant through 2050 and all proposed regulations and controls are included. VMT and CO results are shown in Figure 2.9. VMT increases 10~30% compared with the base year. In spite of VMT increase, CO emissions decrease dramatically because of controls. Emissions decrease much more slowly after 2018 as no new regulations are imposed. This suggests that additional regulations would be needed for reducing emissions for the post-2018 era. According to projections (up to the year 2030) included in the EPA's Tier 2 Regulatory Impact Analysis (EPA 2005), NMVOC emissions will increase post-2018 due to VMT increase and this trend will continue if new regulations or new technologies are not introduced. Therefore, for mobile source projections, a combined approach similar to the "other source types" is used by first adopting Regional Planning Organization (RPO) 2018 VMT projection and MOBILE6

input scenarios files; and then growing 2018 VMT using IMAGE transportation sector growth factor (i.e. 0.496) to represent post-2018 growth and control.

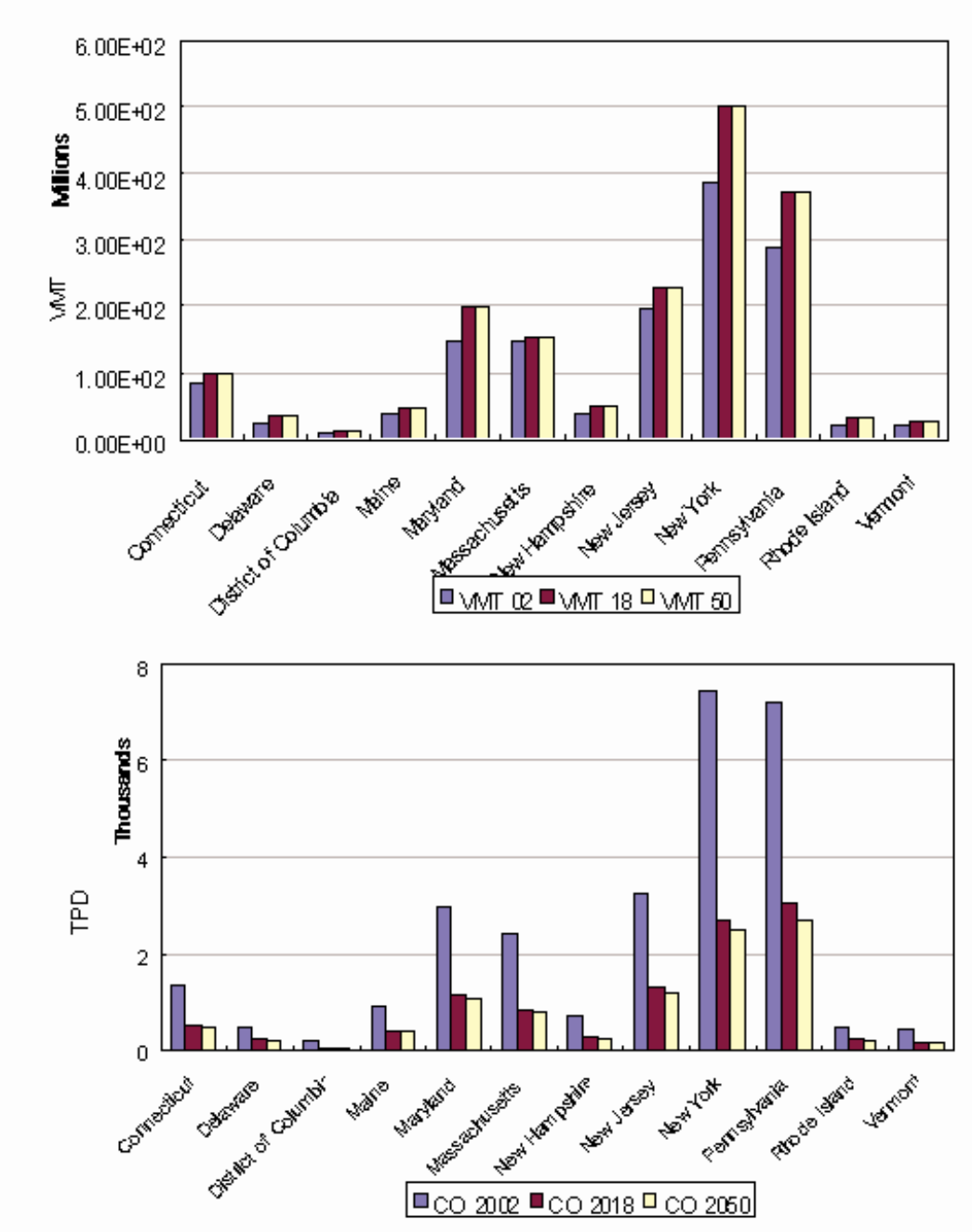


**Figure 2.9: VMT and CO emissions for three years (2002/2018/2050) for MANE-VU states**

The emissions results from IMAGE (2001, 2020, 2050), CAIR (2001, 2020), and this study (2050) are presented in the Table 2.2. For the year 2001, $SO_2$ emissions estimates from IMAGE and CAIR are the same but $NO_x$ and VOCs emissions show differences of -22.5 and 11%, respectively. The differences result from the fact that the IMAGE 2001 emissions are projected from the year 1995 data. $SO_2$ emissions show very little discrepancy in the base year (i.e. 2001) because $SO_2$ major emission sector is power generation which has very firm near term growth and control plans. The year 2050 $SO_2$ emissions from this study, however, are almost twice as much as IMAGE's because IMAGE assumes faster fuel transient than CAIR. $NO_x$ emissions show bigger discrepancy than in $SO_2$ case for the starting point (23% in the year 2001) but show less (41%) in the year 2050. In this case, CAIR shows faster reduction of NOx from onroad, nonroad mobile, and area sources but IMAGE shows bigger reduction only in transportation sector. The year 2050 $NO_x$ emissions estimates from this study are lower than pure IMAGE estimate, as a result. VOC estimates show moderate difference (11%) initially but end up very close (4%) because CAIR estimates a little more reduction in the 2001-2020 period. For $NO_x$ emissions in the year 2050, Wu et al. (2007) estimated about 40% reduction on the continental U.S. scale which is quite similar to IMAGE estimates because both approaches use the same IPCC A1B scenario [*Wu, et al.*, 2007]. Our year 2050 $NO_x$ estimate, which showed 15% more reduction than IMAGE, may be more reasonable because it includes more updated emission activities and control measures for the U.S.

**Table 2.2: Emissions results from IMAGE (2001, 2020 and 2050), CAIR (2001, 2020)**

| Tg/yr | 2001 | | 2020 | | 2050 | |
|---|---|---|---|---|---|---|
| | IMAGE | CAIR | IMAGE | CAIR | IMAGE | This Study |
| $SO_2$ | 16.0 | 16.0 | 4.8 | 10.2 | 3.9 | 7.6 |
| $NO_x$ | 28.9 | 22.4 | 24.0 | 13.3 | 16.8 | 9.9 |
| VOC | 16.0 | 17.8 | 13.4 | 13.1 | 10.8 | 10.3 |

### 2.3.2 Present and Future Emissions in Canada and Mexico

For Canada, the present emissions inventory was developed by combining Environment Canada (EC)'s emissions (year 2000 for point sources and year 2020 for area, nonroad, on-road mobile, available at http://www.epa.gov/ttn/chief/net/canada.html. last access: May 11, 2008) and New York State Department of Environmental Conservation (NYS DEC)'s year 2002 point source inventory, which is based on EC's National Pollutant Release Inventory (NPRI) data (http://www.ec.gc.ca/pdb/npri/npri_home_e.cfm. last access: May 11, 2008). NYS DEC's EI is scaled using EC's province subtotal to avoid inconsistency between the datasets. While $NH_3$ is missing in NYSDEC's point source dataset, $NH_3$ emissions are scaled by $NO_x$ emissions because of high correlation (r=0.9) between two species' emissions found in Canadian point source summary. With the "scaled" point source inventory, growth factors for years 2050/2000 (point source) and 2050/2020 (area, nonroad, on-road mobile) are applied to the datasets. Some source sub-sectors, for example, volcano, fugitive dust, fertilizer application, and fire, are not grown, so as to be consistent with US data. Table 2.3 shows 2000 and 2050 Canadian emissions for all

seven species. Most emissions estimates, except PM, drop by about 30%. PM emissions increase because the surrogate species, EC emissions increase from 2000 to 2020.

**Table 2.3: Year 2000 and Year 2050 Canada point, area, nonroad, and on road mobile source emissions (TPY)**

| Source | Year | CO | $NO_x$ | VOC | $NH_3$ | $SO_2$ | $PM_{10}$ | $PM_{2.5}$ |
|---|---|---|---|---|---|---|---|---|
| Point | 2000 | 1.33 | 0.73 | 0.29 | 0.03 | 2.30 | 0.26 | 0.14 |
| Area | 2000 | 1.87 | 0.44 | 1.94 | 0.59 | 0.20 | 5.31 | 0.84 |
| Nonroad | 2000 | 2.92 | 0.77 | 0.35 | 0.00 | 0.06 | 0.07 | 0.06 |
| Onroad | 2000 | 6.31 | 0.94 | 0.45 | 0.02 | 0.03 | 0.02 | 0.02 |
| Sum | 2000 | 12.43 | 2.87 | 3.03 | 0.64 | 2.59 | 5.66 | 1.06 |
| Point | 2050 | 0.65 | 0.45 | 0.14 | 0.02 | 0.51 | 0.15 | 0.08 |
| Area | 2050 | 1.62 | 0.41 | 1.16 | 0.36 | 0.20 | 7.42 | 1.07 |
| Nonroad | 2050 | 2.13 | 0.54 | 0.17 | 0.00 | 0.04 | 0.04 | 0.03 |
| Onroad | 2050 | 2.36 | 0.15 | 0.08 | 0.02 | 0.00 | 0.00 | 0.00 |
| Sum | 2050 | 6.76 | 1.54 | 1.56 | 0.40 | 0.75 | 7.61 | 1.18 |

For Mexico, the present emissions inventory from US EPA's 1999 BRAVO inventory is updated by combining it with MNEI (http://www.epa.gov/ttn/chief/net/mexico.html, last access: May 11, 2008). BRAVO fugitive dust EI values are used since MNEI does not include dust emissions. Then year 2050/1999 growth factors are applied to the merged inventory. $NO_x$ emissions increase by more than a factor of two due to growth of power generation industrial sector (Table 2.4). Emissions of $SO_2$, however, increase at a lower rate due to controls. CO and PM emissions decrease due to improved combustion and emission controls.

**Table 2.4: Year 1999 and year 2050 Mexico point and area source emissions (TPY)**

| Source | Year | CO | $NO_x$ | VOC | $NH_3$ | $SO_2$ | $PM_{10}$ | $PM_{2.5}$ |
|---|---|---|---|---|---|---|---|---|
| Point | 1999 | 2.68 | 0.43 | 1.22 | 0.00 | 2.89 | 0.62 | 0.33 |
| Area | 1999 | 3.00 | 0.34 | 0.86 | 0.35 | 0.14 | 0.76 | 0.23 |
| Sum | 1999 | 5.67 | 0.77 | 2.09 | 0.35 | 3.04 | 1.39 | 0.56 |
| Point | 2050 | 2.23 | 1.04 | 1.29 | 0.00 | 3.55 | 0.32 | 0.17 |
| Area | 2050 | 2.55 | 0.82 | 0.90 | 1.12 | 0.22 | 0.72 | 0.20 |
| Sum | 2050 | 4.78 | 1.86 | 2.19 | 1.12 | 3.78 | 1.04 | 0.37 |

The resulting inventories have been used to simulate changes in regional air quality in the U.S. between now and 2050 [*Tagaris, et al.*, 2007]. Briefly, that study found that emission changes have a greater impact on pollutant concentrations than climate change, emphasizing the importance of accurately forecasting emission trends. Although climate change alone modifies mean summer maximum daily 8-hr ozone levels ($M8hO_3$) by ±3% regionally and mean annual $PM_{2.5}$ concentrations by -3% to 6%, the impact of climate change, growth activity and emissions controls lead to a 20% decrease (regionally varying from -11% to -28%) in the mean summer $M8hO_3$ while mean annual $PM_{2.5}$ concentrations are estimated to be 23% lower (varies from -9% to -32%). Total nitrogen and sulfur deposition in the future is simulated to be lower over the U.S. compared to the historic period considering both climate change and planned controls on precursor emissions. Reductions in the Northeast, Midwest and Southeast sub-regions will be higher compared to West and Plains, responding to emission reductions. Climate change, alone, with no emissions growth or controls has a minor impact on nitrogen and

sulfur deposition rates. Sensitivities of ozone and $PM_{2.5}$ formation to precursor emissions are found to change only slightly in response to climate change. Sensitivities to $NO_x$ and $SO_2$ controls are predicted to be greater in the future due to both the lower emissions as well as climate, suggesting that current control strategies based on reducing emissions will continue to be effective in decreasing ground level ozone and $PM_{2.5}$ concentrations. Uncertainties associated with climate scenarios are found to have a rather moderate effect on the predicted biogenic VOC emissions and ozone concentrations in year 2050 [*Liao, et al.*, 2008]. Differences in concentrations of M8hO3 due to uncertainties in climatic conditions are found up to 10 ppb in some polluted urban areas, though the change in summer-average ozone is minimal (~1 ppb). Differences in annualized $PM_{2.5}$ levels are predicted to range between -1.0 and +1.5 $\mu g\ m^{-3}$. Planned controls for decreasing regional ozone and $PM_{2.5}$ will continue to be effective in the future under the extreme climate scenarios. The trend in pollutant concentrations reveals the key role that emission control strategies may play in future regional air quality, setting forecasting of emissions as key to being able to assess the impact of climate change on pollutant concentrations.

## 2.4 Summary

Mid-21$^{st}$ century U.S., Canadian and Northern Mexican emissions, consistent with near-term regulations and trends (e.g. US EPA CAIR 2020 EI) and longer-term projections (using RIVM's IMAGE modeling with IPCC SRES A1B) are developed to assess global climate impacts on regional air quality over North America. US emissions in the future (Year-2050) are estimated to decrease by 55% each for $NO_x$ and $SO_2$, 30% for $PM_{2.5}$, 40% for VOC, and increase by 20% for ammonia. Without further regulations,

post-2018 emissions from U.S. onroad mobile sources will not decrease significantly because of VMT growth. IMAGE model, however, projects a decrease for this source sector. The Canadian EI shows decrease in emissions of gaseous pollutants but an increase in particle emissions because of fugitive dust. For Mexico, emissions of $NO_x$, $SO_2$, $NH_3$, and VOC are estimated to increase but CO, $PM_{10}$, and $PM_{2.5}$ emissions are expected to decrease. The methods developed here as well as the future projected EI could be directly adopted or refined for policy-relevant assessment of future regional air quality.

# CHAPTER 3

# IMPATCS OF GLOBAL CLIMATE CHANGE AND EMISSIONS ON REGIONAL OZONE AND FINE PARTICULATE MNATTER CONCENTRATIONS OVER THE UNITEAD STATES *

## 3.1 Introduction

Recent observations and future projections suggest that regional air quality will respond to global climate change and the two systems are intrinsically coupled [*Brasseur, et al.*, 2006; *IPCC*, 2001]. However, our understanding of the linkages between air quality and climate change remain incomplete, in part, due to the disparate spatial and temporal scales traditionally used in the study of these fields.

Climate change over the next century is predicted to have a direct impact on meteorology [*IPCC*, 2001]. Leung and Gustafson (2005) discuss the potential for air quality changes in the western and southwestern U.S. in the 2050s based on changes in surface air temperature, downward solar radiation, precipitation frequency, stagnation events and ventilation in future climate simulations for the U.S. Mickley et al. (2004) suggest the reduced cyclone frequency in a future warmer climate could increase the severity of summertime pollution in the Northeastern and Midwestern US, although the increase of hurricane strength and precipitation might counteract this in some regions [*Webster, et al.*, 2005].

---

* This chapter is published in the *Journal of Geophysical Research*, Vol. 112, D14312, doi:10.1029/2006JD008262, 2007. Co-authors are Tagaris Efthimios, Kasemsan Manomaiphiboon, L. Ruby Leung, Jung-Hun Woo, Shan He, Praveen Amar, and Armistead G. Russell.

Hogrefe et al. (2004) estimate that regional climate change alone will increase the summertime average daily maximum 8-hour ozone concentration over the eastern U.S. by 4 ppb in the 2050s. Their results are based on the IPCC A2 emission scenario [*IPCC,* 2001], which is one of the highest future emissions scenarios. Knowlton et al., 2004 estimate that in 2050 there will be a 4.5% increase in ozone-related acute mortality in New York metropolitan area [*Knowlton, et al.,* 2004], although some researchers (e.g. Schwartz et al. (2005)) question their findings. Using a similar approach, Murazaki and Hess (2006) estimate 0-2 ppb decreases in U.S. background ozone and an increase up to 6 ppb within the U.S. in 2100 compared to 2000 due to climate change alone. Recently Langner et al. (2005) have examined the impact of global/regional climate change on surface ozone and deposition of sulfur and nitrogen in Europe [*Langner, et al.,* 2005]. A strong increase in surface ozone and mean of daily maximum over southern and central Europe and a decrease in northern Europe have been estimated. The decrease in wet deposition of sulfate and nitrate over western and central Europe is caused by the reduction in precipitation, but the authors caution that longer simulation periods are necessary to establish the changes in deposition.

Recent studies suggest that, at least for ozone, future pollutant concentrations are more sensitive to the expected changes in precursor emissions than to the expected changes in temperature and photolytic flux (e.g., Bergin et al, 1999; Russell and Dennis, 2000). As the amount of ozone formed per $NO_x$ molecule emitted remains somewhat constant (e.g., Kleinman, 2000), except in areas with very high emissions of $NO_x$ (e.g., [*Ryerson, et al.,* 2001]) or high in reactive VOC emissions and given the small change estimated for VOC emissions, forecast differences in ozone will generally depend on the

forecast $NO_x$ emission changes. This should not be construed as suggesting that ozone will not respond to VOC controls as significant evidence suggests otherwise, even in cities with high biogenic loadings [*Cohan, et al.*, 2006]. Global/regional climate change will have relatively less impact on $NO_x$ emissions since they are largely anthropogenic and they do not show a strong function of temperature. Thus, current policies in the U.S. to reduce $NO_x$ emissions, such as those being pursued now, (http://www.epa.gov/airtrends/nitrogen.html, last access: May 11, 2008) should continue to be effective.

The objective of this study is to assess the impacts of global climate change on regional air quality over the US. Here, both the direct (impact of climate change on meteorology) and indirect impacts (those caused by emission changes due to either/both controls and climate change) are evaluated. We focus on $O_3$ and fine particulate matter (FPM) because of their suspected significant human health effects [*El-Fadel and Massoud*, 2000; *Galizia and Kinney*, 1999; *Pekkanen, et al.*, 1997]. Specifically, we follow $PM_{2.5}$ (particulate matter with an aerodynamic diameter less than 2.5 μm). Future $O_3$ and $PM_{2.5}$ concentrations are compared to historic ones under two different cases: In the first case, impacts of changes on regional air quality in the US by climate change alone are examined by keeping emissions sources, activity levels and controls constant. In the second case we estimate the future pollutant concentrations based on changes in climate and emissions using the IPCC A1B emission scenarios (IPCC, 2001) and planned controls.

## 3.2 Method

Air quality modeling was conducted using the Community Multiscale Air Quality (CMAQ) Modeling System [*Byun and Schere,* 2006] and meteorology downscaled from the Goddard Institute of Space Studies (GISS) Global Climate Model (GCM) [*Rind, et al.*, 1999] using the Penn State/NCAR Mesoscale Model (MM5) [*Grell, et al.*, 1994]. Future-year emissions forecast for North America are developed by forecasting activity growth and application of emission controls, as discussed below.

### 3.2.1 Emissions

The 2001 Clean Air Interstate Rule (CAIR) emission inventory (EI) (http://www.epa.gov/cair/technical.html, last access: May 26, 2008) is used as the U.S. emission inventory for the historic period (i.e., 2000-2002), as well as the basis for projected emissions up to 2020. For Canada, the Environment Canada (EC)'s 2000 inventory has been used for area and mobile sources (http://www.epa.gov/ttn/chief/net/canada.html, last acess: May 11. 2008). For point sources, the 2002 inventory that the New York States Department of Environmental Conservation compiled using National Pollution Release Inventory (NPRI) was scaled using EC's state level summary. For Mexico, the US EPA's 1999 BRAVO inventory has been updated with the Mexico NEI (http://www.epa.gov/ttn/chief/net/mexico.html, last access: May 11, 2008).

Projection of emissions is done in two steps: i) for near future (2001 – 2020), the 2020 CAIR EI of the US EPA is modified using Economic Growth Analysis System

(EGAS) factors (http://www.epa.gov/ttn/ecas/egas5.htm, last access: May 11, 2008); ii) for far future (2020 – 2050) projections are carried out based on the Netherlands Environmental Assessment Agency's IMAGE model (http://www.mnp.nl/en/themasites/image/index.html, last access: May 11, 2008), which uses widely accepted scenarios (i.e. Intergovernmental Panel on climate Change (IPCC) Special Report on Emissions Scenarios (SRES)). The scenario SRES-A1B has been selected for the far future projection in order to be consistent with the climate/meteorological modeling used here. The SRES A1B scenario describes a future world of rapid economic growth and global population. Emissions peak in mid-century and decline thereafter due to rapid introduction of more efficient technologies, and balanced usage between fossil fuels and other energy sources. Emissions are processed by the Sparse Matrix Operator Kernel Emissions (SMOKE v2.1) Modeling System (www.smoke-model.org, last access: May 11, 2008). SMOKE converts the resolution of the data in an emission inventory to the resolution needed by the air quality model. Emission inventories are divided into the following source categories: area sources, non-road mobile sources, on-road mobile sources, point sources and biogenic land use data. MOBILE6 is selected for mobile source emissions (http://www.epa.gov/OMS/m6.htm, last access: May 11, 2008). The BELD3 land use database (http://www.epa.gov/ttn/chief/emch/biogenic, last access: June 02, 2008) is used for estimating biogenic emissions, and is not modified between the historic (i.e., 2001) and future (i.e., 2050) cases due to the lack of information. Historic and future emission inventories include the following compounds: carbon monoxide (CO), nitrogen oxides ($NO_x$), sulfur dioxide ($SO_2$), nonmethane volatile organic compounds (NMVOC),

ammonia ($NH_3$), and speciated particulate matter ($PM_{10}$ and $PM_{2.5}$). A detailed description of the method has been presented by Woo et al. (2008).

### 3.2.2 Meteorology

Meteorological fields are derived from the GISS GCM (Rind et al., 1999), which was applied at a horizontal resolution of $4^o$ latitude by $5^o$ longitude to simulate current and future climate at global scale (Mickley et al. 2004). The simulation followed the IPCC A1B emission scenario for greenhouse gases. Note that for consistency, the same emission scenario is used in projecting future emissions described in 2.1. Leung and Gustafson (2005) downscaled the GISS simulations for 1995-2005 and 2045-2055 using the Penn State/NCAR Mesoscale Model (MM5) (Grell et al., 1994) to the regional scale. MM5 is applied in a nested configuration with 108 km horizontal resolution for the outer domain and 36 km for the inner one. The inner domain covers the continental US, part of Canada, Mexico and ocean (Figure 3.1). The Meteorology Chemistry Interface Processor (MCIP) (http://www.cmascenter.org, last access: May 11, 2008) is used to provide the meteorological data from the hourly MM5 outputs needed for the emissions and air quality models that both have 147x111 horizontal grids of 36 km x 36 km, with nine vertical layers up to approximately 15 km.

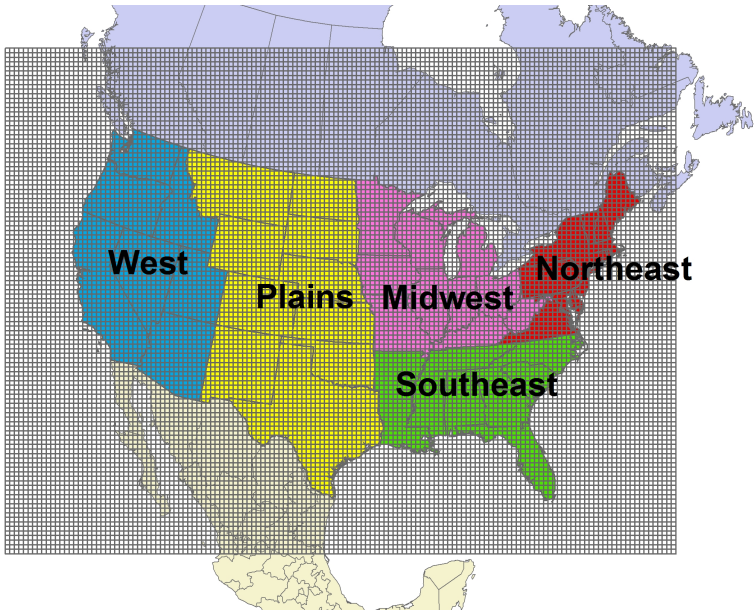


**Figure 3.1: Simulation domain with 111x147 horizontal grid cells which being 36 by 36 km and U.S. regions: West, Plains, Midwest, Northeast and Southeast**

### 3.2.3 Air Quality Modeling

Using meteorology simulated by MM5, both a full historic (2001) and future year (2050) as well as three summer (June-July-August) episodes for historic (2000-2002) and future (2049-2051) $O_3$ and $PM_{2.5}$ concentrations are simulated using the CMAQ Modeling System with the SAPRC-99 chemical mechanism. Predicted pollutant (i.e., $O_3$ and $PM_{2.5}$) concentrations for the historic periods are compared with the observed in order to evaluate the modeling system performance. For the future period two different cases are examined. In the first case the same emission state, i.e., the 2001 inventory, is used for both historic and future simulations in order to estimate the impact to air quality by changes in global climate alone. Although the emission inventory is kept the same, emissions are not, since some pollutant emissions (e.g., biogenic and mobile sources)

depend on meteorology. In the second case the combined impact of future emissions (based on the forecast emissions and climate) and future climate is evaluated to simulate future levels of $O_3$ and $PM_{2.5}$. Average regional concentrations are predicted for the U.S. and five sub-regions (Figure 3.1). In this work, changes in long range transport of pollutants to the U.S. have been neglected as these are uncertain and could mask the impacts of processes investigated here. In both historic and future periods, boundary conditions are kept the same, as there is insufficient information for the emission scenario we use. Keeping the boundary conditions constant makes the impact of regional climate change on pollutant concentrations more transparent. Given the simulated small sensitivity of air quality to climate change, imposing varying boundary conditions would add significant noise to our ability to isolate how climate change impacts compared to emissions changes.

## 3.3 Results and Discussion

### 3.3.1 Emissions

Emissions changes between future (2050) and historic (2001) years show large decreases in $SO_2$ (-51%) and $NO_x$ (-51%) when climate change, growth in human activities and emission controls are simulated (2050 emission inventory and 2050 meteorology) (Figure 3.2). These reductions are due to control strategies applied to anthropogenic US and Canadian sources while the growth of the industrial sector gives higher emissions in Mexico. Emission reductions in anthropogenic VOCs combined with the higher biogenic emissions in the warmer climate results in a small change in VOC emissions (+2%). A detailed description of the regional emissions has been presented by

Woo et al. (2008). For the case where only climatic changes are considered, VOC emissions are higher (+15%) in the future due to temperature effect on biogenic and mobile sources. Minor increases in $NO_x$ (+2%) and $SO_2$ (+4%) are also predicted.

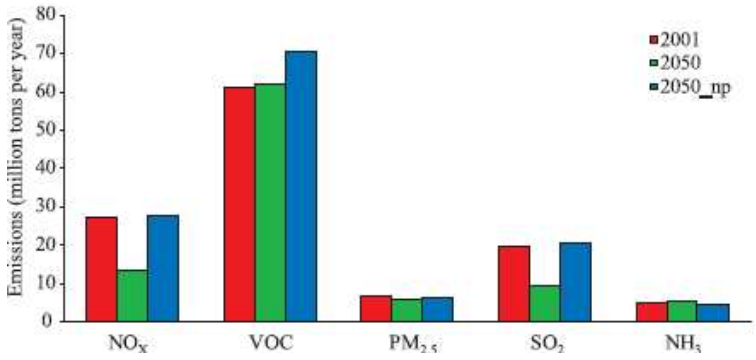


**Figure 3.2: Yearly emissions for 2001, 2050 and 2050 for the ‘‘no emissions projection’’ scenario (2050_np)**

### 3.3.2 Meteorology

Meteorological model performance is evaluated by comparing hourly statistical distributions of observed and predicted temperatures over the US (Figure 3.3) data from more than 1000 monitoring stations (see http://dss.ucar.edu/datasets/ds472.0/, last access: May 11, 2008). Leung and Gustafson (2005) provide details, though a summary is given here. There is a small warm bias of 0.4 K in the average summer temperatures of 2000-2002. Model performance is better for the Northeast region with a small cold bias of 0.1K, and poorest for the Southeast, with a warm bias of 1.5 K. A general cold bias in the 2001 annual temperature is found. Cumulative distribution function (CDF) plots presenting in auxiliary material (Appendix A, Figures A1, A2 & A3) compare observed and predicted

temperatures for 3 consecutive years (2000, 2001 and 2002). A general underprediction is observed in all subregions but the model tends to overpredict maximum temperatures. Model performance is better during the summer months and worst during the transition season of fall, when mesoscale variability is high. As discussed in Leung and Gustafson (2005) data assimilation has not been used. Previously MM5 evaluations (e.g. Zhang et al., 2005) reveal that it reproduces well the diurnal variations for temperature and relative humidity (RH), and the minimum temperatures. It tends to overpredict maximum temperatures and underpredict both maximum and minimum RHs. Moreover, MM5 predicts well the wind speeds but poorly the wind direction and the maximum mixing depths.

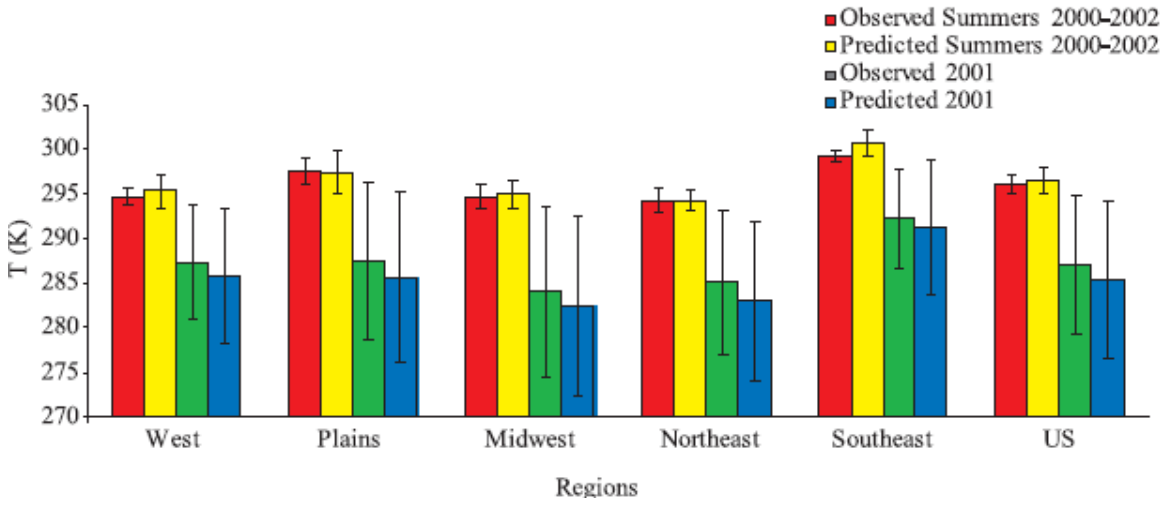


**Figure 3.3 Mean summer (2000–2002) and mean annual (2001) observed and predicted temperatures and monthly standard deviations**

Future summer temperatures (i.e., 2049-2050) compared to the historic ones (i.e., 2000-2002) are simulated to be 1.4 K warmer in the U.S. (Figure 3.4), with small variations by region (± 0.6 K). The minimum increase is noted in the Midwest (0.8 K)

and the maximum in the West (2.0 K). The 2050 annual average temperature is simulated to be 1.7 K warmer than 2001 in the U.S., with small variations by region (± 0.5 K). Maximum warming occurs during fall with simulated average temperature changes up to 4.8 K in the West. The standard deviation calculated on the monthly average temperatures is higher for the annual simulation compared to summers in both observations and predictions. This is caused by the higher variation in temperature during a whole year compared to the summers.

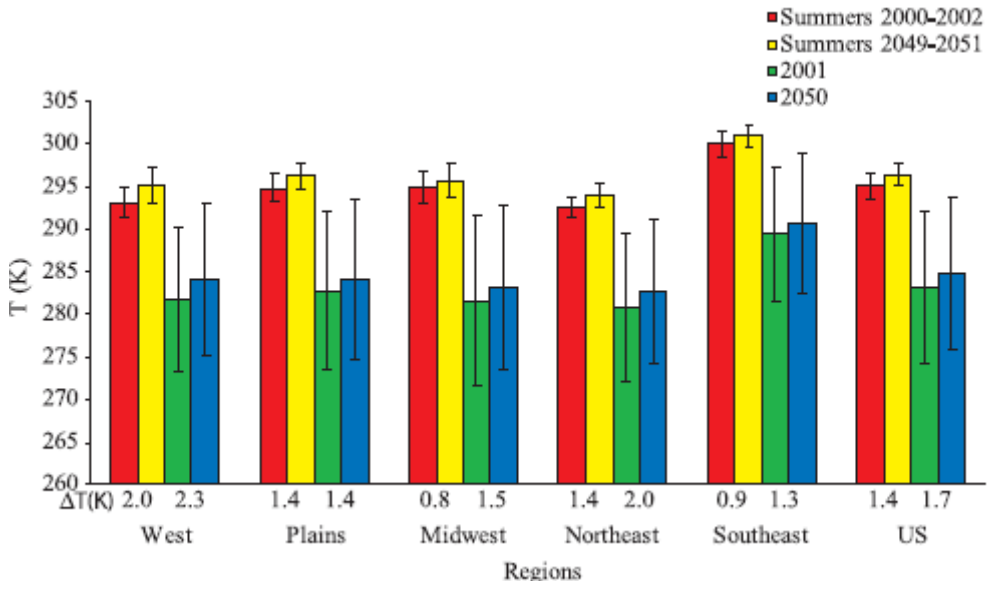


**Figure 3.4: Mean summer and mean annual temperatures and monthly standard deviations for historic and future periods**

One of the most critical questions is if the selected years 2001 and 2050 are representative years for both the historic and future period. In order to answer this question comparison for the cumulative distribution function (CDF) plots and spatial distribution plots is conducted for both historic and future periods. The CDF plots for

temperature and humidity are similar for the three consecutive historic as well as future years but there is an obvious shift to higher values moving from historic to future period (Figures are presented in the Appendix A). Moreover, the spatial distribution plots show similar trend for the consecutive years in both periods. The CDF's plots for the precipitation are similar between the two periods. The spatial distribution plots for the three consecutive years in both periods have the same pattern with only small local changes.

### 3.3.3 Regional Air Quality

Air quality model performance is evaluated by comparing the observed and predicted daily maximum 8-hr $O_3$ ($M8hO_3$) and hourly $PM_{2.5}$ concentrations over the U.S. (Figures 3.5 and 3.6) using data from more than 1000 stations for ozone and about 100 for $PM_{2.5}$ (http://www.epa.gov/ttn/airs/airsaqs/detaildata/downloadaqsdata.htm, last access: May 12, 2008). Around 250 ozone monitoring stations located at the West, Midwest and Southeast sub-regions, 200 at Northeast and 150 at Plains. Regarding $PM_{2.5}$ monitoring stations there are around 45 at Plains, 35 at West and Northeast and 25 at Midwest and Southeast. The three simulated summer mean $M8hO_3$ concentrations for 2000-2002 are about 15% higher, while the $PM_{2.5}$ concentrations are about 30% lower than the observed. Model performance for the $PM_{2.5}$ concentrations is significantly more region dependent than the $M8hO_3$ concentrations. Representation of secondary organic aerosol (SOA) formation is uncertain, and low organic carbon (OC) has been noted in the CMAQ approaches [*Chen and Griffin*, 2005; *Kroll, et al.*, 2006; *Lim and Ziemann*, 2005]. Recent work suggests that this is due to lower yields and higher vapor pressures in

CMAQ [*Morris, et al.*, 2005]. Moreover, the current chemical mechanism neglects isoprene as a SOA precursor, though its role in SOA formation might be quite important [*Claeys, et al.*, 2004a; *Claeys, et al.*, 2004b; *Henze and Seinfeld*, 2006], leading to discrepancies between the predicted and observed $PM_{2.5}$ concentrations. The effect of $NO_x$ on SOA yields, which is highly uncertain, has also been neglected.

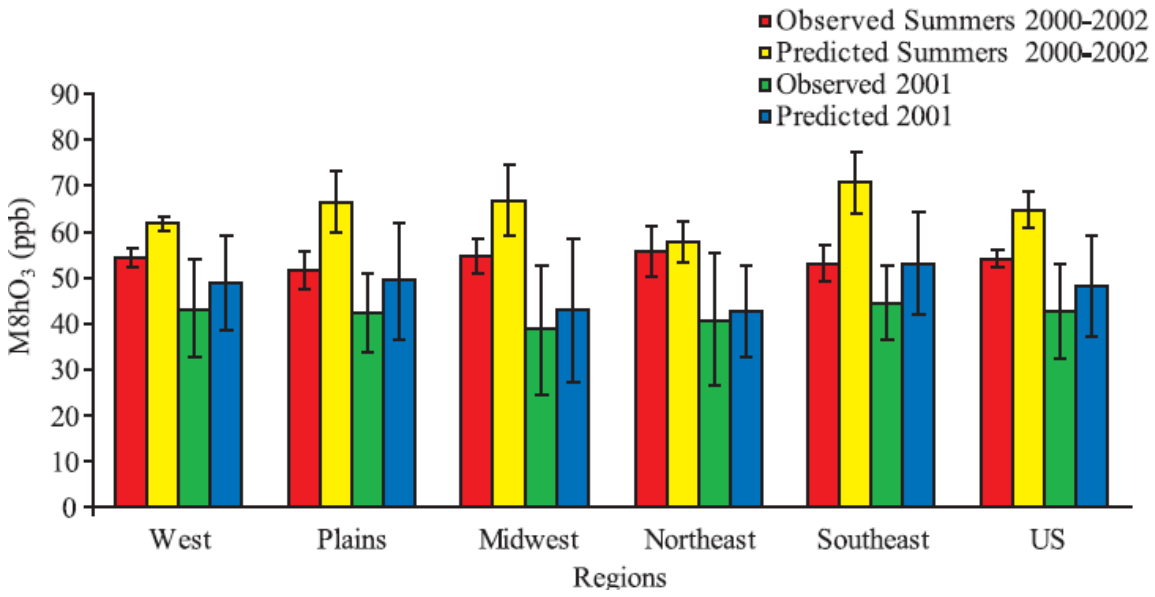


**Figure 3.5: Mean summer (2000–2002) and mean annual (2001) observed and predicted maximum 8-hr $O_3$ ($M8hO_3$) concentrations and monthly standard deviations**

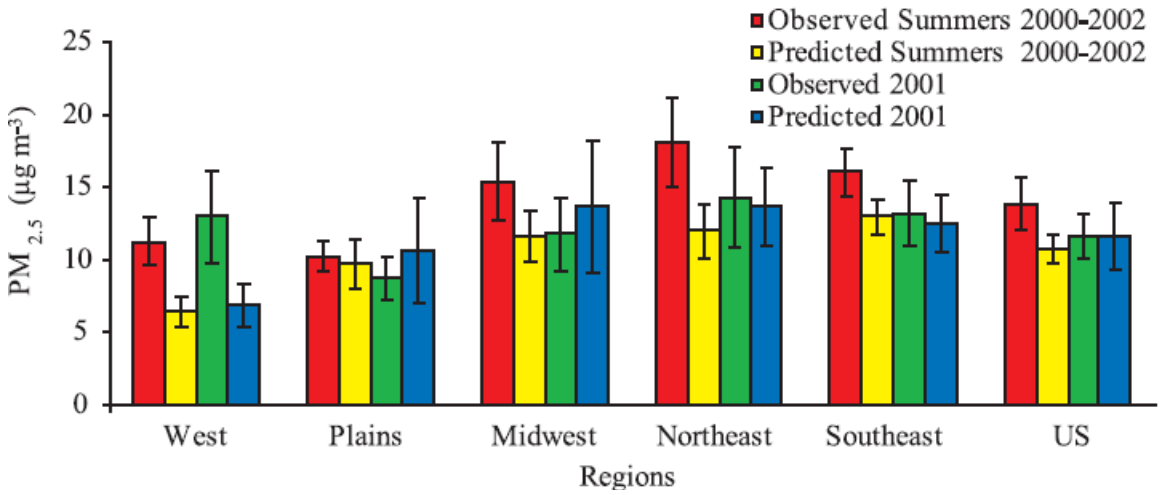


**Figure 3.6: Mean summer (2000–2002) and mean annual (2001) observed and predicted $PM_{2.5}$ concentrations and monthly standard deviations**

Annual mean $M8hO_3$ and $PM_{2.5}$ concentrations are better simulated compared with the three-summer average. Mean annual $M8hO_3$ concentration is slightly (10%) over-predicted. Simulated $PM_{2.5}$ concentrations are low during spring and summer and high during the rest of the year largely due to the under-prediction of organic carbon. The presented standard deviation is calculated for the monthly average concentrations. Ozone concentrations are high during summers and low during the rest of the months resulting in higher annual standard deviation compared to summers in both observations and predictions. The variation in $PM_{2.5}$ concentration during a year is less than ozone as $PM_{2.5}$ high concentrations exist during autumn and winter.

#### *3.3.3.1 Summer pollutant changes*

Global climate change, alone, has a small effect on future summer (i.e., 2049 – 2051) $M8hO_3$ concentrations over the U.S. (Figure 3.7) when compared to the historic summers (i.e., 2000-2002). The average regional changes range from -2.5% to +2.8%

(Table 3.1.a). As noted, Leung and Gustafson (2005) found a small increase in stagnation events, and this, in part, leads to increases in the number of days where concentrations are over 85 ppb in most regions expect the Midwest (Table 3.1.b). Stagnation events are predicted to have the most impact in the West, Northeast and Plains and a small impact in the Southeast. Summer $PM_{2.5}$ concentrations (Figure 3.8) are predicted to be lower in all the U.S. sub-regions (average about 10%), using the same emission inventory, as a result of the increased precipitation and higher temperatures in spite of higher biogenic VOC emissions. The effect of climate change alone in summer $PM_{2.5}$ concentrations seems to be quite important in the Midwest, Southeast and Plains (Table 3.1.a). Higher temperatures lead to increased gas phase partitioning of ammonium nitrate and organics. Sulfate, nitrate, ammonium and organic carbon decrease due to increased precipitation and higher temperatures (Table 3.1.a) but no significant modification in $PM_{2.5}$ composition is predicted (Table 3.1.c).

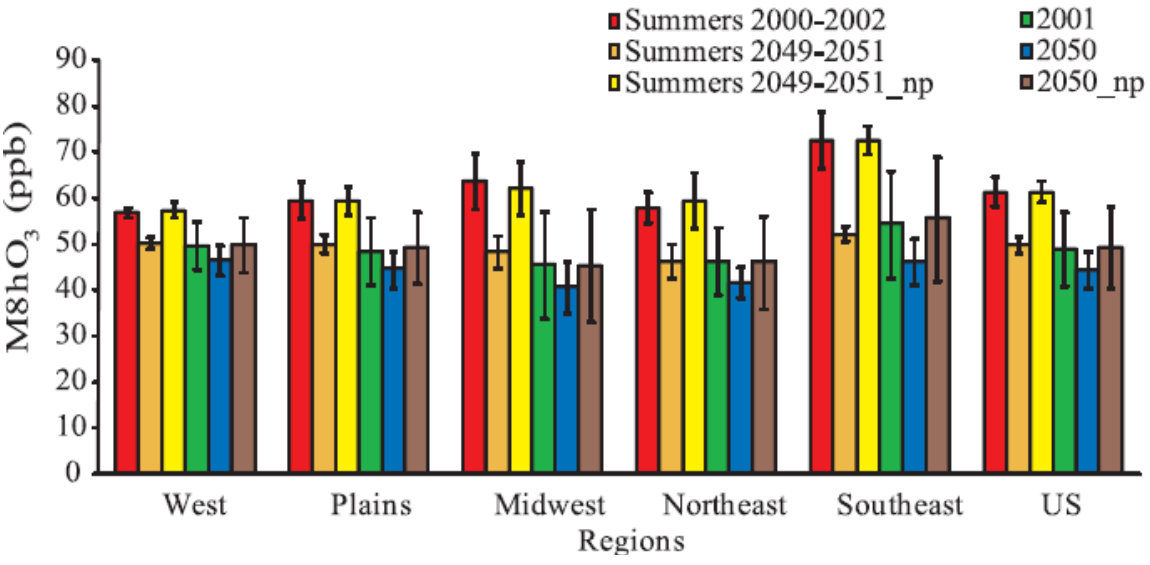


**Figure 3.7: Mean summer and mean annual maximum 8-hr $O_3$ ($M8hO_3$) concentrations and monthly standard deviations for historic and future periods**

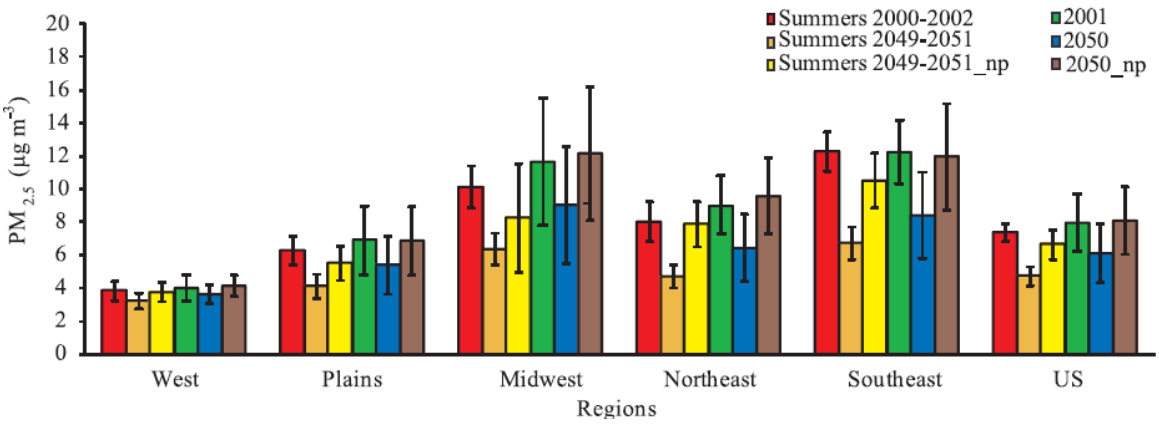


**Figure 3.8: Mean summer and mean annual $PM_{2.5}$ concentrations and monthly standard deviations for historic and future periods**

The impact of climate change, growth activity and emission controls are more pronounced for the $PM_{2.5}$ concentrations than $M8hO_3$ (Figures 3.7 & 3.8). The US summer average concentrations for $M8hO_3$ and $PM_{2.5}$ are predicted to be lower by about 20% and 35%, respectively. Significant reduction is predicted for sulfate, nitrate and ammonium while a smaller reduction is predicted for organic carbon (Table 3.1a). Sulfate will be a significantly lower fraction of $PM_{2.5}$ in the future; nitrate and ammonium will be slightly lower but organic carbon is predicted to be higher (Table 3.1c). Significant reduction is also estimated for the highest $M8hO_3$ concentrations over all US sub-regions along with the average concentrations (Table 3.2). The Midwest is simulated to have the highest peak $M8hO_3$ concentrations in the future as climate change alone has a more significant effect compared to the other US sub-regions. Better air quality is also estimated for the cities and mega-cites (Table 3.2). Significant reduction in the number of days that the $M8hO_3$ concentrations exceed 85 ppb as well as the peak values are

estimated for all the cities examined here. Atlanta in the Southeast US sub-region will benefit more; no days are estimated for the $M8hO_3$ concentrations above 85 ppb. In general, there is little year-to-year variation in region wide $M8hO_3$ concentrations as well as the number of days that the $M8hO_3$ concentrations exceed 85 ppb as well as the peak values for the cities examined (Table 3.2). Spatial distribution plots for mean summer ozone and $PM_{2.5}$ concentrations show the reduction in the higher concentrations simulated at the east comes from emissions control strategies (Appendix A, Figures A.8 & A.9), though lower concentrations may actually increase. Climate change alone leads to increasing concentrations in all cities. Moreover climate change lengthens the stagnations events in these cities, similar to the regional behavior described previously and more days with $M8hO_3$ concentrations over 85 ppb are predicted in Los Angeles, New York and Houston.

#### *3.3.3.2 Annual Average Pollutant Changes*

A separate comparison between the annual average concentrations of $M8hO_3$ and $PM_{2.5}$ is performed for the future (i.e., 2050) and historic (i.e., 2001) years. Annual average $PM_{2.5}$ levels tend to be stable year to year. Comparison of the three consecutive summers reveals only small differences (typically less than 10% for $M8hO_3$ and 15% for $PM_{2.5}$); inclusion of more consecutive yearly data is not expected to change significantly the results of our analysis as no significant weather modification for the consecutive years is estimated (see: Appendix A). Further evidence is found in observations. Monitoring stations in large US cities (e.g. Los Angeles, New York, Chicago) show a small variation (about 1 $\mu g\ m^{-3}$, or 5-10%) in annual average $PM_{2.5}$ levels for the years

2000-2002 (http://www.epa.gov/airtrends, last access: May 11, 2008). This is similar to the observed trend from 1999-2005 showing a decrease of 7% nationwide. The same trend is observed for $M8hO_3$ concentrations showing a decrease of 8% nationwide.

While much of the analysis concentrates on the higher ozone levels found predominantly in the summer, annual statistics are provided as well because some areas have longer ozone seasons, and there is increasing concern over exposures (human and other) to lower ozone levels (EPA, 2006). As is noted, much greater reductions are found for higher ozone levels and in the ozone CDFs (Appendix A, Figure A.12). Others [*Lefohn, et al.*, 1998], have found that intermediate and lower levels of ozone are not as responsive to controls. Further, emission changes can lead to increases in ozone at night and during photochemically less active periods, as seen by examining the low-concentration tail of the CDF (Appendix A, Figure A.12).

Annual average concentrations for both pollutants $M8hO_3$ and $PM_{2.5}$ are predicted to be slightly different over the U.S. in year 2050 compared to 2001, using the 2001 emission inventory (Table 3.1). The sulfate and organic carbon fraction of $PM_{2.5}$ is predicted to be slightly higher while the nitrate fraction lower (Table 3.1.c). This is caused by the higher VOCs and $SO_2$ emissions in a warmer climate, although the same emission inventory is used. The higher $SO_2$ emissions lead to more $H_2SO_4$ formation that quickly reacts with $NH_3$ to form ammonium sulfate. On the other hand, the higher $NO_X$ emissions, although leading to formation of $HNO_3$, do not translate in increase in nitrate concentrations since nitrate aerosol formation depends on the availability of $NH_3$ after neutralization of $H_2SO_4$. Regional changes in future meteorology (e.g., temperature,

precipitation, wind) combined with projected emissions, lead to some regional variation in air quality changes (Tables 3.1.a & 3.1.c). More clouds and precipitation in the Southeast increase aqueous oxidation and wet deposition leading to a net slight increase in sulfate and a decrease in organic carbon concentrations compared with the rest of the regions.

Impacts of climate change, activity growth and emissions controls are more pronounced for regional $PM_{2.5}$ concentrations than $M8hO_3$. The annually average US concentrations for $PM_{2.5}$ and $M8hO_3$ are predicted to be 23% and 9% lower, respectively in 2050 compared to 2001. Significant reductions are predicted for sulfate (-31%), nitrate (-48%), and ammonium (-32%) fractions, while only a small reduction is predicted for organic carbon (-6%) (Table 3.1.a). Controls on NMVOC emissions from area and point sources that are less stringent than for $SO_2$ and $NO_x$ combined with the higher VOC emissions from biogenic sources expected in a warmer future climate are the primary factors. A slight increase in organic carbon in the West is noted due to increase in both primary and secondary organic carbon. Sulfate, nitrate and ammonium fractions of $PM_{2.5}$ are predicted to be lower in the future compared to historic period while organic carbon will be higher (Table 3.1.c). Recent work suggests that SOA formation from both biogenic [*Pun, et al.*, 2003] and anthropogenic [*de Gouw, et al.*, 2003] are larger than have previously been accounted for in atmospheric chemistry models. Further, work by Volkamer et al., (2006) and Mendoza-Dominguez and Russell (2001) also suggests that primary OC emissions may be larger as well [*Mendoza-Dominguez and Russell*, 2001; *Volkamer, et al.*, 2006]. Such findings provide further evidence that OC will be the

dominant fine aerosol species in the future. However, they also show that significant uncertainty remains as to the current and potential future source impacts.

**Table 3.1.a: Mean summer and mean annual changes (percent) in pollutant concentrations for future periods compared to historic ones**

| | $M8hO_3$ (%) | | $PM_{2.5}$ (%) | | $SO_4$ (%) | | $NO_3$ (%) | | $NH_4$ (%) | | OC (%) | |
|---|---|---|---|---|---|---|---|---|---|---|---|---|
| | Summers | Summers_np | Summers | Summers_np | Summers | Summers_np | Summers | Summers_np | Summers | Summers_np | Summers | Summers_np |
| West | -11.6 | 0.9 | -15.7 | -2.0 | -32.2 | -3.7 | -72.8 | -42.8 | -33.0 | -6.9 | -6.7 | 0.7 |
| Plains | -15.8 | -0.1 | -34.3 | -12.1 | -48.7 | -16.4 | -46.4 | -15.2 | -41.8 | -14.1 | -16.2 | -7.7 |
| Midwest | -24.4 | -2.5 | -37.1 | -18.4 | -52.6 | -22.4 | -68.5 | -24.1 | -45.7 | -21.9 | -19.1 | -11.7 |
| Northeast | -20.2 | 2.8 | -41.2 | -1.7 | -56.7 | -2.2 | -79.3 | -28.8 | -44.5 | -0.8 | -25.2 | -0.4 |
| Southeast | -27.9 | 0.3 | -45.2 | -14.3 | -60.5 | -16.5 | -77.1 | -37.1 | -47.9 | -13.3 | -27.5 | -14.8 |
| US | -18.9 | 0.0 | -35.9 | -9.9 | -52.6 | -13.9 | -65.6 | -22.6 | -43.9 | -12.2 | -17.2 | -5.5 |
| | 2050 | 2050np | 2050 | 2050np | 2050 | 2050np | 2050 | 2050np | 2050 | 2050np | 2050 | 2050np |
| West | -6.5 | 0.2 | -9.2 | 2.9 | -20.2 | 4.8 | -41.4 | -17.6 | -24.9 | -3.4 | 4.0 | 8.9 |
| Plains | -7.9 | 1.4 | -22.0 | -0.8 | -29.2 | 5.5 | -45.3 | -17.9 | -31.7 | -3.2 | -3.4 | 4.7 |
| Midwest | -10.5 | -0.2 | -22.7 | 4.2 | -22.2 | 12.6 | -48.5 | -7.7 | -28.7 | 4.2 | -9.3 | 6.6 |
| Northeast | -10.0 | -0.5 | -28.5 | 6.5 | -37.4 | 10.3 | -45.6 | -4.3 | -32.6 | 5.9 | -13.0 | 10.7 |
| Southeast | -14.8 | 2.3 | -31.4 | -2.4 | -41.5 | 0.5 | -54.9 | -12.4 | -37.0 | -1.7 | -14.9 | -3.6 |
| US | -9.2 | 0.9 | -23.4 | 1.1 | -30.8 | 6.2 | -47.8 | -12.4 | -31.6 | -0.2 | -6.4 | 4.4 |

Seasonal variation in $M8hO_3$ concentrations gives higher concentrations during summers at all sub-regions (Appendix A, Table A.1). The differences between summer and the rest of the seasons seem to diminish in the future under the impact of both climate change and emissions projection as higher reduction is estimated during summer. Seasonal variation in $PM_{2.5}$ concentrations gives higher values during winter and autumn and lower during spring and summer at all sub-regions. Reductions are forecast for the average $PM_{2.5}$ concentrations over all US sub-regions (Table 3.3) although climate change can lead to increases. The Midwest is simulated to have the highest daily average $PM_{2.5}$ concentrations in the future. Lower $PM_{2.5}$ concentrations are also forecast for the cities. Reduction in the number of days that the daily average $PM_{2.5}$ exceeds the standard of 35 $\mu g\ m^{-3}$ as well as the peak values are estimated for all the mega cities examined here except the peak value at Los Angeles, although, again, climate change alone leads to increases. Annual average spatial distribution plots for ozone and $PM_{2.5}$ concentrations show again the reduction in the higher concentrations simulated at the east comes from emissions control strategies (Appendix A, Figures A.10 & A.11) Comparison between summers and annual distribution plots confirms that ozone is significant problem during summer especially in the east while $PM_{2.5}$ is important pollutant all over the year.

**Table 3.1.b: Number of days per summer month and per grid cell where $M8hO_3$ concentration is over 85 ppb**

| Region | Summers 2000-2002 | Summers 2049-2051 | Summers 2049-2051_np |
|---|---|---|---|
| West | 0.15 | 0.01 | 0.44 |
| Plains | 1.21 | 0.02 | 1.56 |
| Midwest | 4.52 | 0.08 | 4.22 |
| Northeast | 2.18 | 0.02 | 3.37 |
| Southeast | 6.78 | 0.05 | 7.11 |
| United States | 2.48 | 0.03 | 2.77 |

**Table 3.1.c: Mean summer and mean annual $PM_{2.5}$ composition of pollutants concentrations for historic period, future period and future period_np (historic emissions and future meteorology)**

| | Historic summers | | | | | | 2001 | | | | | |
|---|---|---|---|---|---|---|---|---|---|---|---|---|
| | $SO_4$ (%) | $NO_3$ (%) | $NH_4$ (%) | OC (%) | EC (%) | OTHER (%) | $SO_4$ (%) | $NO_3$ (%) | $NH_4$ (%) | OC (%) | EC (%) | OTHER (%) |
| West | 21 | 2 | 8 | 49 | 5 | 15 | 19 | 11 | 10 | 40 | 5 | 15 |
| Plains | 47 | 1 | 15 | 15 | 3 | 19 | 30 | 17 | 15 | 14 | 2 | 22 |
| Midwest | 44 | 3 | 14 | 13 | 3 | 23 | 27 | 22 | 15 | 11 | 2 | 23 |
| Northeast | 45 | 2 | 13 | 20 | 4 | 16 | 31 | 17 | 15 | 17 | 3 | 17 |
| Southeast | 50 | 1 | 14 | 20 | 3 | 12 | 34 | 13 | 14 | 20 | 3 | 16 |
| US | 44 | 2 | 14 | 20 | 3 | 17 | 29 | 17 | 14 | 18 | 3 | 19 |
| | Future summers | | | | | | 2050 | | | | | |
| | $SO_4$ (%) | $NO_3$ (%) | $NH_4$ (%) | OC (%) | EC (%) | OTHER (%) | $SO_4$ (%) | $NO_3$ (%) | $NH_4$ (%) | OC (%) | EC (%) | OTHER (%) |
| West | 17 | 1 | 6 | 54 | 4 | 18 | 17 | 7 | 8 | 46 | 4 | 18 |
| Plains | 37 | 1 | 14 | 19 | 2 | 27 | 27 | 12 | 13 | 18 | 2 | 28 |
| Midwest | 34 | 1 | 12 | 17 | 2 | 34 | 28 | 15 | 14 | 13 | 1 | 29 |
| Northeast | 33 | 1 | 12 | 26 | 2 | 26 | 28 | 13 | 14 | 21 | 2 | 22 |
| Southeast | 36 | 0 | 13 | 26 | 2 | 23 | 29 | 9 | 13 | 25 | 2 | 22 |
| US | 32 | 1 | 12 | 26 | 2 | 27 | 26 | 11 | 13 | 22 | 2 | 26 |
| | Future summers_np | | | | | | 2050_np | | | | | |
| | $SO_4$ (%) | $NO_3$ (%) | $NH_4$ (%) | OC (%) | EC (%) | OTHER (%) | $SO_4$ (%) | $NO_3$ (%) | $NH_4$ (%) | OC (%) | EC (%) | OTHER (%) |
| West | 21 | 1 | 8 | 50 | 5 | 15 | 19 | 9 | 9 | 42 | 5 | 16 |
| Plains | 45 | 1 | 15 | 15 | 3 | 21 | 32 | 14 | 15 | 15 | 2 | 22 |
| Midwest | 42 | 3 | 14 | 14 | 4 | 23 | 30 | 19 | 15 | 12 | 3 | 21 |
| Northeast | 45 | 2 | 13 | 20 | 4 | 16 | 33 | 16 | 14 | 18 | 3 | 16 |
| Southeast | 48 | 0 | 14 | 20 | 3 | 15 | 35 | 12 | 15 | 20 | 3 | 15 |
| US | 42 | 1 | 13 | 21 | 3 | 20 | 30 | 15 | 14 | 19 | 3 | 19 |

**Table 3.2: Regional and local (cities) predicted maximum 8-hr $O_3$ ($M8hO_3$) concentration characteristics [a]**

| | summers 2000-2002 | | | | | | | | | | summers 2049-2051 | | | | | | | | | | summers 2049-2051_np | | | | | | | | | |
|---|---|---|---|---|---|---|---|---|---|---|---|---|---|---|---|---|---|---|---|---|---|---|---|---|---|---|---|---|---|---|
| | 99.75% | | | # of days over 85 ppb | | | | Peak value | | | 99.75% | | | # of days over 85 ppb | | | | Peak value | | | 99.75% | | | # of days over 85 ppb | | | | Peak value | | |
| | 00 | 01 | 02 | 00 | 01 | 02 | avg | 00 | 01 | 02 | 49 | 50 | 51 | 49 | 50 | 51 | avg | 49 | 50 | 51 | 49 np | 50 np | 51 np | 49 np | 50 np | 51np | avg | 49 np | 50 np | 51 np |
| West / Los Angeles | 91 | 88 | 87 | 54 | 37 | 39 | 43 | 121 | 113 | 118 | 77 | 73 | 75 | 24 | 10 | 17 | 17 | 105 | 94 | 96 | 104 | 94 | 103 | 76 | 67 | 83 | 75 | 146 | 130 | 139 |
| Plains / Houston | 101 | 97 | 95 | 68 | 45 | 36 | 50 | 132 | 116 | 113 | 76 | 77 | 76 | 9 | 12 | 19 | 13 | 100 | 99 | 109 | 102 | 101 | 102 | 47 | 70 | 64 | 60 | 139 | 130 | 143 |
| Midwest / Chicago | 116 | 115 | 116 | 34 | 28 | 32 | 31 | 132 | 140 | 144 | 76 | 78 | 89 | 4 | 5 | 21 | 10 | 100 | 97 | 124 | 110 | 115 | 132 | 17 | 19 | 44 | 27 | 137 | 127 | 165 |
| Northeast / New York | 110 | 108 | 104 | 32 | 24 | 31 | 29 | 119 | 114 | 109 | 71 | 75 | 84 | 0 | 0 | 8 | 3 | 83 | 83 | 89 | 107 | 111 | 124 | 31 | 39 | 54 | 41 | 126 | 124 | 135 |
| Southeast / Atlanta | 116 | 108 | 110 | 78 | 66 | 78 | 74 | 130 | 122 | 102 | 77 | 84 | 83 | 0 | 1 | 0 | 0 | 82 | 85 | 81 | 112 | 116 | 116 | 72 | 75 | 71 | 73 | 149 | 133 | 136 |

[a] The regional value corresponds to the 99.75% of the cumulative distribution function concentrations. The local values correspond to the number of days where $M8hO_3$ concentrations exceed 85 ppb as well as the peak estimated concentrations.

**Table 3.3: Regional and local (cities) predicted daily average $PM_{2.5}$ concentration characteristics [a]**

| Region / City | 2001 | | | 2050 | | | 2050np | | |
|---|---|---|---|---|---|---|---|---|---|
| | Region | City | | Region | City | | Region | City | |
| | 99.75% | # of days over 35 μg $m^{-3}$ | Peak value | 99.75% | # of days over 35 μg $m^{-3}$ | Peak value | 99.75% | # of days over 35 μg $m^{-3}$ | Peak value |
| West / Los Angeles | 21.5 | 5 | 40.5 | 18.6 | 1 | 56.9 | 21.5 | 8 | 67.8 |
| Plains / Houston | 33.5 | 14 | 48.5 | 28.3 | 4 | 46.1 | 34.6 | 11 | 54.0 |
| Midwest / Chicago | 45.2 | 35 | 80.0 | 41.5 | 23 | 63.6 | 48.0 | 44 | 64.0 |
| Northeast / New York | 40.0 | 38 | 88.8 | 32.1 | 12 | 59.3 | 42.9 | 40 | 79.0 |
| Southeast / Atlanta | 40.0 | 38 | 66.0 | 34.0 | 18 | 54.3 | 41.3 | 41 | 63.1 |

[a] The regional value corresponds to 99.75% of the cumulative distribution function concentrations. The local values correspond to the number of days where daily average $PM_{2.5}$ concentrations exceed the standard of 35 μg $m^{-3}$ as well as to the peak estimated concentration.

## 3.4 Conclusions

Regional $O_3$ and $PM_{2.5}$ concentrations for a future period (i.e., summers 2049-2051 and year 2050) are simulated to be lower compared to the historic period (i.e., summers 2000-2002 and year 2001), given the planned controls on precursor emissions, though global warming, alone, does lead to an increase in biogenic emissions. Climate change, alone, with no emissions growth or controls has a small effect on the $M8hO_3$ and $PM_{2.5}$ levels although changes in stagnation events, leading to higher pollutant concentrations over a slightly extended duration, may be regionally important. Future levels of sulfate, nitrate and ammonium are simulated to be significantly lower compared to organic carbon, leaving organic carbon as the likely major constituent of fine particulate matter in the far future. $M8hO_3$ concentrations over all domain sub-regions are simulated to be lower than the historic scenarios; both the number of days with $M8hO_3$ concentrations above the standards and the peak concentrations are reduced for the urban areas.

The trend in pollutant concentrations reveals the key role that emission control strategies may play in future regional air quality, setting forecasting of emissions as key to being able to assess the impact of climate change on pollutant concentrations. One of the most important implications of this study is that the significant reduction predicted for sulfate, nitrate and ammonium concentrations will result in organic carbon as the most important $PM_{2.5}$ component.

These results are used for studying the sensitivity of future pollutant concentrations to emission changes as well as the uncertainties in regional air quality and

changes in sensitivities to climate change uncertainties and source-specific emissions [*Liao, et al.*, 2007; *Liao, et al.*, 2008].

# CHAPTER 4

# THE ROLE OF CLIMATE AND EMISSION CHANGES IN FUTURE AIR QUALITY OVER SOUTHERN CANADA AND NORTHERN MEXICO *

## 4.1 Introduction

Global climate and emission changes are critical factors for future air quality. Although climate change impacts on regional air quality have been examined to some degree [*Hogrefe, et al.*, 2004; *Knowlton, et al.*, 2004; *Langner, et al.*, 2005; *Mickley, et al.*, 2004; *Murazaki and Hess*, 2006] and have been summarized by Tagaris et al. (2007), there are limited studies examining the effect of long term emission changes on air quality. Dentener et al. (2006) recently compared the global atmospheric environment for the years 2000 and 2030 using global atmospheric chemistry models and different emission scenarios. Different emissions scenarios result in different global and regional ozone levels, while climate change alone seems to play a minor role. Tagaris et al. (2007) examined the impacts of global climate and emissions changes on regional ozone and fine particulate matter concentrations over the United States. They found that the impacts of climate change alone on regional air quality are small compared with the impacts from emission control-related reductions, although increases in pollutant concentrations due to stagnation events are found.

---

* This chapter is currently published in the *Atmospheric Chemistry and Physics Discussions* and under review for publication in the *Atmospheric Chemistry and Physics.* Co-authors are Tagaris Efthimios, Kasemsan Manomaiphiboon, Jung-Hun Woo, Shan He, Praveen Amar, and Armistead G. Russell.

Most of the aforementioned studies focus on the United States. However, it is equally important to investigate the impact of the climate and emissions changes to the border U.S. regions, given that a large part of Mexican and Canadian population lives there and will both affect and be affected by pollutant transport. These border regions are some of the most dynamic regions of North America in economic, environmental, demographic and cultural terms. Extending the study by Tagaris et al. (2007), the impacts of global climate and emissions change on regional air quality over northern Mexico and southern Canada are assessed. Future $O_3$ and $PM_{2.5}$ concentrations for northern Mexico and southern Canada are compared to historic ones under two different cases: i) the impacts of changes on regional air quality by climate change alone are examined by keeping emissions sources, activity levels and controls constant; and ii) the future pollutant concentrations are estimated based on changes in both climate and emissions using the IPCC A1B emission scenarios and planned controls. This is the first study examining the impacts of climate and emission changes in these regions and how changes in future U.S. air quality will affect the neighbor countries.

## 4.2 Methods

Following the same methodology as described in details by Tagaris et al. (2007), and summarized below, we use the Goddard Institute of Space Studies (GISS) II' [*Rind, et al.*, 1999] global results downscaled using the Penn State/NCAR Mesoscale Model (MM5) [*Grell, et al.*, 1994], forecast North American emissions and the Community Multiscale Air Quality model (CMAQ) to simulate historic and future air quality [*Byun*

*and Schere*, 2006]. The primary difference between this study and the former is that improved emissions became available for Canada and Mexico.

The Environment Canada's 2000 inventory has been used for area and mobile Canadian sources (http://www.epa.gov/ttn/chief/net/canada.html, last access: May 12, 2008). For point sources, the 2002 inventory that the New York State Department of Environmental Conservation compiled using the Canadian National Pollution Release Inventory (NPRI) was scaled using Environment Canada's state level summary. For Mexico, the U.S. EPA's 1999 Big Bend Regional Aerosol and Visibility Observational (BRAVO) Study Emissions Inventory was updated with the Mexico National Emissions Inventory (NEI). The 2001 Clean Air Interstate Rule (CAIR) emission inventory is used for the U.S. for the early 21st century, as well as the basis for projected emissions up to 2020 [*Woo, et al.*, 2008]. Far future (2020 – 2050) projections of emissions are carried out based on the Netherlands Environmental Assessment Agency's Integrated Model to Assess the Global Environment (IMAGE). IMAGE uses widely accepted scenarios (i.e. Intergovernmental Panel on climate Change (IPCC) Special Report on Emissions Scenarios (SRES)) which are consistent with the scenario IPCC A1B scenario and the climate/meteorological modeling used here.

Meteorological fields are derived from the GISS GCM II', which was applied at a horizontal resolution of $4^{o}$ latitude by $5^{o}$ longitude to simulate current and future climate at global scale [*Mickley, et al.*, 2004]. The simulation followed the IPCC-A1B emission scenario (IPCC, 2001) for greenhouse gases. Leung and Gustafson (2005) downscaled the GISS simulations for 1995-2005 and 2045-2055 using the Penn State/NCAR

Mesoscale Model (MM5) to the regional scale; no data assimilation has been used. Although there are uncertainties in using regionally downscaled climate in air quality simulations, this approach is necessary in air quality models that employ higher resolution meteorological fields produced by regional instead of global climate models [*Gustafson and Leung*, 2007]. CMAQ with SAPRC-99 chemical mechanism is used for the regional air quality modeling. $O_3$ and $PM_{2.5}$ concentrations for three historic (2000-2002) summer (June-July-August) episodes are compared to three future (2049-2051) summer episodes. Regional concentrations are predicted for northern Mexico and western and eastern Canada (Figure 4.1). To quantify the net impact of climate change and the impact of climate change combined with projected emissions; both the historic period and future cases are examined. Future cases are: 1) using the 2001 emissions inventory for historic and future years to quantify the impact of climate change on air quality; and 2) using future forecast emissions along with forecast climate to simulate future pollutant levels over northern Mexico and western and eastern Canada allowing the quantification of both impacts on future air quality.

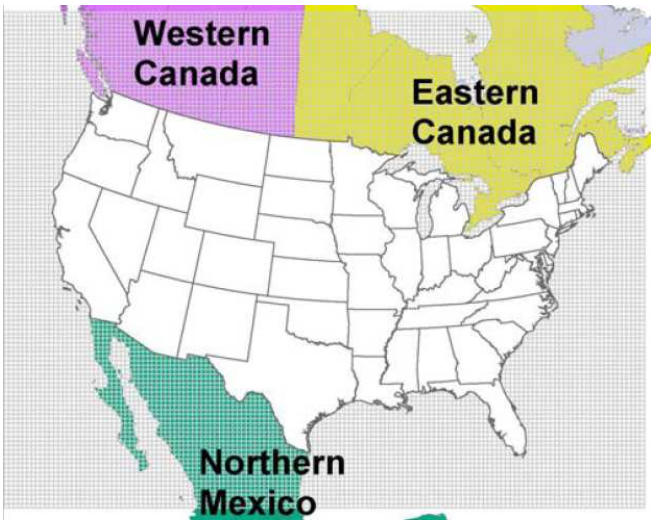


**Figure 4.1 Modeling domain and regions examined**

## 4.3 Results and Discussion

### 4.3.1 Meteorology

Statistics and spatial distributions for forecast temperature, mixing height, insolation and precipitation for northern Mexico and western and eastern Canada (Table 4.1 and Figure 4.2) show higher average temperatures. Northern Mexico is simulated to be the sub-region with the greatest average temperature increase (2.6 K). The average temperature is calculated 1.7 K and 1.5 K higher in western and eastern Canada, respectively. Locally changes up to 4 K in the northern Mexico and up to 3 K for Canada are forecast. The mixing heights are simulated to be higher in most of the northern Mexico (average around +30 m). Maximum increases (around 200 m) are forecast near the US border where the maximum temperature increase is also estimated. For both the Canadian sub-regions mixing height is calculated to be lower in the majority of the domain (average around -30m) except the central part where a small increase is estimated. The average insolation at the earth's surface decreases by 10 W $m^{-2}$ in Canada and increases by 3 W $m^{-2}$ in Mexico. Insolation is simulated to be lower in most of the Canadian sub-regions except the central part, while regional changes are expected in the northern Mexico. Regional changes in daily precipitation are forecast with more precipitation in northern Mexico where the average daily change is up to 6mm locally. Little change is expected for both Canadian sub-regions. Fewer rainy days are estimated for the majority of the northern Mexican and western Canadian sub-regions in contrast to eastern Canada for which more rainy days are predicted (Figure 4.3). All the mentioned local changes in climatic conditions will affect the future local pollutant concentrations.

**Table 4.1: Regional average climatic parameters for the three historic and future summers**

| | Temperature (K) | | Mixing height (m) | | Insolation (Watt/$m^2$) | | Daily Precipitation (mm) | |
|---|---|---|---|---|---|---|---|---|
| | Historic | Future | Historic | Future | Historic | Future | Historic | Future |
| Western Canada | 287.3 | 289.0 | 867.4 | 837.8 | 188.1 | 179.8 | 2.1 | 2.0 |
| Eastern Canada | 287.9 | 289.4 | 919.3 | 884.8 | 168.7 | 158.1 | 2.5 | 2.5 |
| Northern Mexico | 296.1 | 298.7 | 1034.9 | 1062.3 | 282.3 | 285.8 | 1.9 | 2.2 |

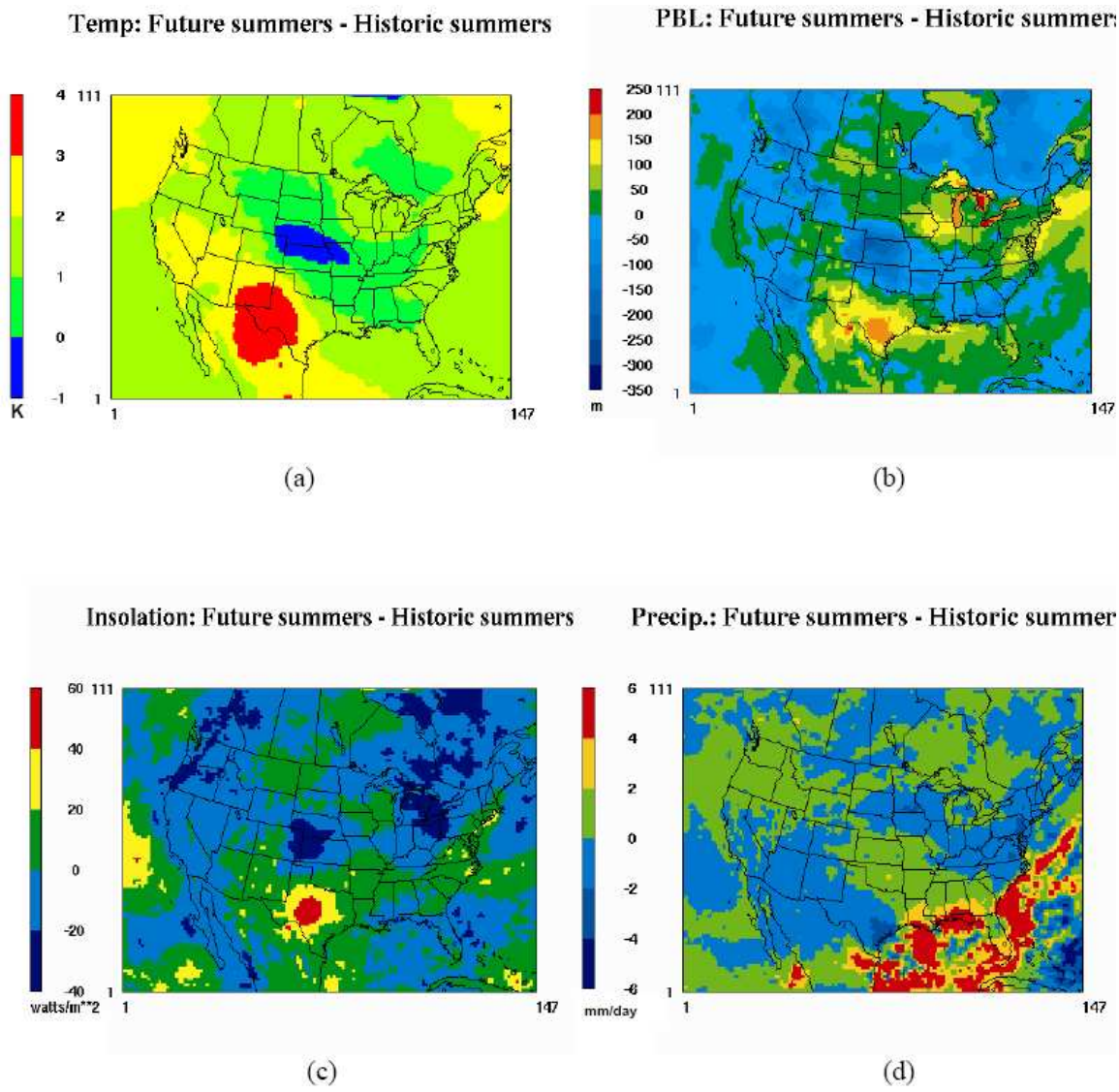


**Figure 4.2: Spatial distribution plots of the average changes in climatic parameters between the three historic and future summers a: temperature, b: planetary boundary level (PBL height), c: insolation, d: precipitation**

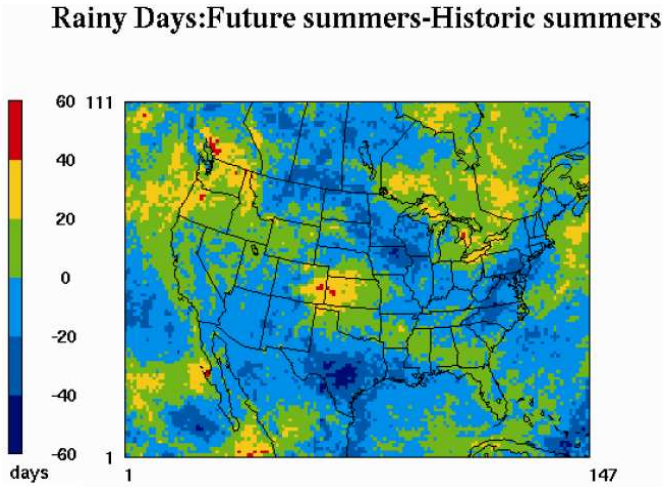


**Figure 4.3: Spatial distribution plots for the change in rainy days between the three historic and future summers**

### 4.3.2 Emissions

Control strategies applied on anthropogenic Canadian sources result in significantly lower $NO_x$, $SO_2$ and $NH_3$ emissions in both Canadian sub-regions (Table 4.2). $NO_x$ emissions are projected to be 32% and 50% lower in western and eastern Canada respectively while $SO_2$ emissions are projected to be 64% and 74% lower in both areas, respectively. $NH_3$ emissions are projected to be 30% and 60% lower in western and eastern Canada respectively. Emissions reduction of anthropogenic VOCs combined with the higher biogenic emissions in the warmer climate results in a small change in VOC emissions: 6% higher in the western Canada and 10% higher in the eastern Canada.

For the case where only climatic changes are considered, although the emission inventory is kept the same, emissions are not, since some pollutant emissions (e.g., biogenic and mobile) depend on meteorology. A minor increase in $NO_x$ emissions in both

Canadian sub-regions is calculated but VOC emissions will be higher in the future (up to 19% in western Canada) due to climate change alone (Table 4.2).

**Table 4.2: Regional average emissions rates (tons/day) for historic and future summers using emissions projections (Future) and no emissions projection (Future_np*) and the relative change (%) based on the historic emissions**

| | $NO_x$ (tons/day) | | | $SO_2$ (tons/day) | | | VOCs (tons/day) | | | $NH_3$ (tons/day) | | |
|---|---|---|---|---|---|---|---|---|---|---|---|---|
| | Historic | Future | Future_np | Historic | Future | Future_np | Historic | Future | Future_np | Historic | Future | Future_np |
| Western Canada | 3.68 | 2.49 (-32.4 %) | 3.72 (1.0 %) | 1.84 | 0.67 (-63.9 %) | 1.84 (0.0 %) | 23.11 | 24.49 (5.6 %) | 27.50 (19.0 %) | 0.92 | 0.65 (-29.6 %) | 0.92 (0.0 %) |
| Eastern Canada | 1.82 | 0.92 (-49.8 %) | 1.84 (0.6 %) | 1.58 | 0.41 (-74.2 %) | 1.58 (0.0 %) | 21.97 | 24.10 (9.7 %) | 25.12 (14.4 %) | 0.38 | 0.16 (-59.2 %) | 0.38 (0.0 %) |
| Northern Mexico | 2.32 | 4.60 (98.8 %) | 2.39 (3.1 %) | 1.88 | 3.53 (87.5 %) | 1.88 (0.0 %) | 29.61 | 36.81 (24.3 %) | 36.78 (24.2 %) | 1.22 | 3.89 (218.9 %) | 1.22 (0.0 %) |

For Mexico, the growth of the industrial sector leads to significantly higher emissions (Table 4.2). $NO_x$, $SO_2$, VOCs and $NH_3$ emissions are projected to be 99%, 88%, 24% and 220% higher in the future summers in the northern Mexico. For the case where only climatic changes are considered a minor increase in $NO_x$ emissions is calculated. VOC emissions are projected to be much higher in the future due to climate change alone (around 24%), but slightly lower when emissions projection is used caused by the higher projected VOC emissions by human activities. Spatial distribution plots of emissions rate changes for the historic and future summers are presented in auxiliary materials.

### 4.3.3 Air quality

#### *4.3.3.1 Ozone*

The impact of climate change alone and the combined effect of climate and emissions changes on $M8hO_3$ are illustrated in Figure 4.4. Under the impact of climate change alone the average $M8hO_3$ concentrations are estimated to be 0.1 ppb higher (0.1%) over western Canada, 0.6 ppb lower (2%) over eastern Canada and 0.5 ppb higher (1%) over northern Mexico (Figure 4.4 & Table 4.3). Global climate change combined with the projected emissions are calculated to reduce the atmospheric pollutant concentrations. Average $M8hO_3$ concentrations are estimated to be 3 ppb lower (6%) over western Canada, 3 ppb lower (8%) over eastern Canada and 2 ppb lower (4%) over northern Mexico (Figure 4.4 & Table 4.3). Interestingly, although future emissions over northern Mexico are projected higher, pollutant concentrations are forecast to be lower. This is caused by the large reduction in US emissions which affect pollutant concentrations over Mexico (Figures are presented in auxiliary materials). Both Canadian

sub-regions are simulated to have lower future M8h$O_3$ concentrations due to emissions reduction (2050s) shown by their Cumulative Distribution Functions (CDFs) (Figure 4.5). Significant reductions are expected for the concentrations above 50 ppb, especially over eastern Canada. The same trend is found for M8h$O_3$ concentrations over northern Mexico with significant reductions in concentrations above 60 ppb.

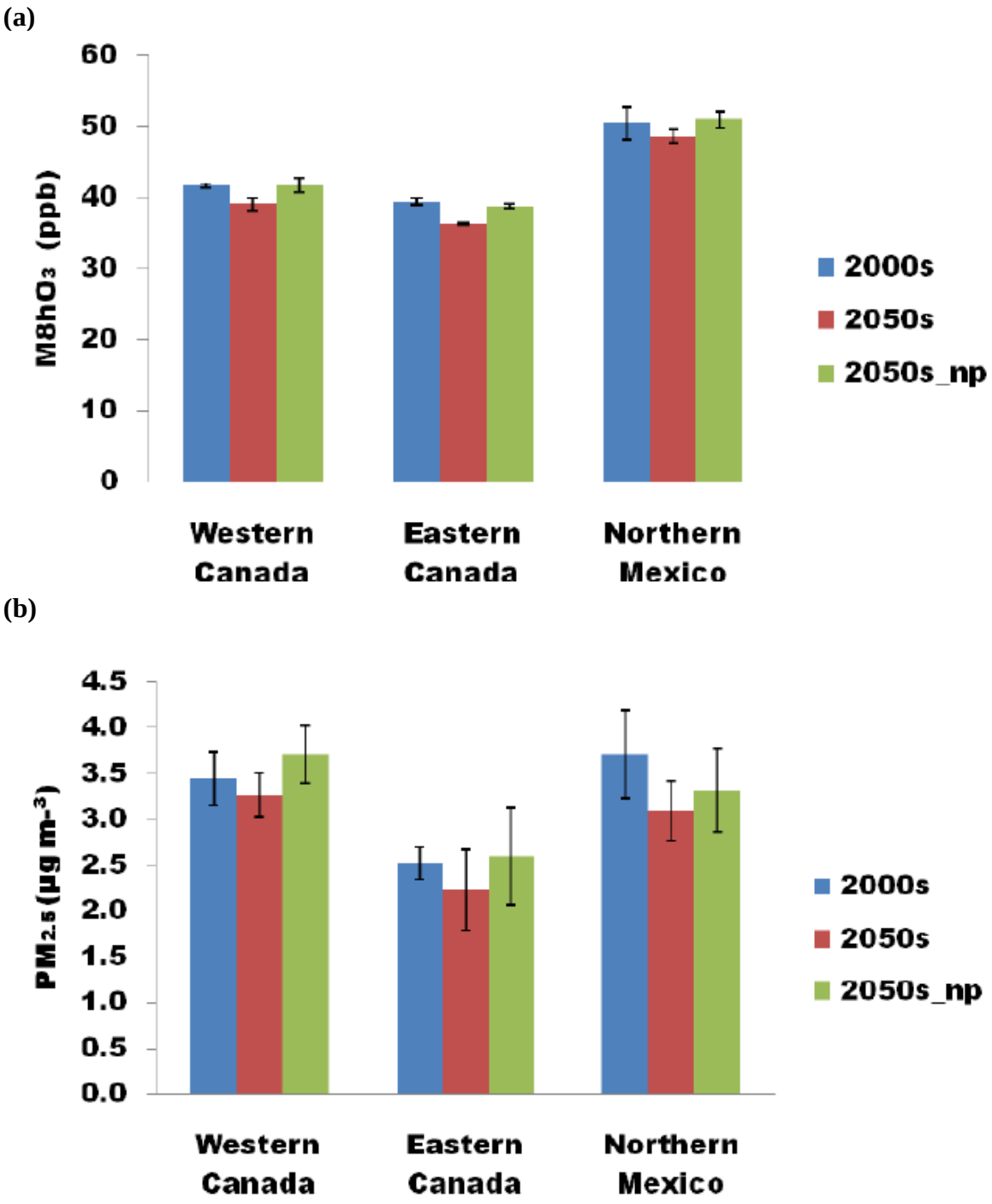


**Figure 4.4: (a) Mean maximum 8 hour ozone concentrations ($M8hO_3$) and standard deviations for historic and future summers (b) Mean daily $PM_{2.5}$ concentrations and standard deviations for historic and future summers (np: 2001 emission inventory and 2050 meteorology)**

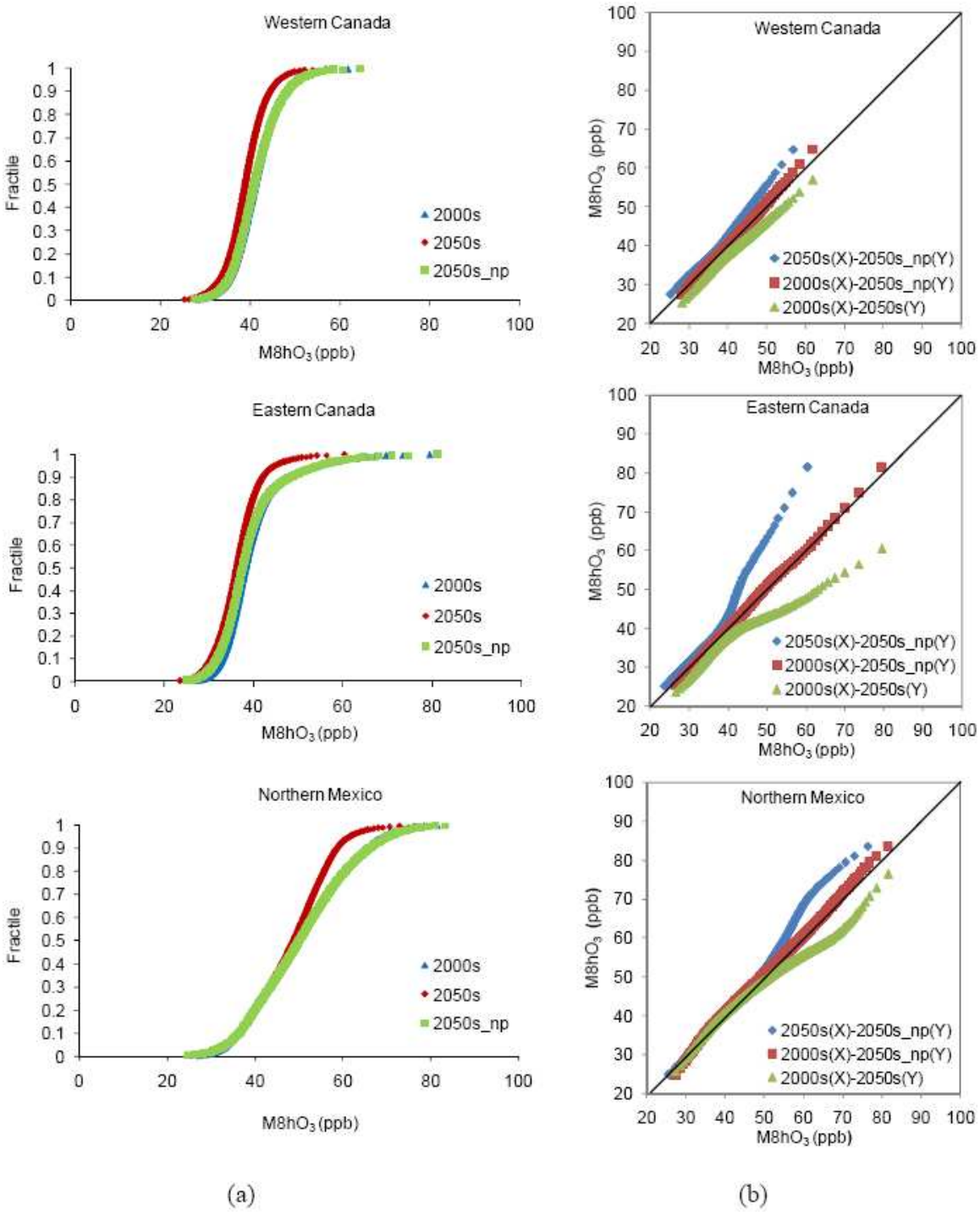


**Figure 4.5: Daily maximum 8 hour ozone concentration cumulative distribution function (CDF) plots (a) for historic and future summers and the correlation (b) between the different examined cases (np: 2001 emission inventory and 2050 meteorology)**

Here, boundary conditions for both historic and future periods are kept the same due to uncertainties in future global changes. Setting varying boundary conditions affect our ability to isolate the impacts of regional climate and emissions changes. Further, calculations were repeated excluding five grid cells deep of the outer perimeter of modeling domain [*Giorgi and Bates*, 1989], with negligible change. Regional average concentrations are similar since the winds typically come from the west well away from the land.

Over Canadian sub-regions, typical $M8hO_3$ concentrations are calculated to be between 30 and 50 ppb (Figure 4.6(a)). Climate change alone is simulated to increase $M8hO_3$ concentrations up to 1 ppb in the center of Canada but a reduction of up to 2 ppb is estimated for the rest of Canada (Figure 4.6(c)). Emission controls are expected to reduce $M8hO_3$ concentrations up to 5 ppb in both Canadian sub-regions (Figure 4.4(d)). The combined effect of climate change and emissions changes is also found to reduce $M8hO_3$ concentrations (up to 5 ppb) in both Canadian sub-regions (Figure 4.6(b)). Over northern Mexico, the highest forecast $M8hO_3$ concentrations are calculated between 50 and 60 ppb near the US border (Figure 4.6(a)). Climate change alone is simulated to increase $M8hO_3$ concentrations up to 4 ppb in the east but to decrease it up to 3 ppb in the west (Figure 4.6(c)). Emissions changes are expected to reduce $M8hO_3$ concentrations up to 5 ppb near the US border while it is expected an increase up to 5 ppb on the west coast due to emission increases (Figure 4.6(d)). The combined effect of climate change and emission changes are found to reduce $M8hO_3$ concentrations up to 5 ppb in the majority of the region expect the east part where an increase up to 2 ppb is predicted. (Figure 4.6(b)).

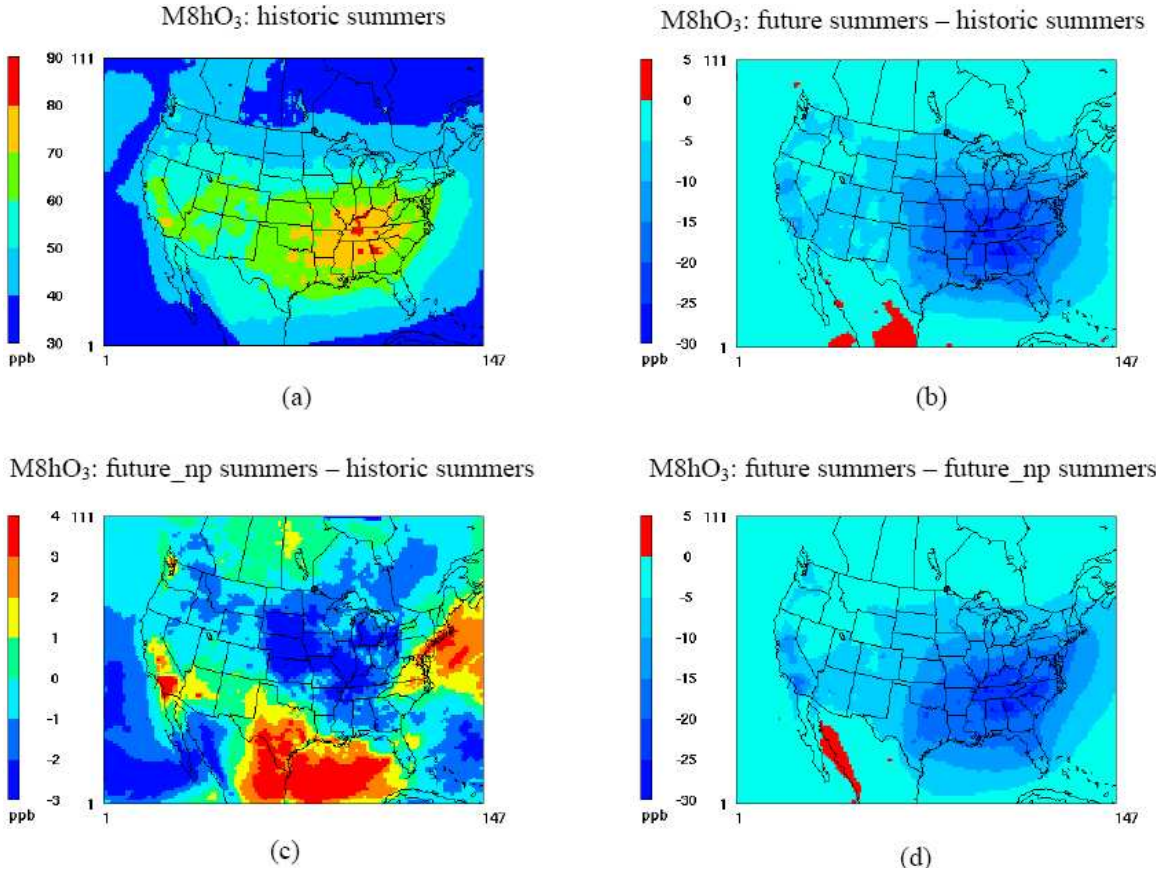


**Figure 4.6: (a) Three-summer-average maximum 8-hr ozone concentrations in historic years; (b) changes in concentrations under the impact of climate change and emission controls; (c) changes in concentrations under the impact of climate change alone; and (d) changes in concentrations under the impact of emission changes alone (np: 2001 emission inventory and 2050 meteorology)**

### *4.3.3.2 Particulate Matter*

Global climate change alone has a significant effect on future summer $PM_{2.5}$ concentrations over western and eastern Canada and northern Mexico as compared to $O_3$, as changes in temperature and precipitation impact gas phase partitioning and wet deposition of particulate matter. Average $PM_{2.5}$ concentrations are estimated to be 0.3 μg $m^{-3}$ higher (8%) over western Canada, 0.1 μg $m^{-3}$ higher (3%) over eastern Canada and

0.4 μg $m^{-3}$ lower (11%) over northern Mexico (Figure 4.4 & Table 4.3). These changes come mainly in $SO_4^=$ and OC over Canada (western Canada: $SO_4^=$ 0.1 μg $m^{-3}$ higher (12%), OC: 0.1 μg $m^{-3}$ higher (7%), eastern Canada: $SO_4^=$ 0.01 μg $m^{-3}$ higher (0.6%), OC: 0.06 μg $m^{-3}$ higher (6%)) and from $SO_4^=$ over northern Mexico (0.3 μg $m^{-3}$ lower (14%)). $PM_{2.5}$ composition will be slightly different due to climate change alone (Figure 4.7 & Table 4.4). Global climate change combined with the projected emission changes is simulated to reduce the atmospheric pollutant concentrations. Average $PM_{2.5}$ concentrations are estimated to be 0.2 μg $m^{-3}$ lower (5%) over the western Canada, 0.3 μg $m^{-3}$ lower (11%) over the eastern Canada (Figure 4.4 & Table 4.3). $PM_{2.5}$ composition is calculated to be significantly modified setting OC as the dominant component followed by sulfate (Table 4.4). Over northern Mexico, average $PM_{2.5}$ concentrations are estimated to be 0.6 μg $m^{-3}$ lower (17%) (Figure 4.4 & Table 4.3). No significant change in $PM_{2.5}$ composition is expected with sulfate to be the dominant component (about 50%) (Table 4.4). Although there is no change in the lower $PM_{2.5}$ concentrations (i.e., below 7 μg $m^{-3}$) there are significant reductions in the higher levels in eastern Canada and northern Mexico when climate change and emissions projection are considered (Figure 4.8).

**Table 4.3: Regional average $M8hO_3$ and $PM_{2.5}$ concentrations and $PM_{2.5}$ composition for the historic and future summers using emissions projection (Future) and no emissions projection (Future_np*) and the relative change (%) based on the historic emissions**

| | Western Canada | | | Eastern Canada | | | Northern Mexico | | |
|---|---|---|---|---|---|---|---|---|---|
| Components ( $\mu g/m^3$) | Historic | Future | Future_np | Historic | Future | Future_np | Historic | Future | Future_np |
| $M8hO_3$ (ppb) | 41.6 | 39.0 (-6.2%) | 41.7 (0.1%) | 39.4 | 36.2 (-8.1%) | 38.8 (-1.6%) | 50.4 | 48.6 (-3.5%) | 50.9 (1.0%) |
| $PM_{2.5}$ ($\mu g/m^3$) | 3.44 | 3.26 (-5.0%) | 3.71 (7.9%) | 2.52 | 2.23 (-11.4%) | 2.60 (3.3%) | 3.71 | 3.09 (-16.7%) | 3.31 (-10.6%) |
| $PM_{2.5}$ components ( $\mu g/m^3$) | | | | | | | | | |
| $SO_4^=$ | 1.07 | 0.76 (-28.5%) | 1.19 (11.7%) | 0.99 | 0.68 (-31.7%) | 1.00 (0.6%) | 1.98 | 1.53 (-22.7%) | 1.71 (-13.7%) |
| $NH_4^+$ | 0.35 | 0.23 (-34.1%) | 0.37 (7.7%) | 0.19 | 0.13 (-30.2%) | 0.19 (1.9 %) | 0.64 | 0.58 (-9.5%) | 0.57 (-11.4%) |
| $NO_3^-$ | 0.09 | 0.04 (-57.8%) | 0.08 (-9.5%) | 0.02 | 0.00 (-78.6%) | 0.02 (-7.6%) | 0.02 | 0.05 (129.3%) | 0.01 (-37.2%) |
| EC | 0.08 | 0.05 (-37.5%) | 0.08 (1.5%) | 0.04 | 0.02 (-45.8%) | 0.04 (2.6%) | 0.07 | 0.04 (-34.8%) | 0.07 (0.4%) |
| OC | 1.16 | 1.19 (2.0%) | 1.25 (7.2%) | 0.93 | 0.93 (0.8%) | 0.98 (6.2%) | 0.46 | 0.41 (-10.2%) | 0.43 (-6.8%) |
| OTHER | 0.70 | 1.00 (43.5%) | 0.74 (6.4%) | 0.34 | 0.45 (32.8%) | 0.36 (4.4%) | 0.54 | 0.48 (-12.6%) | 0.53 (-2.0%) |

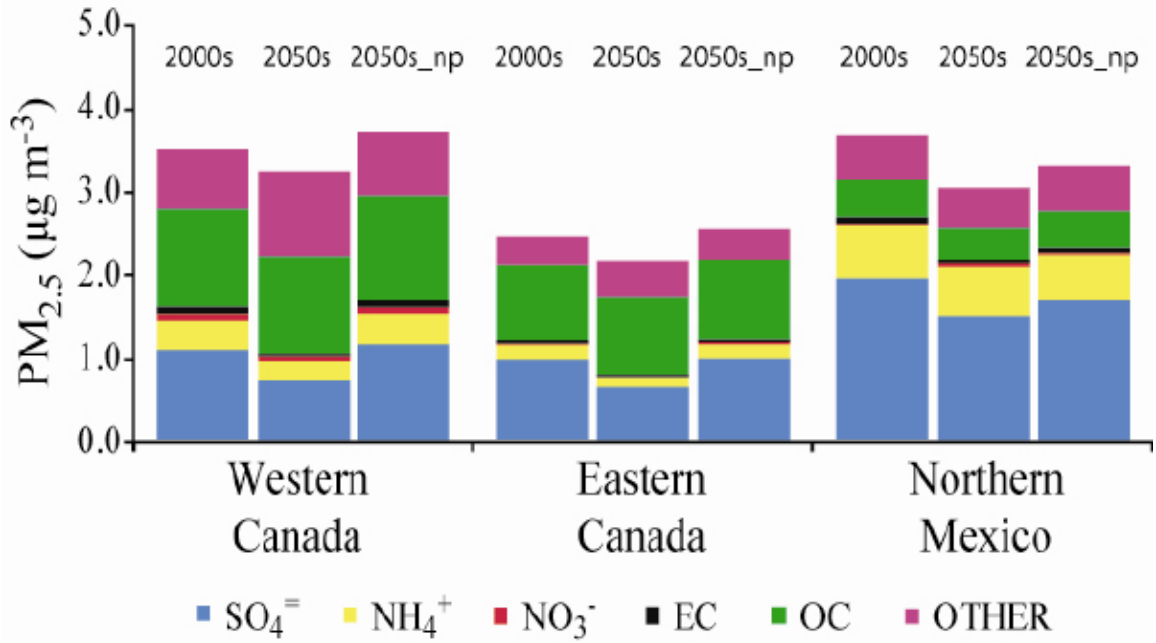


**Figure 4.7: PM $_{2.5}$ composition for historic and future summers**

**Table 4.4: Regional average $PM_{2.5}$ composition (%) for the historic and future summers using emissions projection (Future) and no emissions projection**

| | Western Canada | | | Eastern Canada | | | Northern Mexico | | |
|---|---|---|---|---|---|---|---|---|---|
| Components ( %) | Historic | Future | Future_np | Historic | Future | Future_np | Historic | Future | Future_np |
| $SO_4^{=}$ | 31 | 23 | 32 | 39 | 31 | 38 | 53 | 50 | 52 |
| $NH_4^{+}$ | 10 | 7 | 10 | 7 | 6 | 7 | 17 | 19 | 17 |
| $NO_3^{-}$ | 3 | 1 | 2 | 1 | 0 | 1 | 1 | 2 | 0 |
| EC | 2 | 2 | 2 | 2 | 1 | 2 | 2 | 1 | 2 |
| OC | 34 | 36 | 34 | 37 | 42 | 38 | 12 | 13 | 13 |
| OTHER | 20 | 31 | 20 | 14 | 20 | 14 | 15 | 15 | 16 |

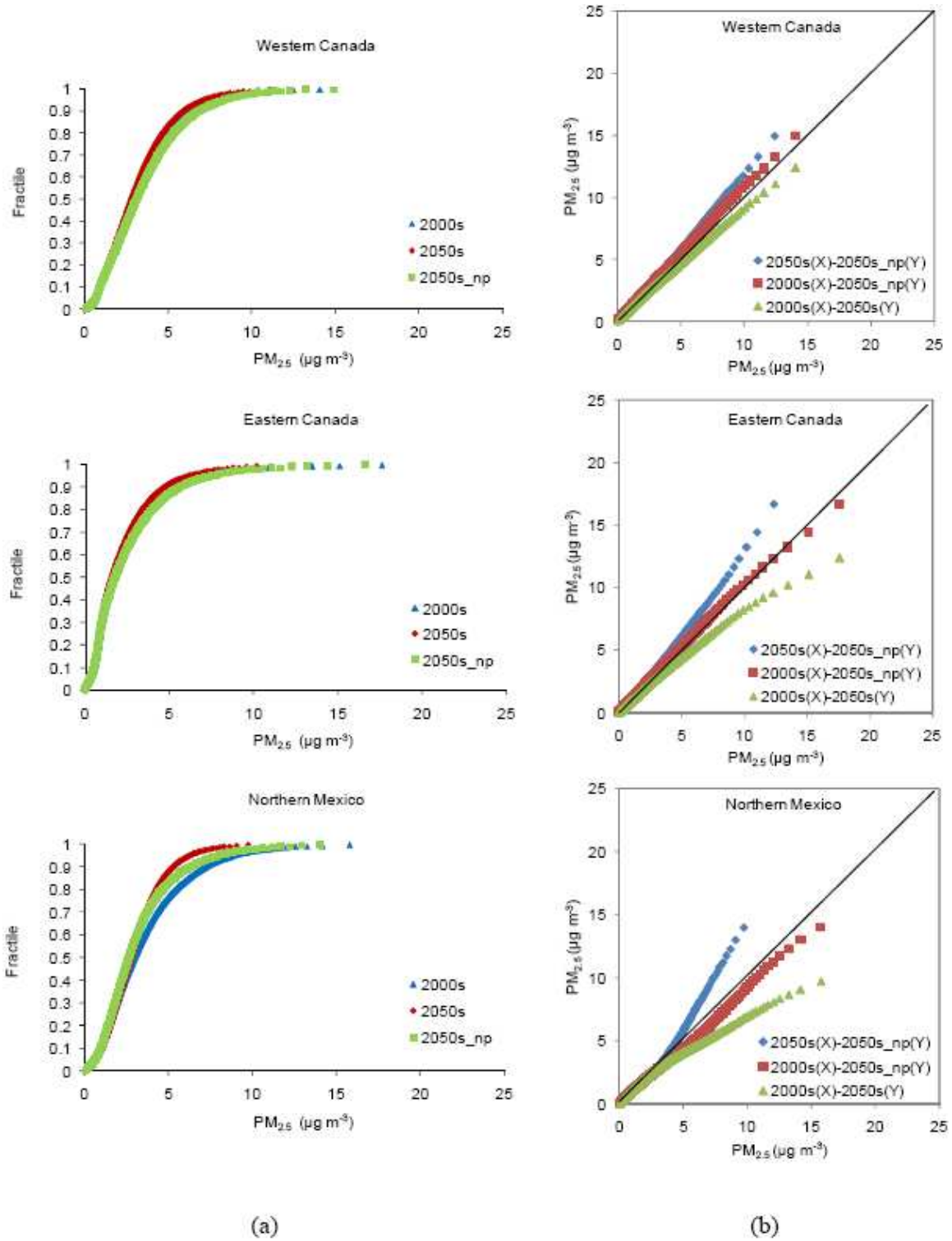


**Figure 4.8: Daily average $PM_{2.5}$ concentration cumulative distribution function (CDF) plots for (a) historic and future summers and the correlation as well as (b) between the different examined cases**

Spatial distribution plots for average $PM_{2.5}$ concentrations for historic years and the changes caused by climate and emission projection are presented in Figure 4.9. Over the majority of both Canadian sub-regions average $PM_{2.5}$ concentrations are calculated between 2.5 and 5.0 μg $m^{-3}$ (Figure 4.9(a)). Climate change alone is simulated to increase $PM_{2.5}$ concentrations up to 0.5 μg $m^{-3}$ in the majority of Canadian sub-regions except the east where a decrease up to 0.5 μg $m^{-3}$ is estimated (Figure 4.9(c)). Emissions projection is expected to reduce $PM_{2.5}$ concentrations up to 1 μg $m^{-3}$ in the major part of both Canadian sub-regions, but there are small areas with reductions up to 2 μg $m^{-3}$ (Figure 4.9 (d)). The combined effect of climate change and emissions projection is estimated to reduce $PM_{2.5}$ concentrations up to 1 μg $m^{-3}$ in both Canadian sub-regions but there are small areas where increase up to 1 μg $m^{-3}$ is projected (Figure 4.9(b)). Over northern Mexico average $PM_{2.5}$ concentrations are simulated higher in the northeast part with average concentrations up to 7.5 μg $m^{-3}$ (Figure 4.9(a)). Climate change alone is calculated to decrease $PM_{2.5}$ concentrations up to 1 μg $m^{-3}$ in the central part (Figure 4.9(c)). Emissions projection is expected to reduce $PM_{2.5}$ concentrations up to 1 μg $m^{-3}$ near US borders while an increase up to 1 μg $m^{-3}$ is expected in the west coast (Figure 4.9 (d)). The combined effect of climate change and emissions projection is estimate to reduce $PM_{2.5}$ concentrations up to 2 μg $m^{-3}$ in the north eastern region close to U.S. borders while small increases are expected in the west (Figure 4.9(b)).

Comparing the effects caused by climate and emission changes between the sub-regions examined here and the U.S. sub-regions (Tagaris et. al., 2007) it is revealed that climate change alone is not expected to significantly modify summer $M8hO_3$ concentrations over Canadian, Mexican and U.S. sub-regions. The effect of climate

change on $PM_{2.5}$ concentrations is expected to reduce summer concentrations over the U.S. and Mexico, they are more important over the Plains, Midwest and Southeast U.S. sub-regions and Northern Mexico where significant reductions are expected in $PM_{2.5}$ levels, but over both Canadian sub-regions small increases are forecast. The combined effect of climate change and projected emissions changes are simulated to reduce $M8hO_3$ and $PM_{2.5}$ concentrations over Canadian and Mexican sub-regions, but this reduction is much lower compared to the reduction simulated for the US sub-regions due to the projected greater emissions reductions in the latter.

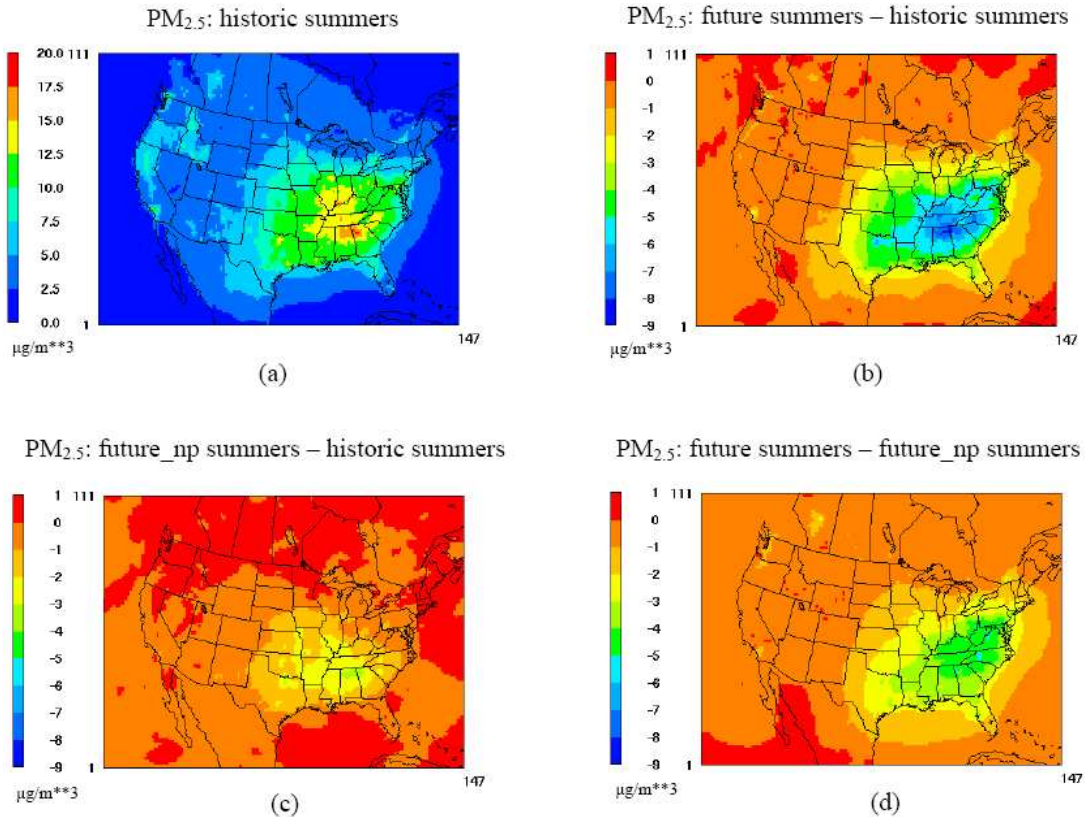


**Figure 4.9: (a) Three-summer-average $PM_{2.5}$ concentrations in historic years; (b) changes in concentrations under the impact of climate change and emission controls; (c) changes in concentrations under the impact of climate change alone; and (d) changes in concentrations under the impact of emission changes alone**

## 4.4 Conclusions

Global climate change impacts on air quality over western and eastern Canada and northern Mexico are simulated to change future summer $PM_{2.5}$ concentrations but have little impact on $O_3$ levels. Global climate change combined with projected emission changes is simulated to reduce pollutants concentrations in all examined sub-regions. One of the most important findings of this study is that although future emissions over northern Mexico are projected to be higher, future pollutant concentrations are not as reductions in the US provide benefits to the south. $PM_{2.5}$ composition is calculated to be slightly different due to climate change alone but when projected emissions are considered, it is calculated to be significantly changed over Canadian sub-regions setting OC as the dominant component followed by sulfate. Over northern Mexico sulfate is simulated to continue to be the dominant $PM_{2.5}$ component.

# CHAPTER 5

# IMPACTS OF FUTURE CLIMATE AND EMISSION REDUCTIONS ON NITROGEN AND SULFUR DEPOSITION OVER THE UNITED STATES *

## 5.1 Introduction

Deposition of nitrogen and sulfur containing compounds on the earth's surface affects terrestrial and aquatic ecosystems. The resulting eutrophication and acidification caused by this deposition leads to changes in species distributions and a loss of biodiversity [*Sanderson, et al.*, 2006]. Sala et al. (2000) rank nitrogen deposition as the third greatest driver after land use and climate change for terrestrial ecosystem biodiversity [*Sala, et al.*, 2000]. Jang et al. (2006) suggest water and inorganic nitrogen soil components as the key factors controlling methane oxidation rates in forest soils [*Jang, et al.*, 2006]. Bragazza et al. (2006) link peat bog decomposition rates with atmospheric nitrogen deposition [*Bragazza, et al.*, 2006]. As peat bogs are exceptional carbon sinks (their extremely low decomposition rates can accumulate plant remnants as peat), increased nitrogen deposition poses a serious risk to the valuable peatland carbon sink.

---

* This chapter is published in the *Geophysical Research Letters*, VOL. 35, L08811, doi:10.1029/2008GL033477, 2008. Co-authors are Tagaris Efthimios, Kasemsan Manomaiphiboon, Jung-Hun Woo, Shan He, Praveen Amar, and Armistead G. Russell.

Recent studies examined the effect of climate change on future deposition using global models [*Dentener, et al.*, 2006; *Phoenix, et al.*, 2006; *Sanderson, et al.*, 2006]. Sanderson et al. (2006) found an increasing risk of acidification in parts of the USA and southeast Asia between the present (1990s) and a century later (2090s) considering both climate change and pollutant emission increases under the Intergovernmental Panel on Climate Change (IPCC) IS92a emissions scenario [*IPCC*, 2001], but noted acid deposition fluxes are subject to large uncertainties. Dentener et al. (2006) estimate that in 2000 the deposition of total reactive nitrogen ($NO_y$+$NH_x$) exceeds 2000 mgN $m^{-2}$ $yr^{-1}$ in much of the world, while 1000 mgN $m^{-2}$ $yr^{-1}$ is viewed as the critical nitrogen load above which changes in sensitive natural ecosystems may occur. Phoenix et al. (2006) compare recent (mid-1990) and future (2050) nitrogen deposition to 34 world biodiversity hotspots keeping climate constant and projected emissions for $NO_x$ and $NH_3$ based on the IPCC IS92a emissions scenario. They found that the average deposition rate across these areas was 50% greater than the global terrestrial average in the middle-1990s and could more than double by 2050. 33 of 34 hotspots receive greater nitrogen deposition in 2050 compared to 1990. The authors conclude that many areas with significant amounts of the global floristic diversity are located near potential damaging future nitrogen deposition rates. Bergstrom and Jansson found that the atmospheric nitrogen deposition in excess of natural levels since the 20$^{th}$ century has caused nitrogen enrichment, eutrophication and increased mass of phytoplankton in lakes over Europe and North America [*Bergstrom and Jansson*, 2006].

Langer et al. (2005) examined the impact of climate change on nitrogen and sulfur deposition in Europe. Using the IPCC IS92a emission scenario, they estimate that for the

2050-2070 period, deposition will be lower over western and central Europe due to the reduction in annual precipitation, although increased dry deposition partly compensates the decrease in wet deposition [*Langner, et al.*, 2005].

Extending the work of Tagaris et al. (2007) examining the impacts of global climate change and emissions on air quality, this study assesses impacts on nitrogen and sulfur deposition over the U.S. This is the first study comparing future with historic deposition rates based on existing emission regulations and strategies for future emissions reduction and potential climate change; uncertainties in emissions projections and future meteorology are not considered. Two different cases are examined: In the first case impacts of changes on deposition in the U.S. by climate change alone are examined by keeping emissions sources, activity levels and controls constant. In the second case future deposition levels are estimated based on changes in climate and emissions together [*Leung and Gustafson*, 2005; *Woo, et al.*, 2008].

## 5.2 Methods

Emission inventory, meteorology and air quality modeling approaches are presented by Tagaris et al. (2007) and are briefly described here. The 2001 US EPA Clean Air Interstate Rule (CAIR) emission inventory (EI) (http://www.epa.gov/cair/technical.html, last access: May 11, 2008) is used for the early 21st century. Projection of 2050 emissions from the 2001 base-year is done in two steps: 1) near future (2020) emissions projection is based on the 2020 EPA CAIR EI; 2) distant future (2050) emissions projection is carried out based on the Netherlands Environmental Assessment Agency's IMAGE model (http://www.mnp.nl/image, last access: May 11,

2008) [*Woo, et al.*, 2008]. The IPCC A1B emissions scenario is selected for the middle century projection in order to be consistent with the climate/meteorological modeling used here [*IPCC*, 2001].

Meteorological fields for both current and future climate are derived from the Goddard Institute of Space Studies (GISS) Global Climate Model (GCM), which is applied at a horizontal resolution of $4^o$ latitude by $5^o$ longitude [*Mickley, et al.*, 2004]. The simulation covers the period 1950 to 2055. Observed greenhouse gas concentrations are used during 1950-2000 and the IPCC A1B emission scenario [*Nakic´enovic´*, 2000] during 2000-2055 with $CO_2$ as implemented in the Bern-CC model [*IPCC*, 2001]. Leung and Gustafson (2005) downscaled the GISS simulations for 1995-2005 and 2045-2055 using a regional climate model based on the Penn State/NCAR Mesoscale Model (MM5).

The Community Multiscale Air Quality (CMAQ) Modeling System with the Statewide Air Pollution Research Center's chemical mechanism (SAPRC-99) (Carter, 2000) is used for the regional air quality modeling. Predicted total nitrogen (NO, $NO_2$, $NO_3$, $N_2O_5$, HONO, $HNO_3$, $HONO_4$, $RNO_3$, PAN, $NH_3$, particulate $NO_3$ and $NH_4$) and total sulfur ($SO_2$, $H_2SO_4$ and particulate $SO_4$) deposition for a historic period (i.e., annual simulations for 2000-2002) are compared with a future period (i.e., annual simulations for 2049-2051) over the US (Figure 3.1). For the future period two different cases are examined. In the first case, the same emission inventory (i.e., 2001) is used for both historic and future simulations in order to estimate the effect of global climate change, alone, on deposition. Although the emission inventory is kept the same, emissions are not, as some pollutant emissions (e.g., biogenic and mobile sources) depend on meteorology.

In the second case the combined effect of future emissions and climate on deposition is examined. Here, in both historic and future periods, boundary conditions are kept the same due to uncertainties in future global changes and to isolate how regional climate and emission changes drive deposition.

## 5.3 Results and Discussion

A detailed discussion of the potential regional climate change over the U.S. has been presented by Leung and Gustafson (2005). Future temperature is simulated to be higher over the U.S. (Figure 5.1(a)). Maximum average temperature increases are around 3 degrees over Texas, New Mexico, Utah, Nevada, Wisconsin, and Michigan. The minimum temperature increases for the U.S. are between 1.0 and 1.5 degrees for the southeastern States (Florida, Georgia, Alabama, Mississippi, Louisiana), along with Montana.

Regional changes in precipitation up to ±5 cm $yr^{-1}$ are simulated for the majority of the States in 2050s. Changes higher than ±20 cm $yr^{-1}$ are expected over central Texas, south Minnesota (negative values) and the southeastern States (positive values). Extreme positive changes (higher than 50 cm $yr^{-1}$) are simulated over the Atlantic Ocean and Gulf of Mexico (Figure 5.1(b)).

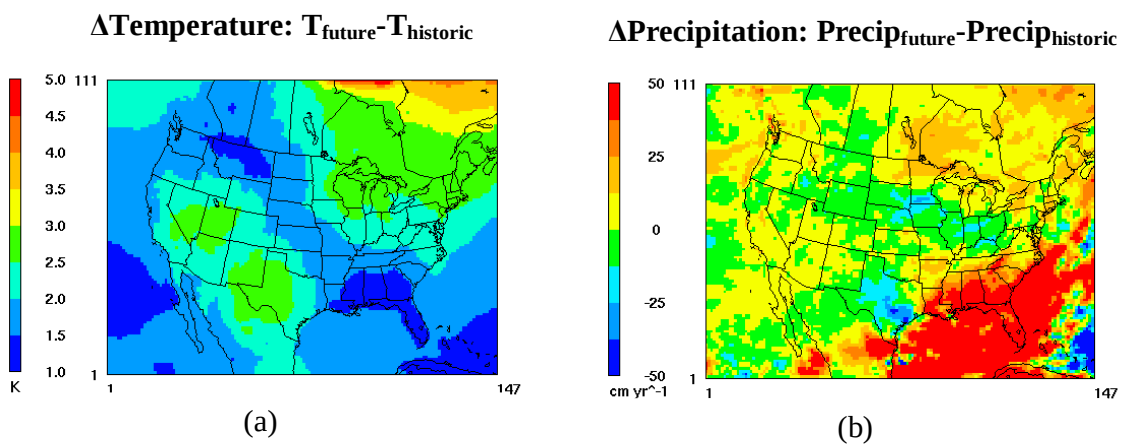


**Figure 5.1 Average changes in temperature (a) and precipitation (b): (2049-2051)-(2000-2002)**

Regional changes in future emissions are detailed by Woo et al. (2008). 2050 emissions of $NO_x$, $SO_2$, $PM_{2.5}$, anthropogenic VOC, and ammonia are expected to change by -55%, -55%, -30%, -40% and +20% for the U.S., respectively, compared with 2001. The biggest reduction is expected over the Midwest, Northeast and Southeast regions as CAIR achieves large reductions in $SO_2$ and $NO_x$ emissions across 28 eastern States. Emission reductions in anthropogenic VOCs combined with the higher biogenic emissions in the warmer climate result in a small change in VOC emissions (+2%). For the case where only climatic changes are considered, VOC emissions are higher (+15%) in the future due to the temperature effect on biogenic and mobile sources; a minor increase in $NO_x$ and $SO_2$ is also predicted.

Model performance is evaluated by comparing observed and predicted annual average total nitrogen and sulfur depositions over the US using data from the Clean Air

Status and Trends Network (CASTNET) (http://www.epa.gov/castnet, last access: May 12, 2008). The simulated three year (2000-2002) average total nitrogen deposition is 48 mgN $m^{-2}$ $yr^{-1}$ overpredicted (9% high bias) for the U.S. domain (ranging from 7 mgN $m^{-2}$ $yr^{-1}$ or 1% high bias in Northeast to 145 mgN $m^{-2}$ $yr^{-1}$ or 25% high bias in Southeast sub-region) (Table 5.1) while the average total sulfur deposition is 60 mgS $m^{-2}$ $yr^{-1}$ underpredicted (9% low bias) (ranging from 2 mgS $m^{-2}$ $yr^{-1}$ or 0.3% low bias in the Southeast to 132 mgS $m^{-2}$ $yr^{-1}$ or 15% low bias in the Northeast sub-region) (Table 5.2). Given that no data assimilation has been used for meteorological fields, model performance provides confidence in our ability to capture typical deposition levels and patterns. Performance (not shown) is better for sulfur wet deposition (27 mgS $m^{-2}$ $yr^{-1}$ underprediction or 7% low bias over U.S. domain), sulfur dry deposition (33 mgS $m^{-2}$ $yr^{-1}$ underprediction or 14% low bias over U.S. domain) and nitrogen wet deposition (88 mgN $m^{-2}$ $yr^{-1}$ underprediction or 23% low bias over US domain). Nitrogen dry deposition is less well captured; over the U.S. domain the model simulates a 70% bias high (~ 130 mgN $m^{-2}$ $yr^{-1}$).

The annual average regional nitrogen deposition and the standard deviation (σ) of the annual average ($\sigma = \sqrt{\frac{1}{N-1}\sum_{1}^{N}(Xi - \overline{X})}$, N=3, $Xi$ stands for the regionally averaged annual deposition and $\overline{X}$ is the three year average value) over the U.S. for the historic period is estimated to be 485±2 mgN $m^{-2}$ $yr^{-1}$ (ranging from 210±9 mgN $m^{-2}$ $yr^{-1}$ in the West to 836±14 mgN $m^{-2}$ $yr^{-1}$ in the Midwest) giving 4.7 Tg as the budget of nitrogen deposited annually onto the continental U.S. (Table 5.1). Holland et al. (2005) estimate a total of 3.7-4.5 Tg nitrogen deposited annually onto the contiguous U.S. [*Holland, et al.*,

2005], close to our estimate. Seasonal variation is noticeable in all the U.S. sub-regions while the oxidized fraction of total nitrogen deposition is greater than reduced due to the elevated $NO_x$ emissions. The dry deposition is greater than the wet deposition in the West and Southeast, but lower in the Midwest and Northeast, resulting in a similar contribution of wet and dry deposition to the total annual deposition averaged over the U.S. No significant change between the three consecutive years examined is noticed for regional average deposition but locally variation can be more pronounced (30% and 50% in interannual variability in nitrogen and sulfur deposition is noticed, respectively).

Climate change alone seems to have a minor effect on the average dry (<6% change in various regions), wet (<9%) and total nitrogen deposition (<3%) (Table 5.1). Wet deposition is modified more in the Southeast (+20 mgN $m^{-2}$ $yr^{-1}$ or 7%), Midwest (-35 mgN $m^{-2}$ $yr^{-1}$ or -7%) and Plains (-17 mgN $m^{-2}$ $yr^{-1}$ or -9%) following the change in precipitation. The same regions have the maximum change in dry deposition: Southeast (-24 mgN $m^{-2}$ $yr^{-1}$ or -6%), Midwest (+17 mgN $m^{-2}$ $yr^{-1}$ or 5%) and Plains (+9 mgN $m^{-2}$ $yr^{-1}$ or 5%). As a result, total nitrogen deposition is expected to change most in the Midwest (-18 mgN $m^{-2}$ $yr^{-1}$ or -2%)).

**Table 5.1 Model Evaluation and Model Simulation for Nitrogen Deposition (in mgN $m^{-2}$ $yr^{-1}$) [a]**

| | Model evaluation | | Model simulation | | | | | |
|---|---|---|---|---|---|---|---|---|
| | Historic | | Historic | | Future | | Future No emissions projection | |
| Region | Observed Total | Predicted Total | Total Seasonal (Win,Spr,Sum,Aut) | Oxidized Reduced Dry - Wet | Total Seasonal (Win,Spr,Sum,Aut) | Oxidized Reduced Dry - Wet | Total Seasonal (Win,Spr,Sum,Aut) | Oxidized Reduced Dry - Wet |
| West | 233±14 | 241±19 | 210±9<br>(57,51,49,53) | 2.2<br>139 - 71 | 165±3<br>(51,43,30,41) | 0.97<br>95 - 70 | 216±2<br>(60,55,47,54) | 2.2<br>140 - 76 |
| Plains | 235±50 | 200±35 | 380±2<br>(56,103,119,102) | 1.4<br>191 - 189 | 294±14<br>(48,79,91,76) | 0.7<br>142 - 152 | 372±12<br>(63,100,115,94) | 1.5<br>200 - 172 |
| Midwest | 803±28 | 898±30 | 836±14<br>(150,225,240,221) | 1.5<br>360 - 476 | 567±8<br>(113,156,145,153) | 0.5<br>214 - 353 | 818±16<br>(162,226,210,220) | 1.6<br>377 - 441 |
| Northeast | 692±65 | 699±62 | 695±13<br>(145,180,196,174) | 2.5<br>331 - 364 | 387±5<br>(91,99,91,106) | 0.7<br>142 - 245 | 700±11<br>(159,181,170,190) | 2.5<br>339 - 361 |
| Southeast | 574±37 | 719±16 | 673±16<br>(183,180,147,163) | 2.4<br>391 - 282 | 434±39<br>(136,116,93,89) | 0.6<br>188 - 246 | 669±51<br>(198,178,146,147) | 2.2<br>367 - 302 |
| US | 558±27 | 606±3 | 485±2<br>(98,129,133,125) | 1.8<br>248 - 237 | 338±11<br>(76,91,86,85) | 0.6<br>150 - 188 | 479±14<br>(105,129,124,121) | 1.8<br>251 - 228 |

[a] Observed and predicted annual average regional total nitrogen deposition for the historic period (2000– 2002) and standard deviation of the annual average for model evaluation, and annual average regional nitrogen deposition data (total, seasonal, wet, dry, oxidized/reduced nitrogen) for the historic (2000– 2002), future (2049 –2051), and future with no emissions projection periods for model simulation. Nitrogen deposition is in mgN $m^{-2}$ $yr^{-1}$.

**Table 5.2 Model Evaluation and Model Simulation for Sulfur Deposition (in mgS $m^{-2}$ $yr^{-1}$) [a]**

| | Model evaluation | | Model simulation | | | | | |
|---|---|---|---|---|---|---|---|---|
| | Historic | | Historic | | Future | | Future No emissions projection | |
| Region | Observed Total | Predicted Total | Total Seasonal (Win,Spr,Sum,Aut) | Oxidized Reduced Dry - Wet | Total Seasonal (Win,Spr,Sum,Aut) | Oxidized Reduced Dry - Wet | Total Seasonal (Win,Spr,Sum,Aut) | Oxidized Reduced Dry - Wet |
| West | 109±16 | 85±5 | 56±3 (21,12,8,15) | 19 - 37 | 46±4 (18,11,5,12) | 12 - 34 | 60±4 (22,14,8,16) | 19 - 41 |
| Plains | 112±21 | 88±24 | 216±8 (30,56,70,60) | 67 - 149 | 150±10 (25,40,47,38) | 42 - 108 | 210±19 (34,57,66,53) | 70 - 140 |
| Midwest | 980±90 | 911±11 | 767±28 (128,208,220,211) | 265 - 502 | 453±15 (92,127,112,122) | 131 - 322 | 737±30 (148,212,184,193) | 274 - 463 |
| Northeast | 894±60 | 762±94 | 770±46 (148,187,243,192) | 239 - 531 | 311±11 (68,77,79,87) | 72 - 239 | 774±32 (165,192,204,213) | 253 - 521 |
| Southeast | 697±40 | 695±14 | 610±42 (166,159,150,135) | 239 - 371 | 304±22 (94,79,73,58) | 83 - 221 | 630±41 (187,161,155,127) | 222 - 408 |
| US | 642±43 | 582±23 | 371±16 (73,97,104,97) | 128 - 243 | 212±7 (48,57,55,52) | 59 - 153 | 368±14 (83,99,96,90) | 129 - 239 |

[a] Observed and predicted annual average regional total sulfur deposition for the historic period (2000– 2002) and standard deviation of the annual average for model evaluation, and annual average regional sulfur deposition data (total, seasonal, wet, dry) for the historic (2000– 2002), future (2049– 2051), and future with no emissions projection periods for model simulation. Sulfur deposition is in mgS $m^{-2}$ $yr^{-1}$.

The effect of climate change, activity growth and emissions controls decreases nitrogen deposition in all sub-regions ranging from -45 mgN $m^{-2}$ $yr^{-1}$ (-21%) in the West up to -308 mgN $m^{-2}$ $yr^{-1}$ (-44%) in the Northeast coming from the reduction in both dry and wet deposition. The total future nitrogen budget deposited annually onto the continental U.S. is estimated to be 3.2 Tg, about 30% less than now. The largest reduction is simulated over the Northeast, Midwest and Southeast regions where the reduction in $NO_x$ emissions is more pronounced. This is the reason for the change in the oxidized nitrogen deposition; reduced nitrogen species are prevalent in all the U.S. sub-regions. Since forest land is the dominant land type covering the eastern U.S., changes in nitrogen fertilizer will mainly affect species biodiversity in these regions. Reduced nitrogen and sulfur loads will be more near pre-industrial conditions. Moreover, since grassland is substantially affected by nitrogen deposition, the reduced loading can decrease the productivity of invasive grasses that may cause less frequent fires [*Sala, et al.*, 2000]. However, the loadings are still above pre-industrial levels and will continue to perturb the ecosystems. The spatial distribution of nitrogen deposition for the historic period (Figure 5.2) shows higher deposition rates in the Midwest States caused by the elevated $NO_x$ emissions in this sub-region [*Woo, et al.*, 2008]. High $NO_x$ emissions result in high nitrogen deposition in the majority of northeastern and southeastern States, as well as eastern Texas. This is in agreement with other studies (e.g., Dentener et al., 2006). For the future period, high nitrogen deposition rates are predicted in areas located in California, Iowa, North Carolina and lakes Michigan and Erie. However, future deposition rates are estimated to be lower compared to historic ones all over the U.S., particularly in the middle and eastern States, except from a small increase simulated

mainly at central California and south Idaho. Climate change alone seems to have a minor impact on nitrogen deposition rates, similar with its impacts on regional air quality [*Tagaris, et al.*, 2007].

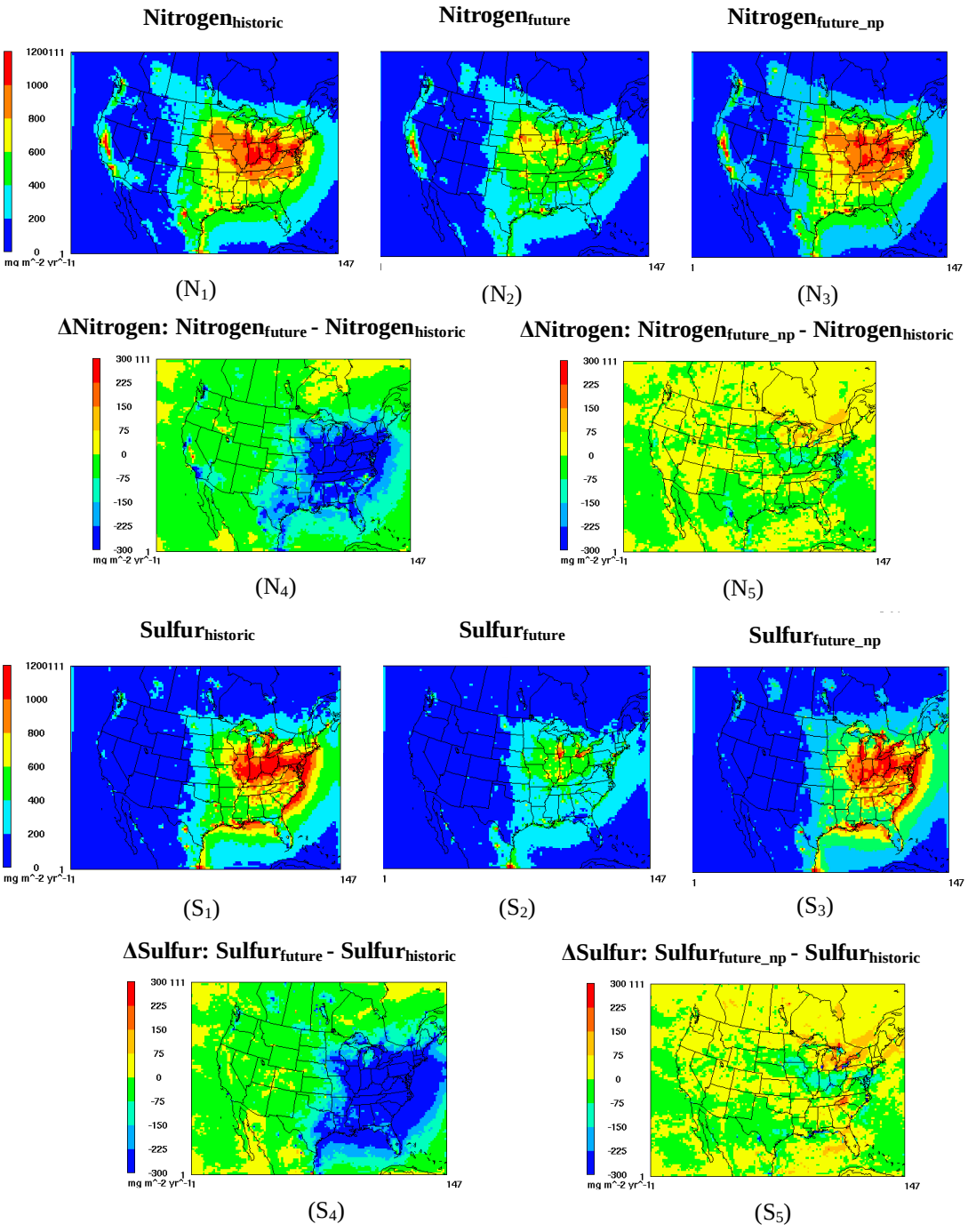


**Figure 5.2: Average nitrogen (N) and sulfur (S) deposition for the historic (2000-2002) ($N_1, S_1$), future (2049-2051) ($N_2, S_2$) and future_np (2049-2051) ($N_3, S_3$) periods and changes caused by the combined effects of future emissions and climate ($N_4, S_4$) as well as by climate change alone ($N_5, S_5$)**

The annual average regional sulfur deposition rates over the US for the historic period are estimated to be 371±16 mgS $m^{-2}$ $yr^{-1}$ (ranging from 56±3 mgS $m^{-2}$ $yr^{-1}$ in the West to 770±46 mgS $m^{-2}$ $yr^{-1}$ in the Northeast) (Table 5.2). No significant change between the three consecutive years examined is noticed for regional average deposition but seasonal variation is noticeable in all US sub-regions. Wet deposition rates are greater than dry deposition.

Climate change alone seems to have a minor effect on the average dry (<7% change in various regions), wet (<10%) and total sulfur deposition (<7%) (Table 5.2). Wet deposition is changed more in Midwest (-39 mgS $m^{-2}$ $yr^{-1}$ or -8%) and Southeast (+37 mgS $m^{-2}$ $yr^{-1}$ or 10%). Southeast appeared as the region with the maximum change in dry deposition (-17 mgS $m^{-2}$ $yr^{-1}$ or -7%) following by Northeast (+14 mgS $m^{-2}$ $yr^{-1}$ or 6%). As a result the total sulfur deposition is expected to change more in the Midwest (-30 mgN $m^{-2}$ $yr^{-1}$ or -4%) and Southeast (+20 mgS $m^{-2}$ $yr^{-1}$ or 3%).

The effect of climate change combined with activity growth and emissions controls decrease sulfur deposition in all US sub-regions ranging from -10 mgS $m^{-2}$ $yr^{-1}$ (-18%) in the West up to -459 mgS $m^{-2}$ $yr^{-1}$ (-60%) in the Northeast due to the reduction in both dry and wet deposition. The biggest reduction is estimated over Northeast, Midwest and Southeast sub-regions due to the future applied $SO_2$ emission strategies in these sub-regions [*Woo, et al.*, 2008].

The spatial distribution plot for the historic period (Figure 5.2) shows higher sulfur deposition rates over Illinois, Indiana, Ohio and Pennsylvania due to the large $SO_2$ emissions in these States [*Woo, et al.*, 2008]. Moreover, $SO_2$ emissions in the eastern US

results in high sulfur deposition over the eastern U.S. coast. For the future period high sulfur deposition rates are predicted over the Midwest and the lakes Michigan and Erie. Similarly to nitrogen, future sulfur deposition is estimated to be lower compared to historic rates over a majority of the U.S. Climate change alone has a minor impact on sulfur deposition rates.

## 5.4 Conclusions and Implications

Total nitrogen and sulfur deposition in the future (i.e., 2049-2051) is simulated to be lower over the U.S. compared with the historic period (i.e., 2000-2002) considering both climate change and planned controls on precursor emissions. Reductions in the Northeast, Midwest and Southeast sub-regions will be higher compared to West and Plains, responding to emission reductions (US EPA Clean Air Interstate Rule (CAIR)). Climate change, alone, with no emissions growth or controls has a minor impact on nitrogen and sulfur deposition rates. As such, climate change will not significantly impact environmental gains achieved from emissions controls.

# CHAPTER 6

# SENSITIVITIES OF OZONE AND FINE PARTICULATE MATTER FORMATION TO EMISSIONS UNDER IMAPCTS OF POTENTIAL FUTURE CLIMATE CHANGE *

## 6.1 Introduction

Climate change is forecast to affect ambient temperatures, precipitation frequency and stagnation conditions [*Karl and Trenberth*, 2003; *Stott, et al.*, 2000], all of which impact regional air quality. Increases in ground-level ozone concentrations are expected in the future due to higher temperatures and more frequent stagnation events [*Hogrefe, et al.*, 2004; *Leung and Gustafson*, 2005; *Mickley, et al.*, 2004; *Murazaki and Hess*, 2006]. Ozone-related health effects are also anticipated to be more significant [*Knowlton, et al.*, 2004]. Prior work suggests $PM_{2.5}$ (particulate matter with an aerodynamic diameter less than 2.5 micrometers) levels will increase in some areas but not in others, largely due to changes in precipitation. Both ozone and $PM_{2.5}$ are also found to impact climate via direct and indirect effects on radiative forcing [*Akimoto*, 2003]. An issue of primary importance for policymakers is how well currently planned control strategies for improving air quality for ozone and $PM_{2.5}$ that are based on the current climate will work under future global climate change scenarios. This can be investigated by quantifying sensitivities of air pollutants (e.g., ozone and $PM_{2.5}$) to their precursors (e.g., nitrogen oxides: $NO_x$ = NO + $NO_2$), volatile organic compounds (VOCs), ammonia, and sulfur dioxides ($SO_2$)) under both historic and potential future climatic conditions.

---

* This chapter is published in the *Environmental Science & Technology* 2007**,** 41, 8355–8361. Co-authors are Efthimios Tagaris, Kasemsan Manomaiphiboon, Sergey L. Napolenok, Jung-Hun Woo, Shan He, Praveen Amar, and Armistead G. Russell.

Sillman et al. [*Sillman, et al.*, 1990] and Milford et al. [*Milford, et al.*, 1994] present sensitivities of ozone formation to its precursors, $NO_x$ and VOCs. They identified the factors that affect sensitivity of ozone to $NO_x$ and VOCs including: the ratio of VOC to $NO_x$ concentrations, reactivity of VOCs, abundance of biogenic hydrocarbons, photochemical aging, and rates of meteorological dispersion [*Sillman*, 1999]. Ambient particulate matter formation, including inorganic components (e.g., ammonium, nitrate and sulfate) and secondary organic aerosols (SOAs), are found to be influenced by ambient temperature, humidity, clouds, and precursor concentrations [*Ansari and Pandis*, 1998; *Chow, et al.*, 1994; *Pun and Seigneur*, 2001; *Russell, et al.*, 1983]. Both anthropogenic and biogenic VOCs contribute to SOA [*Odum, et al.*, 1997; *Seinfeld and Pankow*, 2003], though biogenic VOCs are thought to be more important on a global scale [*Chung and Seinfeld*, 2002; *Kroll, et al.*, 2006]. Since higher ambient temperatures lead to higher biogenic VOC emissions as a result of climate change (assuming no changes in vegetation coverage) [*Lathiere, et al.*, 2005; *Sanderson, et al.*, 2003], future climate-induced emission changes are expected to alter how ozone and PM formation will respond to their precursor emissions (i.e., sensitivities) even if anthropogenic emissions do not change significantly. Recent studies suggest that ozone concentrations are more sensitive to precursor emission changes from controls than to climate-induced effects [*Russell and Dennis*, 2000]. If the same is true for $PM_{2.5}$, this would suggest that current emphasis on local and regional controls should continue to provide air quality benefits.

Responses of future ozone and $PM_{2.5}$ levels to both climate change and to emission changes are quantified using historic (years of 2000-2002) and projected future

(years of 2049-2051) meteorology. The target future period from 2049-2051 is chosen as a compromise between being far enough in the future to experience non-trivial climate modification, yet is still within a reasonable horizon for air quality planning. If the pollutant fields and their sensitivities to anthropogenic emissions in the future are similar to current conditions, the conclusion would be that climate considerations will not significantly impact design of current control strategies that deal with ozone and $PM_{2.5}$ as much as if the relative sensitivities changed markedly. If the sensitivities are similar, but the pollutant levels are significantly different, then control strategies should focus on degree of controls rather than direction. If, however, the sensitivities are significantly different, future control decisions should consider how climate change might be addressed in formulating strategies along with associated uncertainties. This work extends the previous work by Tagaris et al. (2007) to show the sensitivities of different air pollutants to emissions which provides critical information for the air pollution control strategies.

## 6.2 Method

Details of the modeling approach are given in Tagaris et al. (2007), and summarized here. The Fifth-Generation NCAR/Penn State Mesoscale Model (MM5) [*Grell, et al.*, 1994; *Seaman*, 2000] is used to downscale NASA's Goddard Institute of Space Studies (GISS) [*Rind, et al.*, 1999] global climate model results for years of 2000-2002 and 2049-2051 [*Leung and Gustafson*, 2005; *Mickley, et al.*, 2004]. Meteorological model evaluation has been presented by Tagaris et al. (2007) and Leung and Gustafson (2005). Emissions for Canada, Mexico and the U.S. for 2000-2002 are processed using

the Sparse Matrix Operator Kernel Emissions (SMOKE) modeling system (http://www.smoke-model.org/index.cfm, last access: April 29, 2008). For future emissions, we use forecasts accounting for reductions in $NO_x$, $SO_2$ and VOC corresponding to current regulations in the U.S., Canada and Mexico (which include reductions from the Clean Air Interstate Rule (CAIR) controls [*Houyoux*, 2004]) up to 2020. From 2020 to 2050, we use forecasts from the Integrated Model to Assess the Global Environment (IMAGE) model (www.mnp.nl/image, last access: April 29, 2008), based on IPCC A1B scenario (see Woo et al. (2008) for details).

The Community Multiscale Air Quality Model (CMAQ) [*Byun and Schere*, 2006], with SAPRC-99 [*Carter*, 2000] chemical mechanism and decoupled direct method 3D (DDM-3D) [*Dunker*, 1981; 1984; *Dunker, et al.*, 2002; *Yang, et al.*, 1997], are used to simulate historic and future ozone and $PM_{2.5}$ concentrations, and to quantify their sensitivities to specific sets of emissions; including both anthropogenic and biogenic VOC emissions, anthropogenic $NO_x$, total $NH_3$ and total $SO_2$, over a domain covering the United States as well as parts of Canada and Mexico. A uniform grid of 36 by 36 km horizontal cells with 9 vertical layers is employed (Figure 3.1). DDM-3D directly calculates the first-order local sensitivities of both gas- [*Cohan, et al.*, 2005] and condensed-phase [*Napelenok, et al.*, 2006] pollutants to precursor emissions, i.e., the first-order sensitivity ($S_{i,j}$) of pollutant concentration $i$ ($C_i$) to source emissions $j$ ($E_j$) is calculated as:

$$S_{i,j} = E_j \frac{\partial C_i}{\partial E_j} \qquad (2.1)$$

The first-order (linearized) sensitivities, as presented here, have the same units as the corresponding pollutants. These sensitivities represent how pollutant concentrations would respond to a 100% reduction in precursor emissions if the systems were linear, which is typically reasonable for reductions of 25-50% emissions, depending on pollutant and environment [*Cohan, et al.*, 2005].

In this work, two different future scenarios are studied. First, the changes in sensitivities due to the impact of potential future climate change alone are examined by using historic and potential future climates, but keeping future emissions source strengths the same as in historic episodes ("non-projected" or "np" scenario). In the second scenario, potential future meteorological fields and expected future emissions, projected following the IPCC mid-level increase scenario, A1B emission scenario [*IPCC*, 2001], and recent regulatory actions [*Houyoux*, 2004], are applied in the regional air quality simulations. Simulations performed in this study are summarized in Table 6.1. By comparing the results of sensitivity analyses from different scenarios, contributions of ozone and $PM_{2.5}$ precursors and effectiveness of control strategies are quantified.

**Table 6.1: Summary of air quality simulations**

| Scenario | Emission Inventory (E.I.) | Climatic Condition | Future Air Quality Impacting Factor |
|---|---|---|---|
| 2001 | historic (2001) | historic (2001 complete year) | N.A.[a] |
| 2000-2002 summers | historic (2000-2002) | historic (2000-2002 summers[b]) | N.A. |
| 2050_np[c] | historic (2001) | future (2050 complete year) | potential future climate changes |
| 2049-2051_np_summers | historic (2000-2002) | future (2049-2051 summers[b]) | potential future climate changes |
| 2050 | future (2050) | future (2050 complete year) | potential future climate changes & emission controls |
| 2049-2051 summers | future (2049-2051) | future (2049-2051 summers[b]) | potential future climate changes & emission controls |

[a] N.A.: not applicable. [b] Summers include June, July and August. [c] "np" means no projection in emission inventories. Emission inventories for 2049-2051 are the same as 2000-2002.

Simulations using non-projected (np) emissions in the future (i.e., 2050_np and 2049-2051_np summers in Table 6.1) use the same emission inventories as 2001 but the emissions are not identical as some components of emissions (e.g., biogenic VOC and mobile source $NO_x$) have been adjusted to respond to future climate/meteorology (Appendix B, Table B.2).

## 6.3 Results and Discussion

Regional variations are found by dividing the continental U.S. into five large regions, West, Plains, Midwest, Northeast and Southeast (Figure 3.1) taking into account different characteristics of precursor emissions and air pollutant formation processes. Sensitivity results are presented by averaging over the continental U.S. and each region separately for the year 2001, summers (June, July, and August) of 2000-2002, the year

2050, and summers of 2049-2051 with both projected and non-projected emissions. Additionally, the first-order sensitivities of the 2050 scenario are also normalized by 2050 emissions and multiplied by 2001 emissions in order to compare the sensitivities of ozone and $PM_{2.5}$ formation with the 2001 scenario based on "per unit" (e.g. per ton) of precursor emissions ("2050_Norm").

$$S_{2050\_Norm} = S_{2050} \frac{E_{2001}}{E_{2050}} \qquad (2.2)$$

Details of meteorology- and emission-simulation results are given elsewhere [*Leung and Gustafson*, 2005; *Tagaris, et al.*, 2007; *Woo, et al.*, 2008] and are summarized here. Annual average surface temperatures are predicted to increase by about 0-3 K over the simulation domain between 2001 and 2050. The higher temperatures in 2050 are accompanied by increases in absolute humidity in most of the domain (up to 20% compared to 2001). For emissions, $SO_2$ and $NO_x$ emissions are forecast to be reduced 51% each between 2001 and 2050, largely due to current regulations being fully implemented. $NH_3$ emissions are predicted to rise in the future (~ 7%) from increases in population and related activities [*Tagaris, et al.*, 2007; *Woo, et al.*, 2008]. If the effects of increased activities and planned emission controls are not considered, $SO_2$ (+4%) and $NO_x$ (+2%) emissions change only slightly due to temperature dependent processes (e.g., microbial activities, increased exhaust emissions). Without controls of future anthropogenic emissions, VOC emissions are predicted to increase (+15%) due to warmer climate along with temperature-sensitive emissions from biogenic and mobile sources and other evaporative processes. On the other hand, with controls, anthropogenic VOC emissions are predicted to decrease in the future, offsetting increases in biogenic

VOC emissions. Combined effects of those two mechanisms cause total VOC (i.e., anthropogenic and biogenic VOCs) emissions to increase approximately 2% (Table B.2).

### 6.3.1 Ozone Sensitivities

In order to quantify how ozone levels will continue to respond to controls, CMAQ with DDM-3D was used to calculate ozone sensitivities to biogenic VOCs, anthropogenic VOCs and anthropogenic $NO_x$ emissions for the historical and future periods with and without controls. Simulated 2001/2050 yearly and 2000-2002/2049-2051 summer fourth-highest daily maximum 8-hr average ozone ($4^{th}$ MDA8h ozone) is calculated for comparison to EPA's National Ambient Air Quality Standards (NAAQS). Results of sensitivities of annual and summertime (JJA) $4^{th}$ MDA8h ozone to precursor emissions are then averaged by regions as well as for the continental U.S. (Figure 6.1). First-order (linearized) sensitivities suggest each 10% reduction in anthropogenic $NO_x$ emissions causes ~2% to 4% decreases in $4^{th}$ MDA8h $O_3$ concentrations in both 2001 and 2050 when emission controls are not included (Appendix B, Table B.1) on a regional basis. Reductions in VOC emissions are also beneficial for decreasing ozone levels for historic and future episodes without projected emission controls. Overall, ozone and its relative sensitivities to anthropogenic $NO_x$, biogenic VOC and anthropogenic VOC emissions are predicted to increase only slightly in 2050 without considering emission controls as compared with 2001.

For scenarios with projected emissions ("2050" & "2049-2051 summers"), future reductions in anthropogenic precursor emissions decrease the total contributions of anthropogenic $NO_x$ and anthropogenic/biogenic VOCs to ozone formation because of the

51% reduction in $NO_x$ emissions. However, sensitivities of ozone formation to "per unit" (e.g., ton) $NO_x$ emission ("2050_Norm" in Figure 6.1) increase significantly because the reductions in $NO_x$ and steady VOC emissions shift ozone formation towards being more $NO_x$-limited. Conversely, sensitivities of ozone formation to per unit emissions of anthropogenic and biogenic VOCs are both lower in 2050 as compared to 2001. Changes in multi-summer sensitivities of 4$^{th}$ MDA8h ozone formation to precursor emissions between different scenarios (2000-2002_summers, 2049-2051_np_summers and 2049-2051_summers) are found to be in good agreement with the changes in yearly simulations (Figure 6.1). If one looks at regional variations in all sub-regions, sensitivities of 4$^{th}$ MDA8h ozone formation to anthropogenic $NO_x$ emissions are highest in the Southeast because of greater biogenic VOC emissions. Year-to-year variations in sensitivities of 4$^{th}$ MDA8h ozone to anthropogenic $NO_x$ emissions during summers are found to be small for 2000-2002 and 2049-2051 with both projected and non-projected emissions (Table 6.2). Such results suggest more consecutive yearly simulations are not expected to change interpretation of sensitivity analysis significantly.

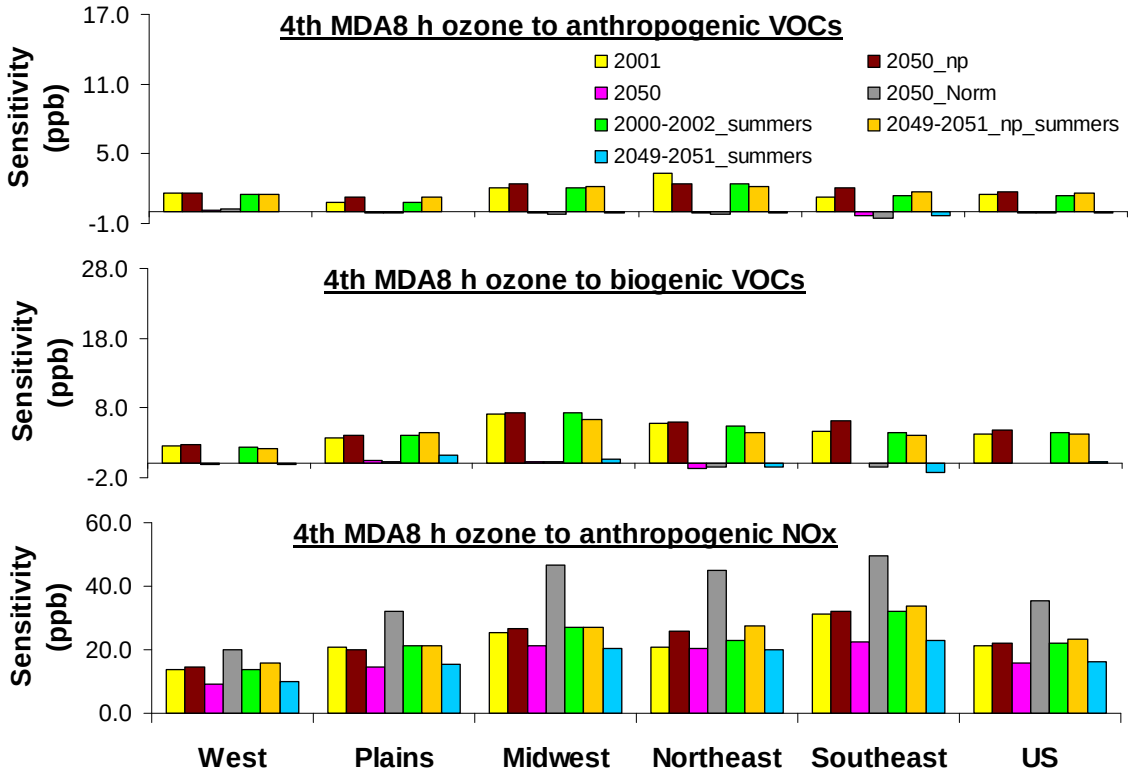


**Figure 6.1: Sensitivities of annual and summertime (JJA) 4$^{th}$ MDA8h $O_3$ to domain-wide emissions of biogenic and anthropogenic VOCs and anthropogenic $NO_x$ for the five regions and U.S. (Note the change in scales)**

**Table 6.2: Sensitivities of summertime (JJA) 4th MDA8h ozone to domain-wide anthropogenic $NO_x$ emissions for the five regions and continental U.S. Unit: ppb**

| | 2000 | 2001 | 2002 | 2049_np | 2050_np | 2051_np | 2049 | 2050 | 2051 |
|---|---|---|---|---|---|---|---|---|---|
| **West** | 13.4 | 14.4 | 13.3 | 15.2 | 15.2 | 17.5 | 9.5 | 9.8 | 10.6 |
| **Plains** | 21.4 | 21.6 | 21.2 | 21.9 | 19.5 | 22.3 | 15.7 | 15.2 | 15.7 |
| **Midwest** | 27.6 | 25.4 | 27.7 | 24.8 | 24.6 | 32.3 | 18.4 | 19.5 | 22.9 |
| **Northeast** | 24.6 | 21.1 | 23.1 | 24.7 | 26.4 | 31.2 | 17.8 | 19.5 | 22.2 |
| **Southeast** | 33.8 | 31.4 | 31.5 | 34.3 | 31.5 | 35.8 | 23.3 | 22.3 | 23.4 |
| **U.S.** | 22.6 | 22.0 | 22.1 | 22.8 | 21.6 | 25.5 | 16.0 | 16.0 | 17.4 |

Spatial distributions of sensitivities of annual 4th MDA8h ozone to anthropogenic $NO_x$ emissions for the scenarios of 2001, 2050_np and 2050 are found to be similar, though the magnitudes of sensitivities of 2001 and 2050_np are higher than 2050 due to controls of anthropogenic $NO_x$ emissions and associated decreases in ozone concentrations in the future (Figure 6.2, (a)-(c)). On the other hand, planned future emission controls are predicted to shift ozone formation to being more $NO_x$-limited in 2050 over the simulation domain. This suggests that reductions in anthropogenic $NO_x$ emissions will continue to be effective for reducing regional ozone concentrations, even more so than is currently the case.

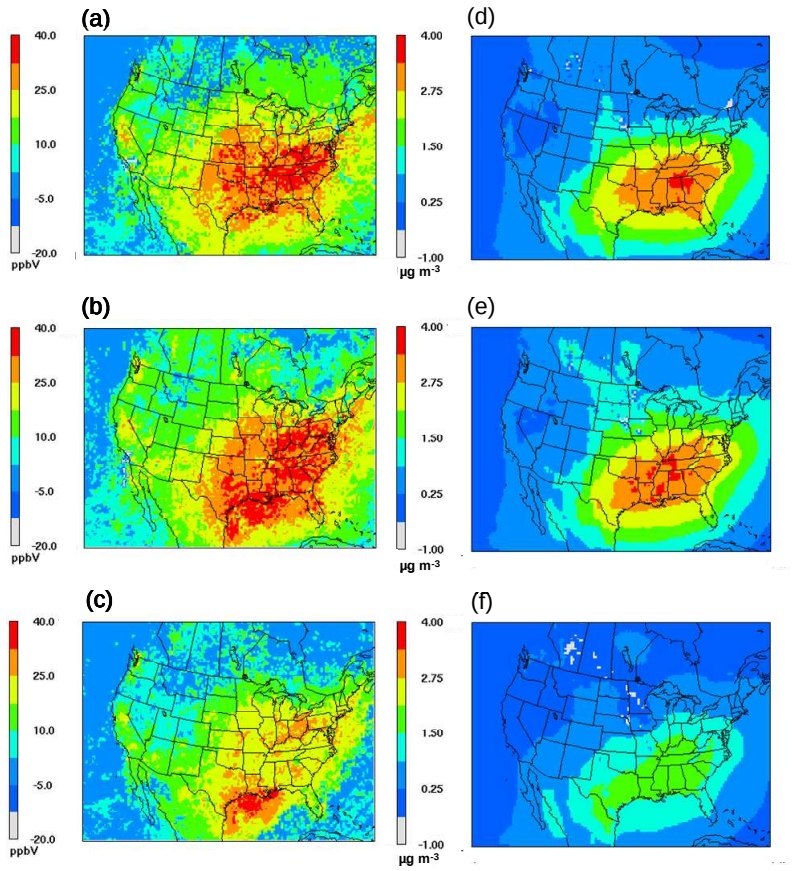


**Figure 6.2: Spatial distribution of sensitivities of annual 4th MDA8h ozone to domain-wide anthropogenic $NO_x$ emissions ((a), (b) and (c)) and annual averaged sensitivities of $PM_{2.5}$ formation to domain-wide $SO_2$ emissions ((d), (e) and (f)) for 2001, 2050_np and 2050 (top to bottom) (sensitivities presented here are first-order sensitivities )**

## 6.3.2 $PM_{2.5}$ Sensitivities

Sensitivities of 2050 annual average speciated $PM_{2.5}$ formation to its precursors are predicted to be similar to 2001 when non-projected emission inventories are simulated ("2050_np") (Figure 6.3), even though climate change influences $PM_{2.5}$ formation in several ways. First, changes in temperatures shift the partitioning of volatile

and semi-volatile compounds between gas and condensed phases. Higher temperatures favor condensable compounds existing as gases, thus decreasing the mass of condensed material. This is true for nitrate and secondary organic aerosols. Increases in absolute humidity due to higher temperature can increase OH concentrations in the atmosphere. Since OH radicals are strong oxidants, higher OH concentrations are expected to favor more rapid oxidation of $SO_2$ and $NO_x$, forming condensable compounds in the atmosphere. Most notable effects, however, relate to meteorological processes affecting dispersion (e.g., stagnation periods) and loss (e.g., wet deposition due to rain). Surprisingly, the net effects of those mechanisms cause only slight changes in $PM_{2.5}$ (see Tagaris et al., 2007) and their sensitivities (Figure 6.3).

Relative sensitivities of sulfate fraction of $PM_{2.5}$ to $SO_2$ emissions ($S_{SO4,SO2}$) and nitrate of $PM_{2.5}$ to anthropogenic $NO_x$ emissions ($S_{NO3,ANOx}$) ("A" presents "anthropogenic") are predicted to decrease with projected emissions in 2050 due to reductions in emissions (Figure 6.3). However, sensitivities of nitrate aerosol formation per unit $NO_x$ emission increase, although the contribution of per unit $SO_2$ emission to sulfate aerosol doesn't change significantly ("2050_Norm"). The increase in sensitivity of nitrate aerosol formation to per unit $NO_x$ emission is due to both higher projected ammonia emissions and reductions in $SO_2$ emissions which make more $NH_3$ available to react with nitric acid to form ammonium nitrate. Sensitivities of sulfate $PM_{2.5}$ formation to ammonia ($S_{SO4,NH3}$) are predicted to increase due to higher, future ammonia emissions. Higher ammonia/ammonium concentrations tend to neutralize cloud water, allowing more rapid $SO_2$ oxidation by ozone. On the other hand, lower $NO_x$ emissions decrease ammonium nitrate formation in the nitrate-limited environment and reduce sensitivities of

nitrate $PM_{2.5}$ to $NH_3$ emissions ($S_{NO3,NH3}$). Overall, changes in sulfate and nitrate lead to less ammonium $PM_{2.5}$ formation and decrease sensitivities of ammonium $PM_{2.5}$ to ammonia emissions ($S_{NH4,NH3}$).

$SO_2$ emission reductions lead to increases in nitrate aerosol formation ($S_{NO3,SO2}$ is negative), while anthropogenic $NO_x$ emission reductions have small impacts on sulfate aerosol formation ($S_{SO4,ANOx}$). Decreases in $SO_2$ emissions make more ammonia/ammonium available for ammonium nitrate formation, though a small increase in nitrate is simulated. Similarly, lower $NO_x$ emissions decrease nitrate aerosol, slightly increasing sulfate, which arises from a decreased atmospheric acidity, increases heterogeneous sulfate formation. Thus, the net effects of $SO_2$ and $NO_x$ reductions are predicted to decrease $PM_{2.5}$ mass under both current and potential future climate conditions. Unlike high ozone levels and their sensitivities, which are consistently observed in the summer, temporal variations, presented by standard deviation of month-to-month variability, of sensitivities of speciated $PM_{2.5}$ are found in a yearly simulation (Figure 6.3). $PM_{2.5}$ sensitivities with the largest variability are $S_{SO4,SO2}$, $S_{NO3,ANOx}$ and $S_{NO3,NH3}$ (Appendix B, Figure B.1). Sensitivities of sulfate $PM_{2.5}$ to $SO_2$ emissions are simulated to be more important during summers than other seasons, while sensitivities of nitrate to $NO_x$ and $NH_3$ emissions are found being the highest in the winter (Figure B.1). This is true because $NH_4NO_3$ has higher vapor pressure and is more sensitive to high temperatures than $(NH_4)_2SO_4$. Gilliland et al. present an underestimation of $NH_3$ emissions in summers and overestimation in winters since seasonal variations of $NH_3$ emissions are not included in current inventories [*Gilliland, et al.*, 2003]. Therefore, seasonal trends of $NH_4NO_3$ and $(NH_4)_2SO_4$ are expected to be more significant if

seasonal variation in $NH_3$ emissions are considered. Those results show that $SO_2$ emissions dominate $PM_{2.5}$ formation in the summer while emissions of $SO_2$, $NO_x$ and $NH_3$ are all comparably important for decreasing secondary $PM_{2.5}$ levels in the winter. Seasonal variability of sensitivity of secondary organic aerosol (SOA) to biogenic VOC emissions ($S_{SOA,BVOC}$) ("B" presents "biogenic") was also found due to higher biogenic VOC emissions and faster oxidation of VOCs in summers. Increases in sensitivity of sulfate to $SO_2$ in the summer are due to an increased photochemical oxidation and stagnation. On the other hand, high temperatures decrease particle-phase ammonium nitrate condensation in summers but the converse is true at other times. Differences in single- and three-summer average (e.g., 2001 vs 2000-2002) sensitivities of $PM_{2.5}$ to $SO_2$ emissions are found to be small (up to ~16%) for 2000-2002 and 2049-2051 with both projected and non-projected emissions (Table 6.3). Spatial distributions of sensitivities of total $PM_{2.5}$ formation to $SO_2$ emissions in 2050 with both projected and non-projected emissions are also examined and found to be similar to 2001 (Figure 6.2, (d)-(f)), showing that the conversion of $SO_2$ to sulfate is only slightly sensitive to climate change. The sensitivity reduction found in some areas is due to precipitation [*Leung and Gustafson*, 2005; *Tagaris, et al.*, 2008].

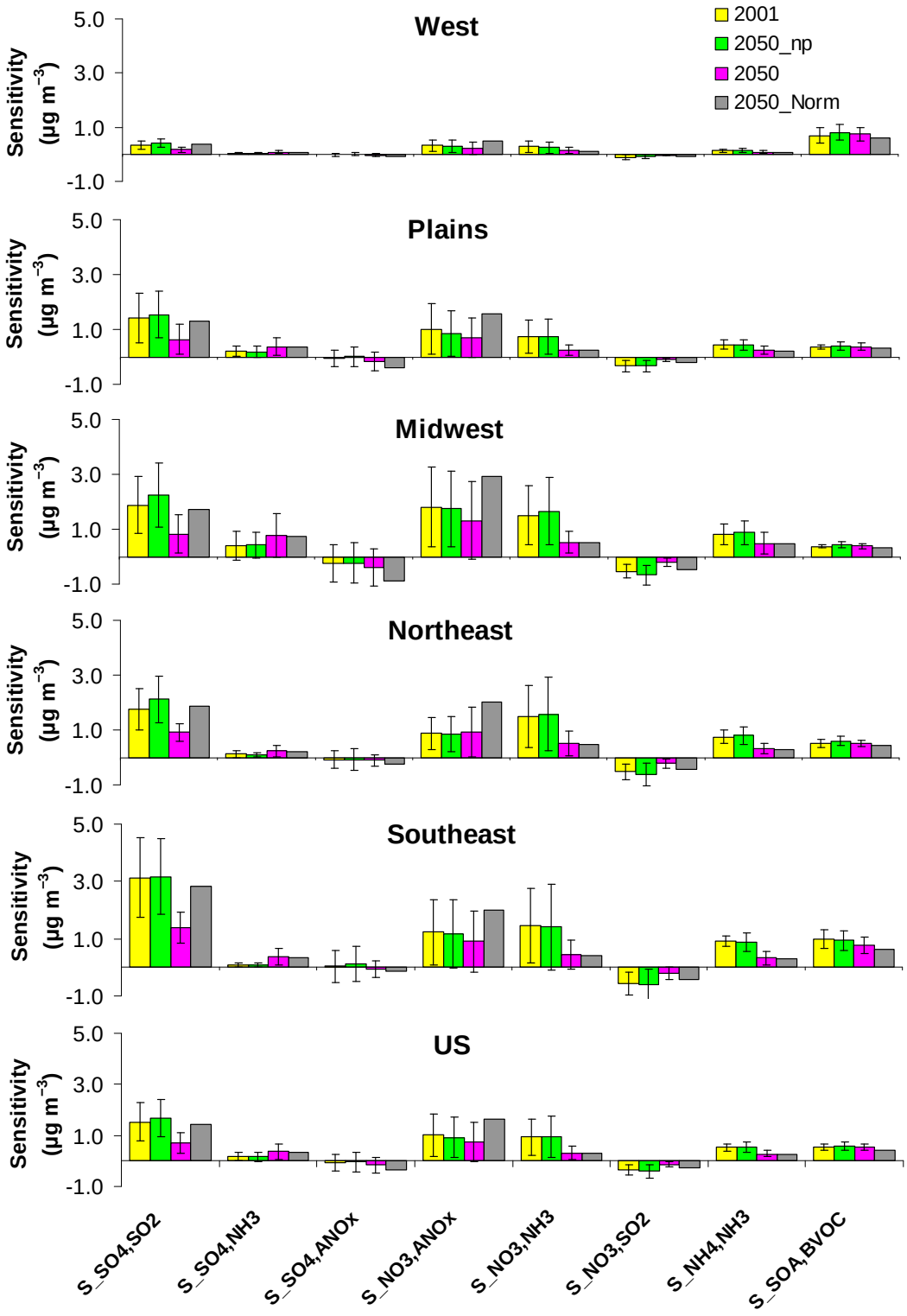


**Figure 6.3: Sensitivities of speciated $PM_{2.5}$ formation to domain-wide precursor emissions for the scenarios of "2001", "2050", "2050_np" and "2050_Norm" (Error bars represent standard deviations of month-to-month variability of sensitivities)**

Contributions of biogenic VOC emissions to $PM_{2.5}$ formation are simulated to be more important in the future because of higher temperatures, resulting in higher biogenic VOC emissions while future emission reductions due to planned controls decrease the sensitivities of $PM_{2.5}$ formation to $SO_2$ and $NO_x$ emissions (Figure 6.3). However, $SO_2$, $NH_3$, anthropogenic $NO_x$ and biogenic VOCs are still found to continue to be important precursors for $PM_{2.5}$ formation in the future with both projected and non-projected emissions. These results also suggest that $PM_{2.5}$ formation is only slightly sensitive to the simulated climate change with the direction of impact ambiguous, and planned controls of $SO_2$ and $NO_x$ emissions will continue to be effective in reducing $PM_{2.5}$ concentrations in the future. Climate–induced changes can slightly increase control effectiveness in some locations ("2050_np" and "2049-2050_np_summers" in Figures 6.1 & 6.3). For ozone and $PM_{2.5}$, the impact of emission controls has a greater effect on sensitivities than simulated climate change between 2001 and 2050.

**Table 6.3: Single- and three-summer average sensitivities of $PM_{2.5}$ to domain-wide $SO_2$ emissions** **Unit: μg $m^{-3}$**

| | Single-summer average | | | Three-summer average | | |
|---|---|---|---|---|---|---|
| | **2001** | **2050_np** | **2050** | **2000-2002** | **2049-2051_np** | **2049-2051** |
| **West** | 0.58 | 0.57 | 0.29 | 0.58 | 0.56 | 0.28 |
| **Plains** | 2.90 | 2.81 | 1.64 | 2.96 | 2.47 | 1.42 |
| **Midwest** | 3.60 | 3.88 | 2.03 | 4.10 | 3.51 | 1.84 |
| **Northeast** | 2.44 | 3.32 | 1.47 | 2.83 | 2.85 | 1.29 |
| **Southeast** | 5.15 | 5.51 | 2.72 | 5.73 | 4.80 | 2.36 |
| **US** | 2.77 | 2.90 | 1.54 | 3.00 | 2.57 | 1.35 |

# CHAPTER 7

# QUANTIFICATION OF IMPACTS OF CLIMATE UNCERAINTIES ON REGIONAL AIR QUALITY *

## 7.1 Introduction

Impacts of future climate change on regional air quality have been investigated for different regions, future climate and future emission scenarios. Due to uncertainties inherent in climate forecasts, the Intergovernmental Panel on Climate Change (IPCC) addresses multiple scenarios associated with different projections of future anthropogenic emissions of greenhouse gases (GHGs) as a qualitative assessment, which are presented in IPCC's Special Report on Emissions Scenarios (SRES) [IPCC, 2001; Nakic´enovic´, 2000]. Hogfere et al. (2004) predict an increase in spatially averaged summertime daily maximum 8-hour $O_3$ concentrations of 4.2 ppb in the 2050s based on the IPCC A2 scenario and assuming anthropogenic precursor emissions and boundary conditions to remain constant. Murazaki and Hess (2006) suggest an increase of up to 12 additional days in the northeast of the continental U.S. each year exceeding daily maximum 8-hr average ozone concentrations of 80 ppb in the decade 2090s compared with 1990s, assuming that future precursor emissions remain at 1990 levels and GHG emissions follow the IPCC A1 scenario.

---

* This chapter is published online in the *Atmospheric Chemistry and Physics Discussions* and under review for publication in the *Atmospheric Chemistry and Physics*. Co-authors are Tagaris Efthimios, Kasemsan Manomaiphiboon, Chien Wang, Jung-Hun Woo, Shan He, Praveen Amar, and Armistead G. Russell.

Racherla and Adams (2006) predict an increase up to 5 ppb in ozone concentrations and a 2%-18% decrease in fine particulate matter levels between 1900s and 2050s assuming climate will follows the IPCC A2 scenario and anthropogenic emissions remain constant. Sanderson et al. (2003) predict a 10-20 ppb increase in ozone concentrations due to a combined effect of changes in vegetation and prescribed IPCC IS92a $CO_2$ emissions in 2090s compared with 1990s.

The objective of this study is to investigate the impact of uncertainties inherent in climate change forecasts on regional air quality predictions over the continental U.S. using multiple climate futures. Given that model inputs (e.g., regional meteorology and precursor emissions) and parameterization/assumption lead to uncertainties in regional downscaling of future climate and air quality modeling (which have been presented elsewhere, e.g., [Bergin, et al., 1999; Gustafson and Leung, 2007; Hanna, et al., 2001; Hanna, et al., 2005; Russell and Dennis, 2000], the purpose of this study is not to specifically forecast future air quality but to quantify the impact of climate uncertainties on regional air quality forecasts, particularly focusing on ground-level ozone and $PM_{2.5}$ (particulate matter with an aerodynamic diameter less than 2.5 μm) due to their adverse health-related effects [*Bernard, et al.*, 2001; *Galizia and Kinney*, 1999; *Johnson and Graham*, 2005]. Of particular interest are the uncertainties associated with the "climate penalty" (increases in levels of air pollutants caused by climate change [*Mickley, et al.*, 2004]) and investigating if uncertainties in climate predictions suggest alternative emission control strategies.

## 7.2. Method

### 7.2.1 Downscaling of Global Climate Models to a Meso-scale Meteorological Model

The meso-scale meteorological model, MM5 (The Fifth-Generation NCAR/Penn State Mesoscale Model) [*Grell, et al.*, 1994; *Seaman*, 2000], is used to downscale outputs from the NASA Goddard Institute of Space Studies (GISS) global climate model (GCM) [*Rind, et al.*, 1999] to regional scale for studying effects of climate on regional air quality in year 2050. 2050 is chosen for this study as a compromise between non-trivial climate modification and a reasonable horizon for regional air quality planning. The GISS-MM5 climate fields, following the IPCC A1B scenario, are used as base-case meteorological fields. Details in GISS global climate simulation and downscaling of GISS global climate to meso-scale climate are described by Mickley et al. (2004) and Leung and Gustafson (2005). IPCC A1B assumes a future world of very rapid economic growth with a balanced case between fossil and non-fossil energy sources [*Nakic´enovic´*, 2000]. For assessing uncertainties in climate projections and their associated effects on regional air quality, it is useful to investigate uncertainties in individual, but covering, climate variables (e.g., temperature, absolute humidity, etc.) in terms of their probabilistic distributions instead of qualitative assessments. In this study, climate fields from MIT's Integrated Global System Model (IGSM) simulations [*Prinn, et al.*, 1999; *Reilly, et al.*, 1999], in the form of probabilistic distributions, are used to quantify uncertainties inherent in forecasts of future changes, and their associated effects on regional air quality.

Temperature and absolute humidity fields from the GISS-MM5 climate are chosen for perturbation as they are strongly correlated with regional ozone and secondary

$PM_{2.5}$ levels [*Nenes, et al.*, 1998; *Sillman and Samson*, 1995; *Strader, et al.*, 1999; *Wise and Comrie*, 2005]. Climate fields used are associated with the, 0.5$^{th}$, 50$^{th}$ and 99.5$^{th}$ percentiles of temperature and humidity from IGSM. Outputs from the two-dimensional 50$^{th}$ percentile IGSM and the base case GISS-MM5 meteorological fields and boundary conditions are used to develop perturbation fields for uncertainty analysis. Details are given in the Appendix C, and briefly described here. Three-dimensional time-dependent variables of the GISS-MM5 climate are decomposed into average and fluctuating terms (equation 7.1).

$$C(y,x,z,t) = \overline{C(y,z,m)} + C'(y,x,z,t) \qquad (7.1)$$

where $C(y,x,z,t)$ is the base case GISS-MM5 climate field (resolved hourly and at a fine scale, three dimensionally; $\overline{C(y,z,m)}$ is the longitudinally and monthly average field, $C'(y,x,z,t)$ is the resulting finer scale fluctuating terms, y is latitude, z is altitude, x is longitude, m is month and t is time (from MM5 simulations). To develop the IGSM-derived fields, the base case average term $\overline{C(y,z,m)}$ is replaced with the 0.5$^{th}$, 50$^{th}$, and 99.5$^{th}$ percentile IGSM fields, and then the fine-scale, fluctuating field is added. The reconstructed meteorological fields are then used as inputs to rerun MM5 in order to get conservative meteorological fields. Fields derived from the 0.5$^{th}$ and 99.5$^{th}$ percentiles climate are defined as "low-extreme" and "high-extreme" scenarios, respectively. The resulting fields were reanalyzed to assure that similar changes in temperature and humidity remained. It is recognized that using MM5 for downscaling may not capture the full range of uncertainty in climate change, though the new fields do capture the

impacts of the temperature and humidity changes, and the precipitation and wind fields are dynamically consistent and responsive to the changes.

### 7.2.2 Emission and Air Quality Modeling

MM5 results are inputs to the Sparse Matrix Operating Kernel for Emissions (SMOKE) (http://www.smoke-model.org/index.cfm, last access: April 28, 2008) for estimating emissions of precursors, and to the Community Multiscale Air Quality Model (CMAQ) [*Byun and Schere*, 2006] for simulating impacts of climate uncertainties on regional air quality. Details of the projections of future emissions and regional air quality modeling approach are given elsewhere [*Tagaris, et al.*, 2007; *Woo, et al.*, 2008], and summarized here. Projections of emissions for Canada, Mexico and the U.S. account for the U.S. Clean Air Interstate Rule (CAIR) controls [*Tagaris, et al.*, 2007; *Woo, et al.*, 2008] and projected growth in population and human activities follow the IPCC A1B scenario in 2050. Although the same projected emission inventories are applied in the uncertainty simulations in 2050, simulated emissions of precursors of pollutants for the three climate scenarios are not identical since emissions (especially, biogenic volatile organic compounds (VOCs)) respond to changes in meteorological fields (e.g., temperature, precipitation, etc.).

The simulation domain in this study covers the continental U.S. as well as parts of Canada and Mexico. For more detailed analysis, the continental U.S is divided into five regions -- West, Plains, Midwest, Northeast and Southeast (Figure 3.1). The highest daily maximum 8-hr average ozone levels, which are often associated with adverse health effects in epidemiologic studies and used for assessing attainment of the U.S. National

Ambient Air Quality Standards (NAAQS) for ozone [*Bernard, et al.*, 2001; *Levy, et al.*, 2001], consistently occur in summer. Three summer months (June, July and August) in the year-2050 are chosen as the target period for studying the impact of climate uncertainties on the average and 4$^{th}$ highest daily maximum 8-h average $O_3$ (4$^{th}$ MDA8h $O_3$) concentrations. The 4$^{th}$ highest value is also chosen as being more stably predicted by chemical transport models than is the maximum in any location. For $PM_{2.5}$, one month from each of the four seasons (i.e., January, April, July and October) in 2050 is chosen for studying the impact of climate uncertainties on annualized $PM_{2.5}$ levels because $PM_{2.5}$ has distinct seasonal variation and has an annual health-based standard (http://www.epa.gov/air/criteria.html, last access: April 28, 2008) .

## 7.3 Results and Discussions

### 7.3.1 Meteorology

The 2050 based case annualized temperatures (average temperatures of January, April, July and October) are predicted to be 0.4-2.4K warmer than 2001, depending on the region, whereas absolute humidity values are simulated to be approximately 9%-14% higher (Table 7.1). On the other hand, annualized temperatures and absolute humidity of the two 2050 extreme scenarios are predicted to change approximately from -0.8 K (low-extreme) to +2.1 K (high-extreme) and -7% (low-extreme) to +19% (high-extreme), respectively, as compared with the 2050 base scenario on a regional basis (Table 7.1). Summer (JJA) temperatures and absolute humidity values are predicted to be higher for the 2050 base case than 2001 climate (Table 7.1). Differences between the high-extreme and base scenarios are found to be larger than differences between the low-extreme and

base scenarios for both temperature and absolute humidity. This reflects that the probability density functions of predicted temperatures and absolute humidity are not normally distributed but have a long right-hand tail in the IGSM outputs (Appendix C, Table C.1) [*Webster, et al.*, 2003]. Annualized precipitation is found to be somewhat different for the three scenarios, with a notable decrease in summer precipitation in the Plains for the high-extreme scenario as compared with the base case (Figure 7.2).

### 7.3.2 Emissions

Both sulfur dioxide ($SO_2$) and nitrogen oxides ($NO_x$) emissions are forecast to be 51% lower in 2050 compared with emissions in 2001, due to planned emission controls. Ammonia ($NH_3$) emissions are simulated to increase by about 7% due to increases in population and related human activities. Total volatile organic compounds (VOC) emissions are predicted to increase by about 2% in 2050 as a net result of increased biogenic VOC emissions and lower anthropogenic VOC emissions for the whole simulation domain [*Tagaris, et al.*, 2007; *Woo, et al.*, 2008]. For the two extreme 2050 scenarios, $SO_2$, $NO_x$ and $NH_3$ emissions are predicted to change very slightly compared with the 2050 base scenario (Table C.2). However, predicted VOC emissions vary significantly as biogenic VOC emissions are much more sensitive to temperature changes than other precursor emissions (Table 7.1). Responses of VOC emissions to the extreme climate scenarios are also found to change spatially. The low-extreme scenario results in an approximately 0-17% decrease in total VOC (= anthropogenic + biogenic VOC) emissions compared with the 2050 base scenario. For the high-extreme scenario, higher biogenic VOC emissions cause an increase of up to about 22% in annualized and 29% in

summer-average total VOC emissions compared with the base case in 2050 on a regional basis (Table 7.1).

### 7.3.3 Summer-average ozone and summertime fourth-highest daily maximum 8-hr average ozone

Summer-average ozone and daily maximum 8-hr average ozone concentrations are found to be slightly sensitive to the extreme climate scenarios in 2050. Differences in summer-average ozone and daily maximum 8-hr average ozone concentrations are about 1-2 ppb between the extreme and base case climate scenarios on a regional basis (Table 7.2). For the peak ozone levels, summertime (JJA) $4^{th}$ MDA8h $O_3$ ($4^{th}$ MDA8h $O_3$ in the summer of 2050) concentrations for the high-extreme scenario are predicted to increase up to 10 ppb as compared with the 2050 base case in urban areas of the Northeast, Midwest and Texas in the continental U.S. (Figure 7.1**).** Such differences are attributed to impacts of meteorological changes, especially temperature, humidity and circulation, on the photochemistry of tropospheric ozone. Sensitivity analyses show that peak ground-level ozone levels and ambient temperatures are positively correlated with each other [*Aw and Kleeman*, 2003; *Baertsch-Ritter, et al.*, 2004; *Dawson, et al.*, 2007; *Menut*, 2003]. Sillman and Samson (1995) found higher temperatures increase decomposition peroxyacyl nitrates (PANs) and generate nitrogen dioxides ($NO_2$) during the daytime and hence cause higher peak ozone levels. Higher absolute humidity (water vapor concentration) increases hydroxyl radicals (OH), resulting in faster oxidation of VOCs, forming peroxy radicals (e.g., $HO_2$, $RO_2$) which react with nitrogen oxides (NO) to form $NO_2$ [*Seinfeld and Pandis*, 1997]. Even when changes in precursor emission are not

considered, concentrations of summertime (JJA) 4$^{th}$ MDA8h $O_3$ in urban are more sensitive to changes in temperatures and humidity due to their higher concentrations of PANs, VOC, $CH_4$ and CO, and are also expected to find a greater simulated impact from the high-extreme scenario than the base case in 2050. Moreover, when temperature-induced increases in VOC emissions (especially biogenic VOC emissions, up to ~29% regionally, Table 7.1) are considered, higher VOC emissions induce more ozone formation in $NO_x$-saturated (or VOC-sensitive) urban areas and the effects of extreme climate scenario are predicted to be more significant. Lower levels of predicted summer precipitation for the high-extreme scenario also lead to more ozone formation and an increase in the differences between the high-extreme and base scenarios in the polluted urban areas (Figure 7.2**)**.

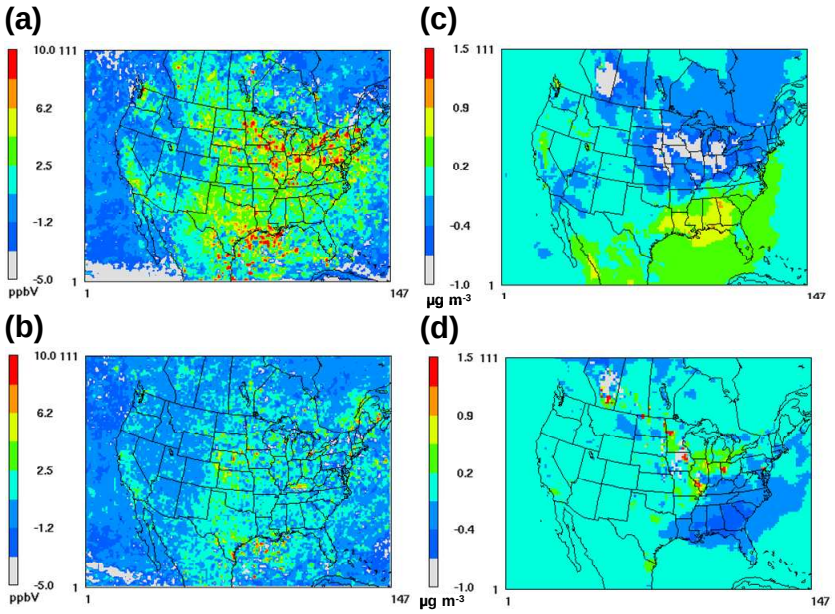


**Figure 7.1: Differences between the 2050 high-extreme & base scenarios (top), and the 2050 low-extreme & base scenarios (bottom) in summertime 4$^{th}$ MDA8h $O_3$ (figures (a) & (b)) and annualized $PM_{2.5}$ (figures (c) & (d)) concentrations, respectively**

**Table 7.1: Differences in summer-average and annualized temperatures (K), absolute humidity (%) and total VOC (=anthropogenic + biogenic VOCs) emissions (%) between the three 2050 climate scenarios and 2001**

| | Summer-average | | | | | | Annualized | | | | | |
|---|---|---|---|---|---|---|---|---|---|---|---|---|
| | **West** | **Plains** | **Midwest** | **Northeast** | **Southeast** | **US** | **West** | **Plains** | **Midwest** | **Northeast** | **Southeast** | **US** |
| **Temperature (K)** | | | | | | | | | | | | |
| Base-2001 | 1.8 | 0.6 | 0.2 | 1.8 | 0.9 | 1.0 | 2.4 | 1.1 | 1.0 | 1.8 | 0.4 | 1.3 |
| Low_extreme-Base | -0.7 | -0.7 | -0.7 | -0.7 | -0.7 | -0.7 | -0.7 | -0.7 | -0.7 | -0.6 | -0.7 | -0.8 |
| High_extreme-Base | 1.9 | 2.1 | 1.8 | 1.7 | 1.6 | 1.9 | 2.1 | 2.1 | 1.8 | 1.7 | 1.7 | 1.9 |
| **Absolute Humidity (%)** | | | | | | | | | | | | |
| Base-2001 | 55.1 | 16.5 | 12.5 | 12.8 | 12.8 | 20.2 | 12.8 | 9.4 | 11.3 | 13.5 | 9.0 | 11.3 |
| Low_extreme-Base | -4.1 | -3.8 | -4.0 | -4.1 | -4.0 | -4.0 | -6.6 | -5.7 | -5.1 | -5.1 | -4.7 | -5.4 |
| High_extreme-Base | 13.3 | 11.6 | 11.3 | 11.6 | 10.8 | 11.7 | 19.1 | 15.7 | 13.6 | 11.9 | 12.6 | 15.1 |
| **Total VOC Emissions (%)** | | | | | | | | | | | | |
| Base-2001 | 16.6 | 3.5 | -16.9 | -3.5 | 5.3 | 2.3 | 11.7 | -9.1 | -26.3 | -19.6 | -16.9 | -11.8 |
| Low_extreme-Base | -17.0 | -10.3 | 0.4 | 0.1 | -6.9 | -8.3 | -13.9 | -9.1 | -1.4 | -2.4 | -4.9 | -7.6 |
| High_extreme-Base | 4.1 | 14.9 | 28.5 | 24.2 | 15.6 | 15.4 | 6.3 | 14.0 | 22.0 | 12.9 | 17.1 | 13.2 |

Differences in concentrations of summertime 4$^{th}$ MDA8h $O_3$ are predicted to be approximately +/-3 ppb between the base case and low-extreme scenario (Figure 7.1). Concentrations of summertime 4$^{th}$ MDA8h $O_3$ are found to be less sensitive to the low-extreme climate scenario than the high-extreme scenario due to smaller differences in meteorological fields between the base case and low-extreme scenario as well as non-linear responses of ozone concentrations to emission changes [*Cohan, et al.,* 2005]. Tagaris et al. (2007) present an about 20% decrease in concentrations of summer-average daily maximum 8-hr ozone and less number of exceedance days of ozone concentrations of 85 ppb in five U.S. cities between 2000-2002 and 2049-2051, mainly due to currently planned emission controls in the future. Here, there is a maximum change of 10 ppb in 4$^{th}$ MDA8h $O_3$ (about one-seventh of the current NAAQS of ozone of 75 ppb) found in 2050 in the extreme climate scenario, which may significantly offset the effectiveness of currently planned emission reductions in urban areas with high concentrations of PANs, VOC, $CH_4$ and CO as well as VOC-sensitive ozone formation regimes.

**Table 7.2: Summer-average ozone concentrations (in ppb) for the three climate scenarios for the five regions and the U.S.**

| Ozone (ppb) | Summer-average ozone | | | Summer-average maximum 8-hr average ozone | | |
|---|---|---|---|---|---|---|
| | **Low-extreme** | **base** | **High-extreme** | **Low-extreme** | **base** | **High-extreme** |
| **West** | 41.7 | 41.8 | 41.6 | 50.3 | 50.3 | 50.5 |
| **Plains** | 40.4 | 40.8 | 41.8 | 48.5 | 49.3 | 50.9 |
| **Midwest** | 35.4 | 35.8 | 36.7 | 44.9 | 46.0 | 47.2 |
| **Northeast** | 37.1 | 37.2 | 37.3 | 44.0 | 44.9 | 45.0 |
| **Southeast** | 42.6 | 42.9 | 43.7 | 52.2 | 52.7 | 54.7 |
| **US** | 39.9 | 40.3 | 40.9 | 48.5 | 49.2 | 50.3 |

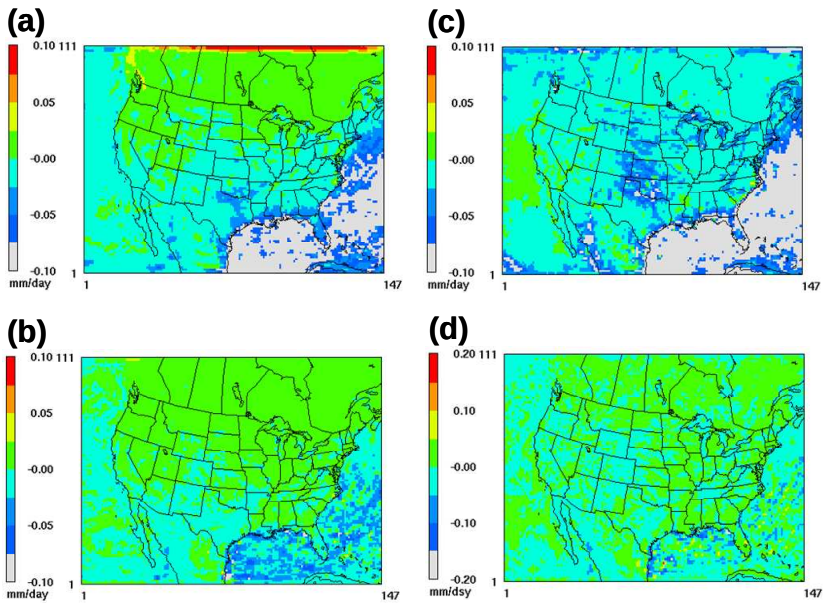


**Figure 7.2: Spatial distribution of difference in precipitation (mm/day) in 2050 for (a) Annualized (high-extreme – base); (b) Annualized (base – low-extreme); (c) Summer-averaged (high-extreme – base); (d) Summer-averaged (base – low-extreme)**

### 7.3.4 Annualized $PM_{2.5}$

$PM_{2.5}$ levels are influenced by the changes between the climate scenarios in several ways. Higher temperatures favor semi-volatile compounds (e.g., secondary organic aerosols (SOAs) and ammonium nitrate ($NH_4NO_3$)) to remain in the gas phase. On the other hand, increases in temperatures and humidity result in higher emissions of SOA precursors and faster oxidation of $SO_2$, $NO_x$ and VOCs, increasing formation of condensable compounds, such as sulfate, nitrate and semi-volatile organic species (SVOCs). Further, changes in precipitation can have a dramatic effect on frequency of washout and fine particle concentrations [*Racherla and Adams*, 2006]. Overall, the net effects of different mechanisms of $PM_{2.5}$ production and loss result in a -1.0 to +1.5 µg

$m^{-3}$ difference in annualized $PM_{2.5}$ levels (average of daily $PM_{2.5}$ levels of January, April, July and October) between the extreme and base scenarios in 2050 (Figure 7.1). Larger differences in $PM_{2.5}$ levels between the extreme and base scenarios are found in the Southeast and Midwest of the continental U.S. due to higher $PM_{2.5}$ precursor emissions (e.g., anthropogenic $SO_2$, $NO_x$, VOC, etc.) in those areas. The changes in $PM_{2.5}$ levels attributed to the extreme climate scenarios are dominated by sulfate and nitrate since SOA formation is not fully captured in current regional air quality models [*Morris, et al.*, 2006; *Pun and Seigneur*, 2007].

Impacts of climate uncertainties on $PM_{2.5}$ concentrations also show a seasonal trend. Monthly-average $PM_{2.5}$ concentrations are predicted to be lower in January but slightly higher in July for the high-extreme scenario compared with the 2050 base case (Table 7.3); this is mainly because temperatures change the partitioning of semi-volatile compounds between the gas-phase and particle-phase. Higher temperature and humidity increase sulfate aerosol formation due to faster gas- and aqueous-phase oxidation rates of $SO_2$. Rae et al. (2007) have shown that increases in temperature and changes in oxidant concentrations are simulated to decrease 1% of Aitken-mode sulfate aerosols but increase of 9.2% of accumulation-mode sulfate in 2100 assuming climate and emission-induced oxidant levels will follow the IPCC SRES A2 scenario. Total sulfate concentrations are expected to increase by 6.8% in 2100 compared with 1990 [*Rae, et al.*, 2007]. Effects of climate on nitrate are more complicated than sulfate due to high vapor pressure for particle-phase ammonium nitrate [*Seinfeld and Pandis*, 1997]. Aw and Kleeman (2003) present that nitrate aerosol may slightly increase with cool temperature (<290K) but decrease with hot temperature (>290K) as temperature increases. The combined effects of

changes in sulfate and nitrates show that the high-extreme climate scenario with associated increases in temperatures in January induces more nitrates to be in the gas-phase lowering $PM_{2.5}$ concentrations. The seasonal trend is reversed in the low-extreme scenario. Wise and Comrie (2005) show that, from a long-term statistical analysis, PM is not as weather-dependent as ozone in the southwestern U.S. since low precipitation is found in the studying region. The results in this study also show that annualized $PM_{2.5}$ levels are not as sensitive as concentrations of summertime peak ozone with respect to the extreme climate scenarios examined since one of the main removal mechanisms of $PM_{2.5}$, precipitation scavenging, is found to slightly affect annualized $PM_{2.5}$ levels between the extreme climate scenarios (Figure 7.2). Our previous study shows that annual average $PM_{2.5}$ levels are predicted to decrease by about 23% as a combined effects of future climate change and CAIR emission controls [*Tagaris, et al.*, 2007]. The results here imply that future emission controls will still be effective with respect to the extreme climate scenarios if precipitation is only slightly affected.

**Table 7.3: $PM_{2.5}$ concentrations (in µg $m^{-3}$) for the three climate scenarios in January, April, July and October of 2050 for the five regions and U.S.**

| | January | | | April | | | July | | | October | | |
|---|---|---|---|---|---|---|---|---|---|---|---|---|
| | **Low-extreme** | **Base** | **High-extreme** | **Low-extreme** | **Base** | **High-extreme** | **Low-extreme** | **Base** | **High-extreme** | **Low-extreme** | **Base** | **High-extreme** |
| **West** | 3.17 | 3.13 | 3.05 | 2.43 | 2.44 | 2.49 | 2.38 | 2.41 | 2.57 | 3.29 | 3.30 | 3.42 |
| **Plains** | 7.23 | 6.96 | 6.50 | 3.39 | 3.37 | 3.42 | 4.26 | 4.31 | 4.73 | 4.18 | 4.21 | 4.45 |
| **Midwest** | 14.53 | 13.53 | 12.21 | 5.80 | 5.78 | 5.79 | 6.70 | 6.65 | 6.72 | 6.39 | 6.38 | 6.64 |
| **Northeast** | 9.94 | 9.62 | 8.70 | 4.40 | 4.36 | 4.32 | 3.54 | 3.56 | 3.76 | 5.25 | 5.23 | 5.48 |
| **Southeast** | 10.46 | 10.23 | 9.83 | 5.68 | 5.69 | 5.85 | 5.65 | 5.62 | 5.78 | 6.90 | 7.08 | 7.72 |
| **US** | 8.20 | 7.86 | 7.32 | 3.99 | 3.98 | 4.03 | 4.39 | 4.40 | 4.65 | 4.83 | 4.87 | 5.14 |

### 7.4 Response of Air Quality to Emission Controls under Extreme Climate Scenarios

In addition to simulating how the alternative extreme scenarios impact pollutant levels, we also investigate the responses of ozone and $PM_{2.5}$ levels to emission controls under the extreme climate scenarios. CMAQ with the Decoupled Direct Method-3D (DDM-3D) [*Dunker*, 1984; *Dunker, et al.*, 2002; *Yang, et al.*, 1997], is used to quantify sensitivities of ozone and $PM_{2.5}$ to precursor emissions. First-order sensitivities ($S_{i,j}$) of pollutant concentration $i$ ($C_i$) (i.e. ozone and $PM_{2.5}$) to source emissions $j$ ($E_j$) (i.e., anthropogenic VOC, anthropogenic $NO_x$ and total $SO_2$ emissions) are defined as [*Yang, et al.*, 1997]:

$$S_{i,j} = E_j \frac{\partial C_i}{\partial E_j}$$

First-order sensitivities represent the locally linear responses of pollutant concentrations to emission changes and have the same units as the concentrations. Sensitivities of summertime 4$^{th}$ MDA8h $O_3$ to anthropogenic $NO_x$ emissions ($S_{4thMDA8hO3,\ ANOx}$) are predicted to slightly decrease for the low-extreme scenario but increase for the high-extreme scenario as compared with the base case in 2050. The differences are mainly attributed to the climate effects on biogenic VOC emissions and photochemistry. The effects of the extreme climate scenarios on sensitivities of summertime 4$^{th}$ MDA8h $O_3$ to anthropogenic VOC emissions ($S_{4thMDA8hO3,\ AVOC}$) are predicted to be small. For the responses of $PM_{2.5}$ to emission changes under the extreme climate scenarios, sensitivities of annualized $PM_{2.5}$ to $SO_2$ emissions ($S_{PM2.5,\ SO2}$) are predicted to slightly increase for the high-extreme scenario because of higher temperature, humidity, decreased rainfall in

some regions, and faster oxidation of precursors as compared with the base scenario. Higher temperatures for the high-extreme scenario favor particulate $NH_4NO_3$ to dissociate to its gas phase precursors and cause slight decreases in sensitivities of annualized $PM_{2.5}$ concentrations to anthropogenic $NO_x$ emissions ($S_{PM2.5, ANOx}$) (Figure 7.3). Overall, on a regional basis, the effectiveness of $NO_x$ and $SO_2$ emission controls for reducing peak ozone and $PM_{2.5}$ levels changes little, though climate-driven increases in extreme ozone levels may require additional controls to reach applicable air quality standards.

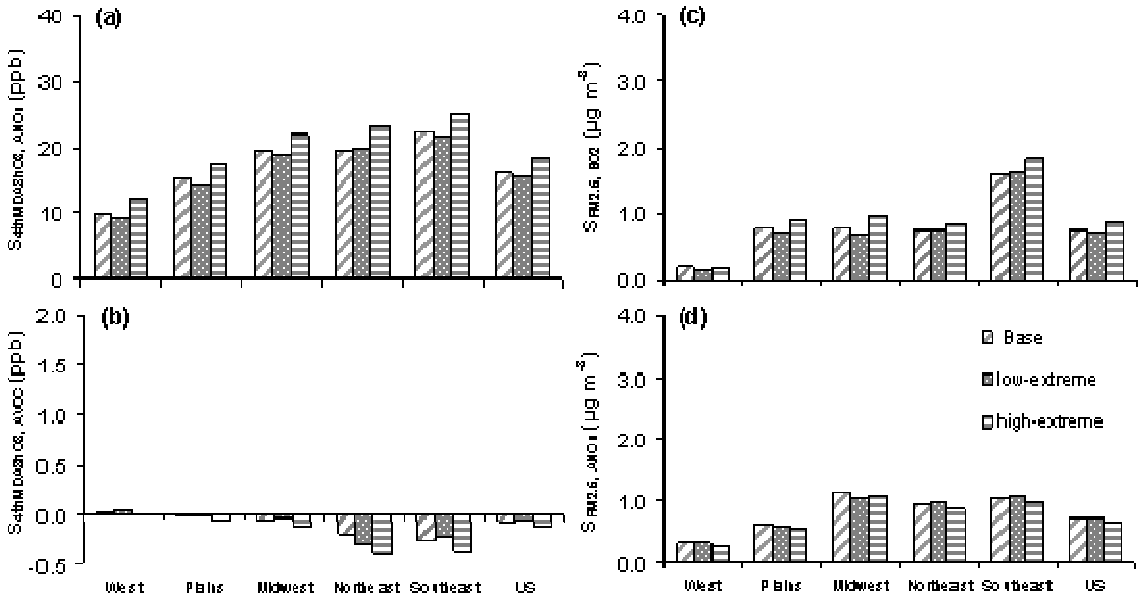


**Figure 7.3: Sensitivities of 4th MDA8h $O_3$ to (a) anthropogenic $NO_x$ ($S_{4thMDA8hO3, ANOx}$) and (b) anthropogenic VOC ($S_{4thMDA8hO3, AVOC}$) as well as sensitivities of annualized $PM_{2.5}$ to (c) anthropogenic $SO_2$ ($S_{PM2.5, SO2}$) and (d) anthropogenic $NO_x$ ($S_{PM2.5, ANOx}$) in 2001 and the 2050 base and extreme scenarios for the five regions and U.S.**

## 7.5 Conclusions

Uncertainties associated with simulations of the extreme climate scenarios are found to have a rather moderate effect on predicted emissions of VOC and concentrations of fourth-highest daily maximum 8-hr average ozone in year 2050. Differences in concentrations of fourth-highest daily maximum 8-hr average ozone between the extreme climate scenarios and base case are found up to 10 ppb (about one-seventh of the current ozone standards) in some polluted urban areas due to higher temperature, absolute humidity and VOC emissions, though the change in summer-average ozone is minimal (~1 ppb). Differences between the extreme and base scenarios in annualized $PM_{2.5}$ levels are predicted to range between -1.0 and +1.5 $\mu g\ m^{-3}$. Future annualized $PM_{2.5}$ is predicted to be less sensitive to the extreme climate scenarios than summertime fourth-highest daily maximum 8-hr average ozone since precipitation scavenging is not significantly changed with the extreme climate scenarios. Planned controls for decreasing regional ozone and $PM_{2.5}$ will continue to be effective in the future under the extreme climate scenarios. However, the impact of climate uncertainties may be substantial in some urban areas and should be included in assessing future regional air quality and emission control requirements.

# CHAPTER 8

# CURRENT AND FUTURE LINKED RESPONSES OF OZONE AND $PM_{2.5}$ TO EMISSION CONTROLS *

## 8.1 Introduction

The formation of ground-level ozone and $PM_{2.5}$ is strongly coupled because of their common sources, secondary nature and interactions of their precursors [*Lamarque, et al.*, 2005]. Changes in both climate and precursor emissions are expected to alter characteristics of ozone and secondary $PM_{2.5}$ (e.g., ammonium sulfate ($(NH_4)_2SO_4$), ammonium nitrate ($NH_4NO_3$), secondary organic aerosols (SOAs), etc.) formation and their interdependencies. Due to interactions between precursors of ozone and secondary $PM_{2.5}$, control measures for one pollutant may lead to increases in others, and reductions in one location may be accompanied by increases in others. For example, decreases in anthropogenic nitrogen oxides ($NO_x$) emissions reduce regional ozone maxima and $PM_{2.5}$ concentrations, but may increase concentrations of ground-level ozone in $NO_x$-rich areas. Likewise, reductions in sulfur dioxide ($SO_2$) emissions decrease sulfate levels but induce more nitrate formation [*Liao, et al.*, 2007]. Unger et al. (2006) suggest that increases in emissions of ozone precursors will enhance sulfate formation up to 20% on a global scale in 2030 climate [*Unger, et al.*, 2006].

---

* This chapter is accepted for publication in the *Environmental Science and Technology*. Co-authors are Efthimios Tagaris, Kasemsan Manomaiphiboon, Sergey L. Napolenok, Jung-Hun Woo, Shan He, Praveen Amar, and Armistead G. Russell.

For evaluating policy options it is important to investigate the interdependencies between ozone and $PM_{2.5}$ formation and how those pollutants respond to emission controls currently and as conditions change in the future. Such information can be used to evaluate how controls developed for one purpose, e.g., meeting an air quality standard for one pollutant metric, might influence levels for other outcomes, e.g., overall health and welfare. Here we examine daily responses of ozone and $PM_{2.5}$ to emission changes for current and future scenarios, including effects of climate change and currently planned emission controls, and investigate their correlations.

Two frequently used indicators of air quality are the daily maximum 8-hr average ozone ($M8hO_3$) and 24-hr average $PM_{2.5}$. For both of these pollutants, National Ambient Air Quality Standards (NAAQS) have been established to protect against adverse human health effects [*Burnett, et al.,* 1997; *Lippmann,* 1993]. Five cities in the continental U.S. – Atlanta, Chicago, Huston, Los Angeles and New York (Appendix D, Figure D.1) – were chosen in this study because each experience elevated ozone and $PM_{2.5}$ levels. Atlanta, Chicago, Los Angeles and New York also have 24-hr average $PM_{2.5}$ levels over the 35 $\mu g\ m^{-3}$ NAAQS (http://www.epa.gov/oar/oaqps/greenbk/, last access: April 28, 2008). Two years are chosen for this study: a "current" year, 2001 and "future", 2050. 2050 provides an opportunity to assess the combined effects of planned emission controls and climate change. Changes in sensitivities of $M8hO_3$ and 24-hr average $PM_{2.5}$ to emissions are primarily due to planned emission changes between 2001 and 2050 as previous results suggest that the effects of emission controls are more significant than climate change alone [*Liao, et al.,* 2007; *Tagaris, et al.,* 2007].

## 8.2 Method

Quantifying sensitivities of air pollutant concentrations is done using EPA's Models-3 regional air quality system, applied as detailed elsewhere [*Liao, et al.*, 2007; *Tagaris, et al.*, 2007], and described briefly here. The Fifth-Generation NCAR/Penn State Mesoscale meteorological Model (MM5) is used to downscale results (i.e., increase the spatial and temporal resolution over the chosen modeling domain) from NASA's Goddard Institute of Space Studies (GISS) [*Rind, et al.*, 1999] global climate model results for years 2001 and 2050 [*Leung and Gustafson*, 2005; *Mickley, et al.*, 2004]. GISS results utilized are for the Intergovernmental Panel on Climate Change (IPCC) A1B scenario, which is generally viewed as a midrange case that assumes a future world of rapid economic growth with a balance between fossil and non-fossil energy sources [*IPCC*, 2001]. Planned controls, e.g., the Clean Air Interstate Rule (CAIR) and others in the U.S. [*Houyoux*, 2004] as well as emission changes in Canada and Mexico [*Woo, et al.*, 2008] are used to forecast emissions to 2020. The Integrated Model to Assess the Global Environment (IMAGE) model (http://www.mnp.nl/image, last access: April 28, 2008) is used to forecast emissions from 2020 to 2050. Emissions are processed by the Sparse Matrix Operator Kernel for Emissions (SMOKE) system version 2.1 (http://www.smoke-model.org/index.cfm, last access: April 28, 2008). Anthropogenic $SO_2$ and $NO_x$ emissions are projected to decrease 51% and 55%, respectively, between 2001 and 2050 over the simulation domain due to currently planned emission controls (Appendix D, Table D.1) [*Woo, et al.*, 2008]. Anthropogenic volatile organic compound (VOC) emissions are predicted to decrease about 38% though total VOC emissions are projected to increase by about 2% as biogenic VOC emissions increase (Table D.1). Ammonia

($NH_3$) emissions are predicted to increase by 7% due to growth in human activities [*Tagaris, et al.*, 2007; *Woo, et al.*, 2008].

The Community Multiscale Air Quality Model (CMAQ) [*Byun and Schere*, 2006] version 4.3 with the SAPRC-99 chemical mechanism and decoupled direct method 3D (DDM-3D) is used to simulate sensitivities of ozone and $PM_{2.5}$ to precursor emissions, including anthropogenic $NO_x$ and VOC, $NH_3$ and $SO_2$ emissions, over the domain covered the continental US and parts of Canada and Mexico in 2001 and 2050. A uniform grid of 36-by-36 km horizontal cells with 9 vertical layers is employed in the simulations (Appendix D, Figure D.1). CMAQ with DDM-3D directly calculates the semi-normalized first-order sensitivities of both gas- and condensed-phase pollutants to precursor emissions [*Cohan, et al.*, 2005; *Napelenok, et al.*, 2006], i.e., the semi-normalized first-order sensitivity ($S_{i,j}$) of pollutant concentration $i$ ($C_i$) to source emissions $j$ ($E_j$) is determined as:

$$S_{i,j} = E_j \frac{\partial C_i}{\partial E_j}$$

The sensitivities, as presented here, have the same units as the corresponding pollutants. These sensitivities are local (accurate for small changes in emissions) and represent how pollutant concentrations respond to precursor emission changes as if the systems were linear. It is recognized that the system is not linear, but extensive testing suggests the first-order (linear) response is accurate up to emission changes of the order of 30% for ozone and 20%-50% for $PM_{2.5}$ (depending on species) [*Cohan, et al.*, 2005; *Napelenok, et al.*, 2006]. Recognizing that changes by percent reductions in a source are more policy-

relevant, here we show the daily sensitivities of ozone and $PM_{2.5}$ to 1% changes in emissions for the two years studied. Sensitivities of ozone and $PM_{2.5}$ are examined for the grid over the city center where population densities are typically highest, and also at the location of the regional ozone maximum (i.e., maximum values among five-by-five grid cells around the city center, Figure D.1). While the ozone response at the city center has increased utility in health-based analyses (city-center monitors are often used in health effects studies, and generally are associated with high population densities), the regional maximum is used in design of strategies to meet the ozone NAAQS.

## 8.3 Results and Discussion

### 8.3.1 Daily Linked Responses of Daily Maximum 8-hr Average Ozone and 24-hr Average $PM_{2.5}$ to Anthropogenic $NO_x$ and VOC Emissions

The response (or sensitivity, S) of daily maximum 8-h $O_3$ to $NO_x$ emissions ($S_{MDA8hO3,ANOx}$) is typically correlated with the corresponding daily maximum 8-h $O_3$ levels (Figure 8.1; Appendix D, Table D.2 provides correlation statistics) when viewed on a daily basis for the years studied. Reductions in anthropogenic $NO_x$ emissions are usually effective in decreasing daily maximum 8-h $O_3$ concentrations on days of higher $O_3$, both at the city center as well as at the regional maximum (Figure 8.1). On the other hand, reductions in anthropogenic $NO_x$ emissions are expected to increase daily maximum 8-h $O_3$ concentrations on days less conducive to ozone formation, a response found more at the city center (where, depending on the city, 215-356 days have this adverse response, Table 8.1) than for the regional daily maximum (where 97-234 days have a negative sensitivity). The forecast 55% reduction in domain-wide anthropogenic

$NO_x$ emissions between 2001 and 2050 is shown to make the formation of moderate-level ozone more $NO_x$-limited and the $S_{MDA8hO3,ANOx}$ more positive in 2050 as compared with 2001 (Figure 8.1). Further, the highest daily maximum 8-h $O_3$ levels are reduced between 2001 and 2050, though levels are simulated to increase on low-ozone days (Figure 8.1). Daily maximum 8-h $O_3$ levels and $S_{MDA8hO3,ANOx}$ are predicted to have a higher correlation in 2050 ($0.53<r^2<0.81$, depending upon city) than 2001 ($0.0<r^2<0.77$) (Figure 8.1 and Table D.2), and the slopes are typically higher as well. Slopes in 2001 range from 0.0 to 0.006 (ppb/%)/ppb, and increase to 0.005 to 0.010 (ppb/%)/ppb in 2050, showing that $NO_x$ controls are more efficient in reducing daily maximum 8-h $O_3$ concentrations in 2050 than 2001 for the five cities (Table 8.1) and there are fewer cases where ozone has a negative response. Based on a 1% change in anthropogenic $NO_x$ emissions in 2001, $S_{MDA8hO3,ANOx}$ is simulated to vary from about -0.3 to +0.4 ppb depending on prevailing $NO_x$ abundance in the five cities (Figures 8.1 & 8.2). Sensitivities of daily maximum 8-h $O_3$ to VOC ($S_{MDA8hO3,AVOC}$) are typically positive (though often small), and negatively correlated with $NO_x$ sensitivities (Appendix D, Figure D.2). VOC sensitivities are greater in 2001 versus 2050. While reductions in anthropogenic VOC emissions always decrease daily maximum 8-h $O_3$ levels in 2001 there are a few days where there is a slightly negative response in 2050 (Figures 8.1 & Appendix D, Figure D.2). For regional maximum daily maximum 8-h $O_3$ in 2001, $NO_x$-sensitive environments become "$NO_x$-starved" and the correlation between the $S_{MDA8hO3,ANOx}$ and daily maximum 8-h $O_3$ concentrations are stronger ($0.1<r^2<0.84$) and slope also increases for four of the five cities as compared with city-center M8h$O_3$ (Figure D.2).

**Table 8.1: Number of days with positive[a] and negative[b] $S_{MDA8hO3,ANOx}$ and daily maximum 8-h ozone over concentration of 85 ppb in 2001 and 2050 for the five cities**

| | 2001 City Center ( +/− ) (number of days over 85 ppb) | 2050 City Center ( +/− ) (number of days over 85 ppb) | 2001 ( +/− ) Regional Maximum (number of days over 85 ppb) |
|---|---|---|---|
| Atlanta | 144 / 215 (66) | 276 / 83 (0) | 224 / 135 (87) |
| Chicago | 31 / 328 (19) | 131 / 218 (6) | 188 / 171 (28) |
| Houston | 117 / 242 (35) | 294 / 65 (3) | 262 / 97 (58) |
| Los Angeles | 87 / 272 (9) | 285 / 74 (1) | 125 / 234 (56) |
| New York | 3 / 356 (0) | 79 / 280 (0) | 173 / 186 (31) |

[a] Positive sensitivity (+): Reductions in anthropogenic $NO_x$ emissions decrease M8h $O_2$ levels
[b] Negative sensitivity (-): Reductions in anthropogenic $NO_x$ emissions increase M8h $O_2$ levels
Note: The first seven days of each year are excluded to minimize the impacts of initial concentrations, leaving 359 days for analysis.

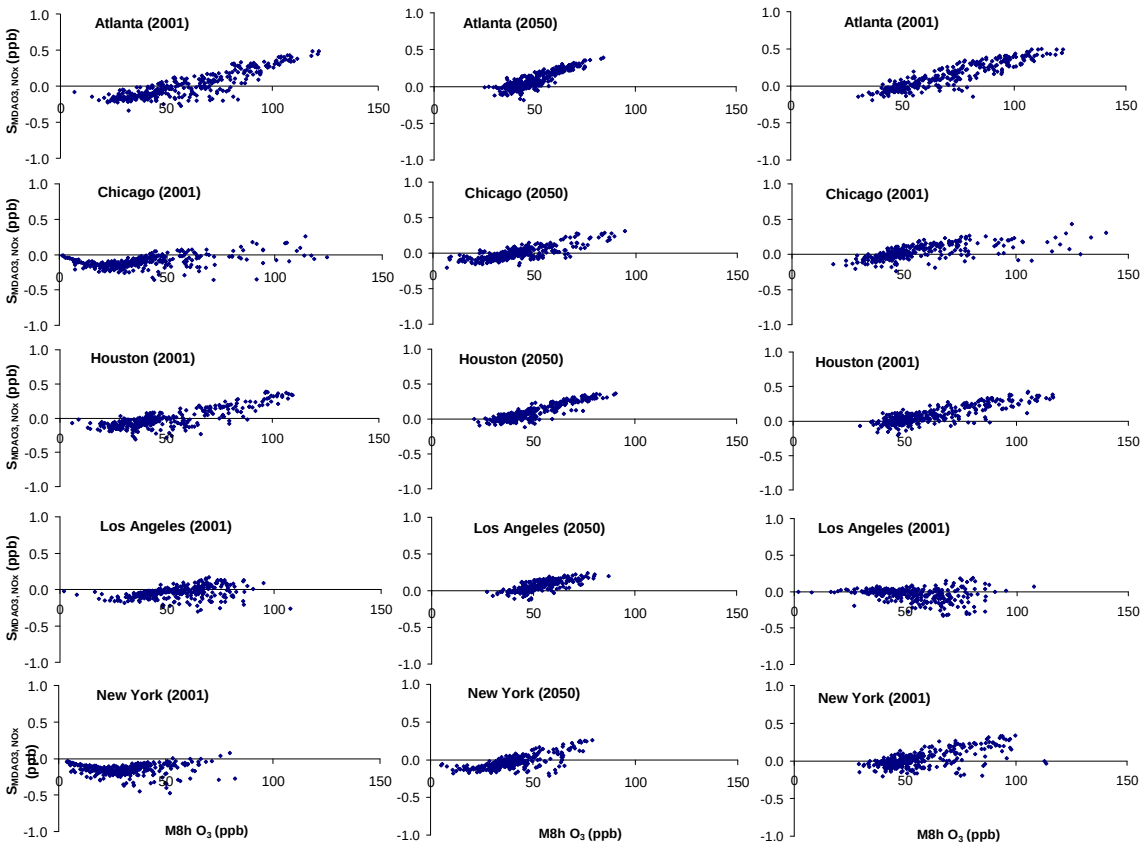


**Figure 8.1: Daily sensitivities of daily maximum 8-h $O_3$ to anthropogenic $NO_x$ emissions ($S_{MDA8hO3,ANOx}$) (in ppb, Y-axis) (based on a 1% change in emissions) versus daily maximum 8-h $O_3$ concentrations (in ppb, X-axis). Shown are the daily maximum 8-h $O_3$ and the corresponding (same day/time, same location) sensitivities in 2001 for city centers and regional maximum values (defined as the maximum over a 5x5 grid around the city) and in 2050 for city centers**

Sensitivities of 24-hr average $PM_{2.5}$ to anthropogenic $NO_x$ emissions ($S_{PM2.5, ANOx}$) are predicted to range from about 0 to 0.1 µg $m^{-3}$ in 2001 and 2050 based on 1% change in anthropogenic $NO_x$ emissions. Reductions in anthropogenic $NO_x$ cause decreases in nitrate but slight increases in sulfate formation [*Liao, et al.*, 2007]. The net effects show a

positive $S_{PM2.5,ANOx}$ in 2001 and 2050 (Figure 8.2) This suggests that reductions in anthropogenic $NO_x$ emissions are expected to continue to be effective in deceasing 24-hr $PM_{2.5}$ (Figure 8.2), and such controls will tend to be more effective and positive for reducing ozone in the future.

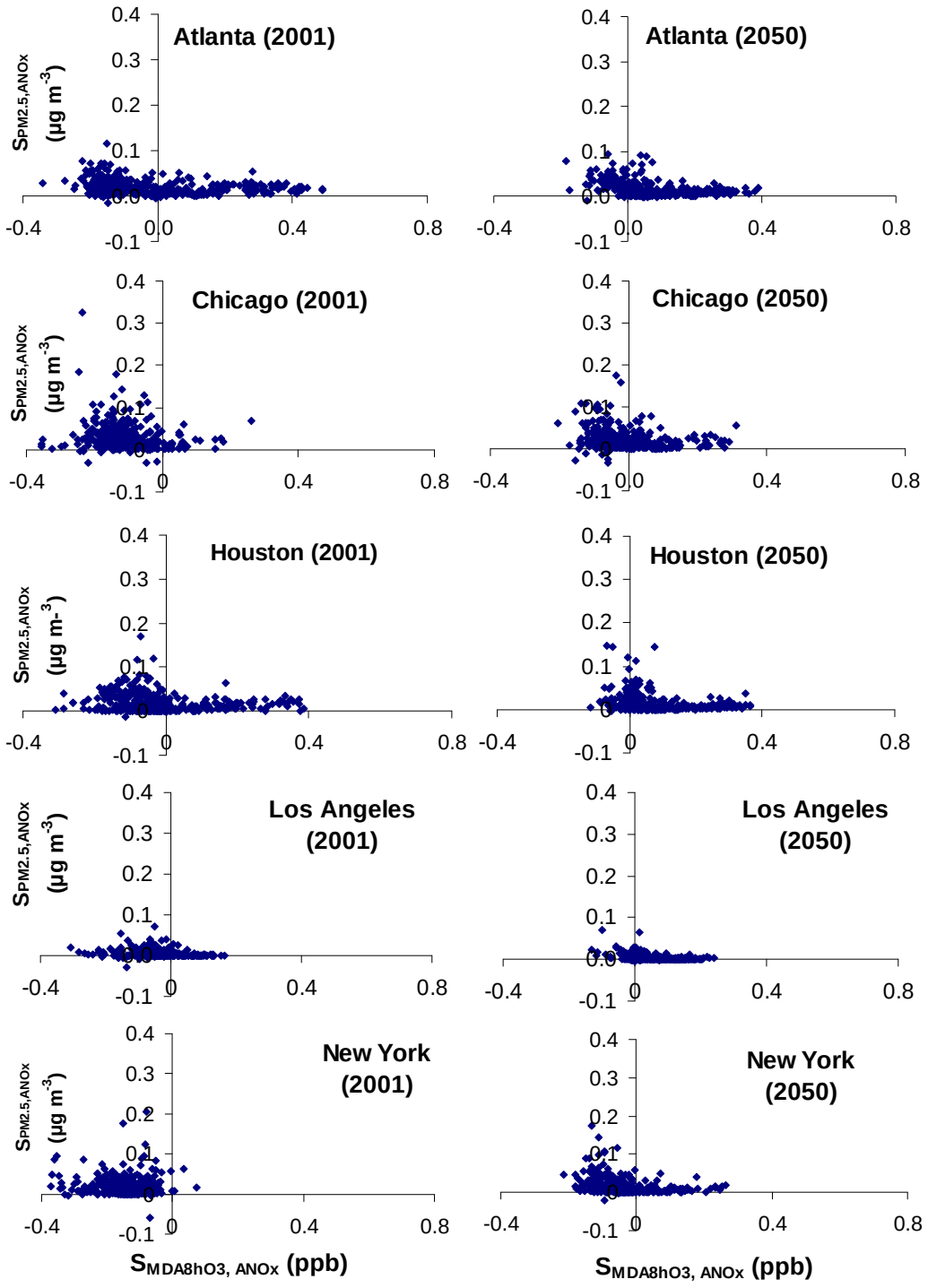


**Figure 8.2: Daily sensitivities of 24-hr $PM_{2.5}$ ($S_{PM2.5,ANOx}$, in µg $m^{-3}$, Y-axis) and daily maximum 8-h $O_3$to anthropogenic $NO_x$ emissions ($S_{MDA8h\ O3,ANOx}$, in ppb, X-axis) in 2001 and 2050 for city centers (each shown as response to a 1% change in anthropogenic $NO_x$ emissions)**

Ozone and PM responses to VOC controls are likewise linked. Sensitivities of daily maximum 8-h $O_3$ concentrations to anthropogenic VOC emissions ($S_{MDA8hO3, AVOC}$) range from about 0 to 0.2 ppb while sensitivities of 24-hr average $PM_{2.5}$ concentrations to anthropogenic VOC emissions ($S_{PM2.5, AVOC}$) are simulated to vary from -0.005 μg $m^{-3}$ to +0.02 μg $m^{-3}$ based on a 1% change in anthropogenic VOC emissions in 2001 (Figure 8.3). Positive sensitivities of daily maximum 8-h $O_3$ to anthropogenic VOC emissions imply that reductions in anthropogenic VOC emissions are effective in decreasing daily maximum 8-h $O_3$ levels. On the other hand, there are a few cases where sensitivities of 24-hr $PM_{2.5}$ to anthropogenic VOC emissions suggest that reductions in anthropogenic VOC emissions may slightly increase 24-hr $PM_{2.5}$ levels. This is attributed to interdependencies between anthropogenic VOCs, radicals, $SO_2$ and $NO_x$ levels in the ambient air [*Napelenok, et al.*, 2006]. Reductions in anthropogenic VOC emissions decrease secondary organic aerosol (SOA) formation but can increase OH radical levels, more rapidly oxidizing $SO_2$ and $NO_x$ which can increase $PM_{2.5}$ concentrations. In 2050, sensitivities of MDA8h $O_3$ and 24-hr average $PM_{2.5}$ to anthropogenic VOC emissions are predicted to decrease mainly due to planned reductions in anthropogenic VOC emissions between 2001 and 2050 (Figure 8.3). It is important to note that current air quality models do not fully capture SOA formation [*Morris, et al.*, 2006], and the actual $PM_{2.5}$ sensitivities are likely to be more positive than simulated, though they highlight the linkage between the responses of $O_3$ and $PM_{2.5}$ to anthropogenic VOC emissions.

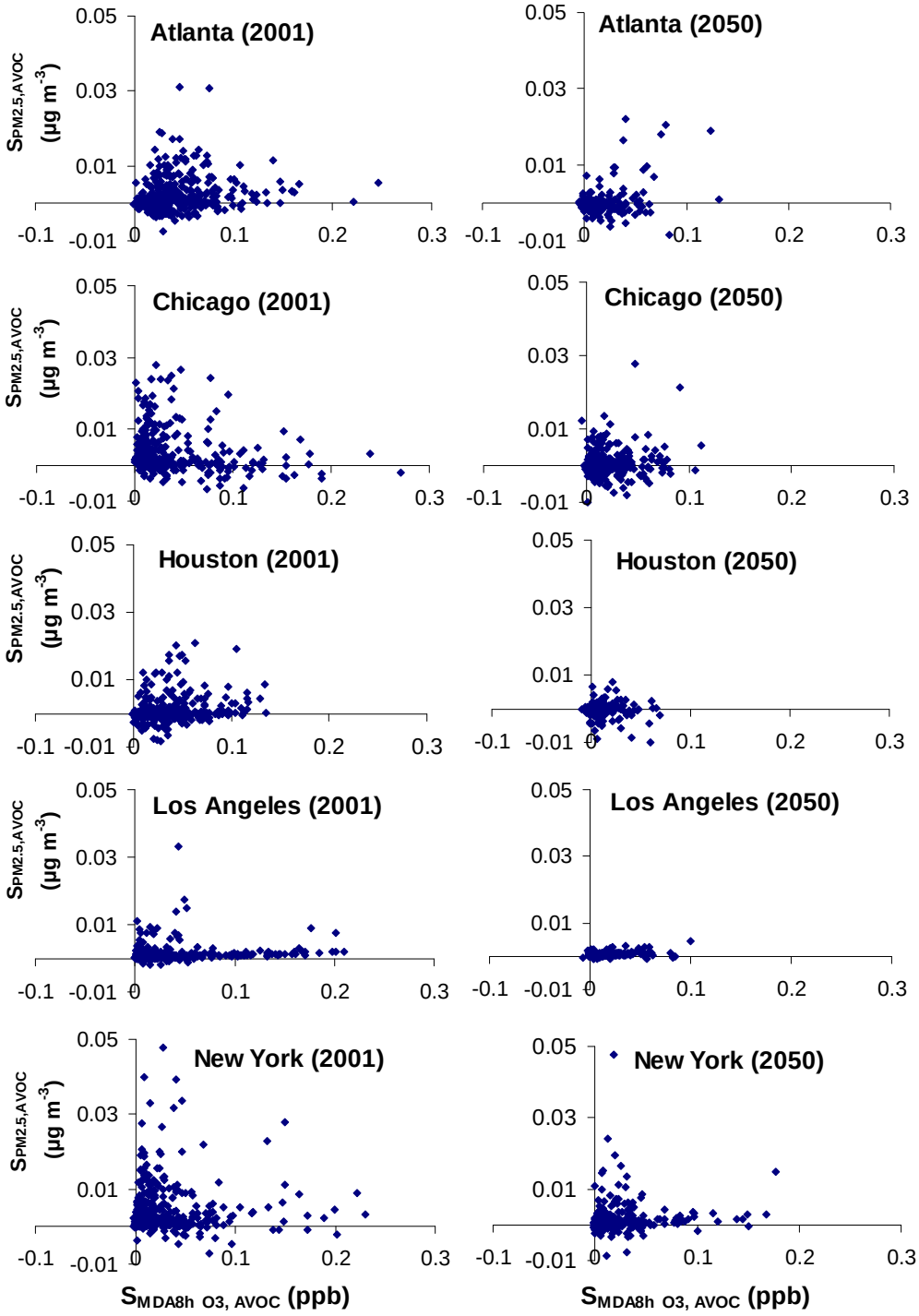


**Figure 8.3: Daily sensitivities of 24-hr $PM_{2.5}$ ($S_{PM2.5,AVOC}$, in µg $m^{-3}$, Y-axis) and daily maximum 8-h $O_3$ to anthropogenic VOC emissions ($S_{MDA8h\ O3,\ AVOC}$, in ppb, X-axis) in 2001 and 2050 for city centers (each shown as response to a 1% change in anthropogenic VOC emissions)**

### 8.3.2 Linked Responses of Sulfate and Nitrate to $NH_3$, $SO_2$, and $NO_x$ Emissions

Sensitivities of nitrate to $NH_3$ emissions ($S_{NO3, NH3}$) (up to about 0.1 μg $m^{-3}$ based on 1% change in $NH_3$ emissions) are found to be much higher than sensitivities of sulfate to $NH_3$ emissions ($S_{SO4, NH3}$) (up to about 0.02 μg $m^{-3}$ based on 1% change in $NH_3$ emissions, which is about one-fifth of the nitrate responses) in 2001 in the five cities (Figure 8.4). High sensitivities of nitrate to $NH_3$ emissions are due to the thermodynamic equilibrium between sulfate, nitrate and ammonium. Formation of $NH_4NO_3$ is limited by availability of ammonium ($NH_3$) after $(NH_4)_2SO_4$ is formed. This is particularly true in areas with high $NO_x$ and $SO_2$ emissions. In 2050, higher temperatures and humidity increase hydroxyl radicals and induce more rapid oxidation of $SO_2$ and $NO_x$. Also, pH-dependent aqueous phase oxidation of sulfate becomes more important. However, higher temperatures also increase gas-phase partitioning of semi-volatile $PM_{2.5}$ compounds, such as $NH_4NO_3$. Overall, lower anthropogenic $SO_2$ and $NO_x$ emissions, and higher ammonia emissions and temperatures cause $NH_4NO_3$ formation to become less ammonia-sensitive in 2050. The increased importance of aqueous-phase oxidation of $SO_2$ causes $(NH_4)_2SO_4$ formation to become more ammonia-sensitive even though $SO_2$ emissions are predicted to decrease in 2050 due to planned emission controls. Overall, the sensitivities of $(NH_4)_2SO_4$ to $NH_3$ increase, a finding that is opposite of the one for $NH_4NO_3$.

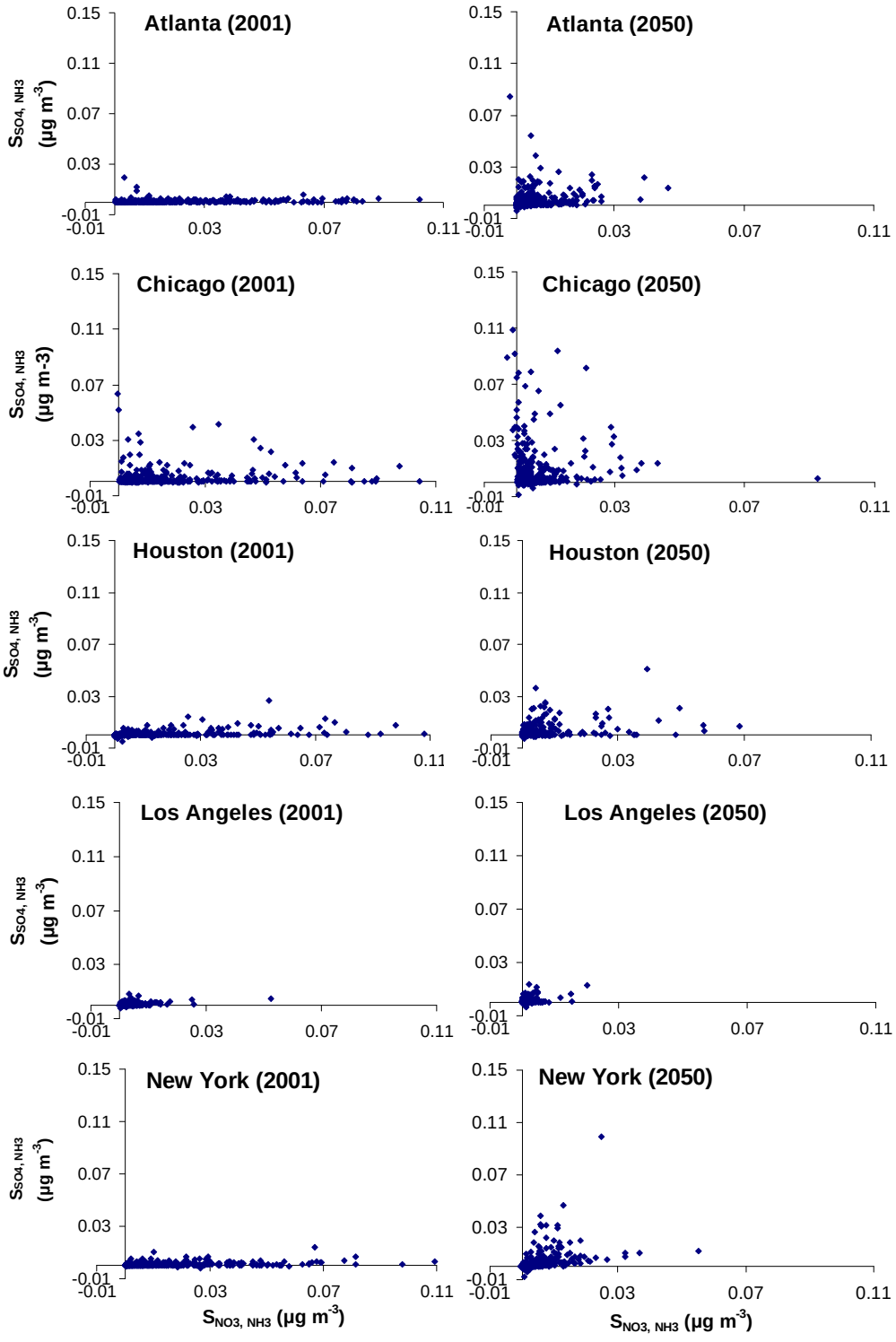


**Figure 8.4: Daily sensitivities of sulfate ($S_{SO4,NH3}$, in µg $m^{-3}$, Y-axis) and nitrate ($S_{NO3,NH3}$, in µg $m^{-3}$, X-axis) to $NH_3$ emissions in 2001 and 2050 for city centers (each shown as response to a 1% change in $NH_3$ emissions)**

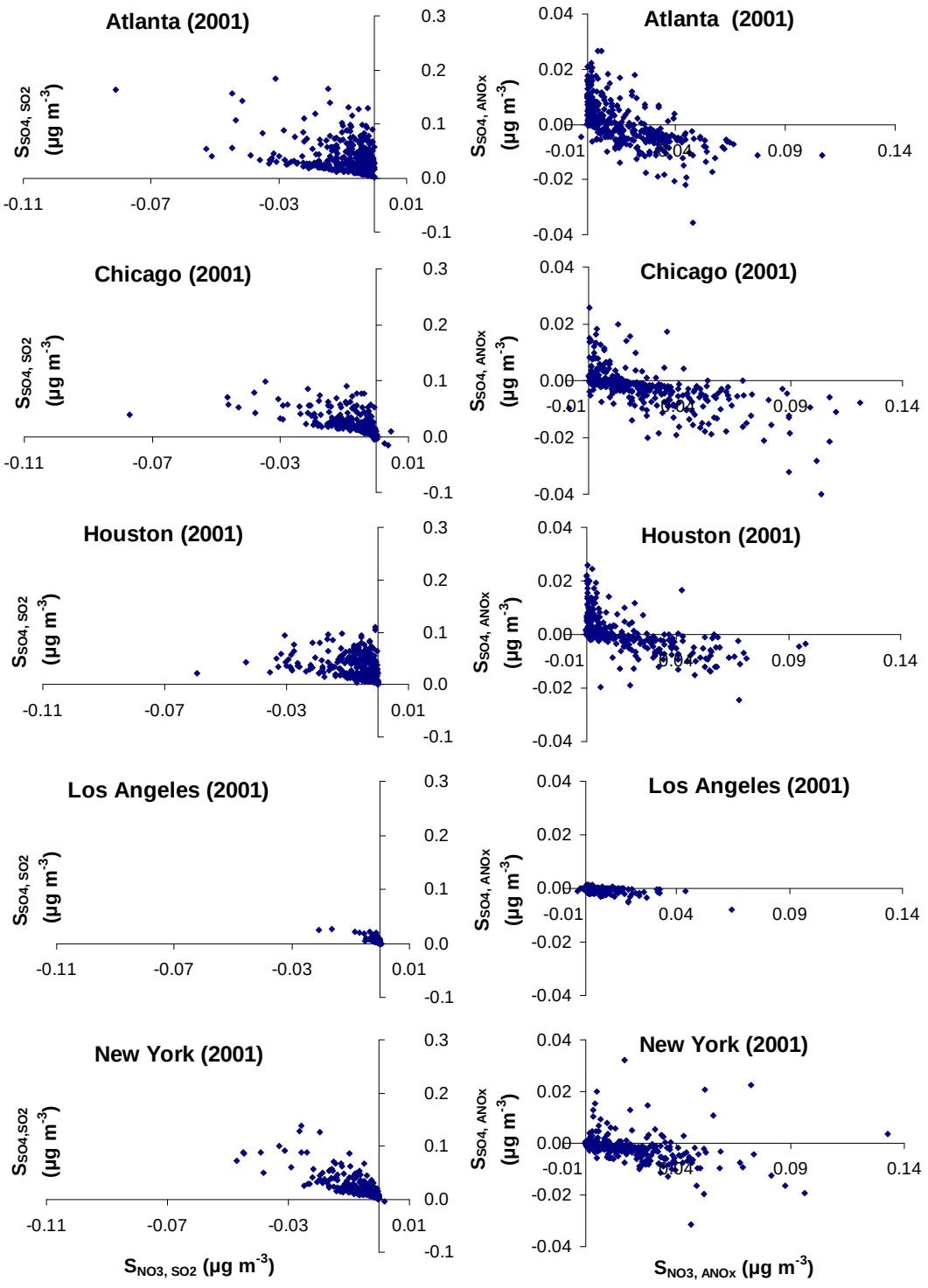


**Figure 8.5: Daily sensitivities of sulfate and nitrate (in µg $m^{-3}$, X-axis) to 1% changes in $SO_2$ emissions ($S_{SO4,SO2}$ and $S_{NO3,SO2}$, in µg $m^{-3}$, left column) and anthropogenic $NO_x$ emissions ($S_{SO4,ANOx}$ and $S_{NO3,ANOx}$, in µg $m^{-3}$, right column) in 2001 for city centers**

Sensitivities of sulfate to $SO_2$ emissions ($S_{SO4, SO2}$) and nitrate to anthropogenic $NO_x$ emissions ($S_{NO3, ANOx}$) are simulated to be mainly positive in 2001 and 2050 (Figures 8.5 & D.3). Reductions in $SO_2$ and anthropogenic $NO_x$ emissions, respectively, are predicted to decrease gas- and aqueous-phase sulfate and nitrate, and lead to less condensable $(NH_4)_2SO_4$ and $NH_4NO_3$ formation in 2050. On the other hand, competition for ammonia/ammonium between nitrate and sulfate causes sensitivities of nitrate to $SO_2$ emissions ($S_{NO3,SO2}$) to be negative and, therefore, reductions in $SO_2$ emission are simulated to increase nitrate formation. Nevertheless, when lowering $NO_x$ emissions reduce oxidant levels (e.g., OH, $H_2O_2$, $O_3$, etc.), sulfate formation can decrease (i.e., when sensitivities of sulfate to anthropogenic $NO_x$ emissions ($S_{SO4,ANOx}$) are positive). Reductions in $SO_2$ and anthropogenic $NO_x$ emissions are simulated to lead to similar decreases in annual 24-hr average $PM_{2.5}$ concentrations (Table D.3). Both future $(NH_4)_2SO_4$ and $NH_4NO_3$ are found to be less sensitive to $SO_2$ and anthropogenic $NO_x$ emissions due to controls (Figures 8.5 & D.3).

## 8.4 Current Annual Average Responses.

While viewing the daily linked sensitivities of ozone and $PM_{2.5}$ to emissions provides a rapid assessment of the complexities in the effects of controls, some health effects are linked to more chronic exposures to these pollutants, and many areas experience annual $PM_{2.5}$ levels above the NAAQS. Further, acute responses to daily maximum ozone levels are found as well [*Bell, et al.*, 2004]. While the sensitivity of the regional maximum 4$^{th}$ highest daily maximum 8-h $O_3$ to $NO_x$ is positive for all the cities except Los Angeles (Appendix D, Table D.3), the annual average of the $NO_x$

sensitivities of the daily maximum 8-h $O_3$ is negative for four of the five cities (from -0.15 ppb/% to -0.01 ppb/%; Atlanta being the exception). Further, the annual average ozone response to $NO_x$ is negative at all locations (from -0.11 ppb/% to -0.05 ppb/%). All of the annual average ozone metrics are found to respond positively to VOC controls. Annual average $PM_{2.5}$ will be reduced by $SO_2$ and $NO_x$ reductions, with sensitivities of 0.0 μg $m^{-3}$/% to 0.04 μg $m^{-3}$/% for $SO_2$ reductions and 0.01 to 0.03 μg $m^{-3}$/% for $NO_x$ reductions (Table D.3).

Consideration of responses of ozone and $PM_{2.5}$ to emission changes shows the complexities in choosing optimum strategies to address air quality problems. While $NO_x$ control is shown to reduce ozone on days with the most elevated ozone levels, it can raise ozone on others. The response of ozone in the city center and the location of the regional maximum are similar in three cities, though not in New York and Chicago. Both ozone and $PM_{2.5}$ are reduced in response to VOC controls, but not in response to $NO_x$. There is an inverse relationship between how sulfate and nitrate respond to both $SO_2$ and $NO_x$ controls. Further, the response of the annual averages is quite different than peak daily levels for both $PM_{2.5}$ and ozone, so health effects associated with acute exposures will respond differently than health effects associated with chronic exposures. This also impacts formulating strategies to meet the various NAAQS, including daily maximum ozone and $PM_{2.5}$, as well as the annual average $PM_{2.5}$.

# CHAPTER 9

# COST ANALYSIS OF IMPACTS OF CLIMATE CHANGE ON REGIONAL AIR QUALITY

## 9.1 Introduction

Climate change has been forecast to influence ground-level ozone and particulate matters levels by affecting meteorological conditions, biogenic precursor emissions, photochemical reactions and thermodynamic equilibriums. Higher volatile organic compound (VOC) emissions, especially biogenic, attributed to higher temperature, increase peak ozone concentrations in VOC-limited urban areas. Some studies show that higher temperatures, faster photochemical rates and more stagnant climate conditions accelerate ground-level ozone formation assuming future climate follows multiple Intergovernmental Panel on Climate Change (IPCC) scenarios [*IPCC,* 2001] [*Hogrefe, et al.*, 2004; *Liao, et al.*, 2006; *Murazaki and Hess*, 2006; *Tagaris, et al.*, 2007]. For another important air pollutant, $PM_{2.5}$ (particulate matter with an aerodynamic diameter less than 2.5 µm), several studies show that impacts of climate change are predicted to influence $PM_{2.5}$ levels via changes in precipitation, rates of photochemical reactions and shifts of thermodynamic equilibriums between gas- and condense-phase semi-volatile compounds [*Liao, et al.*, 2006; *Tagaris, et al.*, 2007]. Climate change and associated influences on regional air quality are also expected to cause adverse health effects and increases in mortality rate due to heat-related effects and elevated ozone levels [*Casimiro, et al.*, 2006].

Air quality managers should be made aware of potential increases in control costs of climate change. The objective of this study is to estimate the additional reductions in precursor emissions required and associated costs for offsetting the impacts of climate change on regional air quality. Here we use a regional air quality model to investigate the impacts of climate change on future air quality and a technology analysis tool to estimate associated costs of emission reductions for offsetting those impacts for five cites in the continental U.S. Future climate change is assumed to follow the IPCC A1B emission scenario, which assumes a future world of rapid economic growth with a balance between fossil and non-fossil energy sources [*IPCC*, 2001]. Specifically, we follow ozone and $PM_{2.5}$ since both cause adverse heath effects [*Levy, et al.*, 2001; *Sarnat, et al.*, 2001] and a number of urban areas violate National Ambient Air Quality Standards (NAAQS) (http://www.epa.gov/air/criteria.html, last access: April 28, 2008).

## 9.2 Regional Air Quality Modeling

Details of air quality modeling approach are given in [*Liao, et al.*, 2007; *Tagaris, et al.*, 2007], and summarized here. The US EPA's Models3 Air Quality Modeling System – MM5, SMOKE and CMAQ – is used for investigating impacts of climate change on air quality. The Fifth-Generation NCAR/Penn State Mesoscale Model (MM5) [*Grell, et al.*, 1994; *Seaman*, 2000] is used to downscale NASA's Goddard Institute of Space Studies (GISS) [*Rind, et al.*, 1999] results for years of 2000-2002 and 2049-2051 assuming climate follows the IPCC A1B emission scenario projections [*Leung and Gustafson*, 2005; *Mickley, et al.*, 2004]. 2049-2051 is chosen as a compromise between non-trivial climate change and still in a reasonable time scale for policy-making.

Emissions for current (2000-2002) and future (2049-2051) episodes are processed using the Sparse Matrix Operator Kernel Emissions (SMOKE) modeling system (http://www.smoke-model.org/index.cfm, last access: April 28, 2008). To assess the impacts of climate change along, emission inventories for 2049-2051 are assumed to remain the same as 2000-2002. However, both biogenic and anthropogenic emissions respond to changes in meteorological conditions, particularly temperature, and those increases are included.

The Community Multiscale Air Quality Model (CMAQ) [*Byun and Schere*, 2006] and the decoupled direct method 3D (DDM-3D) [*Dunker*, 1981; 1984; *Dunker, et al.*, 2002; *Yang, et al.*, 1997] are used to simulate ozone and $PM_{2.5}$ concentrations and quantify pollutant sensitivities to emissions. DDM-3D directly calculates the first-order local sensitivities of pollutants to precursor emissions, i.e. the first-order sensitivity ($S_{i,j}$) of pollutant concentration i ($C_i$) to source emissions j ($E_j$) is calculated as:

$$S_{i,j} = E_j \frac{\partial C_i}{\partial E_j} \tag{8.1}$$

The first-order (linearized) sensitivities have the same units as the corresponding pollutants and represent how pollutant concentrations would respond to a 100% reduction in precursor emissions if the systems were linear.

Five cities in the continental U.S. – Atlanta, Chicago, Huston, Los Angeles and New York – were chosen in this study because each currently experiences high ozone and $PM_{2.5}$ levels (http://www.epa.gov/oar/oaqps/greenbk/, last access: April 28, 2008). Yearly-average concentrations and sensitivities of $PM_{2.5}$ are calculated for the city

centers of the five cities in 2001 and 2050. Ozone levels peak in the summer and downwind of city centers. Here the average concentrations of regional maximum 4$^{th}$ MDA8h $O_3$ (i.e., highest 4$^{th}$ MDA8h $O_3$ among five-by-five grid cells around the city center, see Figure 9.1) are calculated for the summers (June, July and August) of 2000-2002 and 2049-2051.

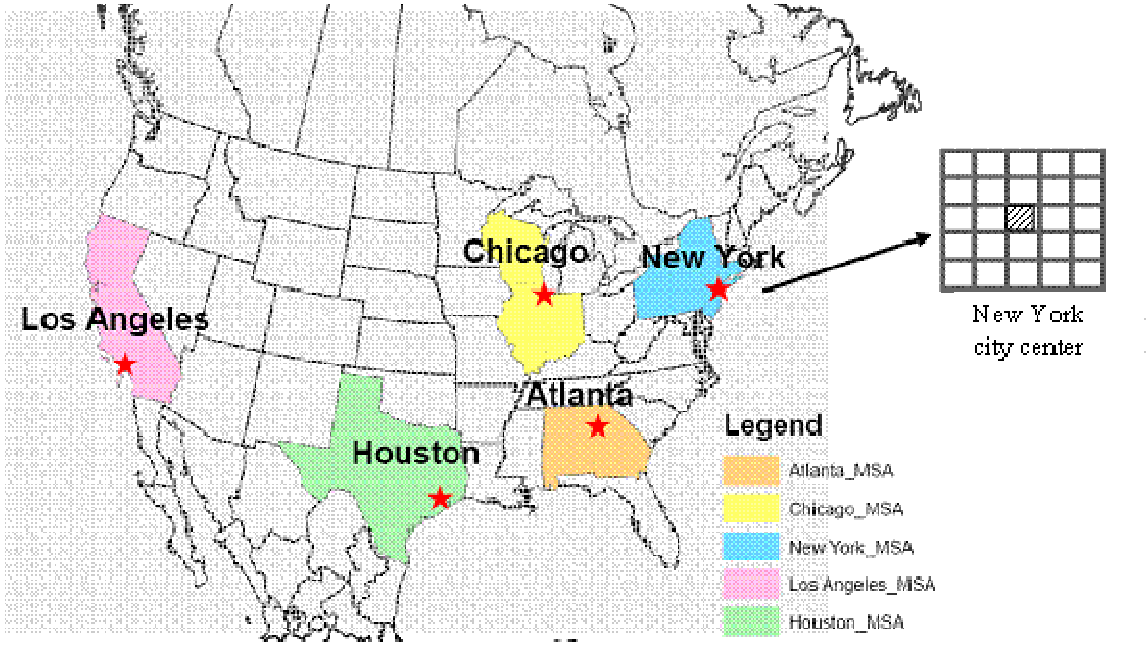


**Figure 9.1**: **Simulation domain and the five U.S. cities studied in this study. Also shown is the five-by-five grid used for identifying the regional maximum, as applied to New York for an example. States include Atlanta in the metropolitan statistical area (MSA) include Alabama and Georgia; Chicago MSA states include Illinois, Indiana and Wisconsin; Houston MSA is solely in Texas; Los Angeles MSA is in California; and the New York MSA states include Connecticut, New Jersey, New York and Pennsylvania**

### 9.3 Effects of Climate Change on Urban Ozone and $PM_{2.5}$ Levels

Average simulated concentrations of the regional maximum 4$^{th}$ MDA8h $O_3$ range from about 75 to 118 ppb in 2000-2002 summers for the five U.S. cities studied. For comparison, three-summer average regional maximum 4$^{th}$ MDA8h $O_3$ concentrations are predicted to increase up to 17.7 ppb in 2049-2051 compared with the 2000-2002 for the cities examined though ozone in Chicago is simulated to decrease (Table 9.1). Slight decreases in future 4$^{th}$ MDA8hr $O_3$ levels in Chicago are related to increases in cloud cover in 2050s in the Midwest of the U.S. [*Leung and Gustafson*, 2005]. Increases in peak ozone concentrations due to impacts of climate change are discussed in other studies (e.g., Hogrefe et al. (2004), Mickley et al. (2004) Murazaki and Hess (2006), Tagaris et al. (2007), etc. Sensitivity results show that reductions in anthropogenic $NO_x$ emissions are more effective for decreasing regional maximum 4$^{th}$ MDA8h $O_3$ levels than VOC emissions for the cities except Los Angeles. Regional maximum 4$^{th}$ MDA8h $O_3$ levels are predicted to be more VOC-sensitive in Los Angeles due to high mobile $NO_x$ emissions (Table 9.1).

**Table 9.1: Regional fourth-highest daily maximum 8-hr average ozone ($4^{th}$ MDA8h $O_3$) in 2000-2002 and 2049-2051 summers as well as sensitivity of $4^{th}$ MDA8h $O_3$ to anthropogenic $NO_x$ ($S_{4th\ MDA8h\ O3,NOx}$) and VOC ($S_{4th\ MDA8h\ O3,VOC}$) Emissions in 2049-2051 summers for the five Cities in the U.S.** **Unit: ppb**

| | 2000-2002 Summer Concentration | 2049-2051 Summer Concentration | 2049-2051 Summer $S_{O3,ANOx}$ | 2049-2051 Summer $S_{O3,AVOC}$ | Δ Concentration (2050s-2001s) |
|---|---|---|---|---|---|
| Atlanta | 113.9 | 123.4 | 51.9 | 2.2 | 9.5 |
| Chicago | 112.8 | 109.4 | 35.0 | 4.7 | -3.4 |
| Houston | 105.9 | 112.2 | 38.2 | 4.5 | 6.3 |
| Los Angeles | 102.1 | 119.8 | 8.5 | 23.1 | 17.7 |
| New York | 95.8 | 106.9 | 18.6 | 10.6 | 11.1 |

Simulated yearly average $PM_{2.5}$ concentrations range from 12.7 to 19.7 $\mu g\ m^{-3}$ in 2001 at the city centers of the five U.S. cities. When the emission inventory is kept constant, in 2050, $PM_{2.5}$ concentrations are predicted to increase in Chicago, Los Angeles and New York but decrease in Atlanta and Houston as compared with 2001. The highest increases in yearly average $PM_{2.5}$ concentrations are predicted to be 1.9 $\mu g\ m^{-3}$ in Chicago. Chemical composition of the yearly averaged $PM_{2.5}$ is predicted to slightly change in 2050 mainly due to shifts in the thermodynamic equilibriums the rate of sulfate formation. Sulfate is predicted to increase while nitrate is predicted to decrease in 2050 due to the effects of climate change (Appendix E, Figure E.1). Higher temperatures and stronger radiation in the projected climate accelerate $SO_2$ oxidation and induce more sulfate formation, while increases in temperature, and less ammonia being available, favor nitrate existing in the gas-phase and decrease the amount nitrate in the $PM_{2.5}$. Sensitivity results show that reductions in anthropogenic $SO_2$ and $NO_x$ emission are more effective for decreasing $PM_{2.5}$ than VOC emissions (Table 9.2).

**Table 9.2: Yearly $PM_{2.5}$ concentrations in 2001 and 2050 and sensitivity of $PM_{2.5}$ to anthropogenic $SO_2$ ($S_{PM2.5,SO2}$), $NO_x$ ($S_{PM2.5,NOx}$) and VOC ($S_{PM2.5,VOC}$) emissions in 2050 for the five cities in the U.S.** **Unit: µg $m^{-3}$**

| | 2001 Concentrations | 2050 Concentrations | 2050 $S_{PM2.5,SO2}$ | 2050 $S_{PM2.5,ANOx}$ | 2050 $S_{PM2.5,AVOC}$ | Δ Concentrations (2050-2001) |
|---|---|---|---|---|---|---|
| Atlanta | 19.7 | 19.0 | 3.4 | 2.1 | 0.2 | -0.7 |
| Chicago | 19.0 | 21.0 | 2.4 | 3.1 | 0.3 | 1.9 |
| Houston | 16.5 | 16.0 | 3.4 | 1.7 | 0.0 | -0.5 |
| Los Angeles | 12.7 | 12.8 | 0.4 | 0.6 | 0.1 | 0.1 |
| New York | 19.7 | 21.2 | 2.2 | 2.1 | 0.5 | 1.5 |

### 9.4 Cost of Offsetting of Impacts of Climate Change on Regional Air Quality

Our previous study shows that anthropogenic $NO_x$ and VOC are the major precursors for controlling the 4$^{th}$ MDA8h $O_3$ levels, while removal of $SO_2$ and $NO_x$ emissions are effective ways for reducing $PM_{2.5}$ concentrations, both now and in the future [*Liao, et al.*, 2007]. Here we use the U.S. EPA's control technology analysis tool, AirControlNet v4.1 [*E.H. Pechan & Associates*, 2006a; b], to estimate the costs of reductions in anthropogenic $SO_2$, $NO_x$ and VOC emissions from different regions in the U.S. AirControlNET uses US EPA's 1999 National Emission Inventories (NEI) (http://www.epa.gov/ttn/chief/net/1999inventory.html, last access: April 28, 2008) and relies on emission control efficiency, fuel use and emission factor data provided in the NEI to perform cost analysis. Costs of emission reductions in the future are presented in 1999 dollars in order to compare with currently estimated costs of emission reductions for improving air quality [*EPA*, 2005]. Results of AirControlNet provide the annual maximum controllable emissions, tons of emissions reduced and annualized associated costs for emission control measures (by species, state, cost per ton, etc.). Costs of emission reductions are calculated as 2$^{nd}$-order polynomial, exponential or power functions of absolute amount of emission reductions depending on species and region. Cost functions of reductions in anthropogenic $SO_2$, $NO_x$ and VOC emissions in Los Angeles and New York are shown as examples in Figure 9.2; results from the other cities are shown in the Appendix E.

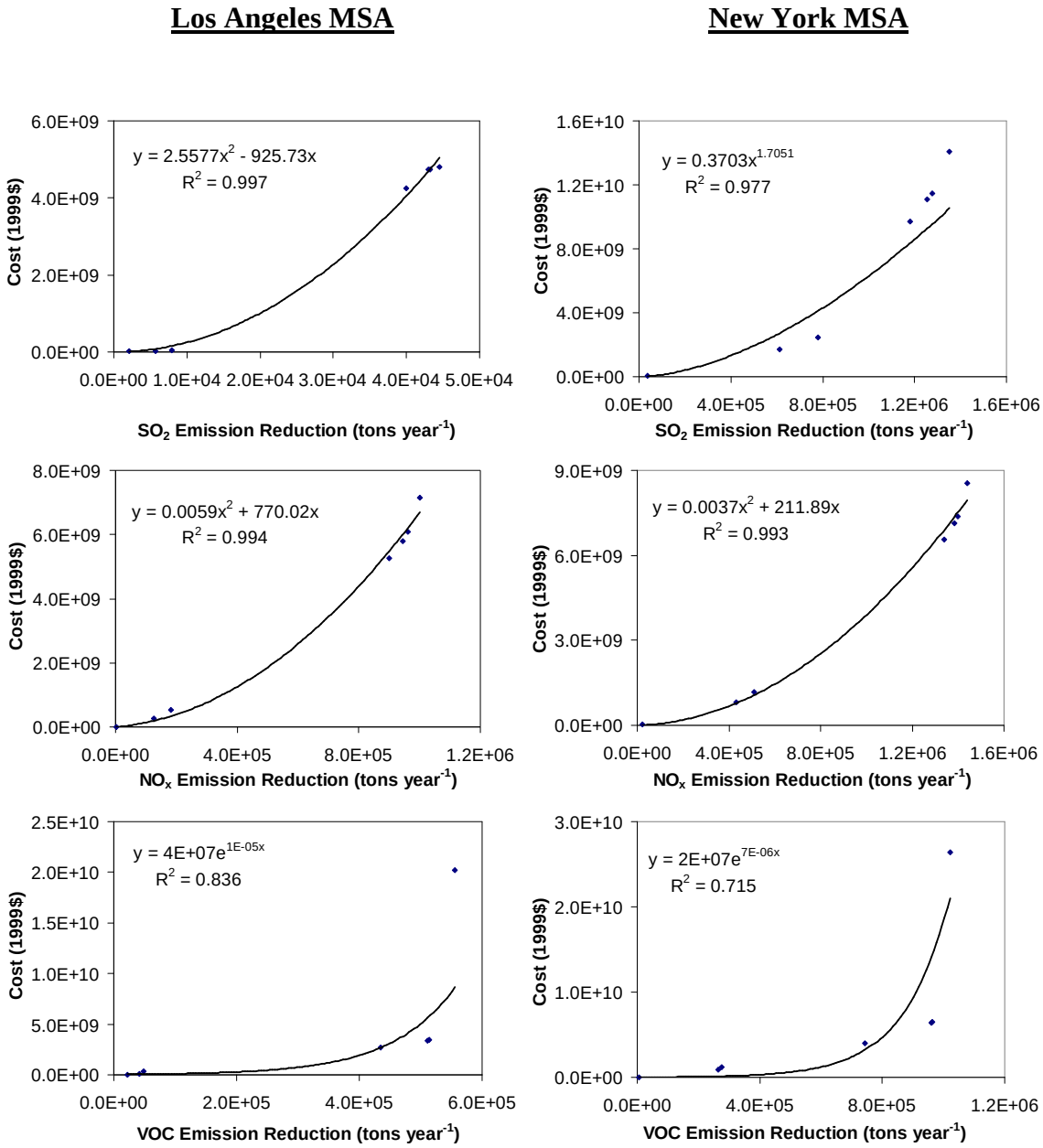


**Figure 9.2: Relationship between costs and amount of reductions in $SO_2$, $NO_x$ and VOC emissions for Los Angeles (left column) and New York MSA states (right column)**

For driving costs functions of emission reductions for offsetting the impacts of climate change on 4$^{th}$ MDA8h $O_3$ and $PM_{2.5}$, we assume that there is no interaction

between emission reductions of species from same or other sources. For example, reductions in $SO_2$ emissions are not expected to decrease $NO_x$ or VOC emissions from the same or other sources, nor are reductions in $SO_2$ emissions from one source expected to affect $SO_2$ emissions from other sources. Therefore, the total costs for offsetting impacts of climate change on ozone and $PM_{2.5}$ are a linear summation of the costs of reductions in $SO_2$, $NO_x$ and VOC emissions for each city (equation 9.1).

$$\begin{aligned}&\textit{Costs of emission reductions for city } i = \sum_j C_{i,j} \\ &\textit{where} \\ &C_{i,j} = \textit{cost of emission reduction of species } j \textit{ for city } i \\ &i = \textit{Atlanta, Chicago, Houston, Los Angeles and New York} \\ &j = \textit{anthropogenic } SO_2, NO_x \textit{ \& VOC from MSA states of city } i\end{aligned} \tag{9.1}$$

Furthermore, prior study shows that impacts of precursor emissions on air quality drop quickly with increases in distance between receptors and sources [*Napelenok, et al.*, 2007]. We assume that air quality in each city is only affected by the emissions from the states which include the metropolitan statistical area (MSA) of that city (Figure 9.1) (for definition of MSA, see http://www.whitehouse.gov/omb/bulletins/fy2007/b07-01.pdf, last access: April 28, 2008), and the levels of controls identified are applied over state(s) containing MSA. This likely increases the control domain the costs MSA states of each of the five cities are shown in the notes of Table 9.3. Future maximum controllable emissions, costs of removal of per unit precursor emissions and maximum control efficiencies for emission sources are assumed to remain the same as their current values.

$$\begin{aligned}&\Delta\varepsilon_{NOx} S_{4thMDA8h\,O3,NOx} + \Delta\varepsilon_{VOC} S_{4thMDA8h\,O3,VOC} \geq C_{4thMDA8h\,O3,2050} - C_{4thMDA8h\,O3,2001} \\ &\Delta\varepsilon_{SO2} S_{PM\,2.5,SO2} + \Delta\varepsilon_{NOx} S_{PM\,2.5,NOx} + \Delta\varepsilon_{VOC} S_{PM\,2.5,VOC} \geq C_{PM\,2.5,2050} - C_{PM\,2.5,2001}\end{aligned} \tag{9.2}$$

where

$\Delta\varepsilon_j$ : *reduction ratios of emission* $j$
$S_{i,j}$ : *sensitivities of species i to emission* $j$ *from MSA states*
$C_i$ : *concentrations of species i*
$i = 4^{th}$ *MDA8h* $O_3$ *and* $PM_{2.5}$ ; $j = SO_2, NO_x$ *and VOC*

Sensitivities of the three-summer average regional maximum 4$^{th}$ MDA8h $O_3$ to anthropogenic $NO_x$ and VOC emissions and yearly-average $PM_{2.5}$ to $SO_2$, $NO_x$ and VOC emissions are used in equation (9.2) in order to calculate the amount of reductions required for offsetting effects of climate change on air quality in 2049-2051 based on least-cost controls. The least-cost controls of emission reductions are found among all the possible control strategies using the cost functions developed from AirControlNet outputs and equation (9.2). Details of development of least–cost control strategies are provided in the Appendix E. Using the least-cost analyses, the costs for offsetting impacts of climate change on both 4$^{th}$ MDA8h $O_3$ and $PM_{2.5}$ concentrations are predicted to range from about $27 million to $5.9 billion in 2050s for the five cities (Table 9.3). The high costs of emission reductions in Chicago ($1.3 billion) are attributed to significant increases in yearly average $PM_{2.5}$ levels (1.9 $\mu g\ m^{-3}$) in 2050 compared with 2001 (Table 9.2). Necessary $SO_2$, $NO_x$ and VOC emission reductions are calculated to be 39%, 30% and 19%, respectively, for the Chicago MSA states for offsetting climate effects based on the least-cost set of controls. High costs in Los Angeles ($5.9 billion) are attributed to significant reductions in anthropogenic $NO_x$ (~ 46%) and VOC (~ 60%) emissions over California. For the New York MSA states, $SO_2$, $NO_x$ and VOC emissions are expected to decrease by about 23%, 42% and 32%, respectively, in order to offset significant

increases in 4$^{th}$ MDA8h $O_3$ and $PM_{2.5}$ in 2050. The associated least-costs are calculated to be $3.6 billion (Table 9.3). Since emission reductions and associated costs are independent among the MSA states of the five cities, total costs of emission reductions for simultaneously offsetting impacts of climate change on 4$^{th}$ MDA8h ozone and yearly-average $PM_{2.5}$ for the five cities are the summation of costs from each of the five cities, but this sum still represents a lower bound of the total nationalwide costs for increased controls to offset climate change. The total costs for simultaneously offsetting climate impacts on air quality in the five cities are calculated to be up to $11 billion in 2050s (Table 9.3), and are mainly attributed to offsetting increases in peak ozone levels in the future in Los Angeles and New York. EPA's currently planned control strategy, Clean Air Interstate Rule (CAIR), projects that annual incremental costs of CAIR are $2.4 billion and $3.6 billion in 2010 and 2015, respectively, without considering effects of climate penalty on air quality management [*EPA*, 2005]. According to our calculation in this study, additional $11 billion (or more) would be added to offset the impacts of climate change on air quality and achieve the currently projected environmental benefits between 2001s and 2050s. The overall costs of emission reductions for offsetting climate change on climate change over the continental U.S. are expected to be higher than calculated values since there are only five cites are investigated in this study.

**Table 9.3: Percentage (%) and Amount (tons year$^{-1}$) of Emission Reductions from the Five MSA States as well as Associated Yearly Costs (in 1999$ year$^{-1}$) for Offsetting Impacts of Climate Change on 4$^{th}$ MDA8h Ozone and $PM_2$.5 for the Five Cities in the U.S. in 2049-2051**

| City | $SO_2$ reduction (%) | $NO_x$ reduction (%) | VOC reduction (%) | $SO_2$ reduction (tons year$^{-1}$) | NOx reduction (tons year$^{-1}$) | VOC reduction (tons year$^{-1}$)) | Cost (1999$ year $^{-1}$) |
|---|---|---|---|---|---|---|---|
| Atlanta[a] | ~ 0 | 18.3 | ~ 0 | 0 | 217194 | 0 | $27,232,000 |
| Chicago[b] | 39.2 | 30.1 | 18.9 | 807868 | 606031 | 204236 | $1,394,500,000 |
| Houston[c] | ~ 0 | 16.5 | ~ 0 | ~ 0 | 291933 | ~ 0 | $210,780,000 |
| Los Angeles[d] | 0.4 | 46.4 | 59.6 | 196 | 580180 | 446242 | $5,887,500,000 |
| New York[e] | 22.7 | 41.5 | 31.9 | 323865 | 759647 | 431837 | $3,626,800,000 |
| All cities | - | - | - | - | - | - | $11,146,812,000 |

Note: maximum controllable emissions and maximum removal efficiencies of $SO_2$, $NO_x$ and VOC; both are calculated in 1999 levels:

[a] Atlanta MSA states (Georgia and Alabama ); maximum controllable emissions: $SO_2$ – 1,181,730 tons year$^{-1}$, $NO_x$ – 1,186,853 tons year$^{-1}$, VOC – 564,837 tons year$^{-1}$; maximum control efficiencies: $SO_2$ – 0.969, $NO_x$ – 0.792, VOC – 0.762

[b] Chicago MSA states (Illinois, Indiana and Wisconsin ); maximum controllable emissions: $SO_2$ – 2,060,889 tons year$^{-1}$, $NO_x$ – 2,013,392 tons year$^{-1}$, VOC– 1,080,612 tons year$^{-1}$; maximum control efficiencies: $SO_2$ – 0.940, $NO_x$ – 0.748, VOC – 0.750

[c] Houston MSA states (Texas); maximum controllable emissions: $SO_2$ – 834,917 tons year$^{-1}$, $NO_x$ – 1,769,293 tons year$^{-1}$, VOC – 941,411 tons year$^{-1}$; maximum control efficiencies: $SO_2$ – 0.801, $NO_x$ – 0.755, VOC – 0.694

[d] Los Angeles MSA states (California); maximum controllable emissions: $SO_2$ – 48,965 tons year$^{-1}$, $NO_x$ – 1,250,388 tons year$^{-1}$, VOC – 748,728 tons year$^{-1}$; maximum control efficiencies: $SO_2$ – 0.910, $NO_x$ – 0.800, VOC – 0.743

[e] New York states (Connecticut, New Jersey, New York and Pennsylvania ); maximum controllable emissions: $SO_2$ – 1,426,718 tons year$^{-1}$, $NO_x$ – 1,830,475 tons year$^{-1}$, VOC – 1,353,720 tons year$^{-1}$; maximum control efficiencies: $SO_2$ – 0.948, $NO_x$ – 0.787, VOC – 0.754

## 9.5 Summary

We calculate the least cost of emission reductions for offsetting impacts of climate change on regional peak fourth-highest daily maximum 8-h average ozone in the summers of 2049-2051 and yearly average $PM_{2.5}$ in 2050 for the five U.S. cities. Impacts of future climate change are predicted to increase peak summertime ozone levels in 2049-2051 for the cities examined, except Chicago, as compared with 2000-2002 summers. Yearly-average $PM_{2.5}$ concentrations are predicted to increase up to 1.9 $\mu g\ m^{-3}$ in 2050. Based on present emission control technologies, least cost emission reductions for offsetting impacts of climate change on regional peak fourth-highest daily maximum 8-h average ozone and yearly average $PM_{2.5}$ are predicted to range from $27 million in Atlanta to $5.9 billion (1999$) in Los Angeles. Total costs of emission reductions for simultaneously offsetting impacts of climate change on air quality for the states containing MSA of the five cities examined are predicted to be about $11 billion (1999$).

# CHAPTER 10

# SUMMARY AND FUTURE RESEARCH

## 10.1 Summary of Main Findings

An approach that integrates the impact of both the current regulations and the longer-term national and global trends is developed to construct an emissions inventory (EI) for North America for the mid-century in support of a regional modeling study of ozone and fine particulate matter. The method developed is based on data availability, spatiotemporal coverage and resolution, and future-scenario consistency (i.e. IPCC SRES A1B), and consists of two major steps: 1) near-future EI projection (to the year 2020), and 2) longer-term EI projection (to mid-century). For the continental United States, the year-2050 emissions for $NO_x$, $SO_2$, $PM_{2.5}$, anthropogenic VOC, and ammonia are projected to change by -55%, -55%, -30%, -40% and +20%, respectively compared to 2001. $NO_x$ and $SO_2$ emission changes are very similar in total amount but different in sectoral contribution. The projected emission trends for Canada and Mexico differ considerably. After taking into account the modeled climate changes, biogenic VOC emission increases from three countries overwhelm the decreases in anthropogenic VOC emissions, leading to a net small increase (about 2%) in overall VOC emissions.

Climate change is predicted to have slight effects on ground-level ozone and $PM_{2.5}$ concentrations as well as nitrogen and sulfur deposition in 2050s over the continental United States. Sensitivities of ozone and $PM_{2.5}$ to precursor emissions are also

found to change slightly in response to climate change. In many cases, mass per ton sensitivities to $NO_x$ and $SO_2$ controls are predicted to be greater in the future due to both the lower anthropogenic emissions as well as climate, suggesting that current control strategies based on reducing such emissions will continue to be effective in decreasing ground-level ozone and $PM_{2.5}$ concentrations. $SO_2$ emission controls are predicted to be most beneficial for decreasing summertime $PM_{2.5}$ levels while controls of $NO_x$ emissions are more effective in winter. Spatial distributions of sensitivities are also found to be only slightly affected assuming no changes in land-use. Contributions of biogenic VOC emissions to $PM_{2.5}$ formation are simulated to be more important in the future because of higher temperatures, higher biogenic emissions, and lower anthropogenic $NO_x$ and $SO_2$ emissions.

Impacts of the extreme climate scenarios on concentrations of summertime fourth-highest daily maximum 8-hour average ozone are predicted to be as high as 10 ppb in some urban areas, although regional average differences in ozone concentrations are predicted to be about 1-2 ppb. Differences between the extreme and base scenarios in annualized $PM_{2.5}$ levels are very location dependent and predicted to range between -1.0 and +1.5 $\mu g\ m^{-3}$. Future, annualized $PM_{2.5}$ is less sensitive to the extreme climate scenarios than summertime peak ozone since precipitation scavenging of particles is only slightly affected by the differences between the extreme climate scenarios examined. However, relative abundances of biogenic VOC and anthropogenic $NO_x$ can significantly impact the response of ambient ozone concentrations to climate change. Since a warmer climate will increase VOC emissions, VOC-limited areas are expected to experience increased ozone in the future. Such areas may find that climate change can significantly

offset air quality improvements from emissions reductions, particularly during the most severe episodes.

Reductions in anthropogenic $NO_x$ emissions decrease 24-hr average $PM_{2.5}$ levels but may either increase or decrease daily maximum 8-hr average ozone levels in 2001 and 2050. Regional ozone maxima for all the cities examined are more sensitive to $NO_x$ reductions than at the city center, particularly in New York and Chicago. Planned controls on anthropogenic $NO_x$ emissions lead to more positive responses to ozone reductions in the future. Sensitivities of ozone and $PM_{2.5}$ to anthropogenic VOC emissions are predicted to decrease between 2001 and 2050. Ammonium nitrate formation is predicted to be less ammonia-sensitive in 2050 than 2001 while the opposite is true for ammonium sulfate. Sensitivity of $PM_{2.5}$ to $SO_2$ and $NO_x$ emissions changes little between 2001 and 2050. Both ammonium sulfate and ammonium nitrate are predicted to decrease in sensitivity to $SO_2$ and $NO_x$ emissions between 2001 and 2050. The complexities, linkages, and daily changes in the pollutant responses to emission changes suggest that strategies developed to meet specific air quality standards should consider other air quality impacts as well.

Climate change alone is predicted to significantly increase urban peak ozone levels in the future for the cities examined, except Chicago. Based on present emission control technologies, least costs of emission reductions for offsetting impacts of climate change on regional peak fourth-highest daily maximum 8-h average ozone and yearly average $PM_{2.5}$ are predicted to range from $27 million in Atlanta to $5.9 billion (1999$) in Los Angeles assuming that emission reductions from different sources are independent.

Total costs of emission reductions for simultaneously offsetting impacts of climate change on regional ozone and $PM_{2.5}$ for the five U.S. cities examined are predicted to be about $11 billion (1999$) in 2050s.

## 10.2 Recommendations for Future Research

### 10.2.1 Quantification of Significance of Emission Uncertainty and Climate Uncertainty

Uncertainties inherent in climate change forecasts are predicted to propagate to projections of regional meteorological conditions. Results in this thesis show that climate uncertainties may be similar in magnitude to the decreases found in response to emissions controls for improving regional air quality in highly polluted areas. In addition to uncertainties in projections of meteorological conditions, precursor emissions are another important source of uncertainties in the regional air quality modeling in this study. It is important to recognize the significance of emission uncertainty impacts on regional air quality and compare it with uncertainties in climate forecasts. By quantifying the uncertainties in climate and precursor emissions, the robustness of the air quality modeling results and the resulting implications on currently planned control strategies can be better understood.

### 10.2.2 Applications of Least-Cost Method for Finding Optimal Control Strategies

Previously implemented control strategies for attaining standards consider multiple pollutants separately despite the fact that the formation of many pollutants is coupled via photochemical reactions in the atmosphere. Traditional approaches for air

quality management use iterative processes for developing attainment strategies. The shortcomings of the traditional approaches are that the iterative processes are inefficient for multiple pollutants and regions and difficult to find the optimal (or most cost-effective) control strategies. The least-cost method used in this study can be applied for finding optimal control strategies for simultaneously reducing air pollutant levels for multiple species and areas. The least-cost method requires cost functions for emission reductions, maximum controllable emissions/efficiencies and understanding of how ambient pollutant concentrations will respond to emission changes.

There are a few steps for implementation of the least-lost method for optimizing air quality control strategies. Reductions in air pollutant concentrations required for attaining air quality standards are firstly determined by calculating the differences between prior air pollutant concentrations and air quality standards. The second step for developing optimal control strategies is to choose candidate emission controls for species from different source categories. The candidate emission controls are those which have major contributions to air pollutant formation and can be found from the results of sensitivities analyses. The last step is to find the optimal control strategies from a pool of potential control strategies; this is done by minimizing the cost of emission controls using the cost functions and sensitivities of pollutants to emission changes. By using the results of air quality modeling and cost analyses of emission reductions, this method can be an efficient and important tool for developing optimal control strategies for reducing air pollutant levels in the future.

### 10.2.3 Quantification of Impacts of Climate Uncertainty on Air Quality Using Probabilistic Distributions of Three-dimensional Climate Fields

Quantification of uncertainties in climate forecasts can be done in several ways. Inter-comparison among multiple climate models is used to quantify the differences in climate estimates arising from choosing different climate models. Uncertainties in climate forecasts can also be quantified by driving probability density functions (PDFs) of key properties of the climate system (e.g., temperature, climate forcing, etc.). The PDFs can be driven using climate model ensembles, uncertainties in model parameters, or both [*Mastrandrea and Schneider*, 2004; *Murphy, et al.*, 2004; *Stott and Kettleborough*, 2002]. In this study, impacts of climate uncertainties on air quality are investigated using probabilistic distributions of climate fields from a two-dimensional (zonal mean) time-dependent global climate model. The two-dimensional climate fields (i.e., temperature and absolute humidity) were expanded into three-dimensional climate in order to perturb the base-case three-dimensional climate for quantifying impacts of climate uncertainty on air quality. Quantification of uncertainties inherent in climate forecasts and their impacts on air quality can also be implemented using observationally-constrained climate predictions [*Stott, et al.*, 2006] and probabilistic distributions of climate fields from three-dimensional climate models (e.g., HadAM3) [*Pope, et al.*, 2000; *Stott and Kettleborough*, 2002]. Further research can apply three-dimensional climate forecasts in the simulations and their probabilistic distributions can be downscaled to meso-scale climate for studying impacts of climate uncertainties on air quality management. The impacts of climate uncertainties on air quality are expected to be better quantified with more comprehensive analyses of uncertainties inherent in climate forecasts.

### 10.2.4 Impacts of Climate Change on Secondary Organic Aerosols

Current regional air quality models neglect some important secondary organic aerosol (SOA) precursors (e.g., benzene and isoprene) and underestimate organic carbons formation in the modeling outputs [*Claeys, et al.*, 2004a; *Henze and Seinfeld*, 2006; *Pun and Seigneur*, 2007]. Recent work also suggests that discrepancies between observational and simulated organic carbon (OC) are partially attributed to simple parameterizations of SOA processes in regional air quality models [*Morris, et al.*, 2006]. SOA formation is sensitive to changes in meteorological fields (e,g, ambient temperature, humidity, precipitation, etc.) because climate change affect rates of SOA precursor oxidation, frequencies of particle washing-out and shifts of thermodynamic equilibrium between gas- and particle- phase organic species [*Sheehan and Bowman*, 2001]. Further studies of climate impacts on regional $PM_{2.5}$ formation using more comprehensive SOA processes in regional air quality models will help poly-makers quantify the effectiveness of control strategies and decrease the uncertainties in the air quality modeling outcomes.

# Appendix A

**Table A.1: Seasonal $M8hO_3$ and $PM_{2.5}$ concentrations over US sub-regions in years 2001, 2050 and 2050_np (2001 emissions inventory and 2050 meteorology)**

| | | West | | Plains | | Midwest | | Northeast | | Southeast | | US | |
|---|---|---|---|---|---|---|---|---|---|---|---|---|---|
| | | $M8hO_3$ (ppb) | $PM_{2.5}$ ($\mu g/m^3$) | $M8hO_3$ (ppb) | $PM_{2.5}$ ($\mu g/m^3$) | $M8hO_3$ (ppb) | $PM_{2.5}$ ($\mu g/m^3$) | $M8hO_3$ (ppb) | $PM_{2.5}$ ($\mu g/m^3$) | $M8hO_3$ (ppb) | $PM_{2.5}$ ($\mu g/m^3$) | $M8hO_3$ (ppb) | $PM_{2.5}$ ($\mu g/m^3$) |
| Winter | 2001 | 46 | 4.0 | 44 | 8.6 | 37 | 16.3 | 39 | 11.1 | 42 | 13.7 | 43 | 9.8 |
| | 2050 | 44 | 3.9 | 42 | 7.6 | 37 | 13.2 | 40 | 8.8 | 41 | 10.6 | 41 | 8.2 |
| | 2050_np | 44 | 4.4 | 43 | 9.2 | 35 | 16.8 | 36 | 12.0 | 40 | 13.7 | 41 | 10.3 |
| Spring | 2001 | 49 | 3.4 | 47 | 5.0 | 45 | 8.9 | 48 | 8.0 | 54 | 10.0 | 48 | 6.2 |
| | 2050 | 46 | 3.1 | 43 | 3.6 | 40 | 6.1 | 42 | 4.9 | 46 | 6.5 | 44 | 4.4 |
| | 2050_np | 49 | 3.5 | 47 | 4.5 | 43 | 8.4 | 46 | 7.4 | 54 | 9.1 | 48 | 5.8 |
| Summer | 2001 | 57 | 3.9 | 59 | 6.2 | 62 | 9.4 | 56 | 7.4 | 69 | 11.6 | 60 | 7.1 |
| | 2050 | 50 | 3.3 | 49 | 4.6 | 46 | 7.3 | 45 | 5.2 | 53 | 7.5 | 49 | 5.2 |
| | 2050_np | 57 | 3.8 | 58 | 6.2 | 59 | 10.6 | 58 | 9.0 | 74 | 11.9 | 60 | 7.4 |
| Fall | 2001 | 47 | 4.9 | 43 | 7.9 | 37 | 12.3 | 42 | 9.5 | 51 | 13.9 | 44 | 8.9 |
| | 2050 | 45 | 4.3 | 43 | 5.9 | 39 | 9.5 | 40 | 6.8 | 45 | 9.1 | 43 | 6.7 |
| | 2050_np | 49 | 4.9 | 48 | 7.6 | 44 | 13.0 | 44 | 10.1 | 54 | 13.2 | 48 | 8.9 |

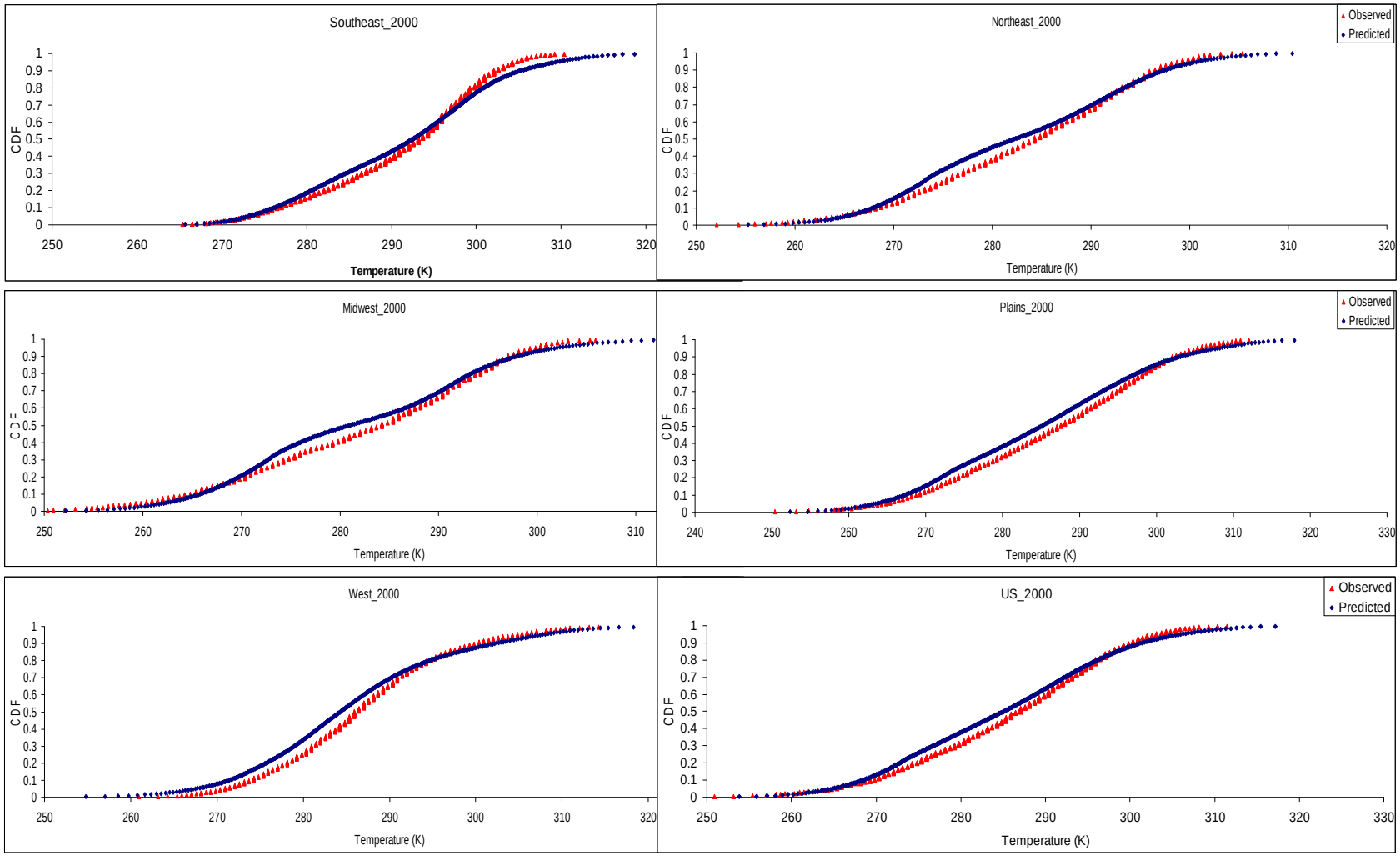


**Figure A.1: Regional CDF plots for temperature in 2000: comparison between observations and predictions**

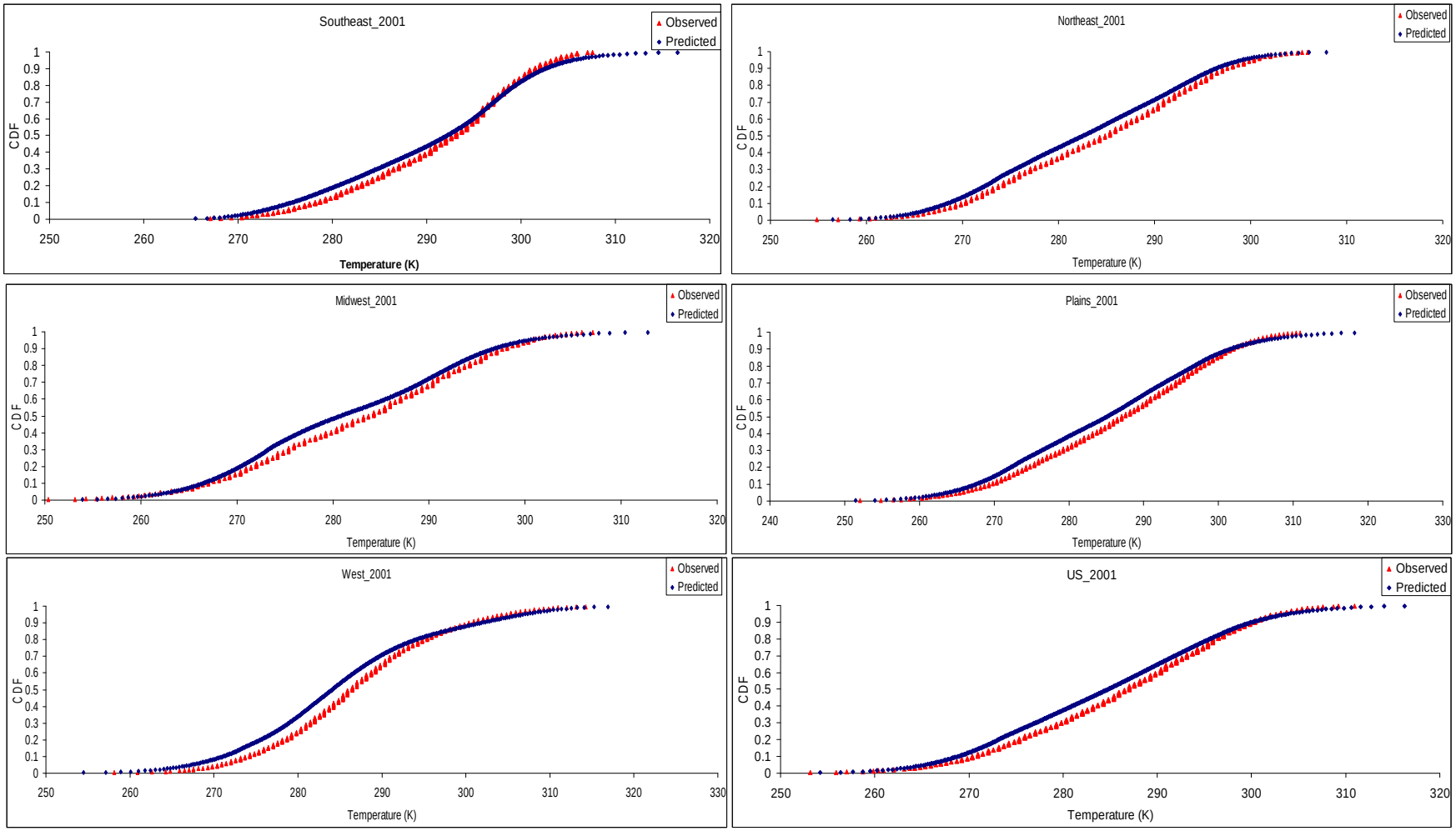


**Figure A.2: Regional CDF plots for temperature in 2001: comparison between observations and predictions**

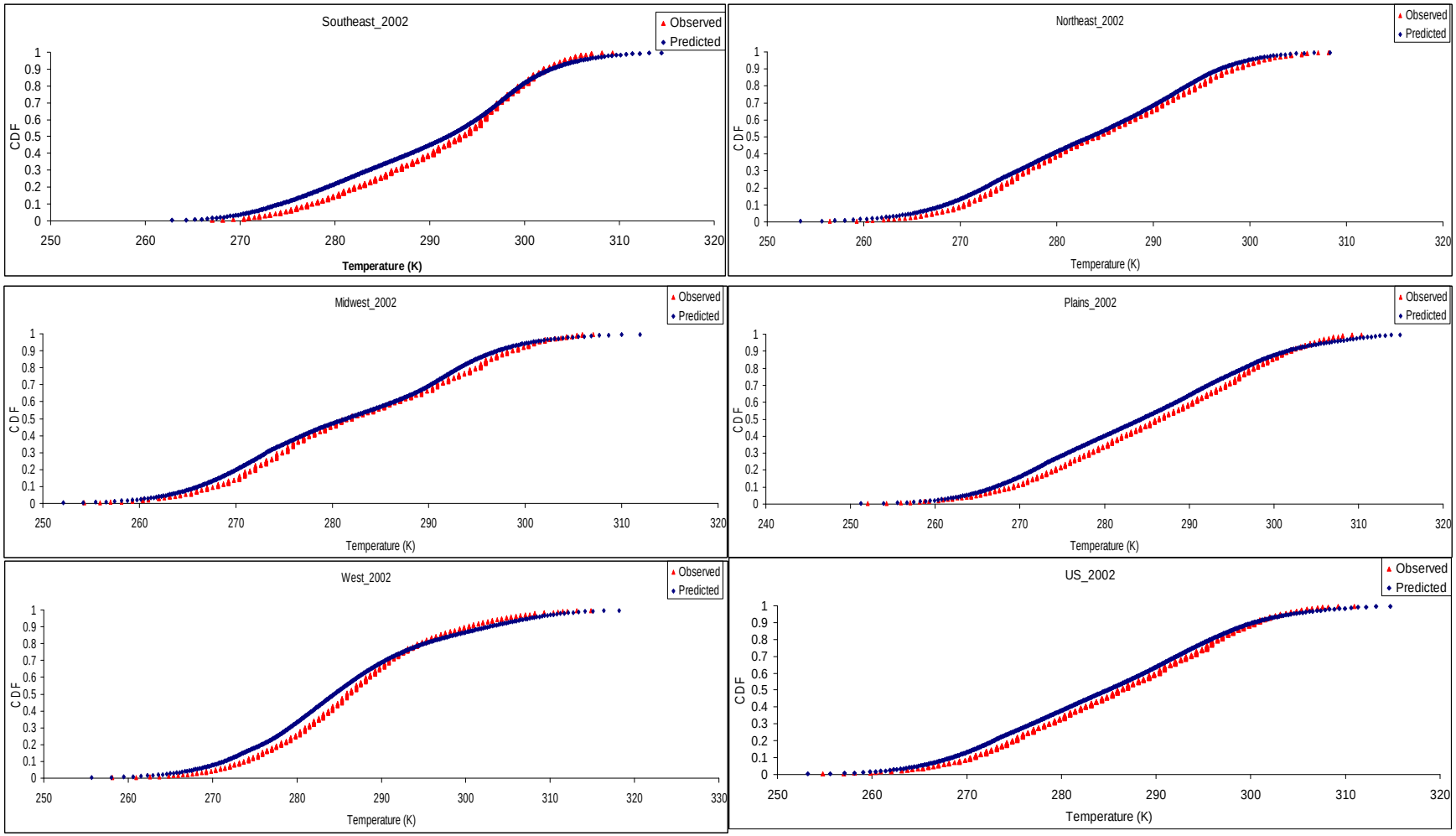


**Figure A.3: Regional CDF plots for temperature in 2002: comparison between observations and predictions**

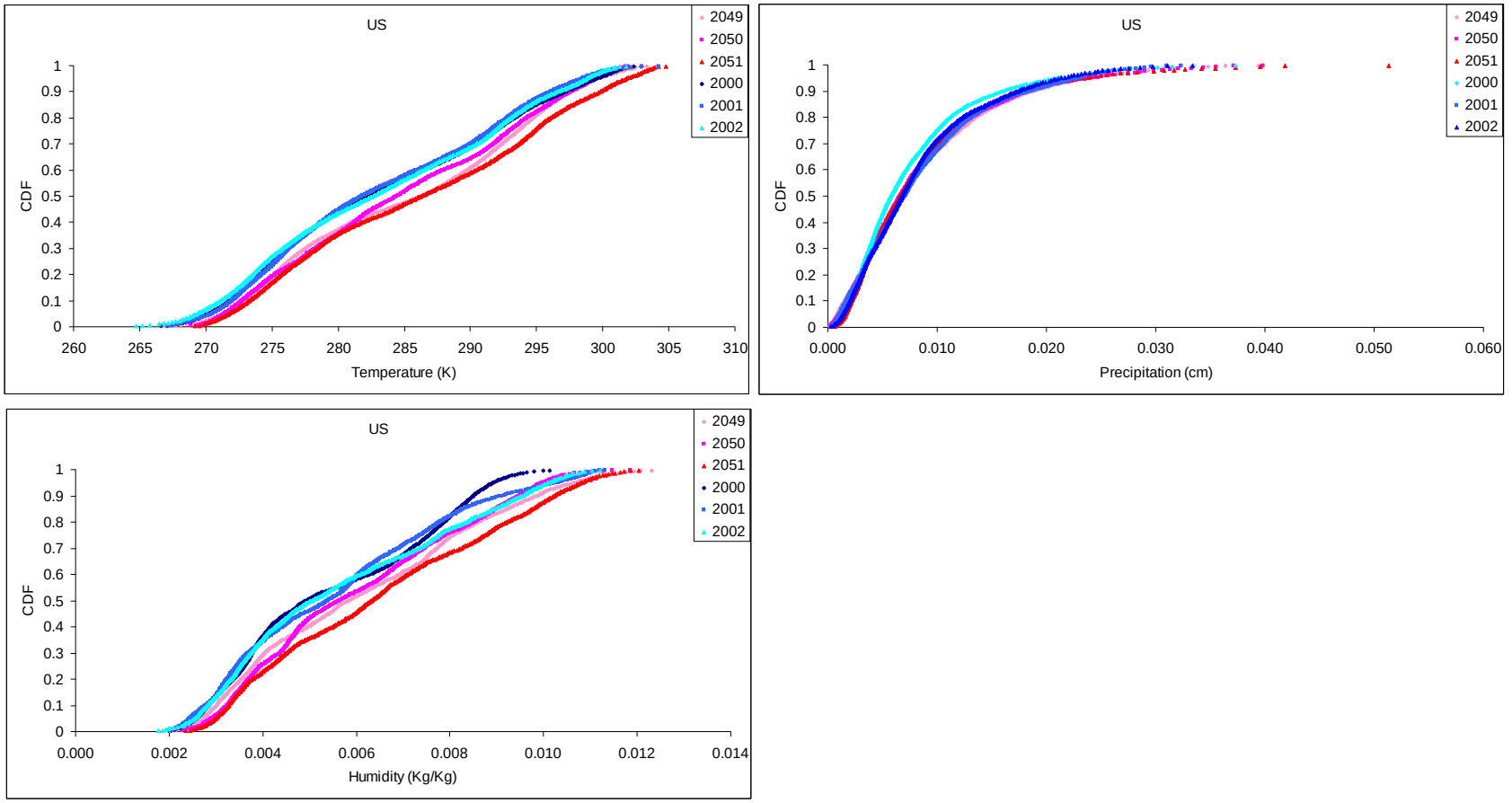


**Figure A.4: CDF plots for temperature, humidity and precipitation over US**

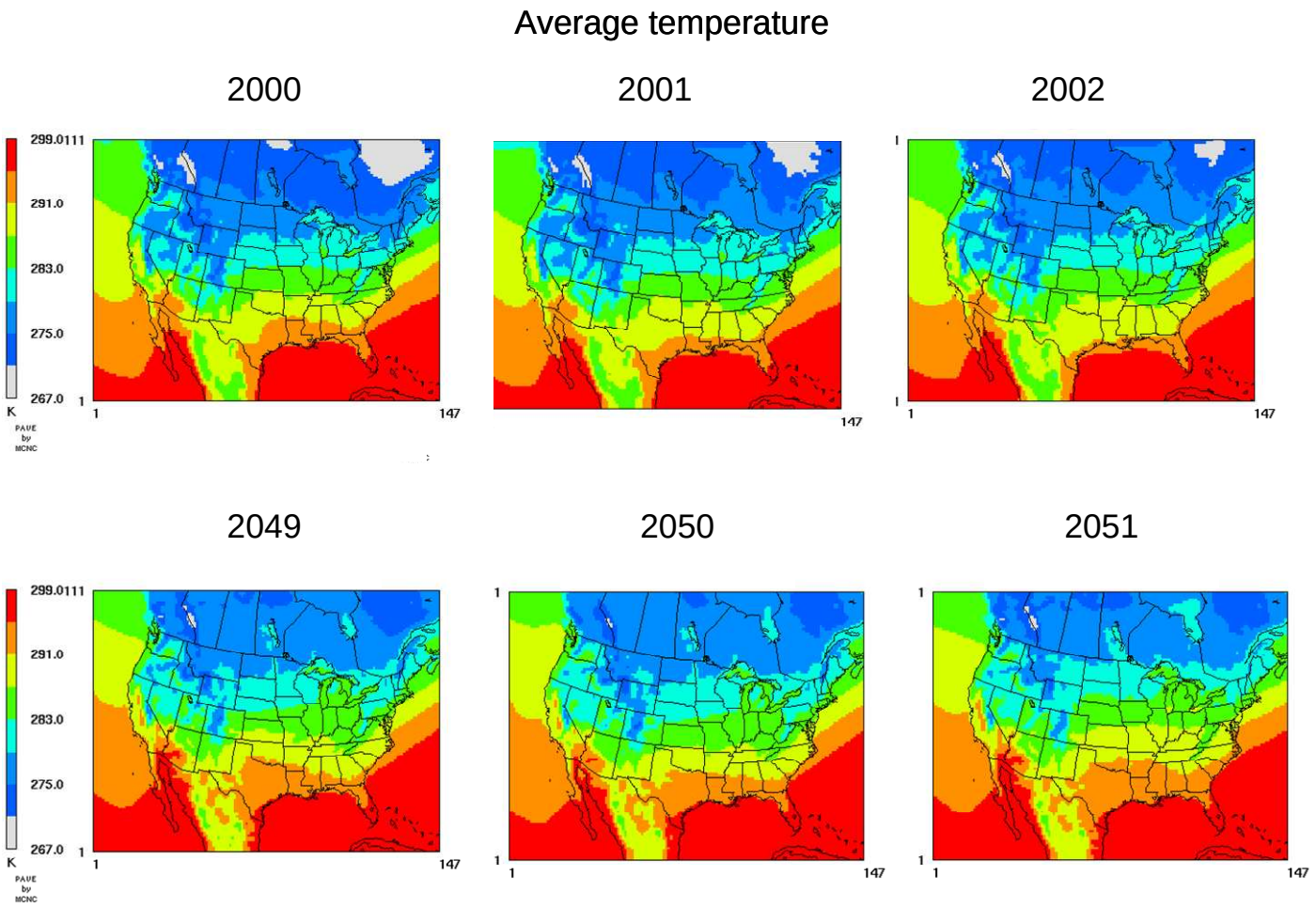


**Figure A.5: Spatial distribution plots of the annual average temperature**

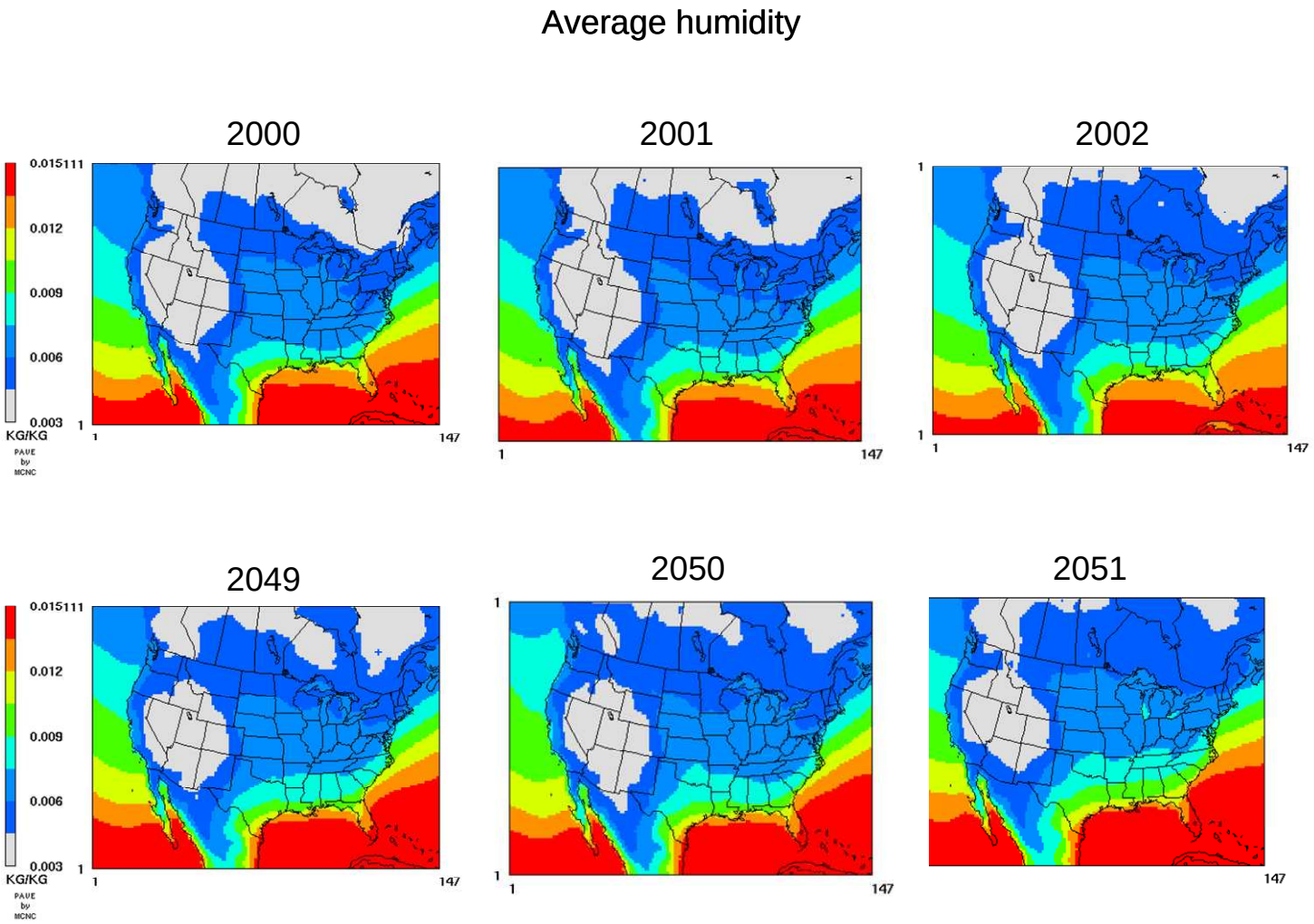


**Figure A.6.: Spatial distribution plots of the annual average humidity**

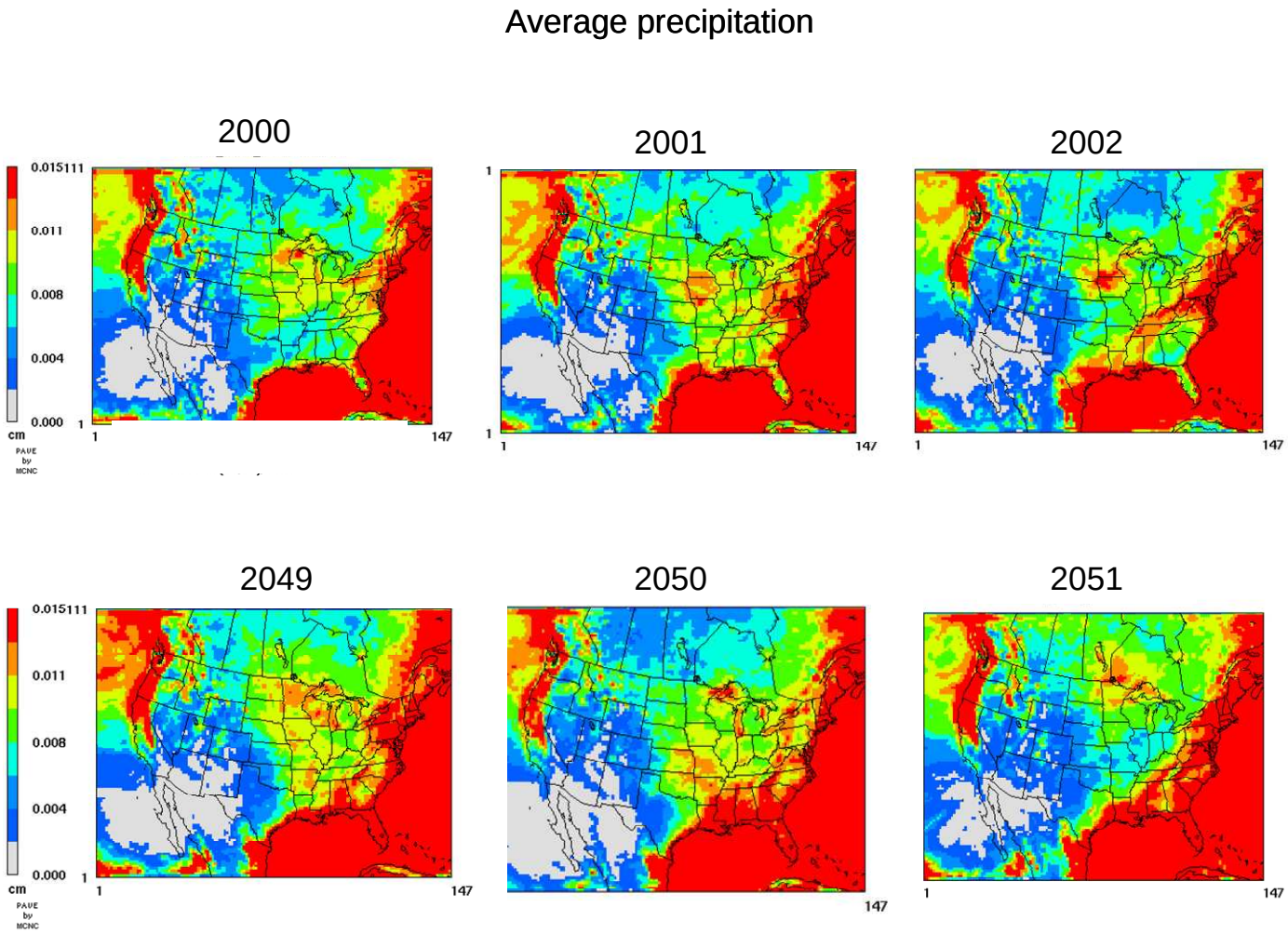


**Figure A.7.: Spatial distribution plots of the annual average precipitation**

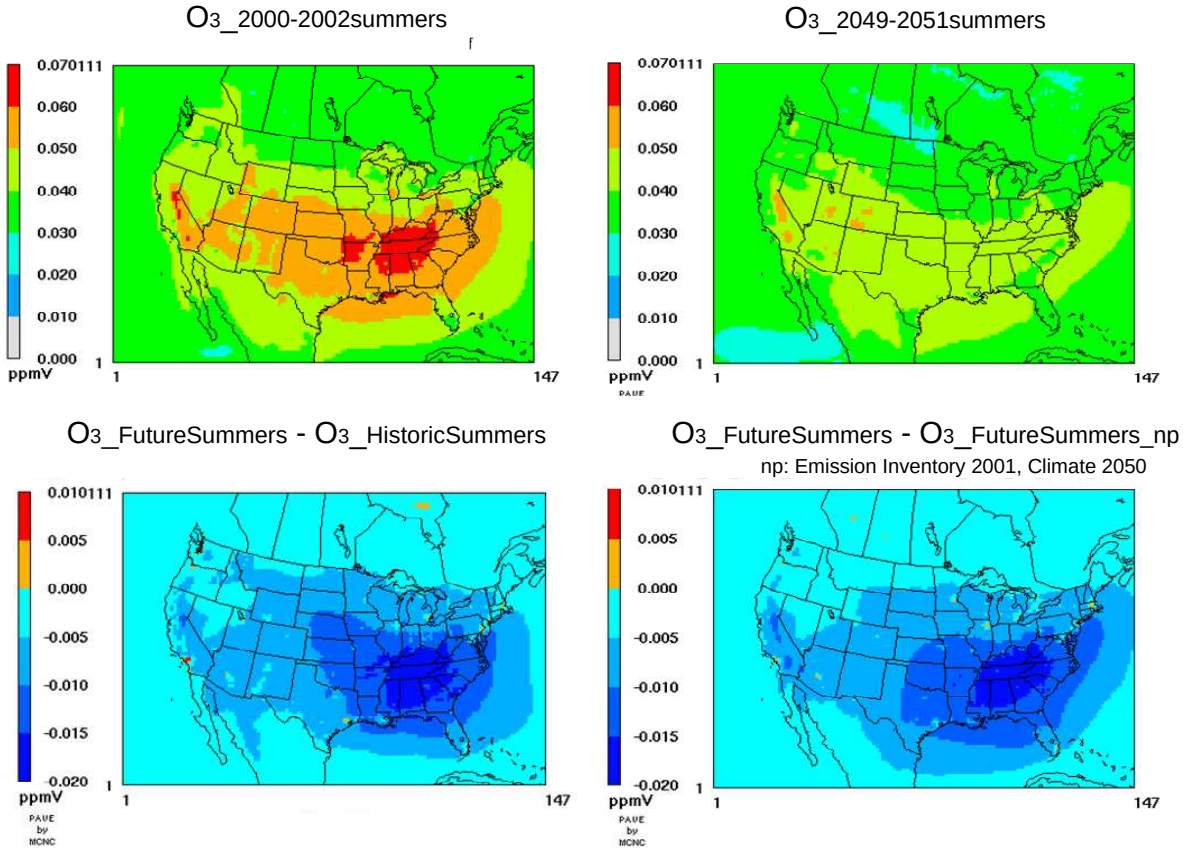


**Figure A.8: Spatial distribution plots of the three summer average ozone concentrations in historic years ($O_3$_2000-2002summers) and future years ($O_3$_2049-2051summers). $O_3$_FutureSummers - $O_3$_HistoricSummers plot presents the effect of climate change and emission controls in future summer ozone concentrations. $O_3$_FutureSummers - $O_3$_ FutureSummers _np plot presents the effect of emission controls**

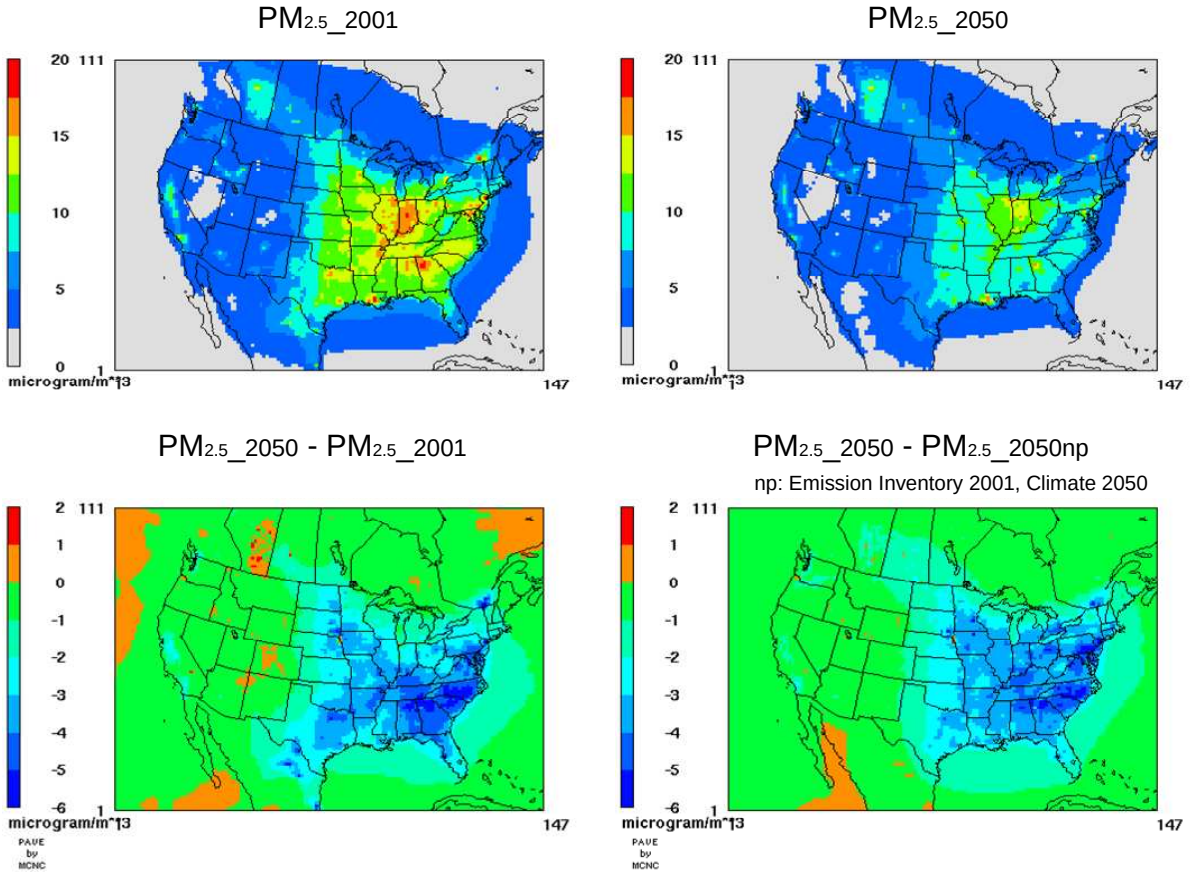


**Figure A.9: Spatial distribution plots of the three summer average $PM_{2.5}$ concentrations in historic years ($PM_{2.5}$_2000-2002summers) and future years ($PM_{2.5}$_2049-2051summers). $PM_{2.5}$_FutureSummers - $PM_{2.5}$_HistoricSummers plot presents the effect of climate change and emission controls in future summer ozone concentrations. $PM_{2.5}$_FutureSummers - $PM_{2.5}$_ FutureSummers _np plot presents the effect of emission controls**

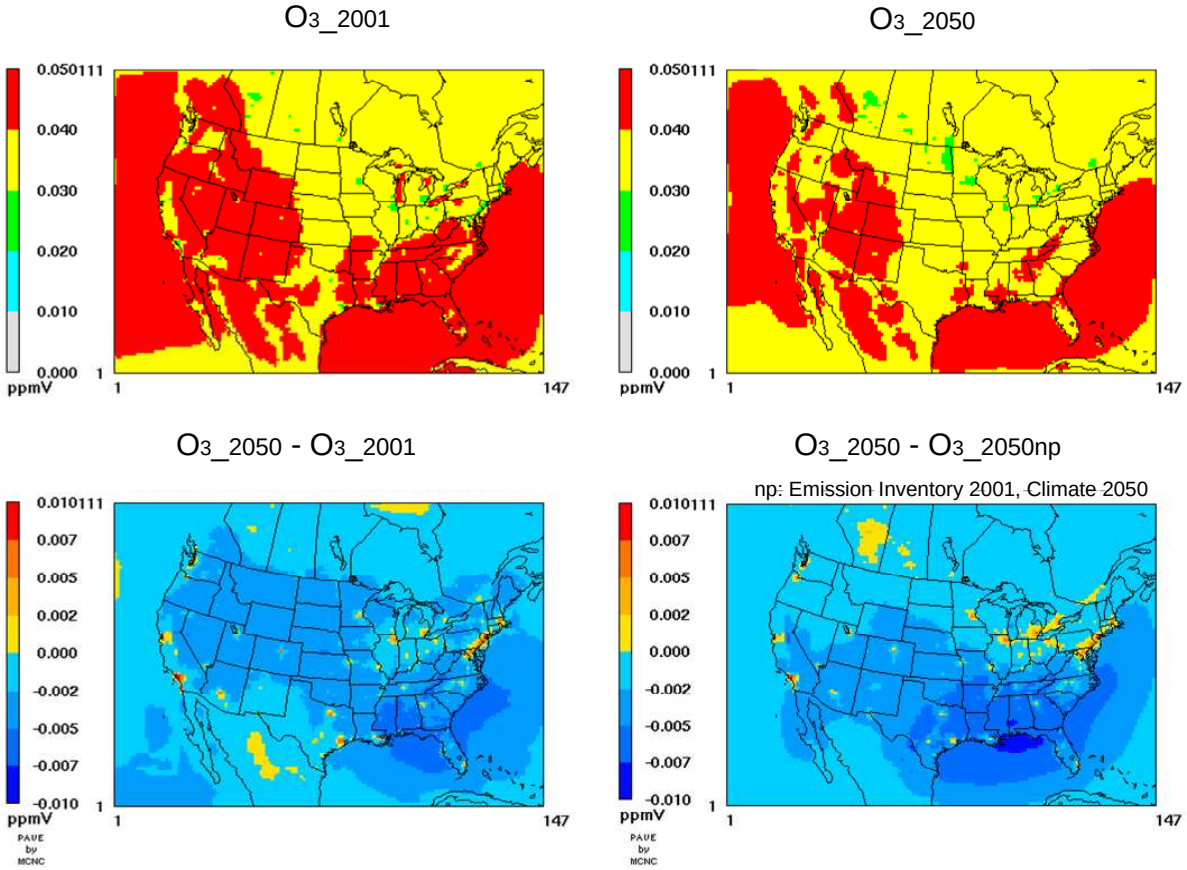


**Figure A.10: Spatial distribution plots of the annual average ozone concentrations in 2001 ($O_3$_2001) and 2050 ($O_3$_2050). $O_3$_2050 - $O_3$_2001 plot presents the effect of climate change and emission controls in future ozone concentrations. $O_3$_2050 - $O_3$_2050_np plot presents the effect of emission controls**

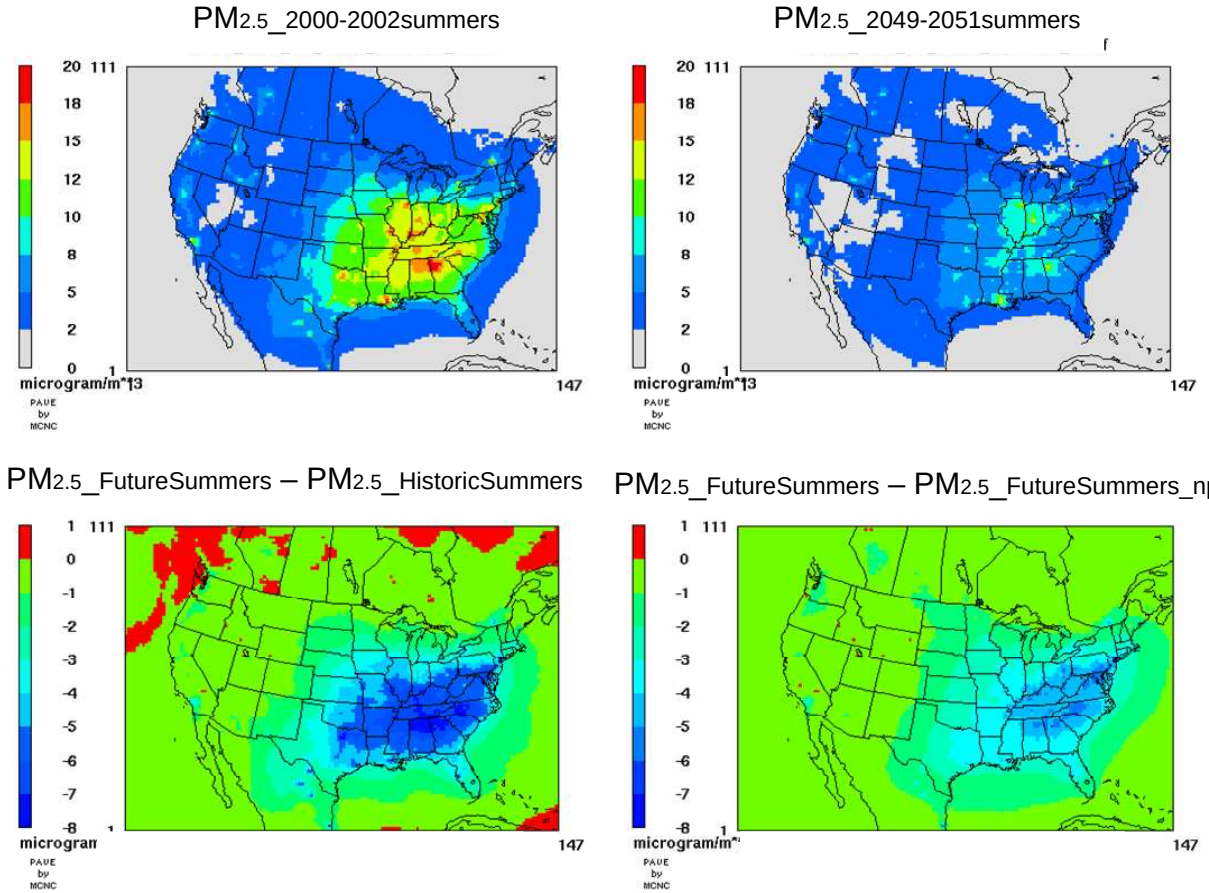


**Figure A.11: Spatial distribution plots of the annual average $PM_{2.5}$ concentrations in 2001 ($PM_{2.5}$_2001) and 2050 ($PM_{2.5}$_2050). $PM_{2.5}$_2050 - $PM_{2.5}$_2001 plot presents the effect of climate change and emission controls in future ozone concentrations. $PM_{2.5}$_2050 - $PM_{2.5}$_2050_np plot presents the effect of emission controls**

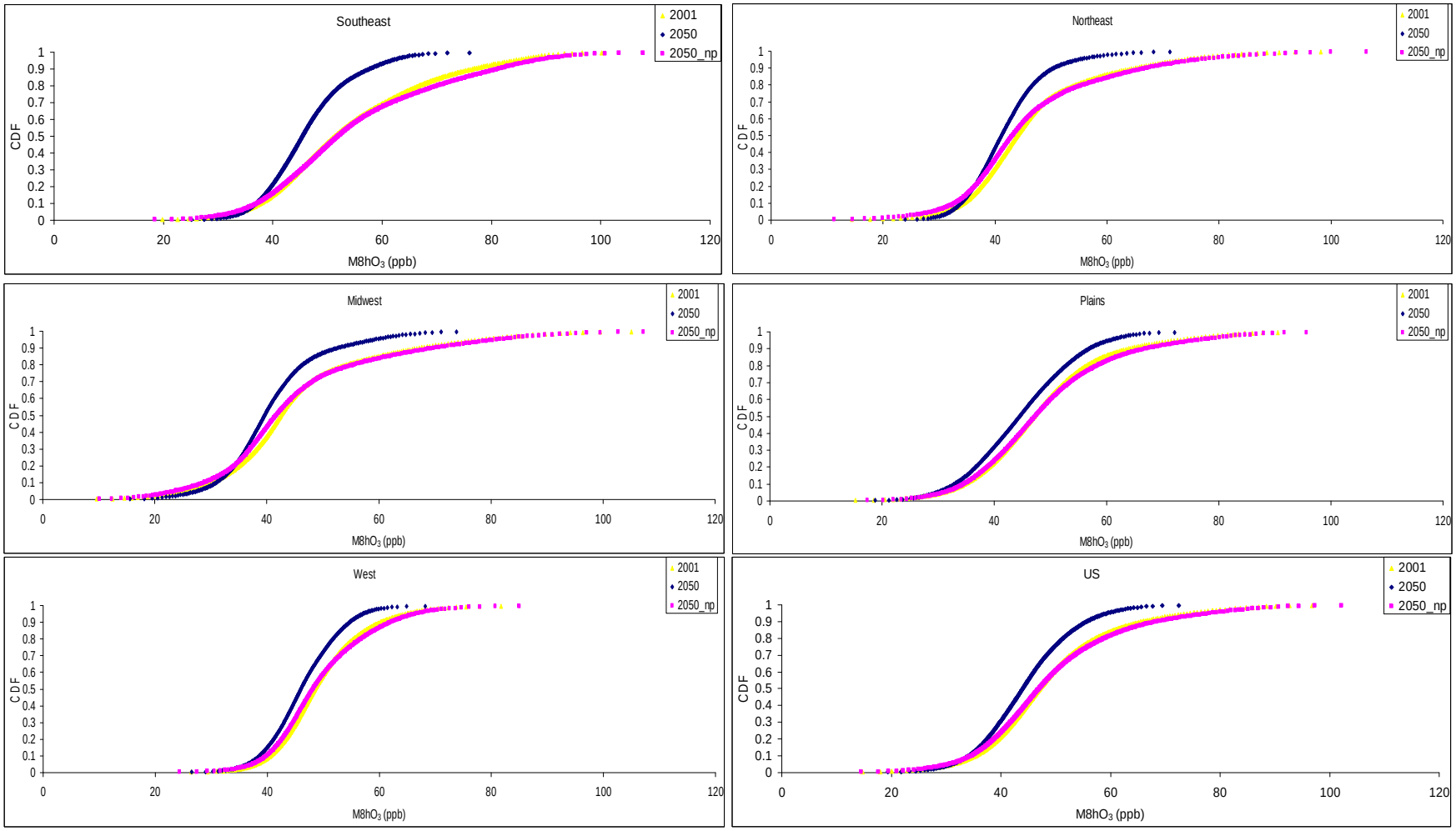


**Figure A.12: Daily maximum 8 hour ozone concentration CDF plots in 2001, 2050 and 2050_np (2001 emission inventory and 2050 meteorology)**

# APPENDIX B

**Table B.1: $4^{th}$ MDA8h ozone concentrations and associated sensitivities: $4^{th}$ MDA8h Ozone to anthropogenic $NO_x$ ($S_{4th\ MDA8h\ O3,NOx}$), anthropogenic VOC ($S_{4th\ MDA8h\ O3,AVOC}$) and biogenic VOC ($S_{4th\ MDA8h\ O3,BVOC}$) emissions (in "ppb"). Percentage (%) of contribution of precursors to $4^{th}$ MDA8h ozone levels are listed at last three columns**

| | ppb | 2001 | 2050_np | 2050 | 2050_Norm | 2000-2002 summers | 2049-2051_np summers | 2049-2051 summers | 2001(%) | 2050_np(%) | 2050 (% ) |
|---|---|---|---|---|---|---|---|---|---|---|---|
| **West** | $4^{th}$ MDA8 h $O_3$ | 65.3 | 66.6 | 56.7 | - | 64.4 | 66.3 | 56.0 | - | - | - |
| | $S_{4th\ MDA8h\ O3,NOx}$ | 13.6 | 14.6 | 9.1 | 20.1 | 13.7 | 16.0 | 10.0 | 20.8 | 21.8 | 15.9 |
| | $S_{4th\ MDA8h\ O3,AVOC}$ | 1.6 | 1.7 | 0.2 | 0.3 | 1.5 | 1.6 | 0.1 | 2.5 | 2.4 | 0.3 |
| | $S_{4th\ MDA8h\ O3,BVOC}$ | 2.6 | 2.8 | 0.0 | 0.00 | 2.4 | 2.20 | -0.2 | 4.0 | 4.1 | -0.1 |
| **Plains** | $4^{th}$ MDA8 h $O_3$ | 72.0 | 72.6 | 59.8 | - | 71.3 | 72.0 | 58.8 | - | - | - |
| | $S_{4th\ MDA8h\ O3,NOx}$ | 20.6 | 19.8 | 14.4 | 32.0 | 21.4 | 21.2 | 15.6 | 28.7 | 27.3 | 24.1 |
| | $S_{4th\ MDA8h\ O3,AVOC}$ | 0.8 | 1.3 | -0.1 | -0.1 | 0.9 | 1.3 | 0.0 | 1.1 | 1.7 | -0.1 |
| | $S_{4th\ MDA8h\ O3,BVOC}$ | 3.8 | 4.1 | 0.40 | 0.3 | 4.1 | 4.5 | 1.3 | 5.2 | 5.7 | 0.7 |
| **Midwest** | $4^{th}$ MDA8 h $O_3$ | 82.7 | 86.1 | 62.6 | - | 85.1 | 84.1 | 61.1 | - | - | - |
| | $S_{4th\ MDA8h\ O3,NOx}$ | 25.4 | 26.8 | 21.1 | 46.8 | 26.9 | 27.2 | 20.3 | 30.7 | 31.1 | 33.6 |
| | $S_{4th\ MDA8h\ O3,AVOC}$ | 2.1 | 2.4 | -0.1 | -0.2 | 2.1 | 2.2 | -0.1 | 2.5 | 2.8 | -0.2 |
| | $S_{4th\ MDA8h\ O3,BVOC}$ | 7.0 | 7.4 | 0.3 | 0.2 | 7.3 | 6.3 | 0.6 | 8.5 | 8.6 | 0.4 |
| **Northeast** | $4^{th}$ MDA8 h $O_3$ | 77.8 | 82.2 | 58.5 | - | 78.0 | 82.5 | 58.5 | - | - | - |
| | $S_{4th\ MDA8h\ O3,NOx}$ | 20.7 | 25.7 | 20.3 | 45.0 | 22.9 | 27.4 | 19.8 | 26.6 | 31.3 | 34.6 |
| | $S_{4th\ MDA8h\ O3,AVOC}$ | 3.3 | 2.5 | -0.1 | -0.2 | 2.4 | 2.2 | -0.1 | 4.2 | 3.0 | -0.2 |
| | $S_{4th\ MDA8h\ O3,BVOC}$ | 5.7 | 6.0 | -0.7 | -0.6 | 5.4 | 4.5 | -0.4 | 7.3 | 7.3 | -1.2 |
| **Southeast** | $4^{th}$ MDA8 h $O_3$ | 87.2 | 91.9 | 63.4 | - | 89.4 | 90.5 | 62.3 | - | - | - |
| | $S_{4th\ MDA8h\ O3,NOx}$ | 31.3 | 31.9 | 22.4 | 49.7 | 32.2 | 33.8 | 23.0 | 35.9 | 34.7 | 35.3 |
| | $S_{4th\ MDA8h\ O3,AVOC}$ | 1.3 | 2.1 | -0.3 | -0.5 | 1.4 | 1.8 | -0.3 | 1.5 | 2.3 | -0.5 |
| | $S_{4th\ MDA8h\ O3,BVOC}$ | 4.6 | 6.1 | -0.7 | -0.6 | 4.5 | 4.0 | -1.3 | 5.2 | 6.6 | -1.1 |
| **US** | $4^{th}$ MDA8 h $O_3$ | 74.9 | 77.1 | 60.0 | - | 75.2 | 76.2 | 59.0 | - | - | - |
| | $S_{4th\ MDA8h\ O3,NOx}$ | 21.4 | 22.0 | 15.9 | 35.3 | 22.3 | 23.3 | 16.5 | 28.5 | 28.5 | 26.5 |
| | $S_{4th\ MDA8h\ O3,AVOC}$ | 1.5 | 1.8 | -0.1 | -0.1 | 1.4 | 1.7 | -0.1 | 1.9 | 2.3 | -0.1 |
| | $S_{4th\ MDA8h\ O3,BVOC}$ | 4.3 | 4.8 | 0.0 | 0.00 | 4.4 | 4.2 | 0.3 | 5.8 | 6.2 | 0.1 |

**Table B.2: Changes in Emissions between 2001 and 2050 with and without Emission Projections *(Tagaris et al., 2007 and Wool et al., 2008)***

| | Differences between 2001 and 2050 | |
|---|---|---|
| | 2050 with emission projections | 2050 without emission projection |
| $NO_x$ | -51 % | +2 % |
| $SO_2$ | -51 % | +4 % |
| VOCs | +2% | + 15% |

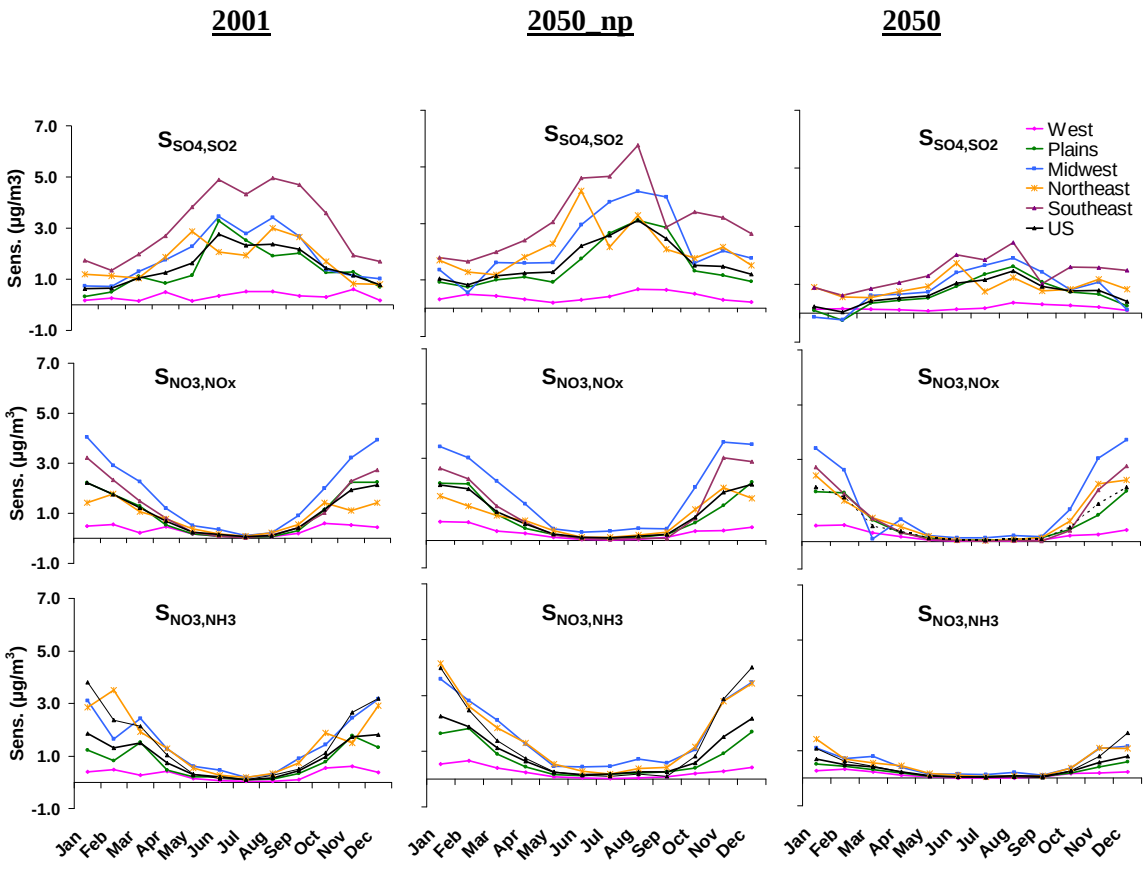


**Figure B.1: Seasonal variation of sensitivities of sulfate to $SO_2$, nitrate to $NO_x$ and nitrate to $NH_3$ for the scenarios of 2001, 2050_np and 2050**

# Appendix C

**Perturbations of the three-dimensional GISS-MM5 climate fields using the two-dimensional IGSM climate fields**

The two-dimensional (latitude and vertical) IGSM fields are expanded into the three-dimensional climate fields and are applied to perturb GISS-MM5 fields using the following steps:

Step 1: Decompose a three-dimensional time-dependent variable of the GISS-MM5 climate $C(y,x,z,t)$ into average and fluctuating terms:

$$C(y,x,z,t) = \overline{C(y,z,m)} + C'(y,x,z,t)$$

where

$C(y,x,z,t)$: Original GISS - MM5 climate

$\overline{C(y,z,m)}$: Longitude - average term of $C(y,x,z,t)$ (steady component of $C(y,x,z,t)$)

$C'(y,x,z,t)$: Fluctuating term of $C(y,x,z,t)$ *and* $\sum_t C'(y,x,z,t) = 0$

y: latitude, z: altitude, x: longitude

m: monthly-averaged values

t: MM5 temporal resolution of every 6-hr

Step 2: Replace the longitude-average term $\overline{C}$ with the 0.5$^{th}$, 50$^{th}$ and 99.5$^{th}$ percentile cases of meteorological fields from IGSM results

Step 3: Reversely convert the new $\overline{C}$ back to C using C' to derive needed three-dimensional meteorological fields

**Table C.1: Annual average zonal (longitude-average) temperatures and their difference from the IGSM outputs for percentiles of 0.5$^{th}$, 5$^{th}$, 50$^{th}$, 95$^{th}$ and 99.5$^{th}$ for five latitudes in 2050**

| | | 2050 Average Zonal Temperature (K) | | | | |
|---|---|---|---|---|---|---|
| Latitude Index | Latitude | 0.5% | 5% | 50% | 95% | 99.5% |
| 1 | 19.6 | 295.3 | 295.3 | 295.9 | 296.6 | 297.5 |
| 2 | 27.4 | 292.0 | 291.9 | 292.8 | 293.1 | 294.1 |
| 3 | 35.2 | 288.2 | 288.4 | 288.6 | 290.0 | 291.1 |
| 4 | 43.0 | 282.4 | 282.8 | 283.3 | 284.2 | 285.4 |
| 5 | 50.9 | 277.3 | 277.8 | 278.2 | 279.1 | 279.8 |
| | | 2050 Average ΔT (K) | | | | |
| Latitude Index | Latitude | 0.5%-50% | 5%-50% | - | 95%-50% | 99.5%-50% |
| 1 | 19.6 | -0.6 | -0.6 | - | 0.7 | 1.6 |
| 2 | 27.4 | -0.8 | -0.9 | - | 0.3 | 1.3 |
| 3 | 35.2 | -0.4 | -0.2 | - | 1.4 | 2.5 |
| 4 | 43.0 | -0.9 | -0.5 | - | 0.9 | 2.1 |
| 5 | 50.9 | -0.9 | -0.4 | - | 0.9 | 1.6 |

**Table C.2: Annualized and summer-averaged emissions of $NO_x$, $SO_2$ and $NH_3$ (tons/day/grid) for the base, low-extreme and high-extreme scenarios in 2050**

| | | Annualized (ton/day/grid) | | | Summer average (ton/day/grid) | | |
|---|---|---|---|---|---|---|---|
| | | Base | Low-extreme | High-extreme | Base | Low-extreme | High-extreme |
| **WS** | $NO_X$ | 2.47 | 2.46 | 2.49 | 2.90 | 2.86 | 2.91 |
| | $SO_2$ | 0.61 | 0.61 | 0.61 | 0.75 | 0.75 | 0.75 |
| | $NH_3$ | 1.47 | 1.47 | 1.47 | 1.66 | 1.66 | 1.66 |
| **PL** | $NO_X$ | 3.41 | 3.38 | 3.50 | 4.11 | 4.09 | 4.24 |
| | $SO_2$ | 1.81 | 1.81 | 1.81 | 2.12 | 2.12 | 2.12 |
| | $NH_3$ | 1.64 | 1.64 | 1.64 | 1.96 | 1.96 | 1.96 |
| **MW** | $NO_X$ | 6.19 | 6.17 | 6.28 | 6.51 | 6.50 | 6.67 |
| | $SO_2$ | 8.22 | 8.22 | 8.22 | 8.74 | 8.74 | 8.74 |
| | $NH_3$ | 3.44 | 3.44 | 3.44 | 3.95 | 3.95 | 3.95 |
| **NE** | $NO_X$ | 7.30 | 7.30 | 7.29 | 6.78 | 6.76 | 6.78 |
| | $SO_2$ | 4.96 | 4.96 | 4.96 | 4.43 | 4.43 | 4.43 |
| | $NH_3$ | 2.46 | 2.46 | 2.46 | 2.88 | 2.88 | 2.88 |
| **SE** | $NO_X$ | 6.58 | 6.55 | 6.60 | 6.81 | 6.77 | 6.83 |
| | $SO_2$ | 5.13 | 5.13 | 5.13 | 5.69 | 5.69 | 5.69 |
| | $NH_3$ | 3.24 | 3.24 | 3.24 | 4.19 | 4.19 | 4.19 |
| **US** | $NO_X$ | 4.42 | 4.39 | 4.47 | 4.83 | 4.81 | 4.91 |
| | $SO_2$ | 3.35 | 3.35 | 3.35 | 3.63 | 3.63 | 3.63 |
| | $NH_3$ | 2.21 | 2.21 | 2.21 | 2.63 | 2.63 | 2.63 |

# Appendix D

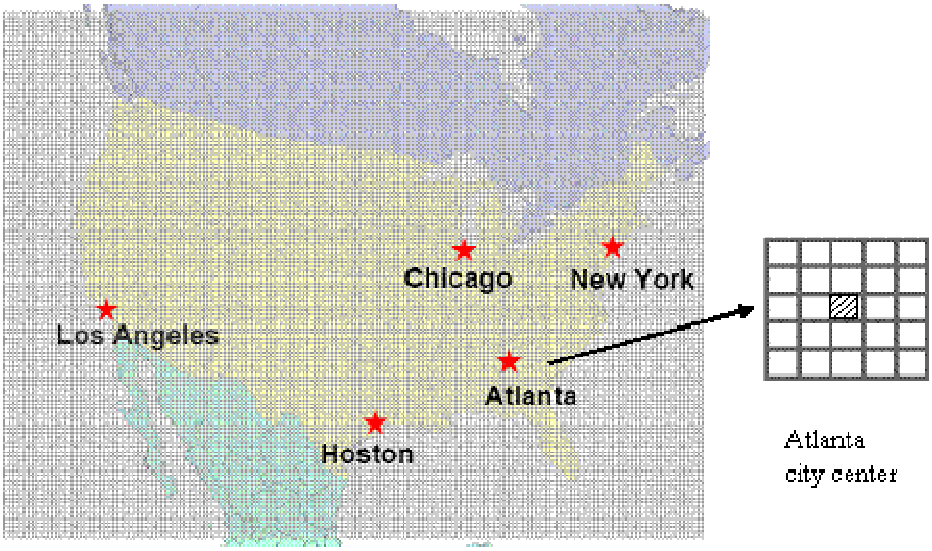


**Figure D.1: Simulation domain and the five cities examined. Also shown is the 5x5 grid used for identifying the regional maximum, as applied to Atlanta for an example.**

2001 City Center 2050 City Center 2001 Regional Maximum

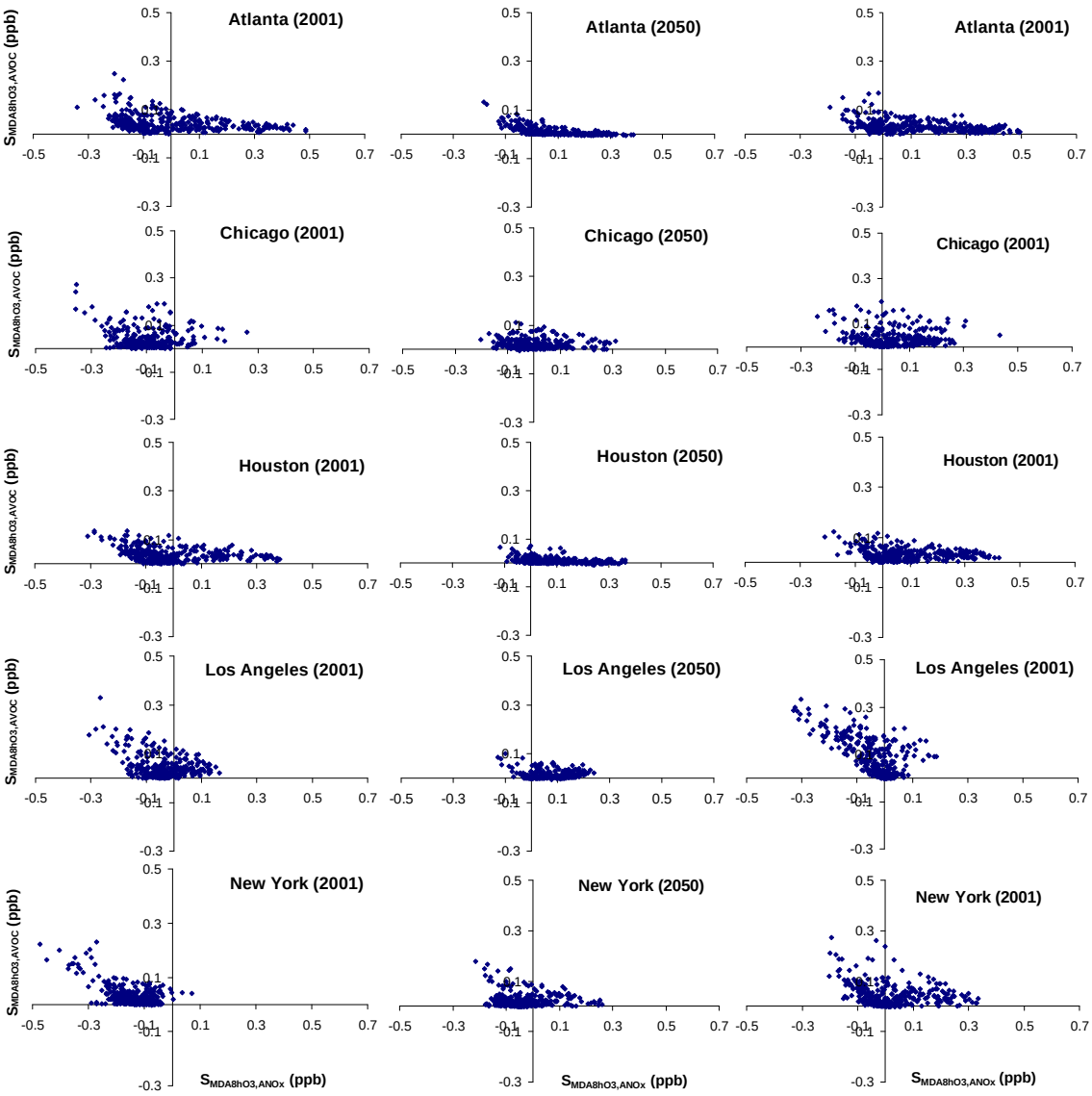


**Figure D.2: Sensitivity of MDA8h ozone to anthropogenic $NO_x$ (X-axis, in ppb/%) and VOC (Y-axis, in ppb/%) emissions for 2001 (left column) and 2050 (middle column) city centers and 2001 regional maximum levels**

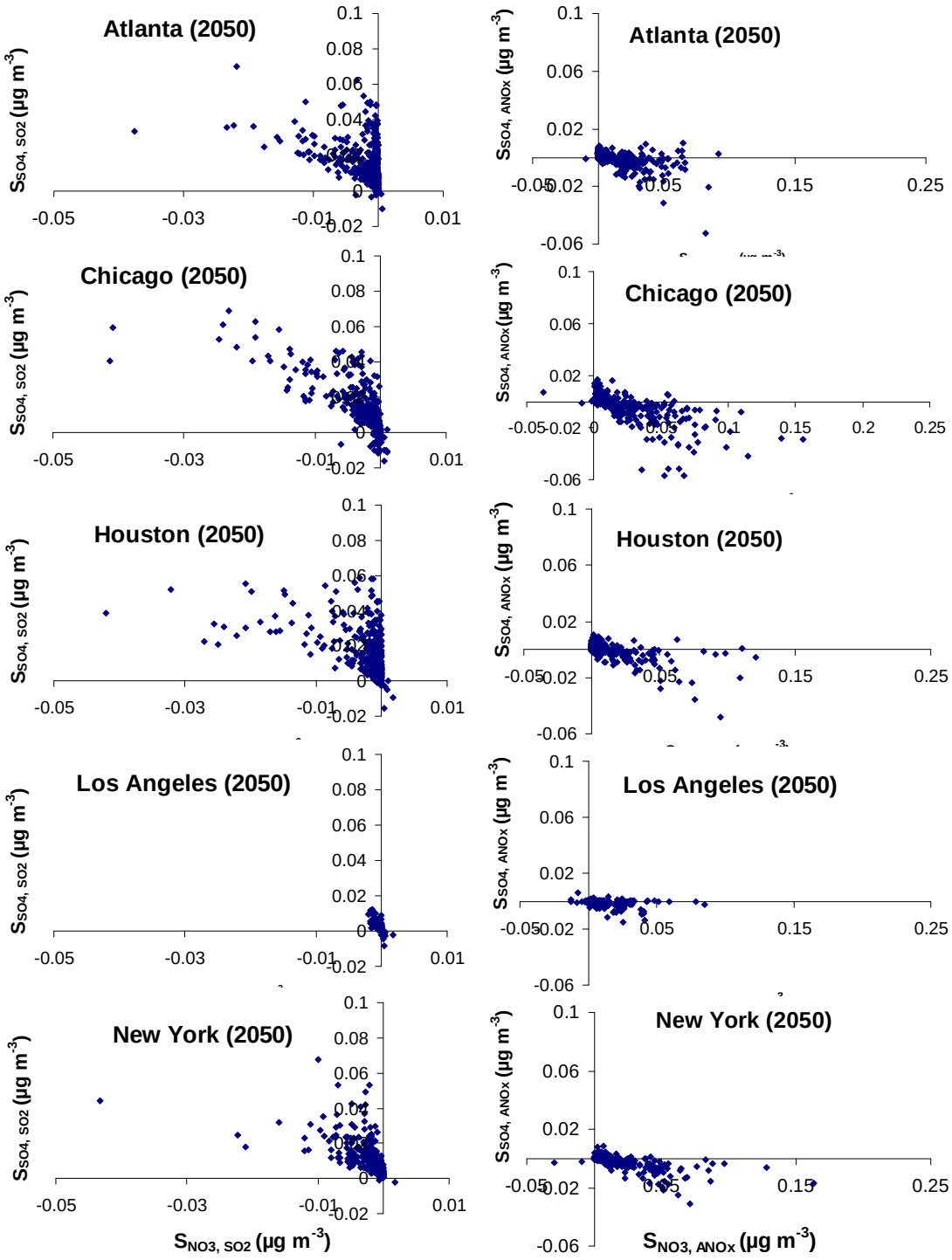


**Figure D.3: Sensitivities of sulfate and nitrate $PM_{2.5}$ (in µg m$^{-3}$, X-axis) to a 1% change in anthropogenic $NO_x$ emissions ($S_{SO4,ANOx}$ and $S_{NO3,ANOx}$, in µg m$^{-3}$, right figures) and to a 1% changes in $SO_2$ emissions ($S_{SO4,SO2}$ and $S_{NO3,SO2}$, in µg m$^{-3}$, left figures) in 2050 for city centers**

**Table D.1: Domain-wide Daily-average total $SO_2$, $NH_3$ as well as Anthropogenic, Biogenic and Total VOC Emissions (in tons/ day) in 2001 and 2050 and Differences (in %) in Emission between 2001 and 2050**

| | 2001 (tons/day) | 2050 (tons/day) | Difference (%) [a] |
|---|---|---|---|
| Anthropogenic $NO_x$ [b] | 69953 | 31512 | -55 |
| Total $SO_2$ | 53832 | 26266 | -51 |
| Total $NH_3$ | 13582 | 14566 | +7 |
| Anthropogenic VOC | 57067 | 35333 | -38 |
| Biogenic VOC | 111909 | 135839 | +21 |
| Total VOC [c] | 168978 | 171172 | +2 |

[a] Difference (%) = $\left(\frac{2050\ Emission - 2001\ Emission}{2001\ Emission}\right) * 100\%$

[b] Total $NO_x$ emissions are predicted to decrease 51% in 2050. (6)

[c] Total VOC emissions are predicted to increase 15% in 2050 without emission controls. (6)

**Table D.2: Slopes[1] ((ppb/%)/ppb), Intercepts[2] (ppb/%), Correlation Coefficients[3] ($r^2$) of Sensitivity of MDA8h $O_3$ to Anthropogenic $NO_x$ Emissions ($S_{MDA8hO3, NOx}$) (Y-axis) versus MDA8h $O_3$ (X-axis) and MDA8h $O_3$ values[4] at which regression suggests $NO_x$ reduction is effective for decreasing MDA8h $O_3$ for city center and regional maximum MDA8h $O_3$ 2001 and city center in 2050**

| | 2001 city center | 2050 city center | 2001 regional maximum |
|---|---|---|---|
| Atlanta | 0.006[1] / -0.37[2] / 0.77[3] / 61.7[4] | 0.010 / -0.37 / 0.76 / 37.0 | 0.007 / -0.37 / 0.84 / 52.9 |
| Chicago | 0.002 / -0.17 / 0.22 / 85.0 | 0.005 / -0.19 / 0.63 / 38.0 | 0.003 / -0.16 / 0.44 / 53.3 |
| Houston | 0.005 / -0.26 / 0.67 / 52.0 | 0.007 / -0.25 / 0.81 / 35.7 | 0.005 / -0.25 / 0.71 / 50.0 |
| Los Angeles | 0.002 / -0.14 / 0.13 / 70.0 | 0.006 / -0.24 / 0.62 / 40.0 | -0.001 / 0.03 / 0.07 / 30.0 |
| New York | 0.000 / -0.15 / 0.00 / N.A.[a] | 0.005 / -0.23 / 0.53 / 46.0 | 0.004 / -0.22 / 0.42 / 55.5 |

[a] N.A. = Not applicable

**Table D.3: Sensitivities of the Regional Maximum and City-center 4th MDA8h ozone ($S_{4thMDA8h\ O3,ANOx}$ & $S_{4thMDA8h\ O3,AVOC}$) and City-center Annual-average of the MDA8h ozone ($S_{MDA8h\ O3,ANOx}$ & $S_{MDA8h\ O3,AVOC}$), Annual-average of Ozone to Anthropogenic $NO_x$ and VOC Emissions ($S_{O3,ANOx}$ & $S_{O3,AVOC}$) and Sensitivities of Annual 24-hr Average $PM_{2.5}$ to $SO_2$ ($S_{PM2.5,SO2}$) and Anthropogenic $NO_x$ ($S_{PM2.5,ANOx}$) Emissions**

| **2001** | Regional max. $S_{4thMDA8hO3,ANOx}$ (ppb/%) | Regional max. $S_{4thMDA8hO3,AVOC}$ (ppb/%) | City-center $S_{4thMDA8hO3,ANOx}$ (ppb/%) | City-center $S_{4thMDA8hO3,AVOC}$ (ppb/%) | City-center $S_{MDA8hO3,ANOx}$ (ppb/%) | City-center $S_{MDA8hO3,AVOC}$ (ppb/%) | City-center $S_{O3,ANOx}$ (ppb/%) | City-center $S_{O3,AVOC}$ (ppb/%) | City-center $S_{PM2.5,SO2}$ ($\mu g\ m^{-3}$/%) | City-center $S_{PM25,ANOx}$ ($\mu g\ m^{-3}$/%) |
|---|---|---|---|---|---|---|---|---|---|---|
| Atlanta | 0.42 | 0.04 | 0.42 | 0.04 | 0.00 | 0.04 | -0.06 | 0.03 | 0.04 | 0.02 |
| Chicago | 0.43 | 0.05 | 0.26 | 0.07 | -0.10 | 0.04 | -0.11 | 0.02 | 0.02 | 0.03 |
| Houston | 0.32 | 0.04 | 0.28 | 0.06 | -0.01 | 0.04 | -0.05 | 0.02 | 0.03 | 0.02 |
| Los Angeles | -0.31** | 0.33 | 0.05 | 0.10 | -0.04 | 0.04 | -0.07 | 0.02 | 0.00 | 0.01 |
| New York | 0.15 | 0.12 | -0.29 | 0.20 | -0.15 | 0.03 | -0.11 | 0.01 | 0.02 | 0.02 |
| **2050** | | | | | | | | | | |
| Atlanta | 0.37 | 0.01 | 0.35 | 0.00 | 0.10 | 0.01 | 0.04 | 0.00 | 0.02 | 0.02 |
| Chicago | 0.24 | 0.04 | 0.19 | 0.06 | 0.00 | 0.02 | -0.05 | 0.01 | 0.01 | 0.02 |
| Houston | 0.38 | 0.01 | 0.30 | 0.02 | 0.10 | 0.01 | 0.04 | 0.06 | 0.02 | 0.01 |
| Los Angeles | 0.16 | 0.09 | 0.17 | 0.05 | 0.06 | 0.01 | 0.02 | 0.01 | 0.00 | 0.00 |
| New York | 0.31 | 0.01 | 0.11 | 0.08 | -0.04 | 0.02 | -0.08 | 0.01 | 0.01 | 0.02 |

**Sensitivities of the 4th highest ozone levels to NOx scatter about zero for ozone levels above about 75 ppb, with both positive and negative values.

# Appendix E

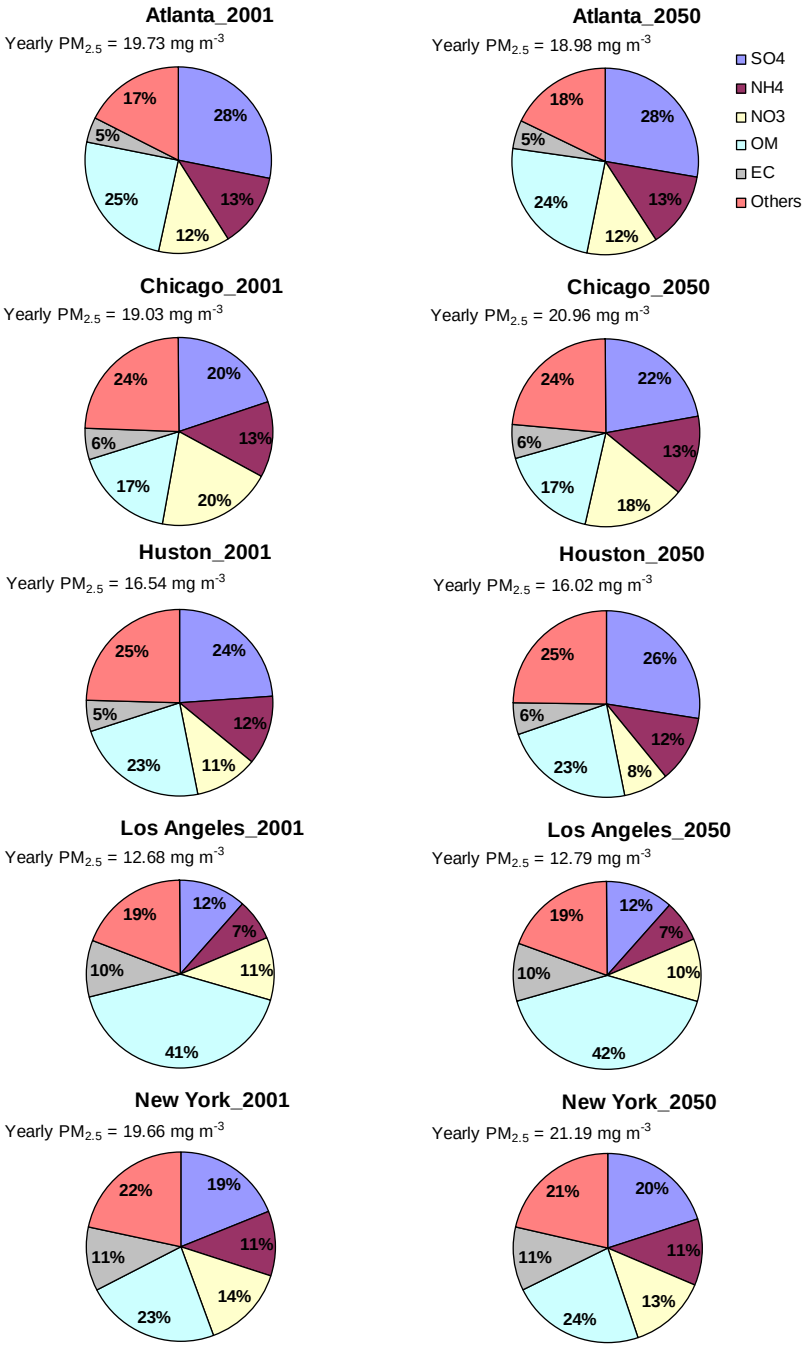


**Figure E.1: Yearly-average $PM_{2.5}$ composition in 2001 and 2050 for the five cities; including $SO_4$: sulfate, $NH_4$: ammonium, $NO_3$: nitrate, OM: organic matter, EC: elementary carbon and others species**

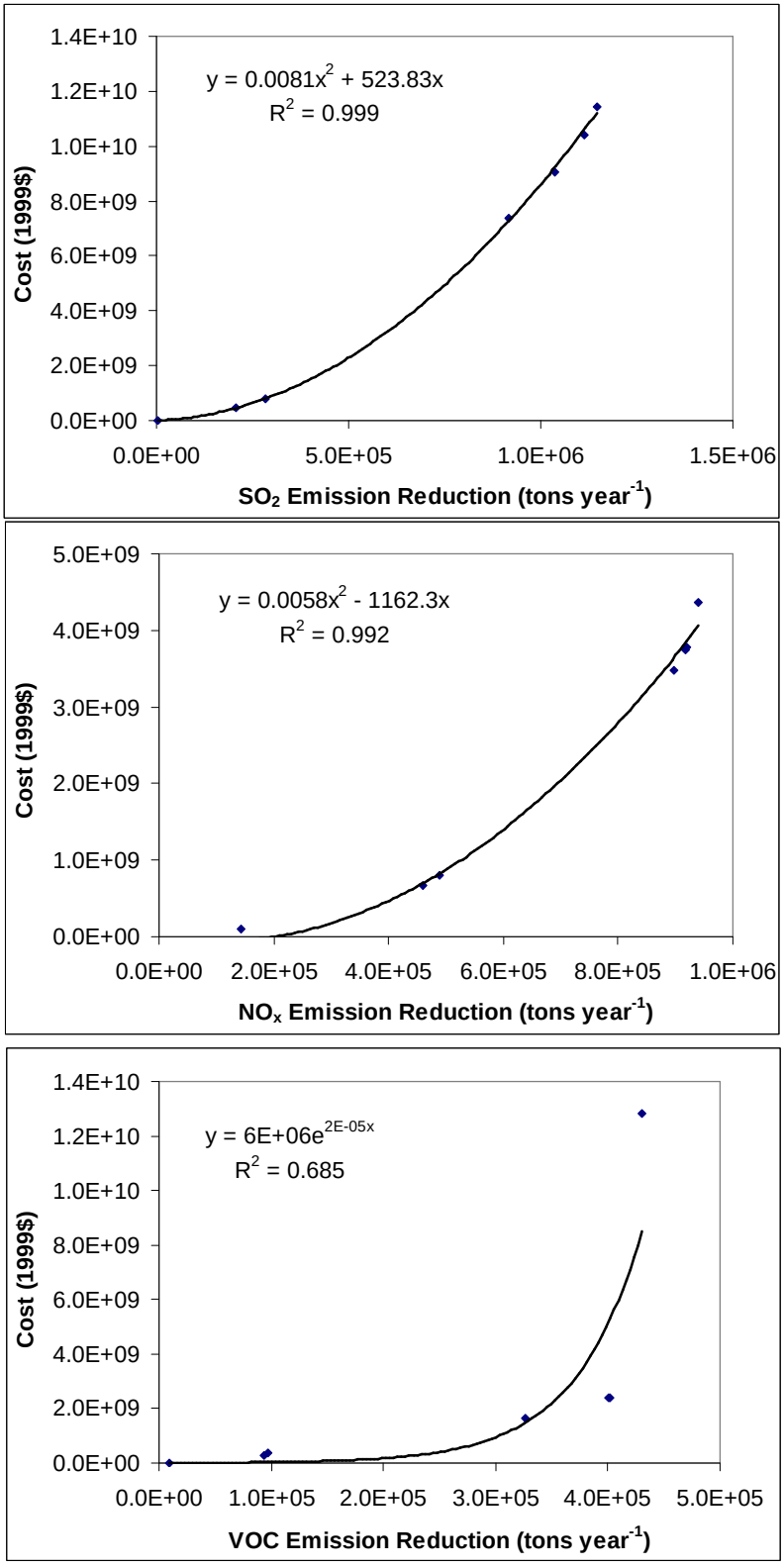


**Figure E.2: Relationship between cost and emission reductions in Atlanta MSA states**

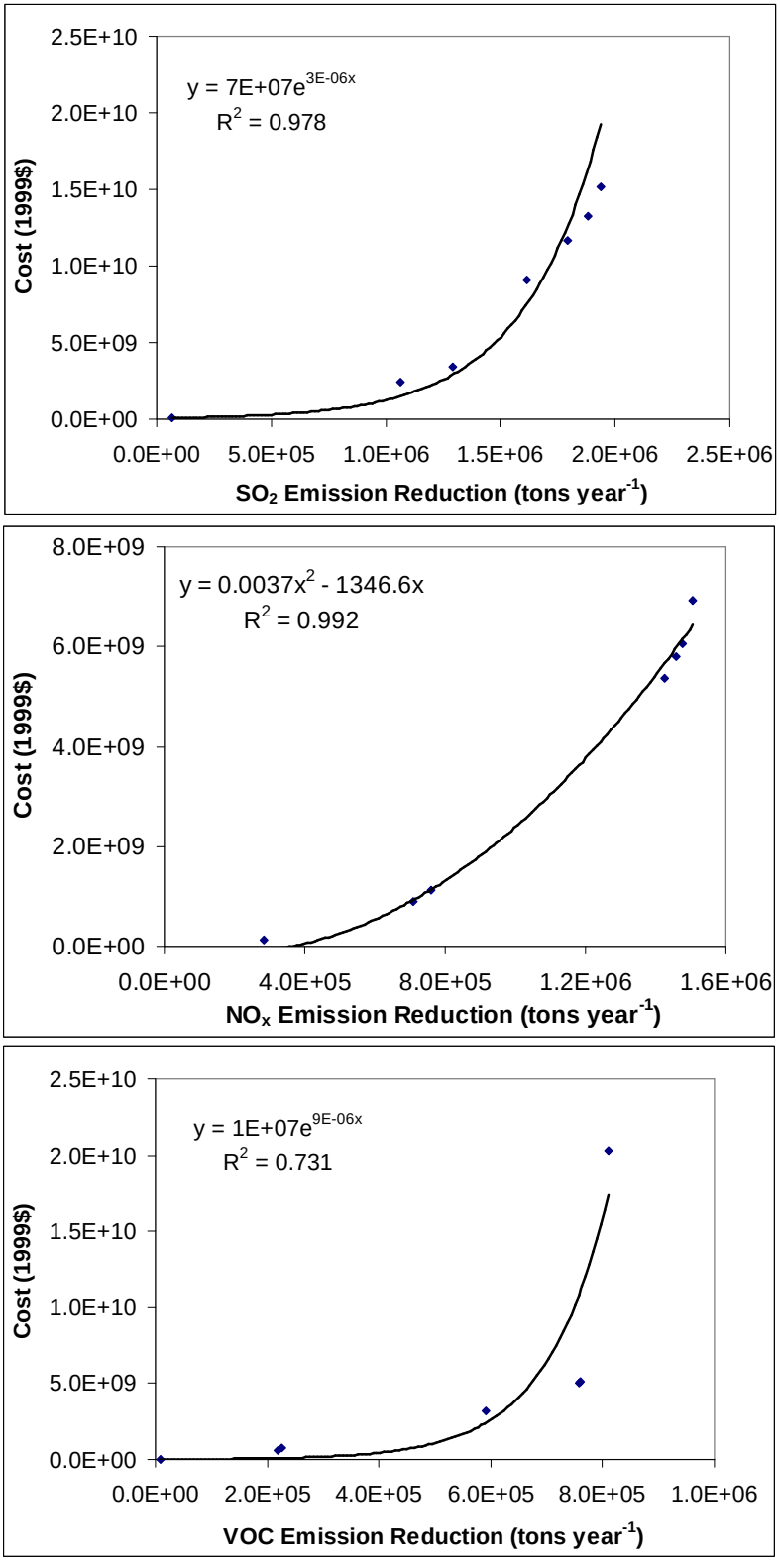


**Figure E.3: Relationship between cost and emission reductions in Chicago MSA states**

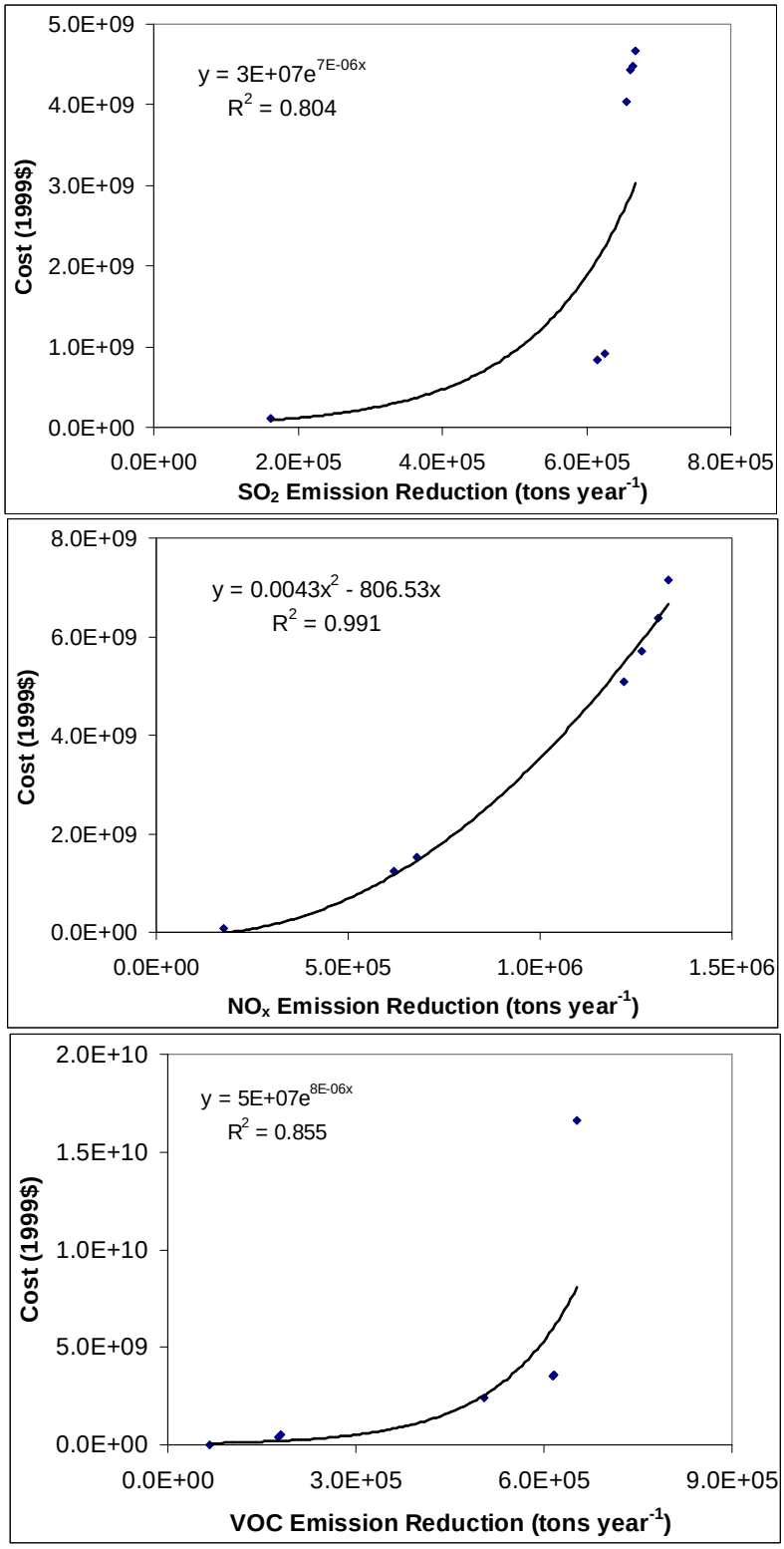


**Figure E.4: Relationship between cost and emission reductions in Houston MSA states**

**Development of Least-cost Cost Control Strategies**

1. Development of cost function for $SO_2$, $NO_x$ and VOC reductions

$$Toal\ Cost = \cos t\ of\ SO_2\ reductions + \cos t\ of\ NOx\ reductions + \cos t\ of\ VOC\ reductions$$

2. Setting up constraints of optimization problems using sensitivities results from CMAQ-DDM simulations

$$\Delta\varepsilon_{ANOx} S_{O3,ANOx} + \Delta\varepsilon_{AVOC} S_{O3,AVOC} \geq C_{O3,2050} - C_{O3,2001}$$
$$\Delta\varepsilon_{SO2} S_{PM\,2.5,SO2} + \Delta\varepsilon_{ANOx} S_{PM\,2.5,NOx} + \Delta\varepsilon_{VOC} S_{PM\,2.5,VOC} \geq C_{PM\,2.5,2050} - C_{PM\,2.5,2001}$$

3. Minimization of cost of emission reductions for offsetting the impacts of climate change on air quality

$\min imize$ *Cost Function*

*subjective to*:

$$\Delta\varepsilon_{ANOx} S_{O3,ANOx} + \Delta\varepsilon_{AVOC} S_{O3,AVOC} \geq C_{O3,2050} - C_{O3,2001}$$
$$\Delta\varepsilon_{SO2} S_{PM\,2.5,SO2} + \Delta\varepsilon_{ANOx} S_{PM\,2.5,NOx} + \Delta\varepsilon_{VOC} S_{PM\,2.5,VOC} \geq C_{PM\,2.5,2050} - C_{PM\,2.5,2001}$$
$$0 \leq \Delta\varepsilon_{SO2} \leq R_{SO2}$$
$$0 \leq \Delta\varepsilon_{ANOx} \leq R_{ANOx}$$
$$0 \leq \Delta\varepsilon_{AVOC} \leq R_{AVOC}$$

*where*

$\Delta\varepsilon_{SO2}$, $\Delta\varepsilon_{ANOx}$ *and* $\Delta\varepsilon_{AVOC}$ *are reduction ratios of* $SO_2$, $NO_x$ *and VOC emissionsfor offsetting impacts of* $c\lim ate$ *change on ozone and* $PM_{2.5}$

$R$: *Maximum available removal efficiency*; $R_{SO2} = 0.712$; $R_{ANOx} = 0.670$; $R_{AVOC} = 0.450$

# REFERENCES


Akimoto, H. (2003), Global air quality and pollution, *Science, 302*, 1716-1719.

Ansari, A. S., and S. N. Pandis (1998), Response of inorganic PM to precursor concentrations, *Environmental Science & Technology, 32*, 2706-2714.

Aw, J., and M. J. Kleeman (2003), Evaluating the first-order effect of intraannual temperature variability on urban air pollution, *Journal of Geophysical Research-Atmospheres, 108*.

Baertsch-Ritter, N., et al. (2004), Effects of various meteorological conditions and spatial emission resolutions on the ozone concentration and ROG/NOx limitation in the Milan area (I), *Atmospheric Chemistry and Physics, 4*, 423-438.

Bell, M. L., et al. (2004), Ozone and short-term mortality in 95 US urban communities, 1987-2000, *Jama-Journal of the American Medical Association, 292*, 2372-2378.

Bergin, M. S., et al. (1999), Formal uncertainty analysis of a Lagrangian photochemical air pollution model, *Environmental Science & Technology, 33*, 1116-1126.

Bergstrom, A. K., and M. Jansson (2006), Atmospheric nitrogen deposition has caused nitrogen enrichment and eutrophication of lakes in the northern hemisphere, *Global Change Biology, 12*, 635-643.

Bernard, S. M., et al. (2001), The potential impacts of climate variability and change on air pollution-related health effects in the United States, *Environmental Health Perspectives, 109*, 199-209.

Bragazza, L., et al. (2006), Atmospheric nitrogen deposition promotes carbon loss from peat bogs, *Proceedings of the National Academy of Sciences of the United States of America, 103*, 19386-19389.

Brasseur, G. P., et al. (2006), Impact of climate change on the future chemical composition of the global troposphere, *Journal of Climate, 19*, 3932-3951.

Burnett, R. T., et al. (1997), The role of particulate size and chemistry in the association between summertime ambient air pollution and hospitalization for cardiorespiratory diseases, *Environmental Health Perspectives, 105*, 614-620.

Byun, D. W., and K. L. Schere (2006), Review of the governing equations, computational algorithms, and other components of the Models-3 Community Multscale Air Quality (CMAQ) modeling system, *Appl. Mech. Rev.*, 51-77.

Carter, W. P. L. (2000), *Documentation of the SAPRC-99 Chemical Mechanism for VOC Reactivity Assessment. Final Report to California Air Resources Board, Contract No. 92-329, and 95-308*.

Casimiro, E., et al. (2006), National assessment of human health effects of climate change in Portugal: Approach and key findings, *Environmental Health Perspectives*, *114*, 1950-1956.

Chen, J. J., and R. J. Griffin (2005), Modeling secondary organic aerosol formation from oxidation of alpha-pinene, beta-pinene, and d-limonene, *Atmospheric Environment*, *39*, 7731-7744.

Chow, J. C., et al. (1994), Temporal and Spatial Variations of Pm(2.5) and Pm(10) Aerosol in the Southern California Air-Quality Study, *Atmospheric Environment*, *28*, 2061-2080.

Chung, S. H., and J. H. Seinfeld (2002), Global distribution and climate forcing of carbonaceous aerosols, *Journal of Geophysical Research-Atmospheres*, *107*.

Claeys, M., et al. (2004a), Formation of secondary organic aerosols through photooxidation of isoprene, *Science*, *303*, 1173-1176.

Claeys, M., et al. (2004b), Formation of secondary organic aerosols from isoprene and its gas-phase oxidation products through reaction with hydrogen peroxide, *Atmospheric Environment*, *38*, 4093-4098.

Cohan, D. S., et al. (2005), Nonlinear response of ozone to emissions: Source apportionment and sensitivity analysis, *Environmental Science & Technology*, *39*, 6739-6748.

Cohan, D. S., et al. (2006), Control strategy optimization for attainment and exposure mitigation: Case study for ozone in Macon, Georgia, *Environmental Management*, *38*, 451-462.

Dawson, J. P., et al. (2007), Sensitivity of ozone to summertime climate in the eastern USA: A modeling case study, *Atmospheric Environment*, *41*, 1494-1511.

de Gouw, J. A., et al. (2003), Validation of proton transfer reaction-mass spectrometry (PTR-MS) measurements of gas-phase organic compounds in the atmosphere during the

New England Air Quality Study (NEAQS) in 2002, *Journal of Geophysical Research-Atmospheres, 108*.

Dentener, F., et al. (2006), The global atmospheric environment for the next generation, *Environmental Science & Technology*, *40*, 3586-3594.

Dunker, A. M. (1981), Efficient Calculation of Sensitivity Coefficients for Complex Atmospheric Models, *Atmospheric Environment, 15*, 1155-1161.

Dunker, A. M. (1984), The Decoupled Direct Method for Calculating Sensitivity Coefficients in Chemical-Kinetics, *Journal of Chemical Physics*, *81*, 2385-2393.

Dunker, A. M., et al. (2002), The decoupled direct method for sensitivity analysis in a three-dimensional air quality model - Implementation, accuracy, and efficiency, *Environmental Science & Technology*, *36*, 2965-2976.

E.H. Pechan & Associates, I. (2006a), AirControlNet Version4.1 Document Report.

E.H. Pechan & Associates, I. (2006b), AirControlNet Version4.1 Documentation Report.

E.H. Pechan & Associates, I. (2006c), Technical Support Document for 2002 MANE-VU SIP Modeling Inventories, Version 3.

El-Fadel, M., and M. Massoud (2000), Particulate matter in urban areas: health-based economic assessment, *Science of the Total Environment, 257*, 133-146.

EPA (2005), Regulatory Impact Analysis for the Final Clean Air Interstate Rule, Office of Air and Radiation, U.S. Environmental Protection Agency.

Galizia, A., and P. L. Kinney (1999), Long-term residence in areas of high ozone: Associations with respiratory health in a nationwide sample of nonsmoking young adults, *Environmental Health Perspectives, 107*, 675-679.

Gilliland, A. B., et al. (2003), Seasonal NH3 emission estimates for the eastern United States based on ammonium wet concentrations and an inverse modeling method, *Journal of Geophysical Research-Atmospheres, 108*.

Giorgi, F., and G. T. Bates (1989), The Climatological Skill of a Regional Model over Complex Terrain, *Monthly Weather Review*, *117*, 2325-2347.

Grell, G., et al. (1994), A description of the fifth generation Penn State/NCAR mesoscale model (MM5), NCAR Tech. Note, NCAR/TN-398+STR, Natl. Cent for Atmos. Res., Boulder, Colorado.

Gustafson, W. I., and L. R. Leung (2007), Regional downscaling for air quality assessment - A reasonable proposition?, *Bulletin of the American Meteorological Society, 88*, 1215-1227.

Hanna, S. R., et al. (2001), Uncertainties in predicted ozone concentrations due to input uncertainties for the UAM-V photochemical grid model applied to the July 1995 OTAG domain, *Atmospheric Environment, 35*, 891-903.

Hanna, S. R., et al. (2005), Monte Carlo estimation of uncertainties in BEIS3 emission outputs and their effects on uncertainties in chemical transport model predictions, *Journal of Geophysical Research-Atmospheres, 110*.

Henze, D. K., and J. H. Seinfeld (2006), Global secondary organic aerosol from isoprene oxidation, *Geophysical Research Letters, 33*.

Hogrefe, C., et al. (2004), Simulating changes in regional air pollution over the eastern United States due to changes in global and regional climate and emissions, *Journal of Geophysical Research-Atmospheres, 109*.

Holland, E. A., et al. (2005), Nitrogen deposition onto the United States and western Europe: Synthesis of observations and models, *Ecological Applications, 15*, 38-57.

Holzer, M., and G. J. Boer (2001), Simulated changes in atmospheric transport climate, *Journal of Climate, 14*, 4398-4420.

Houyoux, M. (2004), *CAIR Emissions Inventory Overview, US EPA*.

IPCC (2001), Climate change 2001: The Science of Climate Change, IPCC(Intergovernmental Panel on Climate Change) Cambridge, UK.

Jang, I., et al. (2006), Methane oxidation rates in forest soils and their controlling variables: a review and a case study in Korea, *Ecological Research, 21*, 849-854.

Johnson, P. R. S., and J. J. Graham (2005), Fine particulate matter National Ambient Air Quality standards: Public health impact on populations in the northeastern United States, *Environmental Health Perspectives, 113*, 1140-1147.

Karl, T. R., and K. E. Trenberth (2003), Modern global climate change, *Science, 302*, 1719-1723.

Kleinman, L. I. (2000), Ozone process insights from field experiments - part II: Observation-based analysis for ozone production, *Atmospheric Environment, 34*, 2023-2033.

Knowlton, K., et al. (2004), Assessing ozone-related health impacts under a changing climate, *Environmental Health Perspectives*, *112*, 1557-1563.

Kroll, J. H., et al. (2006), Secondary organic aerosol formation from isoprene photooxidation, *Environmental Science & Technology*, *40*, 1869-1877.

Lamarque, J. F., et al. (2005), Response of a coupled chemistry-climate model to changes in aerosol emissions: Global impact on the hydrological cycle and the tropospheric burdens of OH, ozone, and NOx, *Geophysical Research Letters*, *32*.

Langner, J., et al. (2005), Impact of climate change on surface ozone and deposition of sulphur and nitrogen in Europe, *Atmospheric Environment*, *39*, 1129-1141.

Lathiere, J., et al. (2005), Past and future changes in biogenic volatile organic compound emissions simulated with a global dynamic vegetation model, *Geophysical Research Letters*, *32*.

Lefohn, A. S., et al. (1998), The difficult challenge of attaining EPA's new ozone standard, *Environmental Science & Technology*, *32*, 276A-282A.

Leung, L. R., and W. I. Gustafson (2005), Potential regional climate change and implications to US air quality, *Geophysical Research Letters*, *32*.

Levy, J. I., et al. (2001), Assessing the public health benefits of reduced ozone concentrations, *Environmental Health Perspectives*, *109*, 1215-1226.

Liao, H., et al. (2006), Role of climate change in global predictions of future tropospheric ozone and aerosols, *Journal of Geophysical Research-Atmospheres*, *111*.

Liao, K. J., et al. (2007), Sensitivities of ozone and fine particulate matter formation to emissions under the impact of potential future climate change, *Environmental Science & Technology*, *41*, 8355-8361.

Liao, K. J., et al. (2008), Quantification of impact of climate uncertainty on regional air quality, *published in the Atmospheric Chemistry and Physics Discussions and under revire for publishing in the Atmospheric Chemistry and Physics*.

Lim, Y. B., and P. J. Ziemann (2005), Products and mechanism of secondary organic aerosol formation from reactions of n-alkanes with OH radicals in the presence of NOx, *Environmental Science & Technology*, *39*, 9229-9236.

Lippmann, M. (1993), Health-Effects of Tropospheric Ozone - Review of Recent Research Findings and Their Implications to Ambient Air-Quality Standards, *Journal of Exposure Analysis and Environmental Epidemiology, 3*, 103-129.

Mastrandrea, M. D., and S. H. Schneider (2004), Probabilistic integrated assessment of "dangerous" climate change, *Science, 304*, 571-575.

Mendoza-Dominguez, A., and A. G. Russell (2001), Emission Strength Validation Using Four-Dimensional Data Assimilation: Application to Primary Aerosol and Precursors to Ozone and Secondary Aerosol, *Journal of the Air & Waste Management Association (1995), 51*, 1538-1550.

Menut, L. (2003), Adjoint modeling for atmospheric pollution process sensitivity at regional scale, *Journal of Geophysical Research-Atmospheres, 108*.

Mickley, L. J., et al. (2004), Effects of future climate change on regional air pollution episodes in the United States, *Geophysical Research Letters, 31*.

Milford, J. B., et al. (1994), Total Reactive Nitrogen (No(Y)) as an Indicator of the Sensitivity of Ozone to Reductions in Hydrocarbon and Nox Emissions, *Journal of Geophysical Research-Atmospheres, 99*, 3533-3542.

Morris, R. E., et al. (2006), Model sensitivity evaluation for organic carbon using two multi-pollutant air quality models that simulate regional haze in the southeastern United States, *Atmospheric Environment, 40*, 4960-4972.

Morris, R. E., et al. (2005), Preliminary evaluation of the community multiscale air, quality model for 2002 over the southeastern United States, *Journal of the Air & Waste Management Association, 55*, 1694-1708.

Murazaki, K., and P. Hess (2006), How does climate change contribute to surface ozone change over the United States?, *Journal of Geophysical Research-Atmospheres, 111*.

Murphy, J. M., et al. (2004), Quantification of modelling uncertainties in a large ensemble of climate change simulations, *Nature, 430*, 768-772.

Nakic´enovic´, N. (2000), Special Report on Emissions Scenarios, Cambridge University Press, Cambridge, UK.

Napelenok, S. L., et al. (2006), Decoupled direct 3D sensitivity analysis for particulate matter (DDM-3D/PM), *Atmospheric Environment 40*, 6112-6121

Napelenok, S. L., et al. (2007), Area of influence (AOI) sensitivity analysis: Application to Atlanta, Georgia, *Atmospheric Environment*, *41*, 5605-5617.

Nenes, A., et al. (1998), ISORROPIA: A new thermodynamic equilibrium model for multiphase multicomponent inorganic aerosols, *Aquatic Geochemistry*, *4*, 123-152.

Odum, J. R., et al. (1997), The atmospheric aerosol-forming potential of whole gasoline vapor, *Science*, *276*, 96-99.

Pekkanen, J., et al. (1997), Effects of ultrafine and fine particles in urban air on peak expiratory flow among children with asthmatic symptoms, *Environmental Research*, *74*, 24-33.

Phoenix, G. K., et al. (2006), Atmospheric nitrogen deposition in world biodiversity hotspots: the need for a greater global perspective in assessing N deposition impacts, *Global Change Biology*, *12*, 470-476.

Pope, V. D., et al. (2000), The impact of new physical parametrizations in the Hadley Centre climate model: HadAM3, *Climate Dynamics*, *16*, 123-146.

Prinn, R., et al. (1999), Integrated global system model for climate policy assessment: Feedbacks and sensitivity studies, *Climatic Change*, *41*, 469-546.

Pun, B. K., and C. Seigneur (2001), Sensitivity of particulate matter nitrate formation to precursor emissions in the California San Joaquin Valley, *Environmental Science & Technology*, *35*, 2979-2987.

Pun, B. K., and C. Seigneur (2007), Investigative modeling of new pathways for secondary organic aerosol formation, *Atmospheric Chemistry and Physics*, *7*, 2199-2216.

Pun, B. K., et al. (2003), Uncertainties in modeling secondary organic aerosols: Three-dimensional modeling studies in Nashville/Western Tennessee, *Environmental Science & Technology*, *37*, 3647-3661.

Racherla, P. N., and P. J. Adams (2006), Sensitivity of global tropospheric ozone and fine particulate matter concentrations to climate change, *Journal of Geophysical Research-Atmospheres*, *111*.

Rae, J. G. L., et al. (2007), Sensitivity of global sulphate aerosol production to changes in oxidant concentrations and climate, *Journal of Geophysical Research-Atmospheres*, *112*.

Reilly, J., et al. (1999), Multi-gas assessment of the Kyoto Protocol, *Nature*, *401*, 549-555.

Rind, D., et al. (1999), Use of on-line tracers as a diagnostic tool in general circulation model development 2. Transport between the troposphere and stratosphere, *Journal of Geophysical Research-Atmospheres, 104*, 9151-9167.

Russell, A., and R. Dennis (2000), NARSTO critical review of photochemical models and modeling, *Atmospheric Environment, 34*, 2283-2324.

Russell, A. G., et al. (1983), Mathematical-Modeling of the Formation and Transport of Ammonium-Nitrate Aerosol, *Atmospheric Environment, 17*, 949-964.

Ryerson, T. B., et al. (2001), Observations of ozone formation in power plant plumes and implications for ozone control strategies, *Science*, *292*, 719-723.

Sala, O. E., et al. (2000), Biodiversity - Global biodiversity scenarios for the year 2100, *Science*, *287*, 1770-1774.

Sanderson, M. G., et al. (2006), Present and future acid deposition to ecosystems: The effect of climate change, *Atmospheric Environment*, *40*, 1275-1283.

Sanderson, M. G., et al. (2003), Effect of climate change on isoprene emissions and surface ozone levels, *Geophysical Research Letters*, *30*.

Sarnat, J. A., et al. (2001), Gaseous pollutants in particulate matter epidemiology: Confounders or surrogates?, *Environmental Health Perspectives*, *109*, 1053-1061.

Seaman, N. L. (2000), Meteorological modeling for air-quality assessments, *Atmospheric Environment*, *34*, 2231-2259.

Seinfeld, J. H., and S. N. Pandis (1997), *Atmospheric Chemistry and Physics - From Air Pollution to Climate Change*, John Wiley & Sons, Inc.

Seinfeld, J. H., and J. F. Pankow (2003), Organic Atmospheric Particulate Material, *Annual Review of Physical Chemistry*, *54*, 121-140.

Sheehan, P. E., and F. M. Bowman (2001), Estimated effects of temperature on secondary organic aerosol concentrations, *Environmental Science & Technology*, *35*, 2129-2135.

Sillman, S. (1995), The Use of Noy, H2o2, and Hno3 as Indicators for Ozone-Nox-Hydrocarbon Sensitivity in Urban Locations, *Journal of Geophysical Research-Atmospheres*, *100*, 14175-14188.

Sillman, S. (1999), The relation between ozone, NOx and hydrocarbons in urban and polluted rural environments, *Atmospheric Environment*, *33*, 1821-1845.

Sillman, S., et al. (1990), The Sensitivity of Ozone to Nitrogen-Oxides and Hydrocarbons in Regional Ozone Episodes, *Journal of Geophysical Research-Atmospheres*, *95*, 1837-1851.

Sillman, S., and F. J. Samson (1995), Impact of Temperature on Oxidant Photochemistry in Urban, Polluted Rural and Remote Environments, *Journal of Geophysical Research-Atmospheres*, *100*, 11497-11508.

Stott, P. A., and J. A. Kettleborough (2002), Origins and estimates of uncertainty in predictions of twenty-first century temperature rise, *Nature*, *416*, 723-726.

Stott, P. A., et al. (2006), Uncertainty in continental-scale temperature predictions, *Geophysical Research Letters*, *33*.

Stott, P. A., et al. (2000), External control of 20th century temperature by natural and anthropogenic forcings, *Science*, *290*, 2133-2137.

Strader, R., et al. (1999), Evaluation of secondary organic aerosol formation in winter, *Atmospheric Environment*, *33*, 4849-4863.

Streets, D. G., et al. (2004), On the future of carbonaceous aerosol emissions, *Journal of Geophysical Research-Atmospheres*, *109*.

Streets, D. G., and S. Fernandes (2002), Development of Future Emission Scenarios for Global Atmospheric Models, Argonne National Laboratory, Argonne.

Tagaris, E., et al. (2008), Impacts of future climate change and emissions reductions on nitrogen and sulfur deposition over the United States, *Geophysical Research Letters*, *35*.

Tagaris, E., et al. (2007), Impacts of Global Climate Change and Emissions on Regional Ozone and Fine Particulate Matter Concentrations over North America *Journal of Geophysical Research-Atmospheres*, *112*.

Unger, N., et al. (2006), Cross influences of ozone and sulfate precursor emissions changes on air quality and climate, *Proceedings of the National Academy of Sciences of the United States of America*, *103*, 4377-4380.

USEPA (2003), National Mobile Inventory Model (NMIM) Base and Future Year County Database Documentation and Quality Assurance Procedures, prepared by Eastern

Research Group, Inc., for U.S. Environmental Protection Agency, Office of Transportation and Air Quality, Ann Arbor, MI.

Volkamer, R., et al. (2006), Secondary organic aerosol formation from anthropogenic air pollution: Rapid and higher than expected, *Geophysical Research Letters*, *33*.

Webster, M., et al. (2003), Uncertainty analysis of climate change and policy response, *Climatic Change*, *61*, 295-320.

Webster, P. J., et al. (2005), Changes in tropical cyclone number, duration, and intensity in a warming environment, *Science*, *309*, 1844-1846.

Wise, E. K., and A. C. Comrie (2005), Meteorologically adjusted urban air quality trends in the Southwestern United States, *Atmospheric Environment*, *39*, 2969-2980.

Woo, J. H., et al. (2008), Development of Mid-Century Anthropogenic Emissions Inventory in Support of Regional Air Quality Modeling under Influence of Climate Change, *J. of Air & Waste Mag. Asso. (accepted).*

Wu, S., et al. (2007), Effect of 2000-2050 Global Change on Ozone Air Quality in the United States, paper presented at GCAP presentation, Harvard University.

Yang, Y. J., et al. (1997), Fast, direct sensitivity analysis of multidimensional photochemical models, *Environmental Science & Technology*, *31*, 2859-2868.

# VITA

## KUO-JEN LIAO

Kuo-Jen Liao was born in June 1978 in Pingtung, Taiwan where he received his bachelor degree in Earth Sciences from the National Cheng-Kung University in 2000 and master degree in Environmental Engineering from the National Taiwan University in 2002. Before going to the Georgia Institute of Technology for his Ph.D. studies, he did his military service and worked as an Environmental Engineer between 2002 and 2004. He began his Ph.D. studies in the School of Civil and Environmental Engineering at the Georgia Institute of Technology in 2004. After joining Dr. Ted Russell's research group, he started his research focusing on air quality studies. During that period, his studies have concentrated on air pollution modeling with considerations of impacts of climate change. He has been participating interdisciplinary cooperative projects with colleagues at the Environmental Protection Agency, the Massachusetts Institute of Technology, NESCAUM and the Pacific Northwest National Laboratory. As part of his work, he has been involved with air quality management and identification of optimal control strategies for improving air quality.